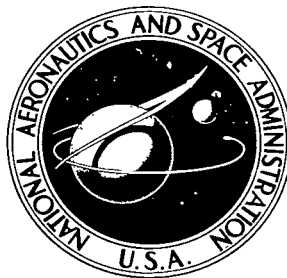


NASA TECHNICAL NOTE



NASA TN D-2240

6.1

LOAN COPY: RETU
AFWL (WLL-
KIRTLAND AFB, NM

0154805



TECH LIBRARY KAFB, NM

NASA TN D-2240

**INVESTIGATION OF MECHANISMS OF
POTENTIAL AIRCRAFT FUEL TANK
VENT FIRES AND EXPLOSIONS CAUSED
BY ATMOSPHERIC ELECTRICITY**

by Melvin Gerstein

Prepared for NASA/FAA under Contract No. NASr-59 by
LOCKHEED-CALIFORNIA COMPANY
Burbank, California



INVESTIGATION OF MECHANISMS OF POTENTIAL
AIRCRAFT FUEL TANK VENT FIRES AND EXPLOSIONS
CAUSED BY ATMOSPHERIC ELECTRICITY

By Melvin Gerstein

Prepared for NASA/FAA under Contract No. NASr-59 by

LOCKHEED-CALIFORNIA COMPANY

Burbank, California

NATIONAL AERONAUTICS AND SPACE ADMINISTRATION

For sale by the Office of Technical Services, Department of Commerce,
Washington D. C. 20230 -- Price \$3.00

ABSTRACT

A study has been conducted to determine the important mechanisms involved in the ignition of fuel vapors issuing from a fuel tank vent under conditions of atmospheric electrical activity. The study included a literature review and experimental and analytical investigations of (a) the mixing of the fuel vent effluent with ambient air for three vent configurations at simulated flight conditions, (b) the electrical environment in the vicinity of an aircraft during lightning activity, including measurements of the far field pressures associated with a high energy discharge, (c) a study of ignition and flame propagation through channels smaller than the normal quenching distance using high energy spark sources, and (d) a study of simulated lightning discharges as to their capability of producing flames capable of propagating through a typical fuel vent with and without a flame arrester.

The various separate programs and final correlating test sequence were performed. Profiles of constant observed fuel-air ratio were mapped using simulated vents installed in a wind tunnel. Characteristics of the electrical environment about an aircraft and the vent exit were derived from literature sources as well as actual probings. Pressure measurements associated with a high energy discharge were measured with pressure transducer and a Schleiren optical system. Flame propagation through normally quenching channels was studied by installing electrodes in a channel and supplying discharge energies of varying magnitudes. Results from these programs were correlated by installing a vent model in a simple wind tunnel and striking the model with simulated lightning discharges.

ABSTRACT (Continued)

The program, as a whole, pointed to certain general useful findings. Mapping of fuel-air mixture profiles near a fuel tank vent exit shows the flammable envelope to be relatively small. The greatest explosion hazard exists when the fuel tank and vent contain a flammable mixture and the vent outflow velocity is low. Pressure studies of high energy discharges show that, except for discharges directly to the vent exit, there is insufficient energy in lightning strike pressure waves to ignite fuel vapors. Finally, installation of flame arresters decreases ignition and propagation hazard under some conditions; however, the ability of a discharge generated plasma to penetrate the arrester and ignite a flammable mixture is a major factor in reducing arrester effectiveness.

TABLE OF CONTENTS

<u>Section</u>	<u>Title</u>	<u>Page</u>
	LIST OF TABLES	v
	FIGURE INDEX	vi
I	INTRODUCTION	1
II	DISCUSSION OF THE PROBLEM	4
III	COMBUSTIBLE ENVIRONMENT	7
	A. Fuel Tank (Effluent Source)	7
	B. Fuel Tank Vents	12
	C. Conclusions	25
IV	ELECTRICAL ENVIRONMENT	27
	A. Introduction	27
	B. Artificial Lightning Discharge Facilities Used in Tests of Aircraft Fuel Vents	28
	C. Lightning Induced Electrical Discharge Streamers at Fuel System Vents	29
	D. Direct Lightning Strikes to Fuel Vent Outlets	30
	E. Interim Considerations for Minimizing Fuel Vent Hazards from the Electrical Environment	31
	F. Concluding Discussion	34
	G. Conclusions	35
V	LIGHTNING INDUCED PRESSURE WAVES	36
	A. Introduction	36
	B. Natural Lightning Discharge Characteristics	36
	C. Laboratory Studies	37
	D. Analysis of Laboratory Measurements	38
	E. Blast Waves from a Natural Lightning Discharge	40

TABLE OF CONTENTS (continued)

<u>Section</u>	<u>Title</u>	<u>Page</u>
V	(continued)	
	F. Reduction of Blast Pressure Waves by Flame Arrester Screens	42
	G. Concluding Discussion	43
	H. Conclusions	44
VI	IGNITION AND QUENCHING	45
	A. Introduction	45
	B. Apparatus and Procedures	46
	C. Results and Discussion	50
	D. Concluding Discussion	56
	E. Conclusions	57
VII	LIGHTNING SIMULATION TESTS	58
	A. Introduction	58
	B. Artificial Lightning Discharge Currents Used in Tests of Aircraft Fuel Vents	58
	C. Apparatus and Procedure	60
	D. Results and Discussion	61
	E. Conclusions	63
VIII	CONCLUSIONS AND RECOMMENDATIONS	64
	A. Conclusions	64
	B. Summary Conclusions	66
	C. Recommendations	67
	REFERENCES	68

LIST OF TABLES

<u>Table</u>	<u>Description</u>	<u>Page No.</u>
I	Summary of Vent Exit Parameters at Maximum Climb Conditions for Several Aircraft	70
II	Comparison of Peak Current, Mechanical Forces, Heating Effect, Energy and Charge Transfer of the Three Types of Surge Current Generators Used in the Tests of Aircraft Fuel Vents	71
III	Summary of Runs in Which Flame Propagation Occurred on Open Vent Exit	72
IV	Summary of Runs in Which Flame Propagation Was Observed with Flame Arrestor Installed	73

FIGURE INDEX

<u>Figure No.</u>	<u>Description</u>	<u>Page</u>
1	Aircraft "A" Saturated Fuel-Air Ratio Inside Fuel Tank Vapor Space During Maximum Rate of Climb. Fuel is 115/145 Aviation Gasoline.	74
2	Aircraft "E" Saturated Fuel-Air Ratio Inside Fuel Tank Vapor Space During Maximum Rate of Climb. Fuel is JP-4 Turbine Fuel.	75
3	Variation of Fuel-Air Ratio in a Test Tank During Simulated Flight. Five Gallons of Hexane in a Fifty Gallon Tank.	76
4	Aircraft "E" Vent Exit Velocity Ratio During a Maximum Climb Profile.	77
5	Summary of Vent Exit Velocity Ratio (Non-Fuel Boiling) for Six Airplanes at Maximum Rate of Climb.	78
6	Vent Exit Velocity Ratio Including Fuel Boiling Effects for Aircraft "A". Fuel is 115/145 Aviation Gasoline.	79
7	Vent Exit Velocity Ratio Including Fuel Boiling Effects for Aircraft "E". Fuel is JP-4 Turbine Fuel.	80
8	Typical Vent Exit Configurations and Locations for One Manufacturer.	81
9	Three General Classes of Fuel Vent Exits.	84
10	Schematic Drawing of Gas Analysis Set-up and Probe Installed at Lockheed's Subsonic Wind Tunnel, Burbank.	85
11	Traverse Mechanism and Control Unit.	86
12	Control Circuit for Probe Traverse and Flap Positioning Mechanisms.	87
13	Model 213B Perkin-Elmer Hydrocarbon Detector.	88
14	Effect of Temperature and Effluent Fuel-Air Ratio on Observed Fuel-Air Ratio.	89
15	Flush Vent Exit Fuel Concentration Profiles	90

FIGURE INDEX (Continued)

Figure No.	Description	Page
16	Wake Vent Exit - Vent Discharging Into Airfoil Wake. Vent Exit Velocity 0.30 Free Stream Velocity.	108
17	Extended Vent Exit Mast Discharging Into Free Stream Airflow. Vent Exit Velocity 0.30 Free Stream Velocity.	109
18	Comparison of Natural Lightning Damage and Laboratory Lightning Damage to Same Type of Unprotected Radome.	110
19	Damaged VHF Transmitter Coil Illustrating Magnetic Forces and Heating of High Energy Natural Lightning Current Components.	111
20	Separation of Vertical Fin Illustrating High Blast Pressures Produced by Lightning Discharge Arcs Which Entered Through Inadequate Antenna Lead-In.	111
21	Natural Lightning Discharge to Jet Transport Wingtip Produces Larger Hole than 300 Coulomb Discharge in Laboratory.	112
22	Diagram of Multiple Generators Which Produce Typical Effects of Natural Lightning Strokes, Individually or as a Composite Single Discharge.	113
23	Oscillograms of Separate Current Components of Combined Discharge for Damage Testing.	114
24	Lightning Stroke Mechanisms	115
25	Induced Streamers off Aircraft Extremities Illustrated by High Impulse Potential Applied to Model Aircraft.	117
26	Gradients of Different Stages of Lightning Discharge Through Aircraft.	118
27	Electric Field Plots About Several Vent Types.	119
28	Test Arrangement for Simulated Vent Tube Streamer Measurements.	120
29	Streamer Discharge Tests	121

FIGURE INDEX (Continued)

<u>Figure No.</u>	<u>Description</u>	<u>Page</u>
30	Vent Tube Streamering With and Without Gradient Ring.	122
31	Fuel Vent Outlet Configurations for Reducing Flame Propagation and Spark Showers.	123
32	Illustration of Diverting Lightning Discharges from a Direct Stroke to a Fuel Vent by Application of Lightning Diverter Rods.	124
33	Test Arrangement and Oscillograms of Arc Current and Associated Blast Wave.	125
34	Blast Wave Front Detail Showing Rise Time of Approximately 10 Microseconds.	126
35	Blast Pressure Waves Recorded for Distance to 15 Feet.	127
36	Blast Pressure Waves to Distances of 3 Feet.	128
37	Blast Waves from Open Air Arc.	129
38	Test Arrangement for Schleiren Measurements of Shock Front Velocity.	130
39	Schleiren Blast Wave Pressure Studies.	131
40	Cylindrical to Spherical Wave Transition in Laboratory Discharge Compared to Natural Lightning Channel.	134
41	Graph of Theoretical and Experimental Distance vs. Time for Blast Waves from Discharge Energies of 1 to 100 Joules.	135
42	Theoretical and Experimental Curves of Strong Shock Transition to Sonic Waves.	136
43	Theoretical Curves of Strong Shock Velocities with Transitory to Measured Sonic Waves.	137
44	Theoretical Curves of Strong Shock Front Temperatures with Transitions to Temperatures Calculated on Basis of Perfect Gas Law and Measured Values of Pressure.	138

FIGURE INDEX (Continued)

Figure No.	Description	Page
45	Rocket Launching Platform on Stern of Ship Equipped with Lightning Current Measuring Shunt and Blast Pressure Gages.	139
46	Natural Lightning Current Oscillograms Triggered by Rocket Supported Wires.	140
47	Oscillograms of Laboratory High Current Discharges.	141
48	Pressures Recorded from Natural and Artificial Lightning Discharge.	142
49	Blast Pressure Waves Measured with and without Flame Arrester Screens.	143
50	Schematic of Spark Gap Electrical Circuit Used for Dynamic Science Corporation's Test Program.	144
51	Paschen Diagram for 5% Propane-Air Mixture Measured with 8.8 Millimeter Gap.	145
52	Quenching Distance for Parallel Plates, at Reduced Absolute Pressure, and 5% Propane-Air Mixture. Geometry Factor = 1.0.	146
53	Ignition and Quenching Apparatus Used in Test Program at Dynamic Science Corp.	147
54	Comparison of Discharges in Air at an Absolute Pressure of 500 Millimeters of Mercury for Three Discharge Energies.	148
55	Spark Volume in 5% Propane-Air Mixture for Various Discharge Energies at Several Pressures.	151
56	Spark Volume in Helium and Air for Various Discharge Energies at Several Pressures.	152
57	Plasma Volume in a 5% Propane-Air Mixture with 0.20 cm. Diameter Electrodes for Various Discharge Energies.	153
58	Plasma Volume in a 5% Propane-Air Mixture with a 0.40 cm. Diameter Electrode for Various Discharge Energies.	154

FIGURE INDEX (Continued)

<u>Figure No.</u>	<u>Description</u>	<u>Page</u>
59	Plasma Volume in Nitrogen with a 0.20 Dia. Electrode for Various Discharge Energies.	155
60	Plasma Volume in Nitrogen with 0.40 cm. Dia. Electrode for Various Discharge Energies.	156
61	Plasma Length in a 5% Propane-Air Mixture with 0.40 cm. Dia. Electrodes for Various Discharge Energies.	157
62	Plasma Length in a 5% Propane-Air Mixture with 0.20 cm. Dia. Electrodes for Various Discharge Energies.	158
63	Plasma Length in Nitrogen with a 0.20 cm. Dia. Electrode for Various Discharge Energies.	159
64	Plasma Length in Nitrogen with 0.40 cm. Dia. Electrode for Various Discharge Energies.	160
65	Relative Plasma Length for Various Gas Velocities and Two Discharge Energies.	161
66	Comparison of Discharges in Air and 5% Propane-Air Mixture at 16 and 80 Joules. Gas Flow is 100 meters/second.	162
67	Comparison of Discharge at Two Velocities for 5% Propane-Air Mixture and a Discharge Energy of 16 Joules.	166
68	Effect of Tube Length on Plasma Characteristics.	168
69	Expansion of a Plasma Produced in Air Into a Large Volume.	171
70	Schematic - Test Installation at LTRI	172
71	Summary of Discharge Locations for Tests with Flame Arrester Installed. Selected Tests with Open Vent also Shown.	173

I. INTRODUCTION

The effluent from a fuel tank vent may, under certain conditions, provide a source of flammable mixture in and around the fuel vent. The venting of fuel during flight through the atmosphere during periods of electrical activity such as lightning may, therefore, result in an explosion hazard due to the existence of a flammable mixture and a potential ignition source. It is important, therefore, to develop design principles and operating procedures which minimize the probability of a fire hazard due to ignition of the effluent from a fuel tank vent by atmospheric electricity. The work reported herein represents one phase of the total problem directed toward obtaining a better understanding of some of the basic processes which can lead to a fire hazard.

The objective of the investigation was to study the mechanisms of potential aircraft fuel tank vent fires and explosions caused by atmospheric electricity. The work represents a fundamental approach to fill some of the voids in existing knowledge and was not directed toward developing specific vent designs. The scope of the study included a survey of existing scientific and engineering data as a means of selecting the areas requiring further investigation. The results of the survey were reported in reference 1. In addition, inquiries were sent to over forty industrial organizations engaged in the production of aircraft and aircraft components to determine the status of knowledge concerning design principles and basic information related to fuel tank vent design and location to minimize fire hazards. The replies to these inquiries indicated that all manufacturers attempted to design and locate the fuel tank vents to minimize the hazards associated with lightning but that adequate basic knowledge was lacking. In particular, little information existed concerning the nature of the

fuel-air mixtures existing near a vent exit, the nature of the electrical environment resulting from atmospheric electrical phenomena, and the nature of the ignition processes under conditions approximating actual aircraft operating conditions.

On the basis of previous experience with aircraft fire hazard problems, the literature survey, and the replies to the inquiries, the scope of the information was formulated to include:

- a. Measurement of the fuel-air mixture profiles near the exit of representative fuel tank vents;
- b. Measurements of the properties of high energy discharges, including the generation of pressure waves;
- c. Measurements of ignition and flame propagation potential of high energy sparks, including a study of quenching phenomena;
- d. Measurement of ignition potential of simulated lightning strikes as a means of synthesizing the observations obtained in the previous experiments; and
- e. Analytical studies to support the experimental work.

As mentioned previously, the objectives of the program were to obtain basic scientific data and not to develop specific fuel tank vent designs. Because of the well-defined application of the data, however, the experimental and analytical work was limited to obtaining answers to questions pertinent to vent design and were not intended to be comprehensive scientific studies. The research program reported here thus represents an initial effort to fill some of the voids in the knowledge necessary to minimize the fire hazard associated with fuel tank venting.

The results of this program are presented in three forms. First there are certain conclusions which may be drawn from information already published. The work performed under this contract leads to additional

conclusions. Finally, overall conclusions leading to vent exit design were drawn from the literature, results of present contract and the experiences of the project personnel, including unpublished information.

The work was performed jointly by personnel from Lockheed-California Company, Lightning and Transients Research Institute, and Dynamic Science Corporation under joint sponsorship of NASA and FAA.

II. DISCUSSION OF THE PROBLEM

Fuel tanks on aircraft are vented to the atmosphere to prevent excessive pressure differences from occurring between the internal and external surfaces of the tank. As the aircraft changes altitude there is a flow either out of or into the tank, depending upon whether the aircraft is ascending or descending or, more exactly, upon whether the internal pressure is higher or lower than the pressure at the vent outlet. As a result of this "breathing" process, flammable fuel-air mixtures may exist within the vent line and tank itself. The occurrence of flammable mixtures within the tank-vent system would be strongly dependent on changes in external ambient pressure and temperature and on fuel volatility. The existence of flammable mixtures at or near the vent exit will depend on the nature of the vent flow and the surrounding air flow. A summary of the results of measurements of fuel-air ratio contours in the vicinity of three typical vent configurations is presented in the section dealing with the combustible environment.

The existence of a flammable mixture is, by itself, not a hazardous situation unless a source of ignition is present and a flame can be initiated and propagated into the fuel tank. The occurrence of an electric discharge in the vicinity of a vent exit can occur in several ways. The most obvious, of course, is a direct lightning strike. A second mechanism, occurring before and during a lightning strike at some other point on the aircraft, creates a charged condition on the aircraft's surface. Possible discharges from the vent exit in the form of a resulting corona or streamer can also represent another mechanism. A third source of electrical discharge is a lightning strike occurring at some point and traveling along the skin of the aircraft. If the

path of the discharge includes the vent exit then, as before, a possible source of ignition exists. The relationship of vent design and location to the occurrence of a discharge at the vent exit is discussed in the section on the electrical environment. This section also describes the status of knowledge with regard to the pressure field generated by a lightning discharge. The pressure wave associated with the discharge is important because it may affect the flow in and around the vent, thus altering the combustible environment; it may change local temperature and pressure conditions affecting ignition probability and, if sufficiently intense, may itself be a source of ignition. Unfortunately, as the subsequent discussion points out, a satisfactory knowledge concerning the pressure wave and other energy forms associated with a lightning discharge is still not available.

It is evident from the preceding discussion that a source of flammable mixture and sources of ignition may exist in the vicinity of the vent exit. The fact that the flammable mixtures and ignition sources exist only as transients greatly minimizes but does not eliminate the fire hazard associated with these sources. The likelihood of ignition will depend on the nature of the combustible mixture, the energy of the discharge, location of the discharge, local ambient conditions, vent velocity, and free stream velocity. A fairly extensive literature exists on ignition and quenching phenomena. Most of the scientific data in the literature, however, were obtained with relatively low energy discharges, usually near the minimum energy for ignition. A series of experiments with discharges several orders of magnitude greater than the minimum ignition energy was performed to determine whether any unusual effects were present. The section on ignition and quenching phenomena includes a detailed discussion of these experiments.

The combination of the possibility of having flammable mixtures near the vent exit and the existence of electrical discharges during lightning

activity leads to a condition which is potentially hazardous. The study of the combustible and electrical environment, as well as the study of ignition and quenching phenomena, supplies basic background material for the design of fuel tank vents.

III. COMBUSTIBLE ENVIRONMENT

This section of the report is concerned with the factors which affect the fuel-air mixtures which may exist in and around a vent exit.

A. Fuel Tank (Effluent Source)

Although the specific objectives of the program reported here did not include the study of the fuel-air mixtures existing within a fuel tank, knowledge of the conditions within the tank is desirable for two principal reasons. First, the nature of the mixture within the tank - especially near the vent entrance - determines the fuel-air mixture likely to exist in the vent effluent and, hence, is an important factor in determining the fuel-air ratio pattern in the vicinity of the vent exit. Second, the degree of hazard associated with the existence of an ignition source at the vent exit depends, to a large extent, upon whether or not a damaging explosion can occur within the fuel tank itself. Unfortunately, only the homogeneous, equilibrium fuel-air ratio can be calculated with confidence. As will be shown later, such homogeneous, equilibrium conditions do not necessarily exist within the tank. The idealized calculation, however, does serve as a guide to the average mixture ratio within the tank.

The saturated fuel-air ratio in the tank vapor space can be calculated from the following equation:

$$\frac{F}{A} = \frac{M_f}{M_a} \left(\frac{P_f}{P_{amb} - P_f} \right)$$

where

F/A = fuel-air ratio

M_f = mean molecular weight of fuel vapor

P_f = absolute vapor pressure of fuel at tank temperature

M_a = molecular weight of air

P_{amb} = absolute ambient atmospheric pressure

As a first approximation, the change in fuel vapor pressure with temperature can be obtained from the Clausius-Clapeyron equation (see standard thermodynamics text):

$$\log \frac{P_{f,2}}{P_{f,1}} = \frac{\Delta H_v}{2.3 R} \left(\frac{T_2 - T_1}{T_1 T_2} \right)$$

where

$P_{f,2}$ = fuel vapor pressure at T_2

$P_{f,1}$ = fuel vapor pressure at T_1

T_1 and T_2 = absolute fuel temperature

ΔH_v = heat of vaporization of fuel per mole

R = universal gas constant in thermal units
corresponding to ΔH_v

Where data are not available for specific fuels, rough estimates of ΔH_v can be obtained from Trouton's rule (see standard thermodynamics text):

$$\frac{\Delta H_v}{T_b} = 23$$

where T_b = normal atmospheric boiling point. It is important to point out that these relationships are only useful for very rough estimates, since they apply specifically to pure, single component liquids rather than to the complex mixtures present in most aircraft fuels. Nevertheless, they serve as a useful basis for first, rough estimates.

In order to illustrate the change in fuel-air ratio for two typical climb paths, Figures 1 and 2 present computed values of the homogeneous,

equilibrium fuel-air ratio for two different climb paths and for different assumed tank temperatures.

Figure 1 illustrates the behavior of 115/145 aviation gasoline for the climb path shown at the bottom of the figure, while Figure 2 illustrates the behavior of JP-4 fuel for a somewhat different climb path also shown at the bottom of that figure. The cross-hatched region in both figures represents the approximate flammable zone for both fuels.

Several important observations can be drawn from a study of the data. For both fuels, low temperature tank conditions may lead to flammable conditions within the tank, for which it may be concluded (for fuels of any specified volatility) there is a mean fuel temperature capable of producing flammable mixtures. The specific temperature range over which flammable conditions will exist under equilibrium conditions depends, of course, on the temperature-vapor pressure curve for the specific fuel.

Included in both figures is a curve representing the fuel-air ratio resulting when the tank temperature is equal to the ambient atmospheric temperature at the various altitudes. Such conditions would occur after extended flight at a particular altitude. For 115/145 aviation gasoline a flammable condition is indicated for altitudes above about 13,000 feet and for JP-4 altitudes above about 2,000 feet when the tank temperature and altitude temperature are equal. A sea level ambient temperature of 60°F was assumed for both fuels.

The equilibrium calculations suggest that both fuels produce mixture compositions richer than the flammable range at tank temperature of the order of 60°F and above. It is not unlikely that fuel temperatures in this range could exist for an aircraft leaving the ground with full tanks and climbing to altitude in a relatively short time. Several factors tend to disturb this apparently safe condition, however. As

the fuel cools during flight, the flammable zone is approached and flammable mixtures may result in the tank. Another factor also must be considered for extended flight at a specific altitude. Consumption of the fuel at a rate sufficiently rapid so that normal evaporation of the fuel cannot fill the tank volume will result in a flow of air through the tank vent into the tank. The flow of air into the tank will produce an interface in which the fuel-air ratio may vary from too rich to burn to too lean to burn with an intermediate flammable zone. The size of this flammable zone will depend on the degree of mixing within the tank, a factor which cannot be calculated with sufficient accuracy for practical estimates. Nevertheless, it must be assumed that a flammable mixture can exist in a portion of the tank under these nonequilibrium conditions, despite the fact that equilibrium calculations could indicate a mixture richer than the flammability limit.

An equivalent condition can result if the aircraft reduced altitude. The flow of air into the tank to equalize the pressure within the tank will similarly produce an interface which contains fuel and air within the flammable range as a result of nonequilibrium conditions.

Experimental results exist which confirm the possibility of flammable zones existing within a fuel tank as a consequence of nonequilibrium conditions (Ref. 2). One such experiment (from Ref. 2) is illustrated in Figure 3, which shows a flight plan in terms of altitude as a function of time and the measured fuel-air ratios as a function of time. Again, the approximate flammable zone is shown by a cross-hatched region. It is evident from an examination of Figure 3 that flammable mixtures were observed, although the calculated equilibrium fuel-air ratio was always greater than the rich flammability limit.

On the basis of the discussion presented in the previous paragraphs, it appears realistic to assume that flammable mixtures are present under conditions where the equilibrium fuel-air ratio is above the rich flammability limit.

In general, it appears that fuels of very low volatility may have some advantages in terms of fire hazard within the tank. A fuel with a sufficiently low vapor pressure such that the fuel-air ratio at sea level ambient temperatures is below the lean flammability limit would exhibit a tendency toward richer fuel-air ratios during climb for a constant tank temperature. Equilibration with the ambient temperature at altitude would tend to decrease the fuel-air ratio toward, and possibly below, the lean limit. Breathing of the tank would tend to minimize the hazard, since the introduction of additional air would tend to further reduce the fuel-air ratio in the interface. A complication does exist which prevents a more conclusive statement concerning fuels of very low vapor pressure. Sloshing of the fuel within the tanks, as well as the effects of tank vibrations, could produce a fine mist of fuel droplets which have been shown to represent a fire hazard (Ref. 3) although the actual fuel vapor-air mixture is below the lean flammability limit. There is not sufficient information at the present time to assess the role of fuel mists within a tank in terms of fire hazard, and it was considered beyond the scope of the present investigation to determine the importance of this factor.

In summary, equations and typical data have been presented for determining the homogeneous fuel-air ratios within a fuel tank. On the basis of the data examined, it is concluded that flammable conditions can exist within a tank despite the indications from equilibrium calculations that a fuel-air ratio richer than the flammability limit should theoretically exist. Preliminary considerations indicate that fuels of extremely low volatility may offer some benefits in terms of explosion hazard, although the role of fuel mists suspended in air must be determined before firm conclusions can be drawn.

B. Fuel Tank Vents

1. Flow Parameters

Two different flow fields are important in the evaluation of the fuel-air mixture which may exist in and around the fuel tank vent exit. The first of these is the flow issuing from the vent, which depends on tank volume, quantity and type of fuel in the tank, fuel temperature, rate of change of external pressure, vent geometry, and the ambient altitude. The second flow field of importance is the flow of air around the vent exit, which depends on the aircraft speed and the vent location. The nature of the fuel-air mixture at the vent exit depends on whether the aircraft is ascending or descending. In assessing the existence of a hazardous condition, it would appear that the climb condition is the most serious. It is during climb, while the external ambient pressure is decreasing, that the fuel tank is discharging fuel vapor or fuel vapor-air mixture. Hence, at this time, a flammable mixture may exist in or near the vent exit. During descent, ambient air is flowing into the vent and it is not expected that a flammable mixture would exist at the vent exit. The greatest hazard may exist during a climb or in levelling off after a climb following a descent. As a result of this combination of maneuvers, air has been admitted to the tank during descent and a flammable mixture may exist in the tank and vent lines during the subsequent ascent.

The vent exit flow velocity can be calculated at altitudes below the saturation partial pressure of the fuel by considering the change in volume of the gases within the vapor space in the tank as a result of the change in local ambient pressure. The vent exit flow velocity can be estimated from the following equation:

$$V_v = \left(\frac{Vol}{A_v} \right) \left(\frac{1}{P} \right) \left(\frac{dP}{dh} \right) \left(\frac{r}{c} \right)$$

where

V_v = vent exit flow velocity
 Vol = tank vapor volume
 A_v = vent exit area
 P = tank pressure (assume local ambient pressure)
 dP/dh = change of pressure with altitude
 r/c = rate of climb

Some typical values of the maximum vent exit velocity to free stream velocity ratio are shown in Table I for a variety of aircraft and flight speeds.

The vent mass flow per second is related to vent velocity by the relation

$$W = \rho A_v V_v$$

where

W = vent mass flow per second
 ρ = density, \overline{PM}/RT
 \overline{M} = mean molecular weight

which results in the equation

$$W = \left(\frac{Vol}{RT} \right)_v \left(\frac{dP}{dh} \right) \left(\frac{r}{c} \right) \left(\frac{1 + F/A}{\frac{1}{\overline{M}_a} + \frac{F/A}{\overline{M}_f}} \right)$$

The last term represents the mean molecular weight.

The velocity ratio V_v/V_o is illustrated in Figure 4 as a function of altitude for maximum rate of climb. The curves show the increase in vent rate as the vented volume increases from expansion space only, to expansion space plus evolution of air from the fuel, to that of an almost empty tank. Since the penetration of the vent effluent

into the ambient air stream will be greatest for the highest vent velocities, the altitude variation of "empty tank" vent rates were computed for six representative aircraft. The results are shown in Figure 5.

The vent exit flow changes abruptly when an altitude is reached at which the ambient pressure is below the vapor pressure of the fuel at the bulk fuel temperature. Under these conditions, the fuel boils and the exit flow increases appreciably. The calculation of vent to free stream velocity ratio for altitudes above the fuel boiling altitude involves an iteration process using the vent system pressure drop characteristics and data relating the percent fuel weight loss to pressure on the fuel surface. Typical tank and vent parameters and the vent exit velocity ratio as a function of altitude are illustrated in Figure 6, where the steep rise in V_v/V_o is the result of fuel boiling with 115/145 aviation gasoline. Similar curves for JP-4 are shown in Figure 7. At the altitudes considered, below 35,000 feet the effect of fuel boiling does not appear because of the lower vapor pressure of JP-4. One would expect a similar behavior for JP-4 as we noted for 115/145 fuel but at considerably higher altitudes.

In this section, equations have been presented for the calculation of fuel tank vent gas velocity, and some typical data are shown for a number of different aircraft. In addition, the effect of fuel boiling on vent gas velocity is illustrated. Vent effluent during a fuel boiling condition is almost pure fuel vapor and as such is much too rich to burn.

The velocity of the gases in the fuel tank vent is important in at least two ways. First, the velocity of the effluent gases will be shown to be a principal factor in determining the mixing and, therefore, the local fuel-air ratios near the vent exit. This effect will be treated in detail in the next section. Second, the velocity of the

gases within the fuel tank vent can be important in determining whether or not a flame can propagate against the flow, presupposing that the mixture is flammable.

Laminar flame velocities for hydrocarbon-air mixtures are of the order of 2 - 4 feet per second (Ref. 3). Turbulence may increase the speed of flame propagation to the order of 10 - 20 feet per second (Ref.3).^{*} The greatest flash-back hazard will, therefore, exist at lower vent flow velocities and will decrease as the vent flow velocity increases. The principal inference to be drawn here is that flash-back of a flame through the vent, presupposing an ignition source and a flammable mixture within the vent, is most likely to occur at low rates of climb.

2. Experimental Determination of Mixture Profiles

The physical model under investigation in this study involves the existence of a flammable fuel-air mixture in or around the fuel tank vent which may be ignited by a lightning strike, streamer or corona discharge. Previous sections have reviewed some of the existing knowledge concerning fuel-air ratios and gas flow velocities within the vent. This section is concerned with the mixing processes occurring at the vent exit which determine local fuel-air ratios in the vicinity of the vent exit for various vent flow conditions and flight speeds. Since data were not available on the mixing of the vent effluent with the ambient air stream, an experimental program was undertaken to determine the fuel-air ratios which can exist for various vent flow and flight speed parameters.

* The stabilization of flames by flame holders at stream velocities of several hundred feet per second is not considered here. It is assumed that the vent does not contain sheltered regions which can result in this type of flame propagation. The approximate numbers cited here are for a free flame propagating against the stream velocity much in the manner of a man rowing a boat against the current. It is further assumed that the boundary layer near the wall is too thin to permit a flame to propagate upstream in the boundary layer.

One of the first tasks in setting up the experimental program was to determine a minimum number of vent exit configurations in order to reduce the number of experimental tests required. Inasmuch as vent configuration and location are strongly dependent on airplane design, the fuel tank vents used in practice assume many different appearances and occur in varied locations for different aircraft. Some typical vent exit configurations and locations by one manufacturer are illustrated in Figure 8. These configurations and locations are by no means complete but are shown only as representative for a large number of aircraft. The figures serve as an orientation to the physical situation which may exist near the fuel vent exit.

A close examination of these and other configurations indicated that all of them seemed to be variations of three principal types:

- a. Flush vent discharging into a boundary layer,
- b. Mast discharging into a wake,
- c. Mast discharging into a free stream.

These three vent types, shown schematically in Figure 9, were chosen as the basic configurations for the experimental study of mixing in the vicinity of a fuel tank vent exit.

A study of the mixing problem indicated that the following variables would be important in determining the local fuel-air ratios in the vicinity of a fuel tank vent exit:

- a. F/A of vent flow,
- b. Vent flow velocity and nature,
- c. Free stream flow velocity and nature,
- d. Boundary layer thickness,
- e. Distance of point from vent exit,
- f. Temperature.

In order to minimize the number of data points required to obtain a fuel-air ratio map, the flush vent configuration was used to

determine the most important parameters.

3. Apparatus

Mixture profiles at the exit of the three typical configurations shown in Figure 9 were determined by analysis of continuous gas samples withdrawn, by means of a probe, from the region near the fuel tank vent exit. Details of the probe and analysis set-up are described below.

Probe

A schematic drawing of the probe and its connection to the gas analysis set-up is shown in Figure 10. The probe was designed to permit sampling within flame quenching distance (the order of 0.04 inch) of the model surface. To accomplish this, the probe was constructed from a hypodermic needle having a 0.05 inch outside diameter. While it was originally believed that the sample velocity into the probe should be iso-kinetic with the gas stream ahead of the probe, repeated tests showed that the iso-kinetic condition was not required. The use of the propane as a tracer gas, once the influence of fuel-air ratio on the mixing process had been evaluated, eliminated the need for dilution of the mixture prior to analysis by the hydrocarbon detector.

Traverse Mechanism

A traverse mechanism having three degrees of freedom and precise position control was constructed to permit positioning of the gas sampling probe without shutting down the tunnel between samples. A photograph of the traverse mechanism is shown in Figure 11. Movement and read-out of the probe position is done electrically through the control circuit shown in Figure 12. Linear potentiometers driven by the traversing screws have been individually calibrated with respect to the three dimensional position of the probe against a digital potentiometer in

a null indicating bridge circuit.

The probe attached to the vertical arm of the mechanism can be remotely re-positioned with respect to an initial pre-determined starting point with an accuracy of ± 0.005 " in the vertical, ± 0.010 " in the lateral, and ± 0.012 " in the longitudinal directions through full travel distances of 4.9, 10.8, and 8.8 inches, respectively.

Gas Analyzer

A Perkin-Elmer Model 213B Hydrocarbon Detector (Figure 13) was used for gas analysis. The instrument uses the principle of hydrogen flame ionization for the detection of gaseous hydrocarbons. The test sample is introduced into the instrument under pressure, metered, mixed with hydrogen, and burned in an enclosed chamber. Within the chamber a 300 volt D-C potential exists between the flame jet and an electrode. Hydrocarbons in the sample are ionized by the flame, causing a current to flow which is proportional to the carbon content of the sample gas. The resulting current is read on a calibrated meter or recorded externally. Calibration is obtained from known samples of hydrocarbon-air mixtures.

Wind Tunnel

Two different wind tunnels were used during the investigation. Both tunnels were operated at a tunnel airspeed of 100 knots. Unfortunately, it was not possible to measure the turbulence level in either tunnel. Measurements made in the first tunnel, including tuft studies to observe the flow, indicated the presence of some turbulence in the flow. The second tunnel, in which all of the data presented in this report were taken, had previously been the subject of a turbulence study. The results had indicated a turbulence level below the range of the

hot-wire instrumentation used. Comparison of the data using the flush vent indicated no major effect due to the differences in the two tunnels. Nevertheless, in order to assure consistency between the measured composition profiles, only the second, low turbulence tunnel data are presented.

4. Instrumentation Procedures

The following instrumentation and test procedures were used in obtaining the fuel-air mixture profiles reported.

Boundary Layer Survey

Pressure surveys were taken of boundary layers to determine the degree of flight article simulation by the test equipment.

Instrumentation

- (a) Manometer bank for static pressure survey.
- (b) Pitot tube reading free stream velocity and associated readout manometer.
- (c) Traverse mechanism and position determination equipment.
- (d) Total pressure probe and manometer.

Procedure

- (a) Set boundary layer generator position.
- (b) Record static pressure survey (if applicable).
- (c) Position total pressure probe.
- (d) Vary the probe in the vertical direction.
- (e) Record total pressure variation from the plate under-surface to free stream total pressure.

Fuel-Air Mixture Mapping

Instrumentation

- (a) Six variable area Schutte & Koerting rotameters.
- (b) Two Heise bourdon tube pressure gages for measuring rotameter inlet pressure, 0 to 200 inches of mercury.

- (c) Traversing mechanism assembly and associated positioning equipment.
- (d) Small rotameter for indicating vapor sample flow rate.
- (e) 0 to 160 PSI bourdon tube pressure tube sample pump output pressure.
- (f) Water manometer for measuring air stream total pressures.
- (g) Perkin-Elmer hydrocarbon detector (Ref. 1).

Procedure

- (a) Switch on and calibrate hydrocarbon detector.
- (b) Set boundary layer generator with remote equipment.
- (c) Set air flow on rotameter.
- (d) Set propane flow on rotameter.
- (e) Activate sample pumping apparatus and set to desired flow rate.
- (f) Position probe in vent exit opening.
- (g) Adjust effluent vapor to a 1% or 10,000 PPM reading on the hydrocarbon detector.
- (h) Position traverse probe in the fore and aft direction.
- (i) Set vertical position and traverse laterally. Take data at five to seven positions, each position requiring two to four hydrocarbon detector readings.
- (j) Move to new fore and aft position and repeat (i).
- (k) Upon changing vent exit velocity or boundary layer, repeat items (f) through (j).

5. Results and Discussion

The initial experiments relative to the measurement of mixture profiles were directed toward the determination of the major parameters affecting the mixing process.

Fuel-Air Ratio of Vent Flow

The local fuel-air ratios in the vicinity of a fuel tank vent exit will, of course, depend on the fuel-air ratio of the vent effluent. In practice, the fuel-air ratio of the vented

gas can range from pure fuel to pure air. One would expect that for turbulent mixing the ratio $\frac{f}{f+a} / \frac{F}{F+A}$ would be independent of the fuel concentration and, in fact, independent of the nature of the fuel molecule itself.* These factors would be important only if molecular diffusion was a significant part of the mixing process. The fuel concentration affects the mixing process through the fuel concentration gradient, while the molecular nature of the fuel molecule affects the diffusion coefficient. In order to determine the sensitivity of the measured fuel concentrations to the initial fuel concentrations, a series of tests with the flush mounted vent was performed. Typical results are shown in Figure 14(a) where it is shown that the observed ratio $f/(f+a)$ is a linear function of the vent ratio $F/(F+A)$ such that

$$\frac{\frac{f}{f+a}}{\frac{F}{F+A}} = \text{constant},$$

all other variables being constant. On the basis of data obtained for a variety of velocity ratios and at different locations with respect to the vent exit, it was concluded that molecular diffusion processes played a minor role in the mixing of the vent effluent and the ambient air stream. The experimental data can thus be generalized in terms of the ratio

$$\frac{\frac{f}{f+a}}{\frac{F}{F+A}}$$

* where $f/f+a$ is the local ratio of fuel to total fuel and air, and $F/F+A$ is the ratio of fuel to total fuel and air in vent.

Temperature Ratio

Examination of a large number of flight conditions showed that the fuel tank vent effluent often differed from the temperature of the ambient air stream. The study indicated that the variation of vent effluent temperature, T_v , to free stream temperature, T_o , varied between the limits

$$0.75 \leq \frac{T_v}{T_o} \leq 1.5$$

Series of tests were performed to determine if the temperature ratio influenced the mixing process. Typical results are shown in Figure 14(b), where the observed weight fraction of fuel is plotted against T_v/T_o , all other variables held constant. It is seen that in the range of T_v/T_o from 1.0 to 1.30 this ratio has no effect on the mixing process. Temperature, at least within the range experienced by current aircraft, was therefore not considered an important variable in the mixing process and is not considered further.

Critical Variables

The preliminary study resulted in the conclusion that the ratio

$$\frac{f/f+a}{F/F+A}$$

was dependent on the nature and velocity of the vent effluent, the nature and velocity of the free stream, the vent configuration, and the boundary layer thickness.

Of these variables the local fuel-air ratios appeared to be a rather complex function of the vent effluent and free stream velocities. Under some conditions, the mixing process appeared to be independent of boundary layer thickness. Since an insensitivity to the ratio of boundary layer thickness to vent diameter D , could not be demonstrated for all conditions, variations in δ/D were included in the program for fuel-air

ratio mapping.

Fuel-Air Ratio Maps

In order to determine the nature of the mixing of the fuel tank vent effluent with the surrounding air stream, gas samples were analyzed. The data are presented for three configurations

- (a) Flush vent discharging into a boundary layer,
- (b) Mast discharging into a wake,
- (c) Mast discharging into a free stream,

illustrated schematically in Figure 9. The results are presented as contours for given values of the ratio $f/(f+a) / F/(F+A)$ for different values of the velocity ratio V_v/V_o and boundary layer thickness ratio (where applicable) δ/D in Figures 15, 16, and 17,

where: δ is the boundary layer thickness and
D is the vent line diameter.

The choice of the ratio of vent flow velocity to air stream velocity as the velocity parameter was made for convenience. The mixing of two streams is often more closely related to the velocity difference $V_o - V_v$. The two quantities are easily related since

$$V_o - V_v = V_o \left(1 - \frac{V_v}{V_o} \right)$$

Since many of the experiments were performed as a constant value of V_o , the velocity difference is thus proportional to one minus the velocity ratio.

(a) Flush Vent Discharging Into a Boundary Layer

Examination of the contours for a flush vent discharging into a boundary layer (Fig. 15 (a) through (j)), shows two features of the mixing process immediately. First, the dilution of the vent effluent in a direction normal to the surface

containing the vent exit is extremely rapid. The fuel-air ratio falls to about 2% of the value in the vent in a vertical distance of the order of a vent diameter. As one would expect, the penetration of the vent effluent (in a direction normal to the surface containing the vent exit) increases with increasing values of V_v/V_o . The presence of a surface, however, tends to maintain fairly high values of the ratio $f/(f+a) / F/(F+A)$ near the surface and downstream of the vent exit.

Consider the significance of the contours in terms of the flammability problem. The flammable range for typical hydrocarbon fuels ranges from values of $F/(F+A)$ of .025 to about 0.25. If it is assumed that a hazard requires the existence of a flammable mixture within the vent line itself, then the most severe mixing problem (most difficult air dilution) exists for the fuel rich mixtures. Even for such mixtures the flammable zone is relatively small. Nevertheless, an electrical discharge within the flammable envelope could cause ignition and possibly propagation of a flame into the vent. Whether or not propagation of flame into the vent could occur would depend on the flow velocity in the vent line. The greatest hazard exists for low vent velocities since, under these conditions, the greatest probability exists that a flame can flash back through the vent line into the tank.

(b) Vent Discharging Into a Wake

The second configuration investigated consisted of a vent discharging into a wake. The measured mixture profiles are presented in Figure 16. Comparison of the results with this configuration and the flush mounted vent shows that the absence of the surface reduces the mixing zone, but that the general observations of a relatively small mixing region elongated in the direction of flow is still applicable.

(c) Vent Discharging Into a Free Stream

The maximum mixing efficiency and, therefore, the greatest dilution potential exists for the configuration in which the vent exit is located in the free stream. A mixture profile for this configuration is shown in Figure 17. Examination of the profile shows a greatly reduced mixing zone compared to the two previous configurations. Nevertheless, the possibility of flammable mixtures still exists in the immediate vicinity of the vent exit. A lightning strike at the vent, or a discharge originating from the vent, could still pass through a flammable mixture and cause ignition.

6. Summary of Mixing Study

Mixture profiles have been determined experimentally for three vent configurations. The largest mixing zone was found for the flush mounted vent, and the smallest mixing zone for a vent discharging into a free stream. For all vent configurations the possibility of the existence of a flammable mixture near the vent exit is shown, despite the major changes in the air flow pattern near the vent exit. It appears, therefore, dilution of the vent effluent by the improvement of the mixing processes cannot be depended upon as a method of eliminating the existence of flammable mixtures near the vent exit.

C. Conclusions

1. Fuel Tank (Effluent Source)

(a) Flammable conditions may exist within a fuel tank contrary to equilibrium calculations.

(b) Preliminary considerations indicate fuels of extremely low volatility may offer benefits in terms of reduced explosion hazard (although the role of fuel mists suspended in air must be determined before firm conclusions may be drawn).

2. Fuel Tank Vents

(a) Flash-back of a flame through the vent, presupposing an ignition source and a flammable mixture within the vent, is most likely to occur at low rates of climb (low effluent velocity).

(b) It was determined practically all vent exits on current aircraft fall into three types:

- (1) A flush vent discharging into a boundary layer,
- (2) A mast discharging into a wake, and
- (3) A mast discharging into a free stream.

(c) Iso-kinetic gas stream sampling with a small probe in the order of 0.05 inch diameter is unnecessary as the probe does not significantly disturb the streamlines.

(d) Observed fuel-air ratio, at any point in the fuel-air ratio envelope, is a linear function of the vent fuel-air ratio. Also, molecular diffusion processes are insignificant in the mixing of the vent effluent and ambient air stream.

(e) The temperature ratio between the vent effluent and the free stream, in the range experienced by current aircraft, has no effect upon the mixing process.

(f) From conclusion (d), the use of a tracer gas in the effluent to determine the mixing envelope of a low speed gas jet discharging into a high speed gas flow is valid.

(g) A vent discharging into a free stream exhibits the greatest dilution or smallest mixing zone.

IV. ELECTRICAL ENVIRONMENT

A. Introduction

The thunderstorm electrical environment about an aircraft in flight consists of charge areas with associated intense electric fields which are varying according to the random charge redistributions taking place in the form of slow charge and rapid discharge of cloud areas. The environmental factors presenting possible hazards to aircraft from these charge regions and associated fields are the induced streamer currents from the intense electric fields, the high temperatures, energies and blast waves from the high current lightning discharges and the metal burning or spark showers from the heavy charge transfers. Studies have been undertaken in this NASA/FAA sponsored program on "Mechanisms of Potential Aircraft Fuel Vent Fires by Atmospheric Electricity" to determine the specific mechanisms by which these environmental factors may present a possible hazard to aircraft fuel vents.

The characteristics of natural lightning discharges to ground have been studied over a period of many years by the electrical power transmission industry. The studies have been extended by Lightning & Transients Research Institute (LTRI) over the past fifteen years to aircraft and the cloud-to-cloud type discharges they frequently encounter by means of flight research programs and analysis of flight damaged aircraft parts or the airline reports. It has been found that the standard test wave shapes and magnitudes used in the electrical power industry are completely inadequate to reproduce the damage commonly encountered on aircraft and special high current, high energy facilities have, therefore, been set up to reproduce this more severe damage.

B. Artificial Lightning Discharge Facilities Used In Tests of Aircraft Fuel Vents

A lightning discharge may be described by the typical effects produced by its various components, the intense electric fields and streamering produced by the high voltages, the magnetic forces of the high currents, the heating and blast effects of the high energy intermediate currents, and the metal erosion of the long duration lower currents which continue for periods up to one second following the short duration high energy components. Examples of these effects are shown in the photographs of Figures 18, 19, 20, and 21 illustrating aircraft components damaged in flight. Analysis of the damaged parts permits an estimate of the natural lightning discharge component magnitudes for establishing artificial lightning generation facilities.

These effects have been reproduced in the laboratory by a group of four artificial lightning generators used separately or connected together in such a way as to give a composite single discharge representative of a single, severe natural lightning stroke. A diagram showing the generator circuits, output wave forms, and coupling circuits used for firing the various components as a single discharge is presented in Figure 22. Oscillograms of the output currents are shown in Figure 23.

The circuit constants of the laboratory generators and the output currents, energies and charge transfers of laboratory apparatus utilized in the evaluation program are presented in Table II. The first generator (Figure 22) was not utilized in the evaluation program.

For the studies of streamering off simulated fuel vents, the high voltage generator was used at levels of about two and one-half million volts, the maximum voltage which the electrode-to-vent spacing would support without flashover. This duplicates the electric fields found in flight which, though involving greater potentials over greater distances, cannot exceed the critical sparkover gradient without a discharge taking place.

For the studies of possible flame propagation through fuel vents or flame arresters in the evaluation program, the high and intermediate current components were used to produce the severe blast effects of natural lightning (Table II). The long duration, low current component was used to burn the vent outlet or flame arrester severely enough to present an ignition source of relatively long time duration to the fuel vapor outflow.

C. Lightning Induced Electrical Discharge Streamers at Fuel System Vents

A lightning stroke approaching an aircraft moves in discrete steps known as step leaders. The thunderstorm structure and step leader development are illustrated in Figures 24(a) and 24(b), based on the early work of Simpson and Scrase (Ref. 4) and Schonland (Ref. 5) selected from the extensive literature on this subject. The potential at the tip of the step leader of the advancing stroke produces an intense electric field on the aircraft and induces corona streamer currents off extremities. The approaching stroke contacts one of the aircraft streamers to form the final step leader path to the aircraft. The stroke then passes on through the aircraft to another cloud charge region or to ground. This is illustrated in Figure 24(c). It may easily be shown that so-called "static discharges" which imply stored charge emanating from the aircraft, cannot possibly have the energies required to produce the severe damage frequently reported on aircraft, because of the relatively small electrical capacity of the aircraft.

When an aircraft is contacted by a lightning discharge channel, its potential may be raised to the order of 10^8 volts in less than a microsecond. At this potential, streamers may be generated from almost any point on the aircraft, including fuel vent locations even in relatively shielded regions. This is illustrated in Figure 25 showing streamers

off a model aircraft raised to a potential of two million volts.

The step-by-step sequence of a lightning stroke approach to an aircraft in flight is illustrated in Figure 26, as determined from an electrolytic tank plot about a model aircraft. Measurements of potential and gradient about an aircraft model in a conducting electrolyte are directly analogous to the free space potentials and gradients about the aircraft in flight. As shown in Figure 9, the potential of the aircraft remains nearly constant until just before the stroke contacts the aircraft, at which time it rises abruptly to the stroke potential. Thus the aircraft suddenly rises in potential to about 10^8 volts, producing potential gradients about the vent outlets such as those shown in Figure 27. The equipotential lines are given in percent of aircraft voltage.

A study under a USAF research program (Ref. 6) of the actual aircraft potentials required to produce critical gradients for various vent locations and types has indicated that there are sufficient differences in gradients between vent locations and types that proper vent location and design can reduce the probability of streamering and direct lightning discharges significantly.

The streamer current magnitudes have been studied in the laboratory (Ref. 7) for a simple cylindrical vent geometry, as illustrated in Figure 28. The LTRI artificial lightning impulse generator was used at two and one-half million volts to produce an impulse field about a simple cylindrical simulated vent tube about 4 inches in diameter.

D. Direct Lightning Strikes to Fuel Vent Outlets

The investigation of ignition from lightning strikes to fuel vent outlets was planned with anticipation that the following mechanisms might represent potential ignition sources from the high arc temperature,

compression ignition of fuel vapors from the strong shock waves near the stroke, spark shower production by arc burning of the vent outlet with subsequent spark entry through the vent tube into flammable regions, and internal vent tube sparking of high resistance or intermittent paths from the high stroke currents. For strokes directly to the vent outlet, the discharge channel energy (100 joules/cm of arc length) exceeds by many orders of magnitude the energy required for fuel vapor ignition (0.001 joules).

Poorly bonded vent outlets can channel stroke currents toward the fuel tank, where a high resistance joint can produce internal sparking. This can be prevented by assuring that the vent outlet is bonded to the skin with a resistance of the order of a few milliohms or, preferably, a few hundred micro-ohms. In view of these mechanisms which have not all been thoroughly evaluated, the importance of avoiding direct strikes, for the present, to fuel vent outlets wherever possible can hardly be overemphasized.

E. Interim Considerations for Minimizing Fuel Vent Hazards From the Electrical Environment

There are some interim electrical protection concepts which can be applied to specific aircraft as evolved in current interim lightning protection research programs at LTRI under industry support. Model studies have been carried out by LTRI on different types of current aircraft, and extensive flight damage reports are available to give a fairly complete picture of the points at which lightning strikes can be most often expected. Based on this data, some conclusions can be drawn regarding optimum fuel vent locations from the point of view both of streamers and direct or swept lightning strokes. Vents located near aircraft extremities are most vulnerable to direct lightning strikes, shock wave effects, and streamering. The preferable locations are in low electrical gradient areas with large radii of curvature, such as

the under surface of the wing.

As most strikes to forward sections of an aircraft are swept to the rear, vents should preferably not be located behind sharp, high gradient points such as propellers or jet pods. Strikes to the aircraft nose are common and, as these strikes are nearly always swept back along the fuselage, vent locations should preferably be located with respect to the least likely paths for lightning strokes to be swept along the fuselage. One favorable vent location is midway between the wingtip and the outboard propeller tip or jet pod in the flat area of the wing.

Because of the tremendous potentials involved, the use of insulation or limiting resistances to prevent or limit the streamer currents and energies from vents is not very practical. For example, standard insulated aircraft antenna wire, WS 25/U, with a dielectric strength of one-quarter to one-third of a million volts is easily and frequently punctured in thunderstorm areas, one of the reasons for its coming into disuse. Also, unprotected aircraft radomes are minutely punctured during thunderstorm conditions, sometimes even by friction charging of the surface without direct lightning strikes. Once punctured, the thunderstorm induced discharge energies are channeled through the puncture to provide a streamer. The puncture discharge current acts to some extent as a small lightning rod to locally attract or divert lightning discharges. An illustration of streamering from a plastic vent is shown in Figure 29. The importance of gradient control as a primary method of fuel vent protection is pointed up by an illustration of an effect often observed on tops of flag poles. A lightning strike to a flag pole often does not strike the top of the round ball used at the tip, but passes around the ball to the pole which has a higher gradient by virtue of its smaller radius. Extensive pitting on the pole, with no pitting on top of the ball, is often observed. This

analogy can be extended to an aircraft wing tip. With a typically well rounded, smooth tip and a sharp vent outlet slightly inboard, a stroke may be expected to pass around the tip to the vent outlet. The conclusion drawn is that once any part of the aircraft reaches the ionization threshold, the large thunderstorm potentials will heavily feed the resultant discharge and that the threshold potential for each vent type and location is therefore the most significant information in relation to the degree of hazard from the electrical standpoint.

Among the possibilities which have been considered for reducing the hazard of direct lightning strokes to a fuel vent outlet are the use of gradient reducing rings which help to prevent streamering from taking place directly off the vent outlet. The purpose of the gradient ring is to remove any possible streamering or lightning strokes at least a few inches away from the vent outlet. This is illustrated in the diagram and photograph of Figure 30.

The use of a series of parallel tubes in a vent outlet had been suggested earlier (Ref. 8) for the purpose of withstanding direct arc burning, with possible flame arrester application illustrated in Figure 31. They suffer from the disadvantage that they do not prevent spark shower entrance into the vent interior. Considered for prevention of spark shower entrance into the vent outlet is the use of a baffle system also illustrated in Figure 31. A sequence of baffles act as particle traps such that the particles are blocked from entering the vent outlet while the air fuel vapors may flow unimpeded. It should be emphasized that in each of these systems there exists a great many critical factors such as the bonding to the vent surfaces, the internal current paths, cross sectional requirements, the melting temperatures of the material involved, etc. so that individual high current tests are an absolute necessity for any device of this nature which is intended to withstand direct strokes. In addition, it should

be emphasized that even though adequate prototype designs may be evolved, the test of production systems are also absolutely necessary in view of the repeated experience in which slight production changes have resulted in complete failure of the system to withstand natural lightning discharge current magnitudes. It should also be emphasized that these vent outlet concepts have been proposed in terms of protection from the direct high energy electrical environment and would have to be thoroughly checked for use on aircraft in regard to icing, fuel trappage, etc., as well as for their effectiveness in inhibiting flame or spark passage into a vent tube.

One additional technique for keeping natural lightning discharges away from fuel vents located near obvious strike points is the use of resistive diverter rods. Where a fuel vent could itself be struck by lightning, diverter rods would certainly tend to reduce possible hazards by moving the nearest point of discharge and associated pressure peak at least a foot away, which as shown in the report section of blast pressure, reduces the blast pressures greatly. A hypothetical application of diverter protection is illustrated in Figure 32.

F. Concluding Discussion

Potential hazards to aircraft fuel vents from the thunderstorm electrical environment include induced streamer currents from the intense electric fields, high temperatures, energies and pressures from the lightning stroke currents, and metal burning and sparking from the heavy stroke charge transfers as determined over a period of years by analysis of flight damaged aircraft parts and by flight research programs (Refs. 9 and 10). The studies of the environment indicate that because of the several possible ignition mechanisms with large energies, it is still most important to avoid direct strikes to the vent outlet whenever possible. The relative gradient for each vent type and location is the most significant information in relation to the probability

of direct lightning strikes as well as induced streamering. Once any point on the aircraft reaches the ionization threshold, the large thunderstorm potentials will heavily feed the resultant discharge. Thus, from the purely electrical standpoint, keeping direct strikes away from the vent outlet is more important whether by vent shaping or location or by lightning diverter rod techniques.

Another important factor determining the probability of direct strikes to a vent outlet is the relative motion of the aircraft with respect to the nearly stationary ionized stroke channel. Although it is known that strokes always move to the rear of an aircraft following the air flow pattern, more information on the sweeping mechanisms is badly needed.

The studies to date have reduced the region of uncertainty from a distance of possibly 20 feet to a region about two feet from the ionized channel, but insufficient information has been obtained to date to permit any final conclusions as to ignition hazards in the near zone. Additional laboratory investigations of fuel vapor ignition near the channel are suggested.

G. Conclusions

1. The probability of direct strikes and corona type discharges in the vicinity of a vent exit is influenced by vent exit configuration.
2. Poorly bonded vent outlets or inserted flame arresters can channel stroke currents such that internal sparking may result.
3. Studies indicate ignition is not possible at distances beyond two feet from the ionized channel; at distances less than two feet insufficient information exists to define the probability of ignition.

V. LIGHTNING INDUCED PRESSURE WAVES

A. Introduction

The question has been raised as to the possible hazard from compression ignition of aircraft fuel vapors by blast pressure waves from natural lightning discharges to or near aircraft fuel vents. In a recent Russian paper (Ref. 11) blast pressure waves from natural lightning discharges have been calculated from a special analysis of the lightning channel. The calculations show pressures of the order of one hundred atmospheres near the lightning channel corresponding to temperatures of about five thousand degrees F, and this would suggest a strong possibility of pressure wave ignition of fuel vapors. An experimental investigation has been undertaken to measure pressure waves from high energy artificial lightning discharges, and it has been extended with measurements of triggered natural lightning discharge channels using the LTRI research schooner in thunderstorms off the coast of Florida.

B. Natural Lightning Discharge Characteristics

Studies of natural lightning discharges have indicated that cloud-to-ground discharges have the greatest current crests and current rates of rise while cloud-to-cloud lightning discharges, although often containing greater charge transfers, are generally characterized by much lower current rates of rise, often with little or no associated blast wave. Artificial lightning discharge current components representing the several major types of natural discharges have all been used in this series of pressure wave studies, but probably of most significance are the high current and high energy components which produce the maximum blast pressures. Current crests of 100,000 amperes with charge transfers of nearly two hundred coulombs have been used in the experiments, and these represent severe but not the most severe natural

lightning discharge.

C. Laboratory Studies

Piezo electric blast transducers were used in initial phases of the laboratory studies, with final confirmation of propagation velocities using Schleiren photography. An illustration of the test arrangement for the piezo blast gage measurements is shown in Figure 33, along with oscillograms of the blast pressure and discharge current. Discharge lengths of one to four feet were used to produce a cylindrical wave geometry near the arc such as would be found near a natural lightning discharge channel. The piezo transducer had a rise time of approximately 10 microseconds, as illustrated in Figure 34, showing measurements at 12 and 48 inches from the arc. The 10-microsecond response delay during the piezo voltage rise corresponded to a wave movement of 0.13 inches or an error of only about 1% at 12 inches.

Oscillograms of pressure waves from an arc four feet long (Figure 33), produced by 100,000 ampere discharges (100 joule/cm arc length) triggered by a 0.008 inch copper wire are shown in Figures 35 and 36, along with graphs of the distance vs. time and pressure vs. distance. The graph of distance vs. time indicates a purely sonic wave except for distances closer than one foot which were not checked because of possible flashover to the blast probe. The graphs of pressure vs. distance show the experimental points superimposed on an inverse first power curve, and the correlation indicates that the wave fronts correspond to a cylindrical sonic pressure wave (cylindrical, $p \sim 1/r$) out to a distance equal to the arc length of about four feet. Beyond this distance the pressure falls off more rapidly as it corresponds more to a spherical wave (spherical, $p \sim 1/r^2$). The transitions between spherical and cylindrical waves are illustrated in the next section on analysis of laboratory measurements. Vaporization of the trigger wire used in some of the measurements raises the shock pressure

somewhat. Calculations of Rouse (Ref. 12) have shown that an increase of 40 to 80% in energy input into an arc is required to equal the peak pressures produced by vaporizing a fine wire. The measurements using trigger wires are thus conservative; air discharges such as natural lightning would produce lower pressures for a given energy input without the wire vapor pressure.

Oscillograms of pressure waves from a lower energy, 6 joule, air discharge with no trigger wire are shown in Figure 37, and again the velocity is found to be sonic and the pressure rise much less than one atmosphere at even three inches from the arc. For final confirmation of wave front velocities and a check of the blast gage, Schleiren photographs were taken. An electronic flash tube was used as a light source and was fired at pre-determined time delays after the arc discharge occurred. Oscillograms of a timing wave with the flash lamp output superimposed were recorded with each Schleiren photograph to assure accurate measurement of the travel time of the shock front. The test arrangement is shown in Figure 38 and the Schleiren photographs in Figure 39(a). A photograph relating the blast gage measurements to the Schleiren measurements is shown in Figure 39(b). The graph of distance vs. time is shown in Figure 39(c) and, as may be seen, there is good correspondence between the blast gage and Schleiren measurements.

D. Analysis of Laboratory Measurements

The blast oscillograms and Schleiren studies have shown that for regions beyond five to ten centimeters from the arc, the blast waves travel with the speed of sound and do not, therefore, constitute strong shock waves. To study the regions of strong shock which must exist near the arc and to estimate their extent, calculations have been made based on Taylor's analysis (Ref. 13) of intense spherical shock from nuclear bursts extended to a cylindrical geometry by S. C. Lin (Ref. 14).

In this solution, it is assumed that a finite amount of energy per unit length is instantaneously released along an infinite straight line in the atmosphere. The pressure, velocity, and temperature distribution may be then calculated according to a set of similarity assumptions consistent with the fluid dynamic equations and strong shock conditions. A perfect gas of constant heat capacity is assumed, and heat transfer by radiation and conduction is neglected. Because of the strong shock conditions the analysis is not valid when the shock pressure ratio decays to less than 10 nor when the pressure ratio becomes so high that dissociation and ionization become significant.

When the shock strength decays below 10, the wave degenerates into an acoustic wave. The pressure decay of the acoustic wave depends on the geometry; for a plane wave the pressure wave propagates undiminished (ignoring viscous attenuation), for a cylindrical wave the pressure reduces as $1/r$, for a spherical geometry as $1/r^2$. The pressure reductions correspond to the variations in surface area of a cylinder and sphere as a function of radius. For laboratory studies with short arcs, there exists a cylindrical region out to about one arc length which is directly analagous to the cylindrical geometry of a long natural lightning discharge. Beyond this distance of one arc length for the laboratory discharge, a transition to a spherical wave occurs. This is illustrated in Figure 40. Thus, in laboratory studies the transition between strong shocks and acoustic waves and between cylindrical and spherical regions must be recognized in any attempted correlation of measurements with calculations.

The results of the strong shock calculations are presented in Figures 41, 42, 43, and 44 showing distance vs. time, and temperature, velocity, and pressure vs. distance. The curves show the calculated regions of strong shock and are extrapolated as a cylindrical sonic wave from the region where the strong shock assumption is no longer valid; i.e., where the pressure ratio drops well below 10, the region

where the blast gage and Schleiren studies have shown the pressure wave to be sonic. For comparison, the experimental values are also shown. The curves show a region of uncertainty out to about 5 or 10 cm, beyond which they indicate a pressure of only a few atmospheres and a temperature ratio below two. These theoretical and experimental investigations with severe artificial lightning discharges thus do not indicate high pressures at distances greater than five to ten cm. from the arc.

The experimental studies do not preclude, however, the possibility of a strong blast wave from a lightning discharge directly into a vent outlet being propagated nearly undiminished into a fuel tank, as the strong shock calculations based on the studies of Taylor, Rouse, Line, etc. (which have been partially confirmed experimentally) do indicate high pressure ratios within a few centimeters of the arc channel.

The theoretical calculations have been based on an assumed instantaneous release of energy, whereas finite current and energy rates must exist in all real discharges. The shock wave magnitudes are related to the current and current rates of rise as well as the energy and, although a completely satisfactory theoretical relationship has not yet been obtained to our knowledge, the current and current rate of rise of 100,000 amperes and 30,000 amperes/microsecond represent a severe lightning stroke exceeded by only a small percentage of all natural lightning discharges, as shown by LTRI flight studies and by electrical transmission equipment manufacturers' studies of strikes to transmission lines (Ref. 15).

E. Blast Waves From A Natural Lightning Discharge

For verification of laboratory measurements, piezo electric transducers were installed on the LTRI schooner deck to permit measurements of blast waves from triggered natural lightning discharges. Blast gages were located on the schooner deck at distances of 15 and 45 feet from an expected point of lightning stroke contact. Wire carrying

rockets were fired into the thunderstorms just prior to the time that a natural lightning discharge would be expected to take place, as indicated by the peaks shown on an electric field monitoring device located aboard the ship. A diagram of the rocket platform located on the stern of the ship and of the blast gage locations is presented in Figure 45. The rocket carried a fine stainless steel wire, 0.008 inch in diameter, to approximately 600 feet, a distance just sufficient to trigger a lightning stroke. A lightning stroke to the wire was carried down to the insulated platform which was equipped with current measuring shunts for monitoring the lightning stroke current and wave shape. The blast information recorded from natural lightning discharges was correlated with the current magnitudes and channel characteristics being studied under an Air Force Cambridge Research Center program.

The pressure wave oscillograms and the associated current wave oscillograms are presented in Figures 46(a) and (b). The oscillograms show pressures of the order of 1/10 of a psi at a distance of 15 feet from the stroke.* The peak current magnitude of the lightning stroke was approximately 30,000 amperes, as shown in Figure 46(b), and rose to crest in approximately two microseconds. The separation between the peak pressure on the lower trace and on the upper trace is approximately 22 milliseconds, corresponding to the time required for a sonic wave to travel between the two pressure heads.

A high voltage generator aboard the ship was used to produce an artificial discharge to the rocket platform for calibration purposes. The blast oscillogram and corresponding current wave for the artificial

* Unless noted otherwise, discussions refer to gage pressure rather than absolute pressure; i.e., units from local atmospheric ambient pressure.

lightning discharge are presented in Figures 47(a) and (b). As may be seen in Figure 47(a), the time delay to the first pulse was about 13 milliseconds, and the time separation of the crests for the upper and lower wave again correspond to approximately 22 milliseconds, the time required for a sonic wave to travel between the two heads. The artificial lightning discharge produced by the ship's generator reached a crest of 30,000 amperes, but the current rate of rise was lower, as indicated in the oscillogram of Figure 47(b). A graph of the pressures (psi gage) plotted against distance is presented in Figure 48 along with the experimental pressures measured in the laboratory and with inverse linear and inverse square curves for comparison. It may be seen that extrapolation backward of a $1/r$ pressure curve from the measurement of the natural lightning discharge to a distance of approximately one foot indicates a pressure of about two psi comparable to the laboratory pressure measurements.

F. Reduction of Blast Pressure Waves by Flame Arrester Screens

To determine the effect of screens such as might be used in flame arresters in reducing the pressure wave magnitudes, a cylindrical tube with a replaceable end was placed over the piezo electric blast transducer, and 100 joule per centimeter arc discharges were fired in front of the tube with screens placed over the tube end. These included a solid cover, a coarse screen, a fine screen and, finally, no cover. As shown in Figure 49, even with the fine mesh screens almost no discernible reduction in pressure was noted at the levels measured. The measurements with the end of the tube completely covered showed very low pressure, indicating that the measurements with the arrester screens were not merely the result of the compression of the tube from the passing pressure wave. The conclusion drawn from the tests is that flame arresters do not reduce blast pressure waves significantly.

G. Concluding Discussion

These investigations of blast waves from lightning discharge currents have indicated pressure and temperature ratios of less than two in regions beyond one foot from the arc, using arc discharges which represented severe, but not the most severe, natural lightning discharges. The laboratory measurement techniques were confirmed by measurements of blast waves from triggered natural lightning discharges to the LTRI research vessel.

A pressure ratio of two corresponds to an adiabatic temperature rise of less than 1000°F. As shown by Stout and Jones (Ref. 14), temperatures of the order of 2500 to 3500°F had to be applied for a period of over 40 milliseconds to produce ignition of methane air and hydrogen air mixtures by hot wires. Thus the studies indicate that the shock front peak pressures and corresponding temperatures from a natural lightning discharge are not sufficient to produce direct pressure ignition one foot or farther from the unrestricted channel. It should be noted that within a few millimeters of the arc, the blast pressures are probably very high and that a strike directly to the fuel vent outlet could conceivably drive a high pressure wave through a dry vent outlet nearly undiminished into a fuel tank to produce ignition. Thus the importance of avoiding direct strikes to fuel vent outlets can hardly be overemphasized, both from the standpoint of direct ignition of flammable fuel vapors and blast wave propagation through dry vent tubes into fuel tank areas.

Another important aspect of blast waves is their possible effect in forcing flame fronts through flame arresters. This is discussed in the wind tunnel studies of lightning discharges to fuel vents in another section of this report. An important related question, and one suggested for future study, is the question of fuel vapor ignition in the arc-blast transition region out to one foot from the discharge channel. This could be approached from both directions, arc ignition of fuel

vapors by high voltage discharges with greater ionization extent and less blast (lower currents), and shock tube studies of fuel vapor ignition by blast waves. Also suggested for future study is the possible effect of water vaporization in raising the blast pressure magnitudes, an effect which has recently been suspected in some serious aircraft lightning damage reports.

H. Conclusions

1. For regions beyond 5 to 10 centimeters from a discharge arc the blast wave apparently travels at the speed of sound, which does not constitute a strong shock wave.

2. Screens placed in the path of a shock wave do not significantly reduce blast pressure waves.

VI. IGNITION AND QUENCHING

A. Introduction

The study of fuel-air mixture profiles in the vicinity of a fuel tank vent exit has illustrated that a flammable mixture can exist in the vicinity of the vent exit, if a flammable mixture exists in the vent itself. It has also been shown previously, as well as in the study reported here, that sufficient energy exists in streamers and corona discharges to produce ignition of a mixture in the normal flammable range. There is, of course, no question that a direct lightning strike contains sufficient energy for ignition even of mixtures outside the normal flammable range.

Most of the experimental work in the literature is concerned with ignition of gas mixtures with sparks of fairly low energy, of the order of fractions of a joule. Since this area of electrical ignition has been explored in reasonable detail, the objective of the present program was to investigate whether any different effects are produced with relatively high energy discharges. There seemed little question that ignition would occur with discharges of higher energy than the minimum required under normal experimental conditions. The question which could not be resolved was whether a high energy discharge could drive a flame through a quenching channel. In other words, would a flame arrester designed on the basis of normally propagating flames be effective for flames produced and driven by a large excess of electrical energy? The investigation of ignition in channels of the order of the quenching distance for the mixture under consideration thus became the principal objective of the present work.

B. Apparatus and Procedures

1. The Electrical Circuit

The electrical circuit shown in Figure 50 consists of a DC power supply with a voltage output of 0 to 15 KV and a maximum current output of 1.75×10^{-3} A. The resistor R_f protects the power supply from burnout and provides an additional filter with C_f . S_1 and S_2 are two mechanical high voltage switches. With S_1 closed and S_2 open, the capacitor C is charge; the rate of charge was controlled with a variac. The voltage is measured with an e.c. Voltmeter by means of a high voltage probe. When the desired charge at C is reached, S_1 is opened. For the experiment S_2 is closed and the capacitor C is discharged through the spark gap.

The e.c. Voltmeter is a Simpson Model 270 with 20,000 ohms per volt and $\pm 1.5\%$ accuracy full scale. The capacitor values from 25×10^{-12} Farad up to 9×10^{-6} Farad were available and used either as single capacitors or in combination as a capacitor bank. The leaking current of all the large capacitors was tested repeatedly and was found smaller than 1×10^{-6} amps.

The mechanical switch S_2 was used, since the attempt to trigger the discharge by radiation from a trigger spark failed to work reliably in propane-air mixtures. This latter method would have eliminated switch losses. Studies of the mechanical switch showed that the losses, even with voltages 10 - 20% greater than the statistical breakdown voltage, were not detectable among the other uncertainties of the experiment.

The static breakdown voltage for the mixture - a function of the product of gap distance and gas pressure for the specific gas mixture being tested - was measured and is given in Figure 51. A plot of breakdown voltage versus the product of pressure and gas distance is normally called a Paschen diagram and should give a linear relationship.

The slight curvature noted is attributed to two causes: (1) accumulation of deposits on the electrodes (e.g., carbon), and (2) the electrode shape which produces a nonuniform electric field. Inasmuch as the departures from linearity were not great, no attempt was made to alter the experimental procedure. In order to assure consistency of the results, the ignition experiments were performed under the same conditions as those used to obtain the Paschen diagram of Figure 51. The diagram was obtained under the same conditions as the experiments later on were performed. The electrodes, 2 mm. in diameter, had rounded tips with a radius of 1 mm. and were made of stainless steel. They were inserted into opposite walls of a plexiglass tube with a square shaped cross section with 0.88 cm. side length and the tips flush with the wall surfaces. After the tube was filled with mixture, the voltage was slowly raised until breakdown occurred. Each measurement was repeated three times, and the mean value was used in the diagram. Since the gap distance could not be changed, the gas pressure was changed. The pressure was measured with a closed mercury manometer to ± 1 Torr. Because of the combustion products from the mixture, channel and electrodes had to be cleaned with methyl alcohol after each discharge to obtain good reproducibility. After the cleaning operation, the channels were pumped down to 10^{-1} Torr for about 5 minutes to remove the remaining alcohol. Longer times have proven to give no further change. The discharge time measured with the complete circuitry was of the order of 10^{-5} second.

2. Test Mixture

Propane-air mixtures were chosen for the study, since appreciable data exists for normal ignition and flame propagation. All experiments reported in Section VI have been performed with a mixture containing 5% by volume of propane in air.

For the experiments with quiescent mixtures, about 6 liters of mixture were prepared for every test run by measuring propane and air

separately by volume. The components were introduced into a plastic bag and mixed by circulating the contents of the bag with a diaphragm pump. The mixture was uniform after about 1/2 hour; however, the circulation of the mixture was continued during the whole test run. The propane used had a purity of 99.5% (instrument grade); the relative accuracy of the described volume measurement was better than 0.5% for each component. Prior to introducing the propane-air mixture into the tube, it was passed through a drying tube filled with calcium chloride. For experiments with chambers closed at both ends, the chamber was first evacuated and then filled with the mixture to the desired pressure, controlled by a closed end mercury manometer. For experiments with atmospheric pressure (one end or both open) the mixture was passed through the chamber long enough to assure a uniform mixture.

A different procedure was used for the experiments in which an appreciable mixture flow velocity was maintained during the ignition experiments. Commercial grade propane (93.49% propane, 0.212% methane, 4.00% ethane, 1.90% iso-butane, and 0.26% n-butane) and air were run separately through measuring chambers containing hot wires for flow control. Both hot wires were electrically adjusted for optimum sensitivity in the range of the desired flow rate. The hot wires were calibrated by the conventional water displacement technique. The accuracy was better than 5%. For experiments involving very high air flow rates, the air was metered by pressure measurement, the pressure-flow rate relationship obtained from prior calibration. The accuracy was, again, better than 5%.

The voltage drop of both hot wire probes (in series with a constant resistor) was amplified and observed on a DC oscilloscope. This simplified the control, since the deflection of the beam indicated the flow rate of both contents at the same time. While the power supplies for the hot wire probes were sufficiently stabilized by means of zener diodes and transistorized voltage regulators, the oscilloscope needed

to be controlled periodically by standard voltages, which were correctly adjusted to deflect the beam to zero on the screen of the scope. Any change of the oscilloscope could be readjusted, which was carefully done before each photographic recording.

The propane and air were then mixed and allowed to flow through the ignition tube.

3. Flame Arrester Simulation

A single channel was used to simulate actual arrester conditions, which may actually include many of those channels. Figure 52 shows quenching distance versus pressure for parallel plates and a 5% propane-air mixture (Ref. 17). Since the conversion factors for differently shaped cross sections are known, the quenching distance can be calculated from these data. Specifically, the geometric factor for a square shape is 2.38 and for round 2.67. For the first experiments plexiglass chambers of different lengths and square shaped cross sections were used. A pressure of 280 Torr was used to obtain a bigger gap distance. This form of channel was also used to test and develop observation methods and to find out which measurable thermodynamical phenomena would be suitably related with the electrical excess energy. Some experiments with 180 cm. long plexiglass channels are also reported in this paper. Because of the low pressure used in this chamber, it had to be closed at the ends and disturbances caused by shock waves were found. Figure 53 shows the apparatus with this particular chamber mounted.

Most of the experiments were conducted in glass tubes of circular cross section and at atmospheric pressure. Both ends of the chambers could thus be left open. The electrodes were held in a round plexiglass chamber of about 15 mm length, which was turned on a lathe to exact quenching distance at the inside and also worked out to receive two glass tubes as extensions - one at each side - of the same inner diameter.

4. Observation and Recording

Since flame propagation, in an actual sense of the term, could not necessarily be expected under quenching conditions, it was the prime objective of the first experimental investigations to find an observable and descriptive thermodynamical phenomenon which was clearly related to the amount of excess energy introduced by the electrical discharge. Photographic recording of the discharge and its effects proved to be the most useful observational technique. All photographs reported in this paper were made with Agfa Record film (1200 ASA).

During the experiment, the room was kept dark, and the camera was opened manually after all other experimental preparations had been completed. Then - camera still open - the high tension switch was actuated and the camera closed, after the flash of the discharge disappeared to visual observation.

To prevent overexposure, the necessary f-stop numbers, as a function of discharge energy, were estimated by preliminary experiments and have proven to be not too critical. It may be noted that the pictures taken in the described manner give a time integrated recording of the discharge and the events caused by it.

C. Results and Discussion

1. General Observations

Early observations of the phenomena occurring in the ignition tube show that two distinct types of propagation seemed to exist. The discharge itself produced a hot luminous plasma which could extend for various distances in the channel, depending on discharge energy and channel dimensions. This plasma generally appeared as an intense white zone on color film. Either concurrent with the plasma formation or produced by it, a blue flame could also be observed in some experiments. The rather light blue color of the flame was completely masked by the

plasma so that its existence could not be determined until the flame propagated away from the discharge generated plasma. Whether the flame exists within the plasma or is ignited by it could, therefore, not be determined. The existence of a hot plasma of considerable volume represents one of the principal differences between high energy discharge experiments and the usual ignition experiments using low energy discharges. The study of the discharge generated plasma was thus made a major part of the current program.

The plexiglass chamber with a square cross section (0.88 cm. sides) and a 180 cm. length, and with electrodes mounted in the center of the tube proved very useful for many of the qualitative observations. The following visual phenomena were noted.

For discharge energies of 10^{-3} joule and below, the spark channel appeared as a thin bluish line, generally less than 0.5 mm in diameter. With increasing energy the diameter of this cylinder grew, and the color changed to white. At about 5×10^{-3} joules the discharge reached the side walls of the chamber described above. At even higher energies the plasma began to fill the chamber and extend longitudinally in both directions. For later calculations of plasma volume, the shape of the plasma was assumed to be cylindrical at first, and then cubical after reaching the tube walls.

Figure 54(a), (b), and (c) illustrate discharges in air at 500 mm H_g A (Torr) pressure.* It was observed that the discharge appearances in propane-air mixtures, helium, or nitrogen are quite similar to those observed in air. The characteristics of the plasma do not appear to depend upon whether or not the channel would represent quenching conditions for a given propane-air mixture. For conditions under which quenching is normally not expected, a blue flame could be

* obtained with apparatus shown in Figure 53.

seen propagating away from the plasma extremities. Blue flame propagation was not observed for conditions which would normally quench a flame. Under some conditions, however, such flames appeared to extend the plasma zone rather than propagate as separate flames.

2. Plasma Volume

Figures 55 and 56 show the change in plasma volume with discharge energy for propane-air mixtures and for helium and air. Pressure was varied for the different gases. Attempts to explain the trends observed were made difficult by the fact that pressure waves generated by the discharge and reflected from the closed ends of the tube could affect the spread of the plasma. Nevertheless, certain features of the phenomenon appeared evident. There is a change in slope of the plasma volume versus energy curve which occurs at the point where the plasma touches the tube walls. Although an uncertainty exists in the calculation of the plasma volume, repeated measurements indicated that the observed effect was larger than the uncertainty in volume measurement. Loss of energy to the tube walls seemed a logical explanation for the decreased rate of plasma growth at the higher energy levels. The similarity of the measured plasma volumes for propane-air mixtures and nonreacting gases such as helium, nitrogen, and air, indicates that the energy due to chemical reaction plays a minor role in the plasma development. This observation is further suggested by the absence of a discernible change in the curves below and above quenching pressures for this particular tube.

In order to eliminate the effects of reflected pressure waves, a series of experiments was performed in a tube open at both ends and with the contained gases at atmospheric pressure. The discharge chambers were machined from a 25 mm plexiglass rod with holes for the electrodes and openings for the connection of precision bore glass tubes. Three units having inner tube diameters of 0.32, 0.48, and 0.79 cm. and a total length of 180 cm. were fabricated. The glass was

connected to the plexiglass with epoxy cement to provide seamless, tight junctions. The electrodes were forced into undersized holes until their flat surfaces were tangential with the chamber walls. The smallest diameter tube was found to be below the quenching distance for a 5% propane-air mixture at atmospheric pressure, while the largest tube exceeded the quenching distance. Partial propagation of flame was observed in the intermediate diameter tube, the distance of propagation varying from experiment to experiment.

Two different electrode diameters were used, having diameters of 0.5 cm. and 0.2 cm, to investigate the effect of electrode size and current density.

Plasma volumes as a function of discharge energy are presented in Figures 57 - 60 for the 5% propane-air mixture and for nitrogen, obtained in the apparatus described above. Several general conclusions can be drawn from the data presented. Electrode size within the range tested produced no discernible difference outside of experimental accuracy. The volume of the plasma in nitrogen is lower than for the propane-air mixture at low energy levels, but it has a steeper rate of change with energy. This result is qualitatively in agreement with the explanation that the energy of reaction of the propane with air contributes a small additional increase in volume at low levels of electrical energy, but that is not significant at the higher energy levels. It does not explain, however, higher values for nitrogen at the higher energy levels.

All of the figures show higher values of the plasma volume in the larger tube. This result is consistent with the suggestion, raised previously, that some of the plasma energy is lost to the tube walls.

The general trend of the data suggests that a specific plasma volume is associated with each discharge energy. If this is fact, then the length of the plasma zone should change with energy. This length

variation can be of importance, since the length of the plasma could determine whether the discharge energy could penetrate a quenching channel of a given length and produce ignition on the other side.

Plasma lengths obtained from the same experiments used for the measurement of plasma volume are shown in Figures 61 - 64 as a function of discharge energy. The plasma length varies in much the same manner as plasma volume. In all cases the plasma length becomes greater as the tube diameter decreases, which is consistent with the suggestion that a given volume is associated with each discharge.

The experimental configuration with the spark gap located within the tube itself was chosen so that the amount of energy delivered to the gas could be known. Appreciable plasma lengths are associated with the higher energy discharges. These lengths must be considered maximum values. A discharge occurring at the end of a tube would transmit only a fraction of its energy into the tube and the plasma penetration would be reduced correspondingly. Nevertheless, the discharge generated plasma which propagates readily through a normally quenching channel must be considered as an important part of the ignition hazard.

In propane-air mixtures, flames were observed in addition to the plasma, depending on the experimental conditions. Since the intensity of the flames was much less than that of the plasma, the plasma tended to mask the photographic detection of flames. It was possible, however, to observe the flames visually in a number of experiments. In general, the rate of flame propagation was much slower than the rate at which the plasma spread to its maximum length. The flame speed seemed to increase with discharge energy, but quantitative data could not be obtained. In only one experiment, using a discharge energy of about 0.1 joules, was there a flame observed in the smallest tube which was smaller than the quenching distance. This flame propagated for only about 1 cm. It must be concluded at this stage that the application of ignition energies greatly above the minimum ignition energy does not

tend to drive a flame through a quenching channel.

The previous experiments described had all been performed with nonflowing mixtures. Another aspect of the operation of quenching channels which was not known was whether a flame could be forced through a channel by a flowing gas stream. It was also of interest to determine whether the plasma was affected by gas flow.

In order to investigate the effects of gas velocity, air and a 5% propane-air mixture were passed through a 4 mm glass tube, which is smaller than the quenching diameter at atmospheric pressure. Flow velocities of 10, 20, and 100 m/sec were investigated at two levels of discharge energy, 16 and 80 joules. The effect of flow velocity is illustrated in Figure 65, while photographs of the plasma are shown in Figure 66 (a) through (d). The length of the plasma downstream of the discharge is not affected by the flow, but downstream of the discharge the plasma length increases linearly with increasing velocity. The reversal in the air and propane-air curves is not actually known. A reasonable explanation is, as before, that the propane-air reaction adds energy to the plasma which is significant at the lower energies. Irreversible endothermic reactions could account for the lower values of propane-air plasmas than air plasmas at the higher energies. One can, indeed, observe appreciable carbon formed at the higher energy levels, indicating decomposition of the propane.

Faint flames were observed at flow rates of 10 and 20 m/sec and 16 joule discharge energy (Figure 67 (a) and (d)). There appeared, in these somewhat isolated cases, to be a prolonged combustion zone under quenching conditions. The lack of reproducibility of the event makes it difficult to explain the nature of the phenomenon.

The previous experiments were performed under conditions where the plasma is completely confined in a tube. It was of interest to determine the behavior of the plasma as it left a tube corresponding crudely to the junction between the end of a flame arrester and an

unobstructed tube. Figure 68 illustrates the behavior of the plasma in air under three different experimental conditions. Figure 68(a) shows an approximately 200 joule discharge with only one glass tube (right side) attached to the plexiglass section containing the electrodes. The electrodes are still contained in the plexiglass tube, approximately 15 mm in length; that is, 7.5 mm from the open left end. The air is quiescent. The plasma extends into the glass tube on the right roughly the same distance as in previous experiments. This experiment simulates a discharge near the entrance to a flame arrester.

Figures 68(b) and 68(c) show the plasma extending through the ends of a tube cut at different lengths. The tube diameter is 4 mm, and the air flows from right to left in excess of 100 m/sec. There is no question that the plasma can extend beyond the confining limits of the tube. A similar experiment is shown in Figure 69, where the tube extremity extends into a glass bulb.

The final question to be answered concerned the ignition capability of the plasma. Two different sets of experiments were performed.

Using the shortened tube configuration of Figure 68(c), a propane-air mixture was allowed to flow past the tube end. The glass tube itself, about 30 cm. long, contained only air. The plasma extending from the tip of the tube reliably ignited the propane in each experiment. The second configuration involved the use of the 5% propane-air mixture in the experimental configuration shown in Figure 69. Explosion of the mixture in the glass bulb shattered the bulb. There is no doubt that the plasma generated by the discharge is capable of igniting a flammable mixture.

D. Concluding Discussion

The following conclusions can be drawn. High energy discharges produce a hot plasma which can propagate for considerable lengths through channels which would normally be expected to quench a 5% propane-air

flame. Air flow tends to increase the length of the plasma in the direction of the flow. The plasma appears only slightly dependent on the nature of the gas in which the discharge occurs. The plasma propagates from an open end through a tube and can travel through a tube into a large volume. The plasma generated by a high energy discharge is capable of igniting a flammable mixture at a considerable distance from the source of the discharge. Flame arresters of normal design appear to offer no protection, if the plasma-like discharge occurs.

E. Conclusions

1. Application of ignition energies greatly above minimum ignition energy does not tend to drive a flame through a quenching channel beyond limits of plasma penetration.

2. Discharge generated plasma passes readily through a normally quenching channel and, if the plasma passes into a non-quenching volume, can contain sufficient energy to ignite a combustible mixture. Moreover, there is no doubt the plasma generated by a discharge is capable of igniting a flammable mixture.

3. Flame arresters of normal design appear to offer no protection if the plasma-like discharge occurs.

VII. LIGHTNING SIMULATION TESTS

A. Introduction

The previous discussions covering the efforts devoted to determining the nature of the combustible environment, the electrical environment, and ignition and quenching processes have shown that a combustible mixture can exist in the vicinity of a vent exit for various vent flow conditions and that sufficient energy exists in lightning strikes, streamers, and corona discharges to produce ignition under laboratory conditions. It was further shown that flame propagation can occur under normally quenching conditions when an electrical discharge produces a high energy plasma. The final phase of the program was the testing of vent configurations under simulated flight and lightning conditions to determine whether the combination of all of the individual effects confirmed or altered the conclusions drawn from the separate studies.

For the execution of these final evaluation tests a simulated vent was installed in a ~~simple~~ wind tunnel at Lightning and Transients Research Institute and subjected to simulated lightning discharges as well as relatively low energy sparks. An attempt was made to produce the most severe conditions within the experimental limitations.

B. Artificial Lightning Discharge Currents Used In Tests of Aircraft Fuel Vents

Lightning discharges to aircraft are of two general types: cloud-to-ground discharges characterized by high currents and high current rates of rise, and cloud-to-cloud discharges characterized by intermediate currents and current rates of rise but with greater charge transfers. The discharge currents may be arbitrarily divided into

components which produce the typical effects of natural lightning discharges, the magnetic forces of the high currents, the heating and blast effects of the high energy intermediate currents, and the metal erosion of the long duration lower currents which continue to periods up to one second following the short duration high current components.

The effects may be reproduced in the laboratory by a group of several artificial lightning generators connected in such a way as to give a single discharge representative of a severe natural lightning discharge. The circuit values of the laboratory lightning generator and the output currents, energies, and charge transfers are presented in Table II. A diagram indicating the generator circuits and the current wave forms and coupling circuits used for firing the three current components as a single discharge is presented in Figure 22, along with a graph of the composite output wave form plotted on a logarithmic time scale. Oscillograms of the actual currents are shown in Figure 23. The oscillograms represent the maximum values; the actual values varied somewhat on individual tests. These current wave forms correspond to those specified in Mil-A-9094C, the military specifications for the artificial lightning discharge currents used in testing aircraft lightning arresters. The current requirements are based on analysis of flight damage reports, flight research programs, and examination of damaged aircraft parts over a period of about fifteen years.

In studying the possible propagation of flame fronts through fuel vents or flame arresters, the first two components, the high and intermediate current components, were used to produce severe blast effects and possible momentary reversed flow in the outlet, utilizing the configuration shown in Figure 9(b). The third component was used to burn the vent outlet or flame arrester severely enough to present an ignition source of relatively long time duration to the fuel vapor outflow but did produce little blast effect. With these currents the energy density in the arc is equivalent to a severe, but not the most

severe, natural lightning discharge.

C. Apparatus and Procedure

1. Test Layout

The vent configuration is illustrated in Figure 70. Commercial propane, pre-mixed with air, was passed through the vent at various velocities. Due to difficulties in controlling the fuel-air ratio, spark tests were performed prior to each experiment to assure that a flammable mixture existed in the vent effluent. The air flow past the vent was varied in steps from 0 to 100 miles per hour.

During the preliminary tests it was noted that conditions existed where ignition occurred but flame did not propagate into the vent. In order to observe the behavior within the vent, subsequent experiments were run with a transparent tube leading to the air foil surface.

2. Instrumentation

The instrumentation consisted of

- a. Fuel flow rotameter;
- b. Air flow rotameter;
- c. Pitot tube and airspeed indicator;
- d. Three iron-constantan thermocouples installed in the vent tube as propagation indicators;
- e. Oscilloscope for reading thermocouple output;
- f. Three still cameras consisting of a Polaroid, a 2-1/4 x 2-1/4 black and white, and a 35mm infrared; and
- g. Two motion picture cameras consisting of a 64-frames-per-second Bell and Howell color camera, and a 1000-to-2000-frames-per-second Fastax high-speed camera.

3. Procedure

The following procedure was used for the determination of the ignition probability envelope at zero airspeed with a 15,000 volt

"neon" light transformer.

- a. Start exhaust fan;
- b. Set air rotameter;
- c. Set fuel rotameter;
- d. Activate sparking apparatus; and
- e. Observe oscilloscope for flame propagation indication.

The procedure for using the high energy discharges (elements 1 - 3) involved the following steps:

- a. Start exhaust fan;
- b. Prepare camera film loads and lens settings;
- c. Set air flow on rotameter;
- d. Begin electrostatic charging;
- e. Set propane flow on rotameter;
- f. Open shutters on still cameras;
- g. Start tunnel;
- h. Start motion picture camera(s);
- i. Stop tunnel motor at proper airspeed;
Note: Tunnel motor is a constant speed rotor and airflow throttling was not available.
- j. At the "Stop Tunnel" signal, close electrostatic equipment switch;
- k. One test operator visually observes the clear vent tube segment for visual signs of flame propagation;
- l. Another test operator observes the oscilloscope for thermocouple indication; and
- m. Stop motion picture camera(s) and close the still cameras' shutters.

D. Results and Discussion

A series of tests was run with an open vent exit and a 15,000 volt discharge to check out the setup. These tests verified that ignition and flame propagation could occur under the conditions and with the equipment tested.

Further tests were performed on the open vent configuration (vent exit clear of any structure or arresters) with electrical element (a) only (Table II), elements (a) and (b) only, and elements (a), (b), and (c). With a free stream velocity of 100 miles per hour, propagation occurred only with the discharges directed at the vent exit peripheral lip. When the discharge was directed an inch or more away from the lip, propagation failed to occur.

The number of tests with an open vent, no flame arrester, was limited since it was felt that the most important question to be resolved by the tests was whether or not the existence of a flame arrester could eliminate the fire hazard. A summary of the tests with a flame arrester is given in Table IV.

The most important result is that flame propagation was observed with the flame inhibitor in place. The ignition and propagation of flame was strongly dependent on the location of the discharge and the discharge electrode with respect to the vent exit. The critical discharge locations observed are illustrated in Figure 71. The greatest ignition potential existed when all three supply systems were activated. This condition results in the longest discharge duration and maximum heating of the metal surfaces.* Ignition and flame propagation were noted for both quiescent air conditions and air flow rates past the vent of 100 mph. The vent flow velocity was kept low deliberately, below 1 foot per second, since this represents the most hazardous condition.

In general, although the flame arrester did not completely prevent flame propagation into the vent, it did reduce the tendency for propagations. In several cases spark showers and a plasma were noticed as a

* However, it was also determined that a discharge consisting of elements (a) and (b) with the electrode similarly located to a three element discharge resulted in a propagation in the vent tube.

result of high energy discharges.

The tests confirm that a flammable mixture exists at the vent exit even at air flows of 100 mph. This mixture can be ignited by a simulated lightning discharge. Although the installation of a flame arrester reduced the tendency for flame propagation, a flame arrester cannot be assumed to give complete protection since propagation was observed under a fairly broad range of conditions.

In some experiments, particularly at zero air flow velocity, a flame could be initiated and stabilized at the vent exit. Such a flame heated the flame arrester until flame propagation through the arrester was possible. Such observations, as well as other unreported evidence, suggest strongly that the flame arrester should be installed in a manner which does not produce sheltered zones conducive to flame holding.

The observed flame propagation through the vent was at fairly low velocities, suggesting that high velocity vent flows also inhibit flame propagation.

It was noted during the tests that discharges not normally containing sufficient energy to ignite a flammable upstream of the arrester could drive a flame burning at the arrester face through, causing propagation.

E. Conclusions

1. Flame propagation can occur within a flush type vent with a "flame arrester" in place.
2. If a flame sustains itself on an arrester face, a strike in the near vicinity can push the flame through the arrester and propagate through the vent line.
3. Although the installation of a flame arrester reduced the tendency for flame propagation, a flame arrester cannot be assumed to give complete protection since propagation was observed under a fairly broad range of conditions.

VIII. CONCLUSIONS AND RECOMMENDATIONS

A. Conclusions:

For the reader's convenience, a restatement of the conclusions presented in each of the five previous sections is given.

Section III - Conclusions

1. Fuel Tank (Effluent Source)

(a) Flammable conditions may exist within a fuel tank contrary to equilibrium calculations.

(b) Preliminary considerations indicate fuels of extremely low volatility may offer benefits in terms of reduced explosion hazard (although the role of fuel mists suspended in air must be determined before firm conclusions may be drawn).

2. Fuel Tank Vents

(a) Flash-back of a flame through the vent, pre-supposing an ignition source and a flammable mixture within the vent, is most likely to occur at low rates of climb (low effluent velocity).

(b) It was determined practically all vent exits on current aircraft fall into three types:

- (1) A flush vent discharging into a boundary layer,
- (2) A mast discharging into a wake, and
- (3) A mast discharging into a free stream.

(c) Iso-kinetic gas stream sampling with a small probe in the order of 0.05 inch diameter is unnecessary as the probe does not significantly disturb the streamlines.

(d) Observed fuel-air ratio, at any point in the fuel-air ratio envelope, is a linear function of the vent fuel-air ratio. Also, molecular diffusion processes are insignificant in the mixing of the vent effluent and ambient air stream.

(e) The temperature ratio between the vent effluent and the free stream, in the range experienced by current aircraft, has no effect upon the mixing process.

(f) From conclusion (d), the use of a tracer gas in the effluent to determine the mixing envelope of a low speed gas jet discharging into a high speed gas flow is valid.

(g) A vent discharging into a free stream exhibits the greatest dilution or smallest mixing zone; however, a flammable mixture exists at the exit which means this configuration is vulnerable to direct lightning strikes.

Section IV - Conclusions

1. The probability of direct strikes and corona type discharges in the vicinity of a vent exit is influenced by vent exit configuration.

2. Poorly bonded vent outlets or inserted flame arresters can channel stroke currents such that internal sparking may result.

3. Studies indicate ignition is not possible at distances beyond two feet from the ionized channel; at distances less than two feet insufficient information exists to define the probability of ignition.

Section V - Conclusions

1. For regions beyond 5 to 10 centimeters from a discharge arc the blast wave apparently travels at the speed of sound, which does not constitute a strong shock wave.

2. Screens placed in the path of a shock wave do not significantly reduce blast pressure waves.

Section VI - Conclusions

1. Application of ignition energies greatly above minimum ignition energy does not tend to drive a flame through a quenching channel beyond limits of plasma penetration.

2. Discharge generated plasma passes readily through a normally quenching channel and, if the plasma passes into a non-quenching volume, can contain sufficient energy to ignite a combustible mixture. Moreover, there is no doubt the plasma generated by a discharge is capable of igniting a flammable mixture.

3. Flame arresters of normal design appear to offer no protection if the plasma-like discharge occurs.

Section VII - Conclusions

1. Flame propagation can occur within a flush type vent with a "flame arrester" in place.

2. If a flame sustains itself on an arrester face, a strike in the near vicinity can push the flame through the arrester and propagate through the vent line.

3. Although the installation of a flame arrester reduced the tendency for flame propagation, a flame arrester cannot be assumed to give complete protection since propagation was observed under a fairly broad range of conditions.

B. Summary Conclusions:

1. Mapping of fuel-air mixture profiles near the exit of a fuel tank vent shows, for all vent configurations, the flammable envelopes are relatively small.

2. The greatest explosion hazard exists when the fuel tank and vent contain a flammable mixture and the vent outflow velocity is very low.

3. The ability of a discharge generated plasma to penetrate the arrester and ignite a flammable mixture is a major factor in reducing arrester effectiveness.

4. Although the installation of a flame arrester reduced the tendency for flame propagation, a flame arrester cannot be assumed to give complete protection since propagation was observed under a fairly broad range of conditions.

C. Recommendations:

The following recommendations are presented as a logical outgrowth of the program just completed, general information obtained from the references, unpublished tests performed by some of the experimental personnel, and experience of the personnel conducting this program.

1. Maintaining high vent exit velocities by adding air (at all times) is recommended and appears to be a more certain design feature for safe operation than using an additional airflow to dilute effluent vapors.

2. If flame arresters are used, they should be installed in a manner not conducive to flame holding. A sustained flame at an arrester face tends to heat the arrester to a temperature where the arrester is no longer effective. Although a flame arrester does not completely prevent flame propagation into a vent, it may, under some conditions, reduce the tendency for propagation.

3. The vent exit should be designed not to produce a region of high potential gradients, thereby minimizing direct lightning strikes, streamers, or corona discharges. The vent exit should not be located in a region of high potential gradient nor should it be located in the path of discharges originating elsewhere. The use of "diverters" near the vent exit may be advantageous; however, geometric effects produced by increasing the discharge probability near the vent exit require careful consideration.

4. Flush mounted, slightly recessed or electrically shielded, vents appear to be the most promising design types and are recommended. These configurations minimize discharge probability without greatly increasing the extent of the flammable mixture region.

REFERENCES

1. Gerstein, M., et al: "Investigation of Mechanisms of Potential Aircraft Fuel Tank Vent Fires and Explosions Caused by Atmospheric Electricity," NASA Research Project No. NASr-59, Progress Report No. 1 (1961).
2. R.A.E. Report CH650 as appeared in Cornell Report No. V-449-D-4.
3. Barnett, H. C., and Hibbard, R. R. (editors): "Basic Considerations in the Combustion of Hydrocarbon Fuels in Air," NACA TR 1300, 1957.
4. Simpson, G. C. and Scrase, F. J.: "The Distribution of Electricity in Thunderclouds," Proceedings of the Royal Society, A 161, pp 309-352 (1937).
5. Schonland, B. F. J.: "Polarity of Thunderclouds and Interchange of Electricity Between Thunderclouds and Earth," Proceedings of the Royal Society, A118, p. 233-263 (1928).
6. Newman, M. M. and Robb, J. D.: "Lightning Protection - Aircraft Fuel Vents, " Part II, L&T Report 404 (1962).
7. Newman, M. M., Stahmann, J. R., and Robb, J. D.: "Aircraft Protection From Atmospheric Electrical Hazards," WADD TN-60-35 (AF 33(616)-3991, L&T Report 363), 1960.
8. Newman, M. M. and Robb, J. D.: "Investigation of Minimum Corona Type Currents for Ignition of Aircraft Fuel Vapors," NASA TN-D-440, 1960.
9. Newman, M. M. and Robb, J. D.: "Lightning Stroke Diverting Methods for Aircraft Fuel Tank Areas - 1," L&T Report 393, 1961.
10. Newman, M. M. and Robb, J. D.: "Lightning Protection for Aircraft-Special Effects," Part III, L&T Report 405, 1962.
11. Zhiulyuk, Y. N. and Mandel'shtam, S. L.: "On the Temperature of Lightning and Force of Thunder," V JETP, Vol. 13, No. 2, p. 338 (1960). Journal of Experimental and Theoretical Physics (USSR), Vol. 40, pp 483-487 (1961).
12. Rouse, C. A.: "Theoretical Analysis of the Hydrodynamic Flow in Exploding Wire Phenomena," from "Exploding Wires," Plenum Press, New York (1959).

13. Taylor, G. I.: "The Formulation of a Blast By a Very Intense Explosion," Proceedings of the Royal Society (London) A 201, p. 159 (1950).
14. Lin, S. J.: "Cylindrical Shock Waves Produced by Instantaneous Energy Release," Journal of Applied Physics, Vol. 25, p. 54, (1954).
15. Harder, E. L. and Clayton, J. M.: "Transmission Line Design and Performance Based on Direct Lightning Strokes," AIEE Transactions, Vol. 68, Part I, p. 439-449 (1949).
16. Stout, H. P. and Jones, E.: "The Ignition of Gaseous Explosive Media by Hot Wires," Third Symposium on Combustion Flame and Explosion, Williams & Wilkins Co., Baltimore, p. 329 (1949).
17. Lewis, B. and von Elbe, G.: "Combustion, Flames and Explosion of Gases," Academic Press, Inc., 1951.

TABLE I

Summary of Vent Exit Parameters at Maximum Climb
Conditions for Several Aircraft.

Aircraft Model	Aircraft Speed V_o (knots)	Boundary Layer Thickness at Vent (inches)	Reynolds Number at Vent $Re(x) \times 10^{-6}$	Maximum V_v/V_o
A	160	1.7	18	0.045
B	310	3.7	110	0.017
C ₁	147	0.6	4.7	0.125
C ₂	147	1.9	19	0.0125
D	152	1.0	8.7	0.09
E	190	0.9	11	0.163
F ₁	190	0.9	11	0.092
F ₂	190	0.9	11	0.029

TABLE II

Comparison of peak current, mechanical forces, heating effect, energy and charge transfer of the three types of surge current generators used in the tests of aircraft fuel vents.

	(a) High current generator 3.3 μ f at 150 kv (maximum)	(b) Secondary stroke generator 3000 μ f at 10 kv (maximum)	(c) Long duration current generator 200 amp at 500 v
Peak Current	100,000 amperes duration = 10^{-5} sec to 1/2 value	5000 amperes duration = 10^{-2} sec to 1/2 value	200 amperes duration = 1 sec rectangular wave
Relative Mechanical Force (pro- portional to I^2)	<u>100.0</u>	0.25	0.0004
Heating Effect = $\int_0^{\infty} I^2 dt R$	= 69,000 R	= <u>172,000 R</u>	= 40,000 R
Energy = $\frac{1}{2} CE^2$	33,800 joules	<u>300,000 joules</u>	100,000 joules
Charge Transfer Q	(C) x (E) 3.3 $\times 10^{-6}$ x 15 $\times 10^4$ = 0.5 coulombs	(C) x (E) 3000 $\times 10^{-6}$ x 10,000 = 30 coulombs	(I) x (t) 200 x 1 = <u>200 coulombs</u>

TABLE III

Summary of Runs in which Flame Propagation
Occurred on Open Vent Exit






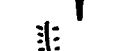





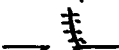

Electrical Supply	F/A	V _v fps	V _o Free Stream mph	Electrode	
				Distance from Plate (inches)	Location
1	.107	3.34	75	30	 inside vent tube
1	.107	3.34	100	30	 inside vent tube
1	.095	4.41	100	30	 inside vent tube
1	.095	4.41	100	30	 inside vent tube
1	.104	4.45	100	30	 inside vent tube
1	.095	4.42	100	30	 inside vent tube
1	.095	4.47	100	30	 leading edge lip
1	.091	4.42	100	30	 inside vent tube
1	.091	4.42	100	30	 inside vent tube
1	.091	4.42	100	30	 inside vent tube
1	.091	4.42	100	30	 inside vent tube
1	.20	.99	0	30	 inside vent tube
1+2+3	.114	.75	100	3/8"	 aft lip

TABLE IV

Summary of Runs in Which Flame Propagation was
Observed with Flame Arrester Installed.

Electrical Supply*	F/A	V _v ft/sec	V _o mph	Electrode Distance inches	Electrode** Location
1	.105	.70	0	1/2	Arrester Center
1	.118	.75	0	1/2	Arrester Center
1	.112	.70	0	1/2	Arrester Center
1 + 2	.128	.70	0	1/2	Arrester Center
1 + 2	.128	.70	0	1/2	Arrester Center
1 + 2	.114	.75	0	3/4	Arrester Center
1 + 2	.088	.70	100	1/4	Arrester Center
1 + 2	.127	.70	100	1/4	Arrester Center
1 + 2	.133	.70	100	1/4	Arrester Center
1 + 2	.127	.70	100	1/4	Trailing Lip
1 + 2	.118	.75	0	3/8	Aft Arrester Face
1 + 2	.118	.75	100	3/8	Aft Arrester Face
1 + 2	.124	.75	100	3/8	Aft Arrester Face
1 + 2	.127	.70	100	3/8	Aft Arrester Face
1 + 2 + 3	.130	.75	0	1/4	Arrester Center
1 + 2 + 3	.119	.75	0	1/4	Forward Edge
1 + 2 + 3	.138	.70	0	1/4	1/2" Left of Lip
1 + 2 + 3	.132	.50	0	1/4	1/2" Left of Lip
1 + 2 + 3	.141	.60	0	1/4	Left of Forward Lip
1 + 2 + 3	.152	.75	100	1/4	Trailing Lip
1 + 2 + 3	.121	.70	100	3/8	Aft Arrester Face
1 + 2 + 3	.121	.70	0	3/8	Aft Arrester Face
1 + 2 + 3	.124	.75	0	3/8	Aft Arrester Face

* Numbers refer to electrical elements (see text)

** See Figure 71 for summary of electrode locations

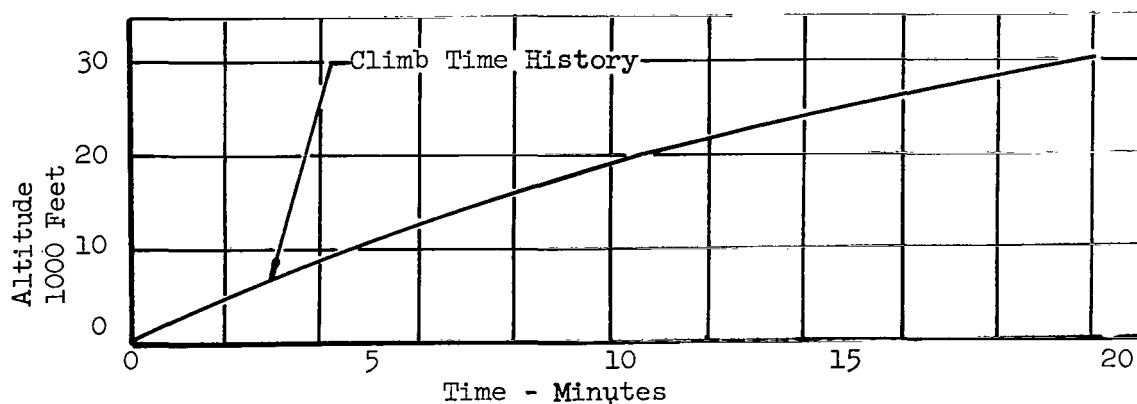
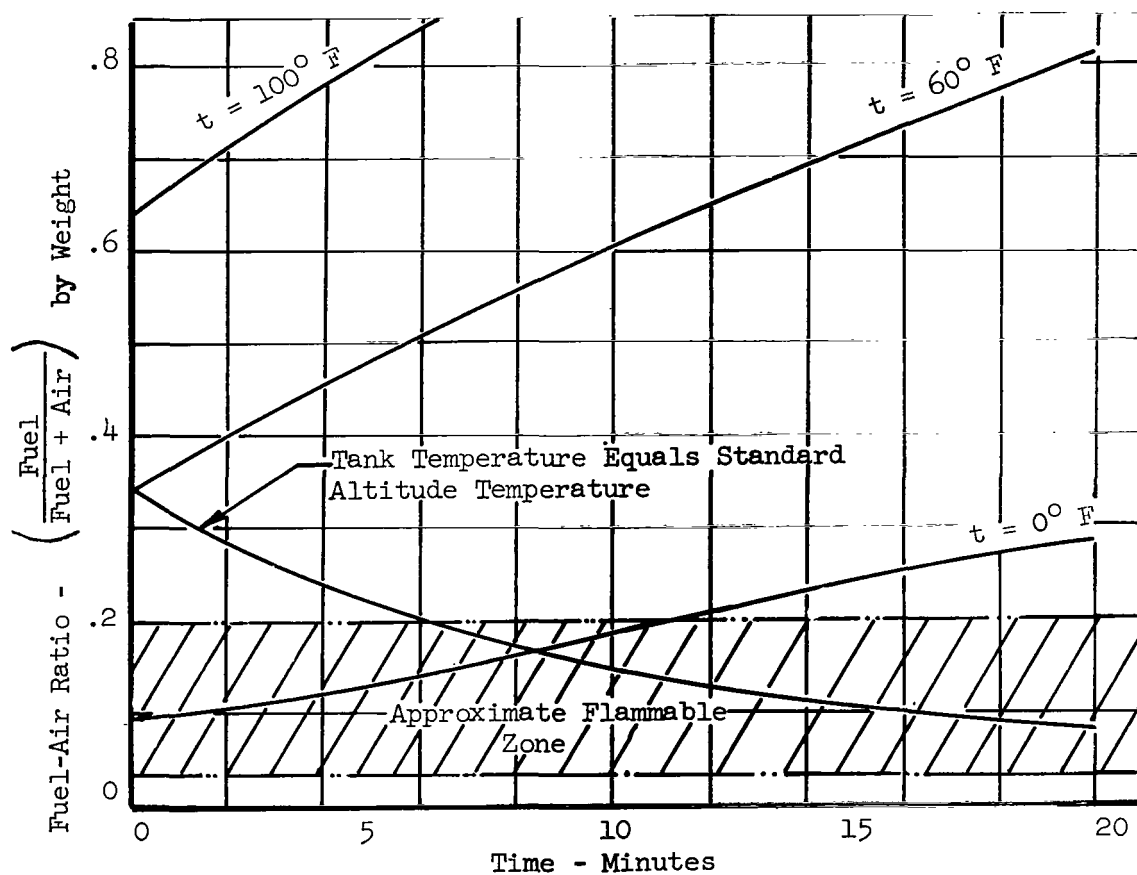


Fig. 1. - Aircraft "A" Saturated Fuel-Air Ratio Inside Fuel Tank Vapor Space During Maximum Rate of Climb. Fuel is 115/145 Aviation Gasoline.

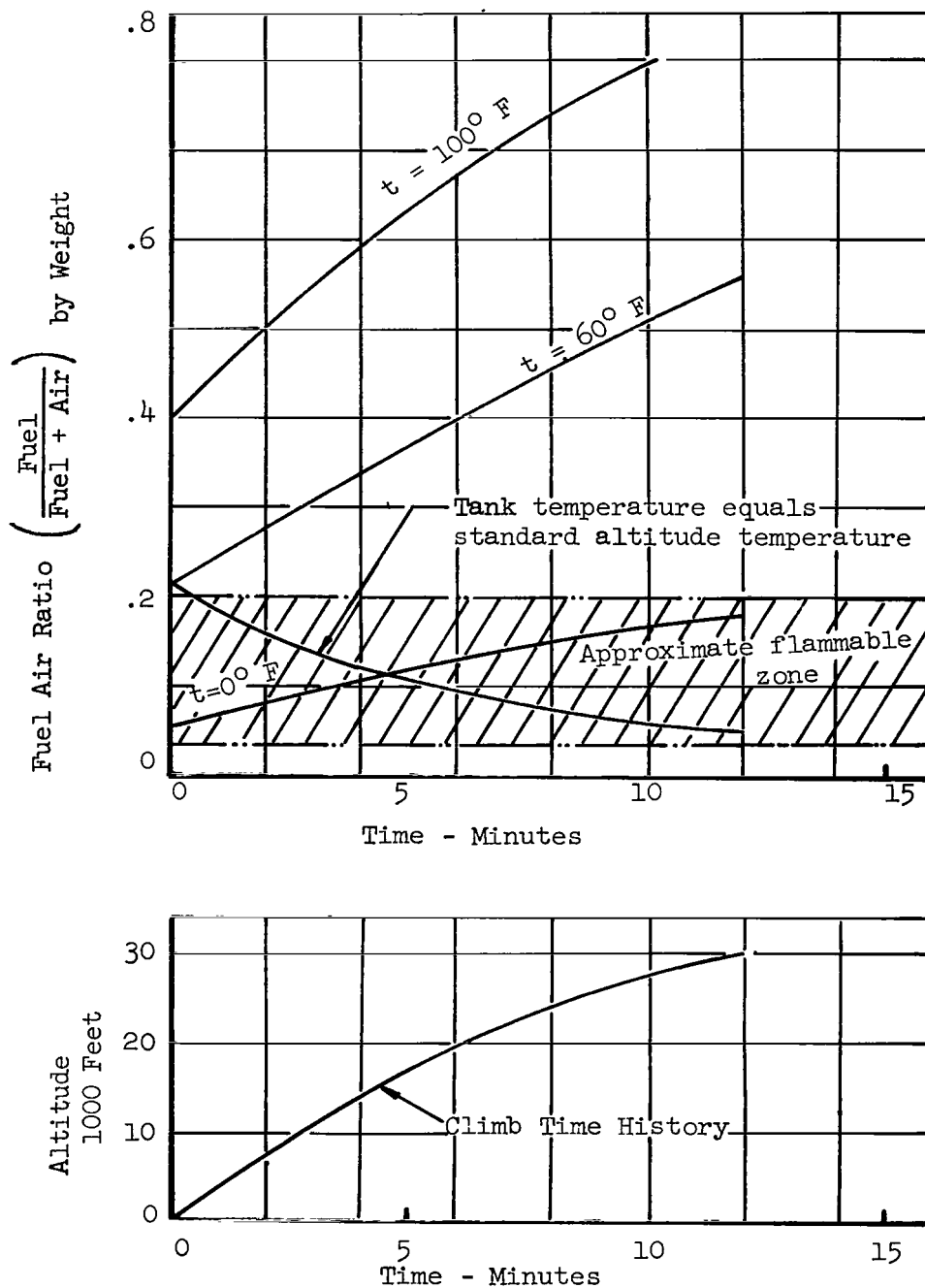


Fig. 2. - Aircraft "E" Saturated Fuel-Air Ratio Inside Fuel Tank Vapor Space During Maximum Rate of Climb. Fuel is JP-4 Turbine Fuel.

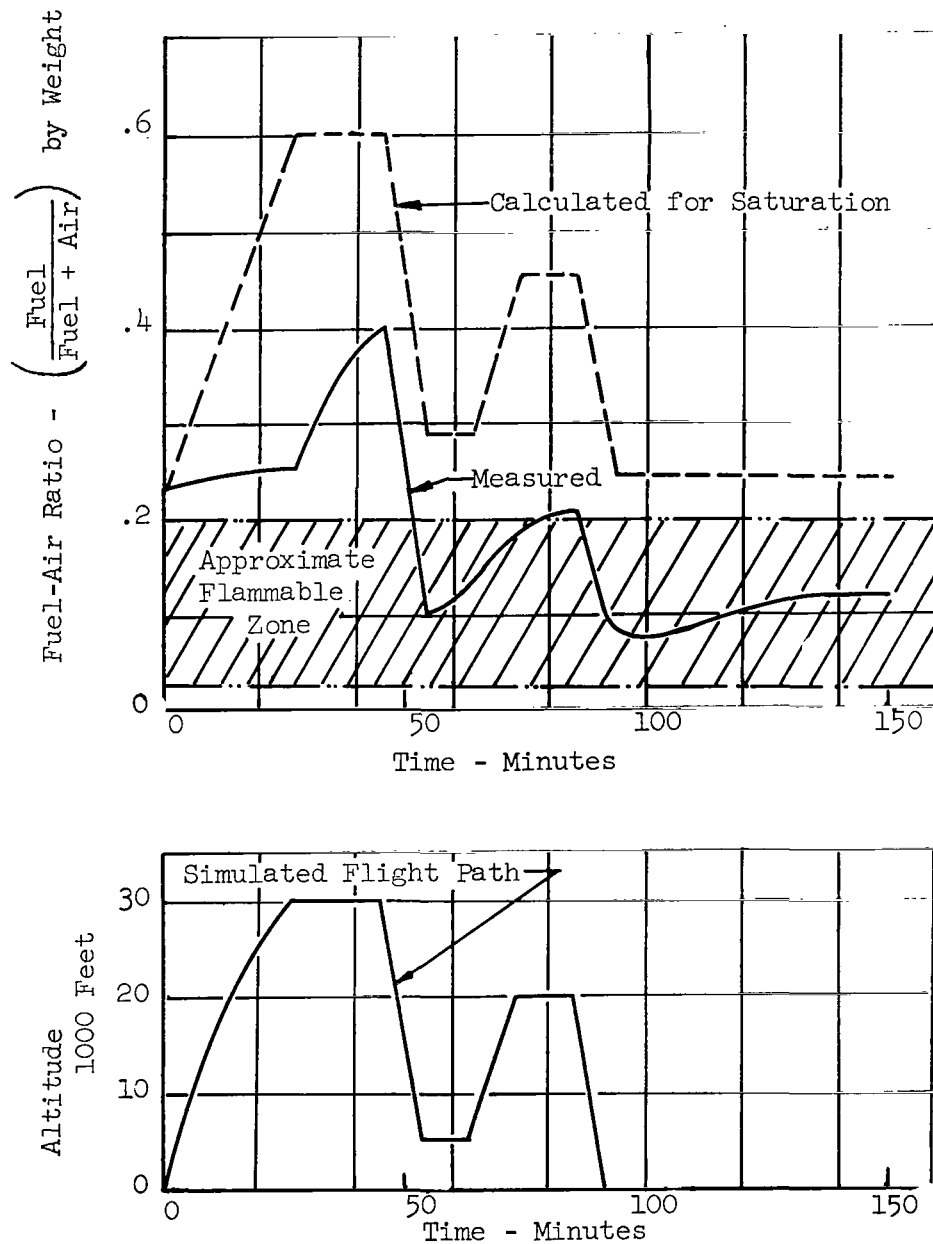


Fig. 3. - Variation of Fuel-Air Ratio in a Test Tank During Simulated Flight. Five gallons of Hexane in a fifty gallon tank. Ref.: British Report R.A.E. CH650.

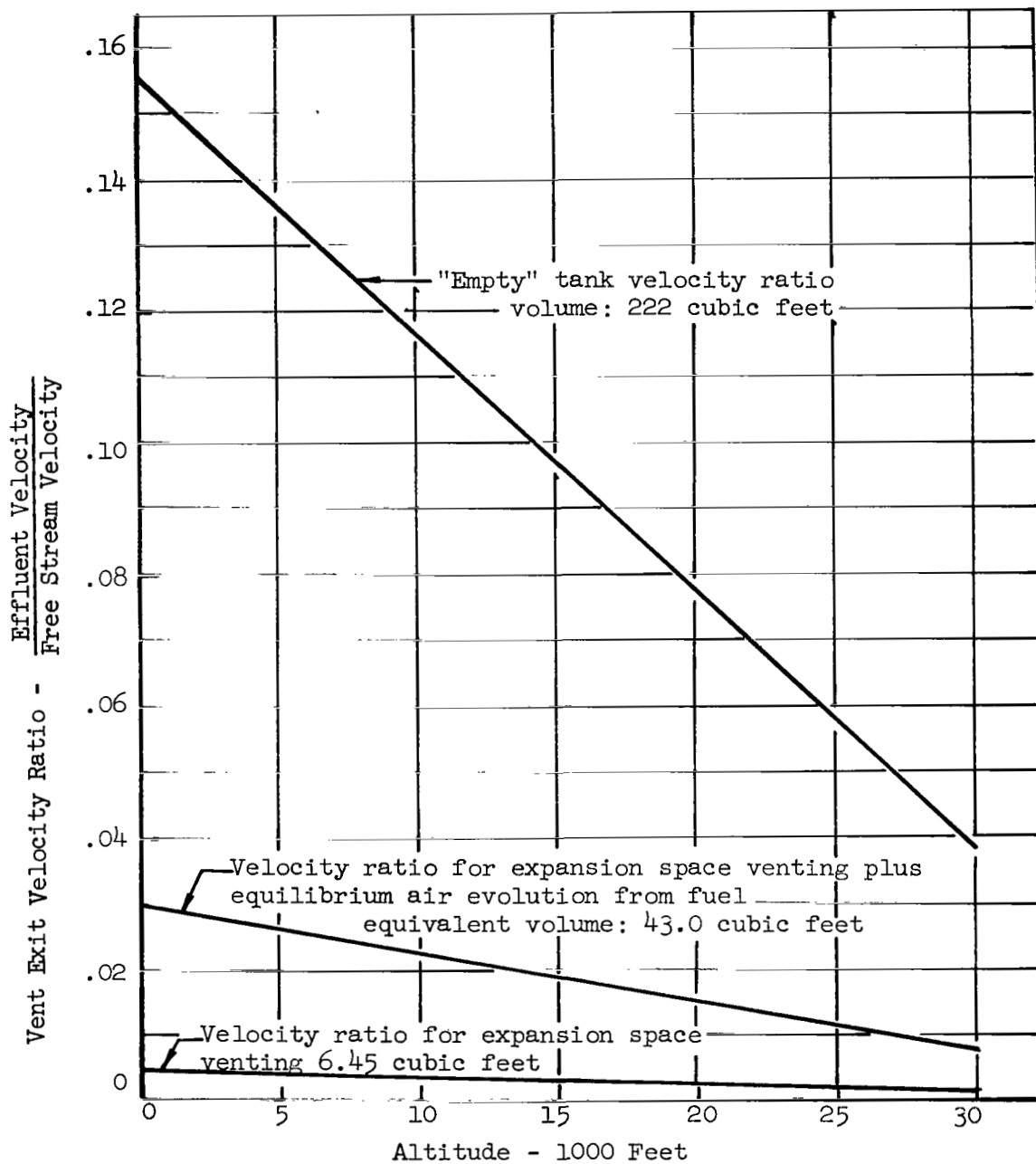


Fig. 4. - Aircraft "E" Vent Exit Velocity Ratio During a Maximum Climb Profile.

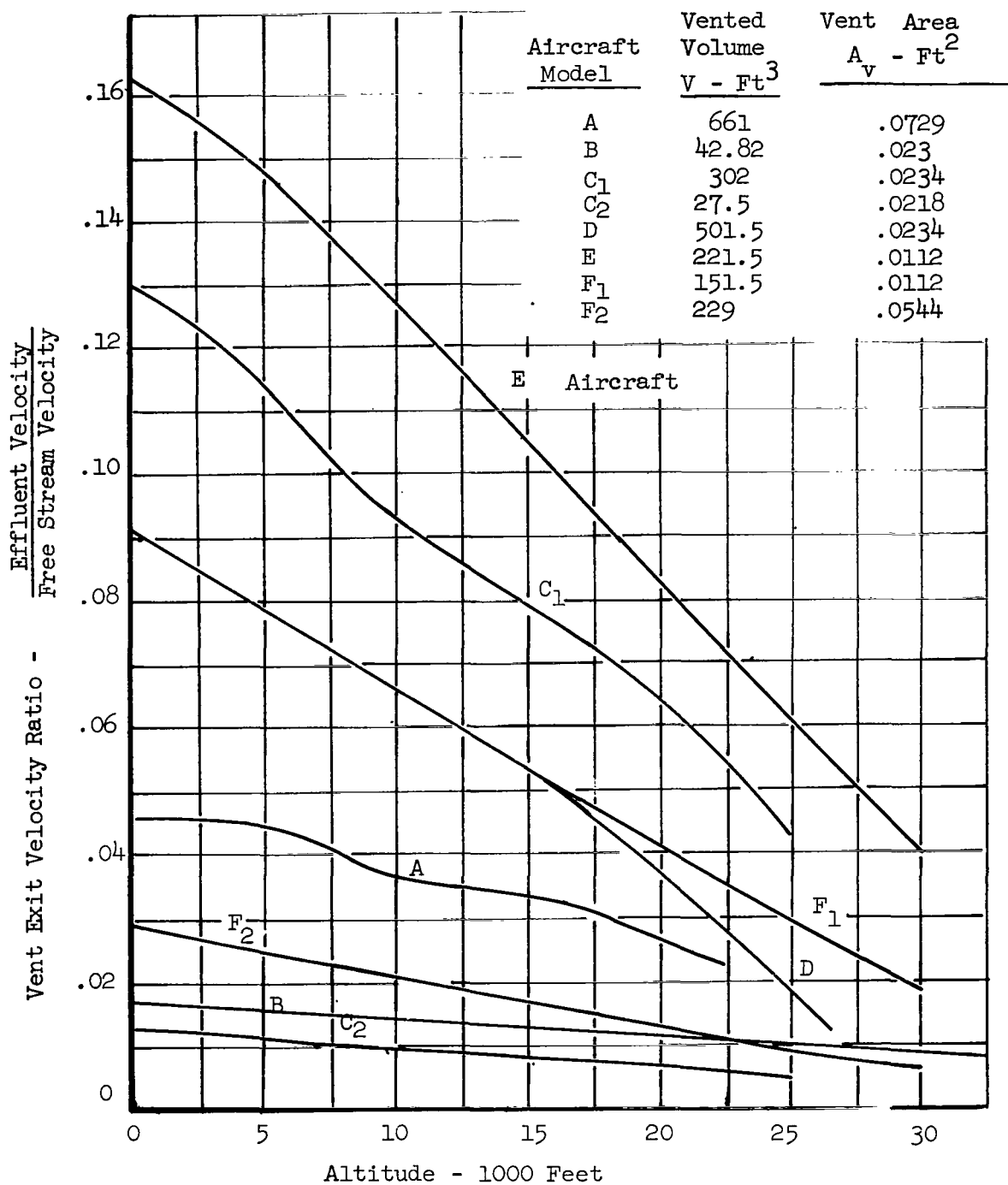


Fig. 5. - Summary of Vent Exit Velocity Ratio (non-fuel boiling) for six airplanes at maximum rate of climb.

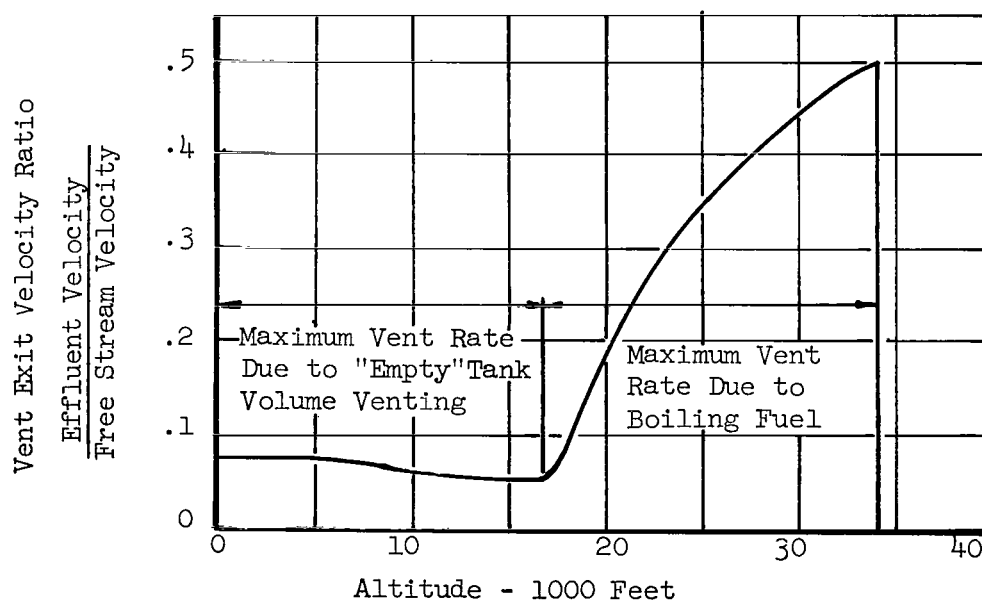
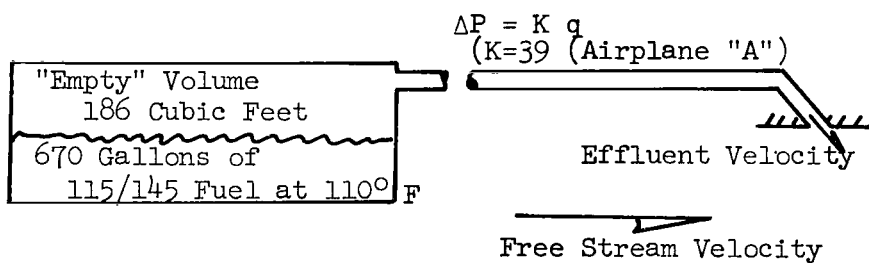
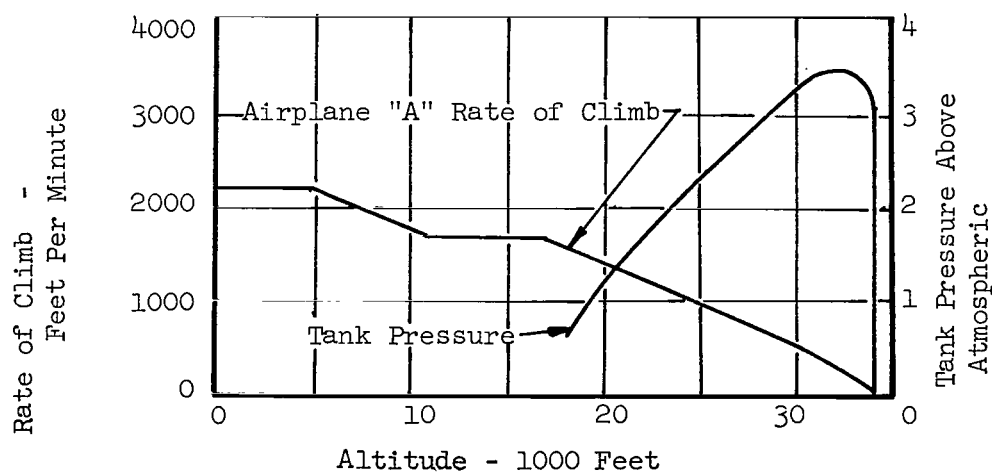


Fig. 6. - Vent Exit Velocity Ratio Including Fuel Boiling Effects for Aircraft "A". Fuel: 115/145 Avgas

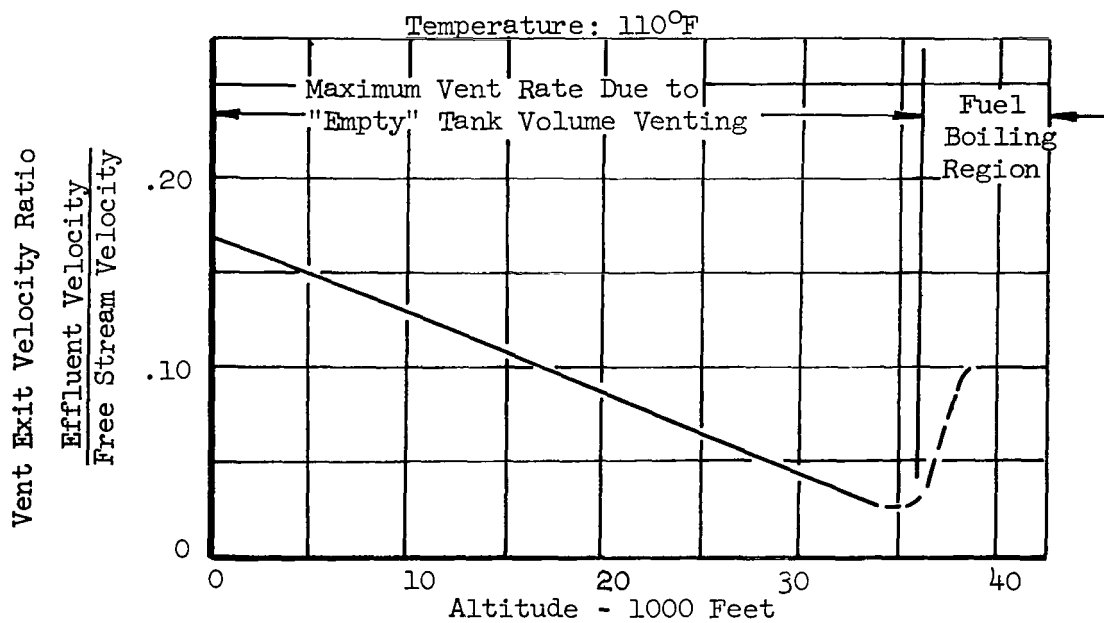
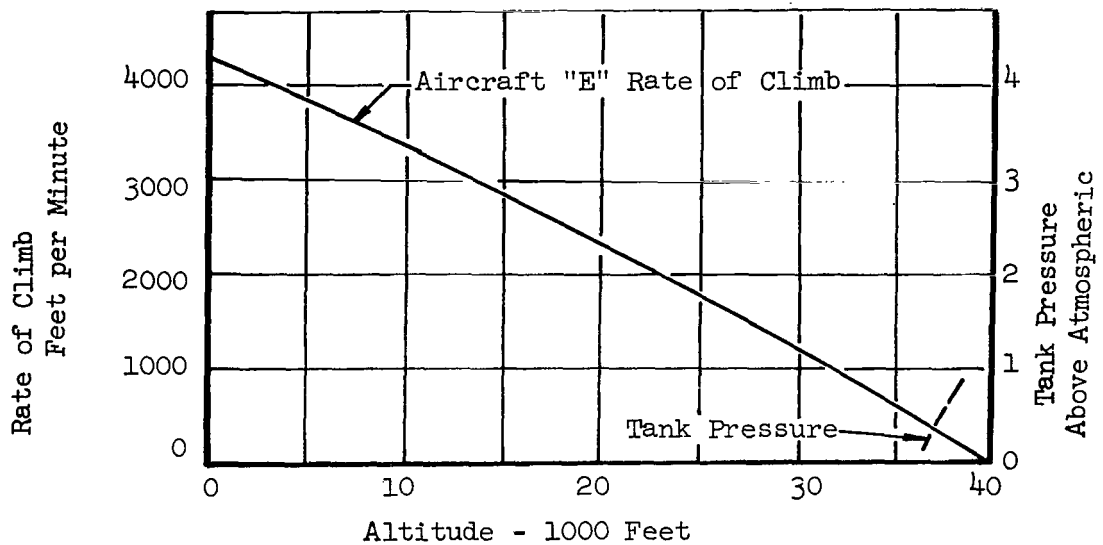


Fig. 7.- Vent Exit Velocity Ratio Including Fuel Boiling Effects for Aircraft "E". Fuel: JP-4

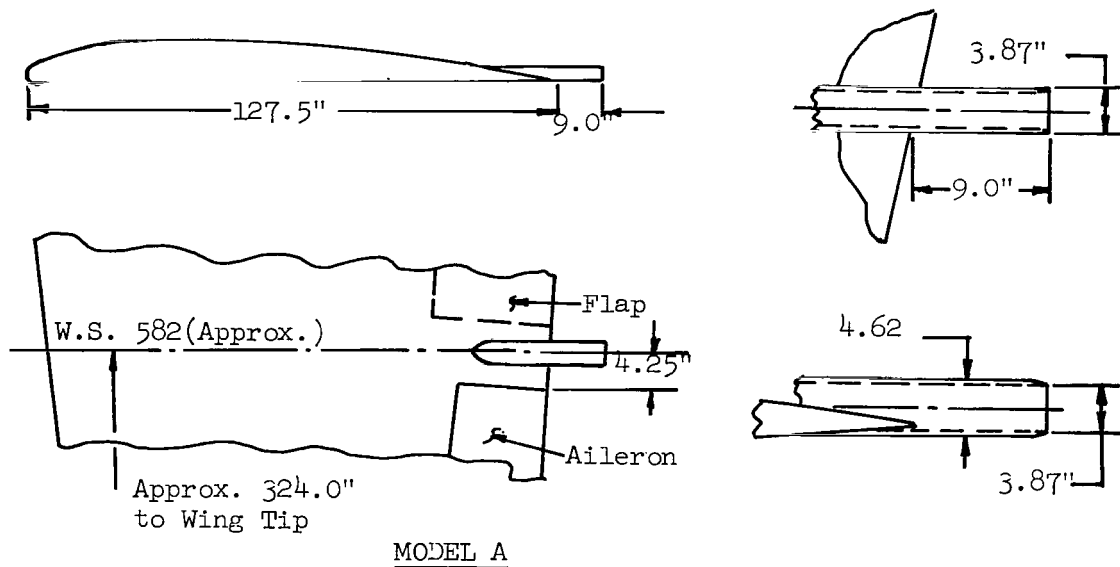


Fig. 8(a). - Mast Discharging Into Wake.

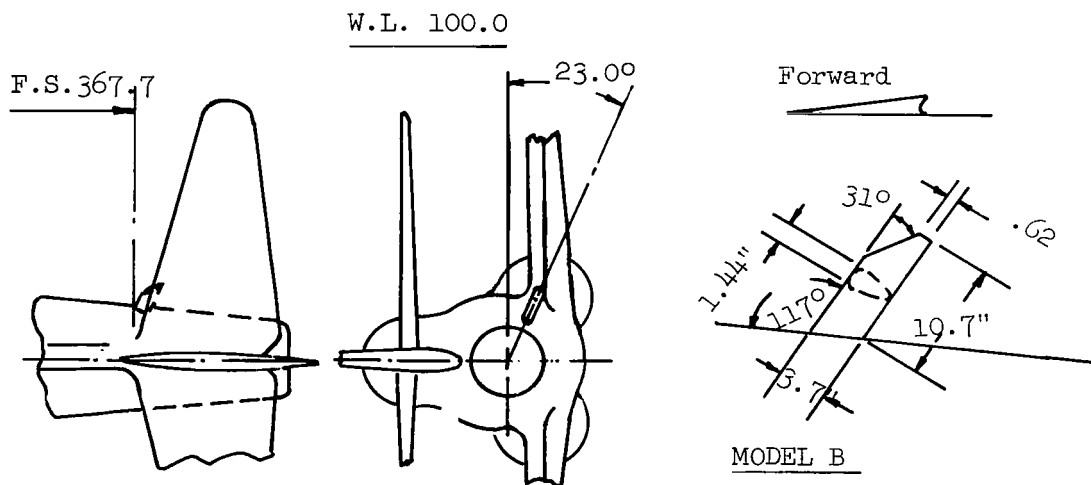


Fig. 8(b). - Mast Discharging Into a Free Stream.

Figure 8. - Typical Vent Exit Configurations and Locations for One Manufacturer.

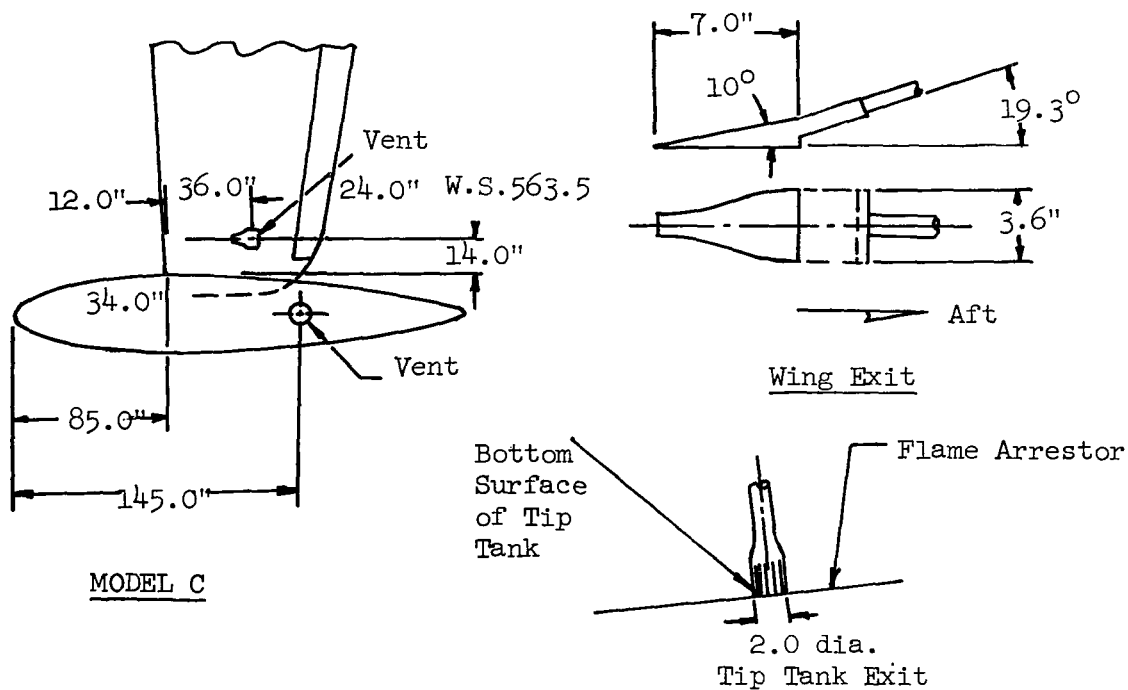


Fig. 8(c). - Flush Vent Discharging Into a Boundary Layer.

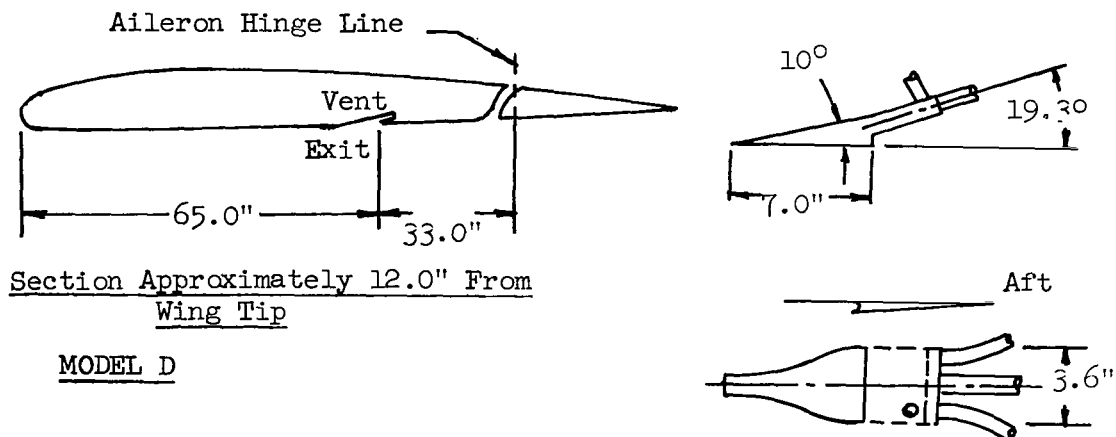


Fig. 8(d). - Flush Vent Discharging Into a Boundary Layer.

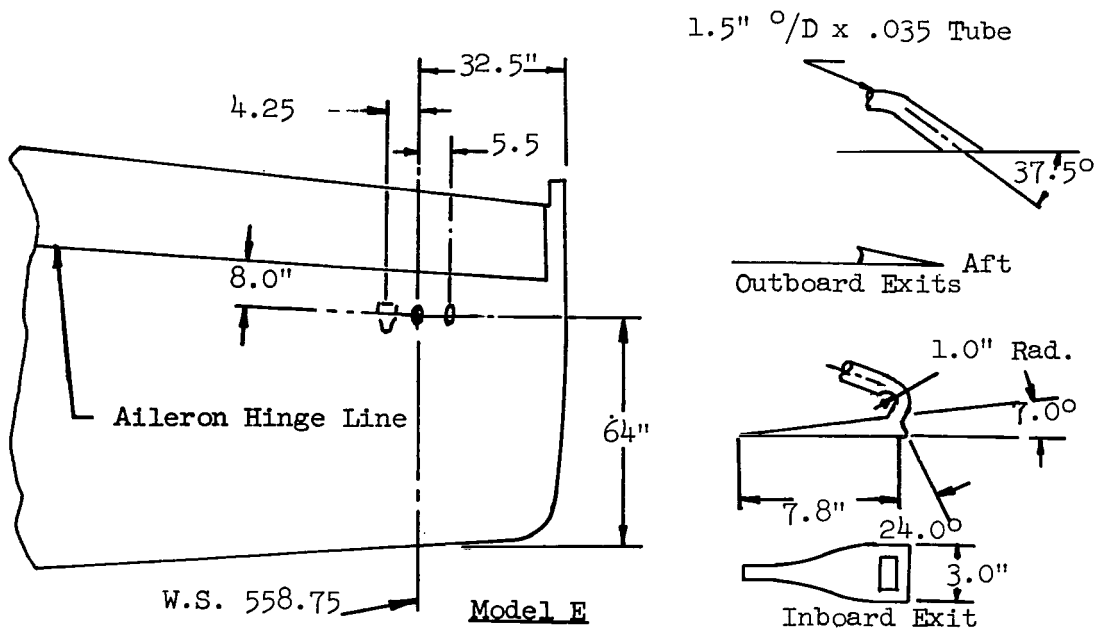


Fig. 8(e). - Flush Vent Discharging Into a Boundary Layer.

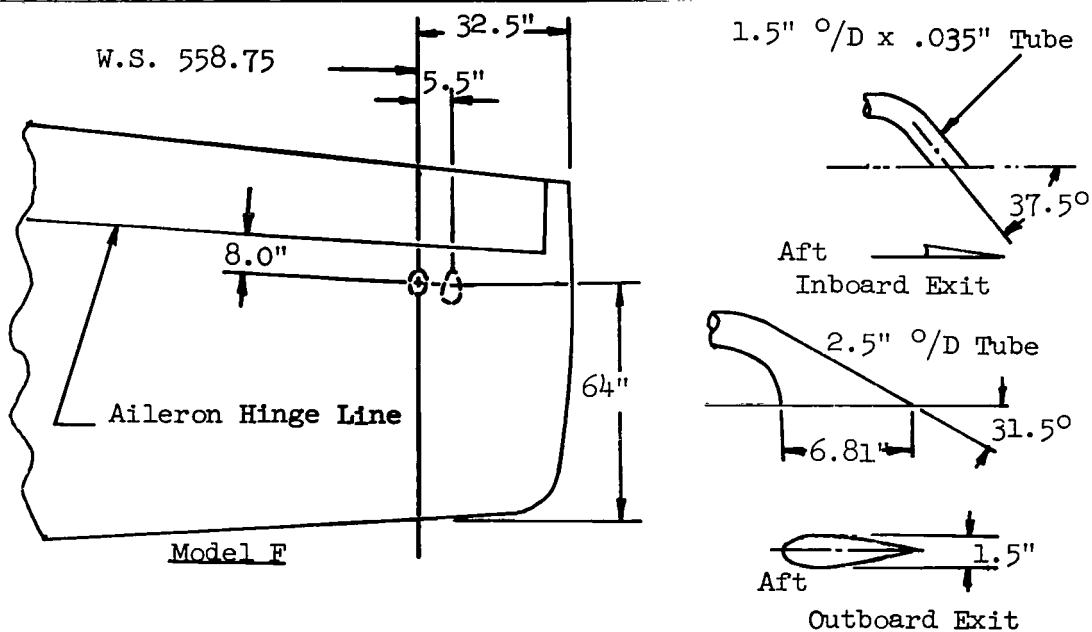
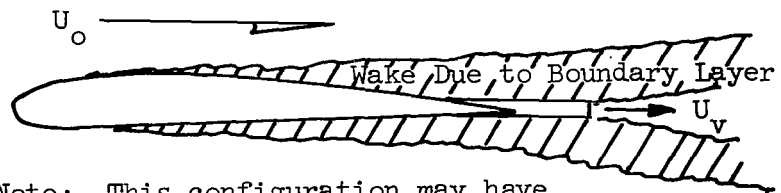


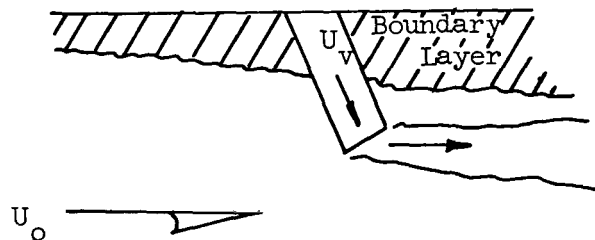
Fig. 8(f). - Flush Vent Discharging Into a Boundary Layer.

A. Mast Discharging Into a Wake.



Note: This configuration may have flap, aileron, or both, adjacent to the vent mast to disturb flow pattern.

B. Mast Discharging Into Free Stream.



C. Flush Vent Discharging Into Surface Boundary Layer.

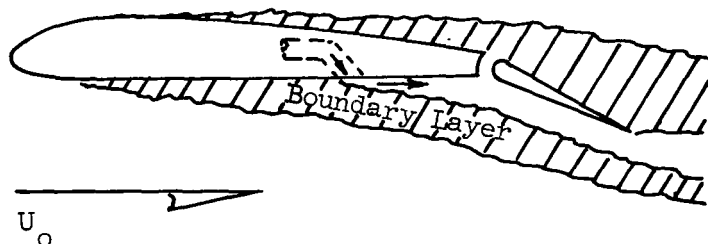
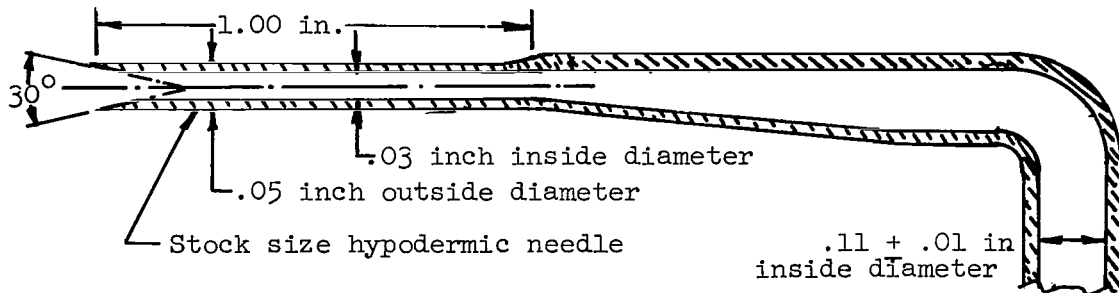


Fig. 9. - Three General Classes of Fuel Vent Exits.



PROBE DETAIL

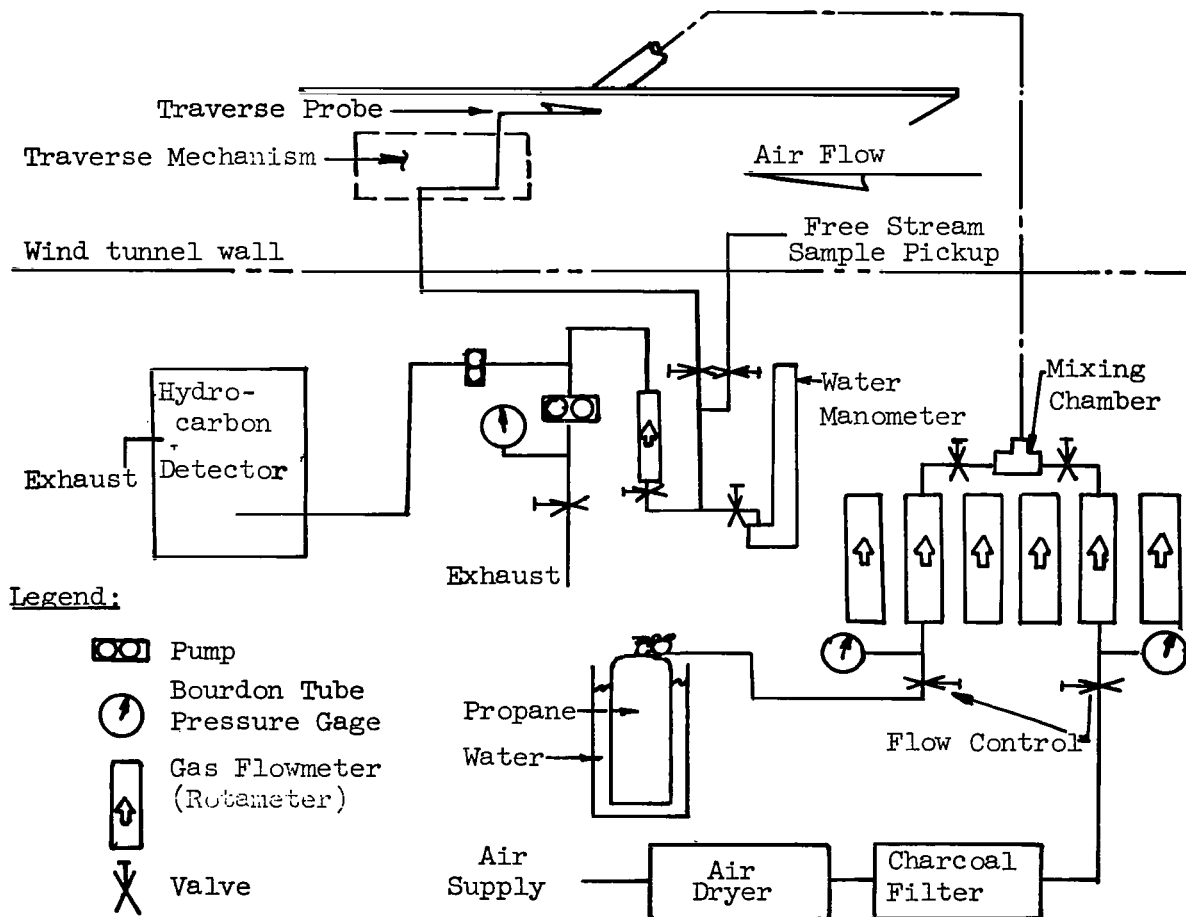
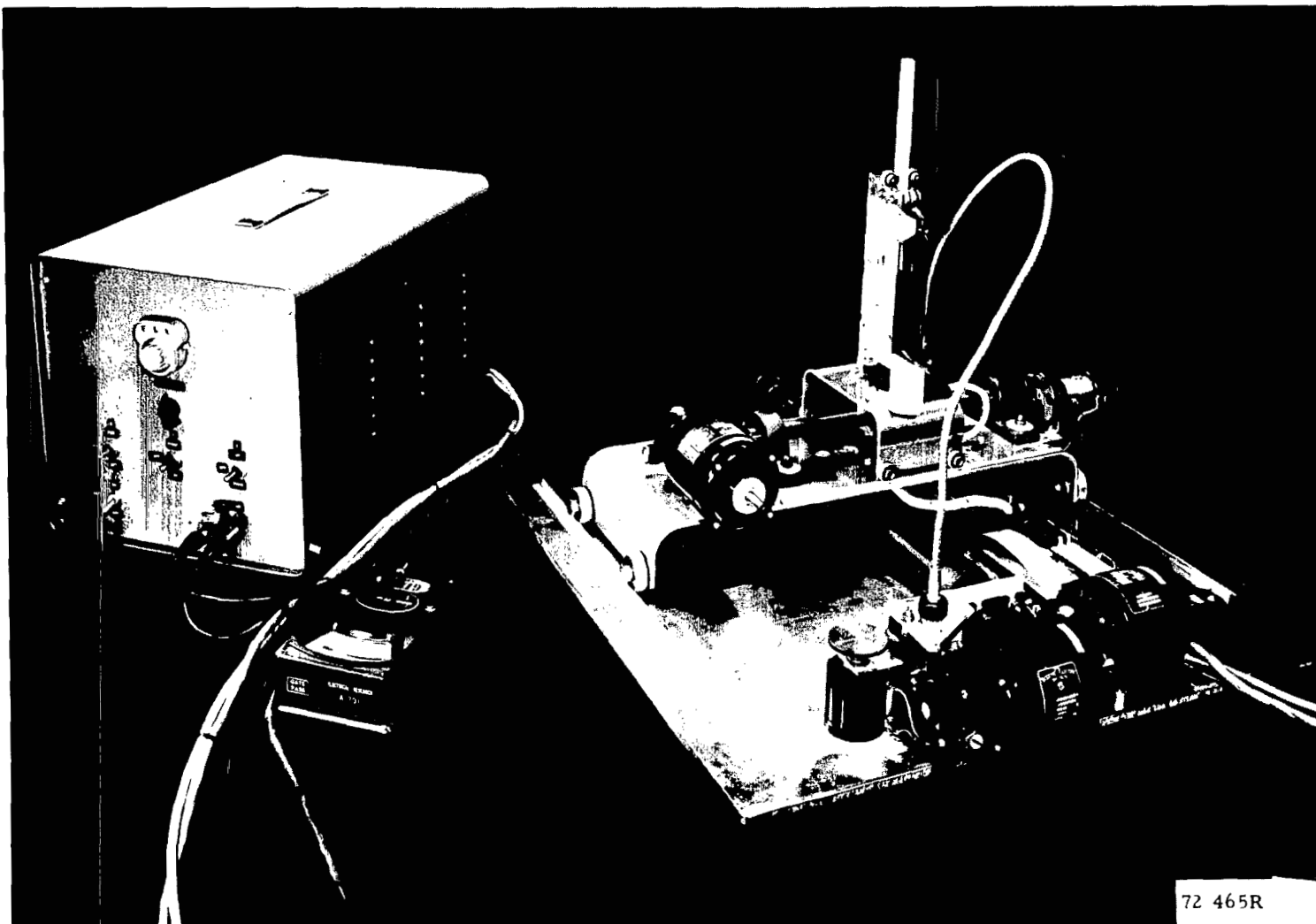


Figure 10. - Schematic Drawing of Gas Analysis Set-Up and Probe Installed at Lockheed's Subsonic Wind Tunnel, Burbank.



72 465R

Figure 11. - Traverse Mechanism and Control Unit.

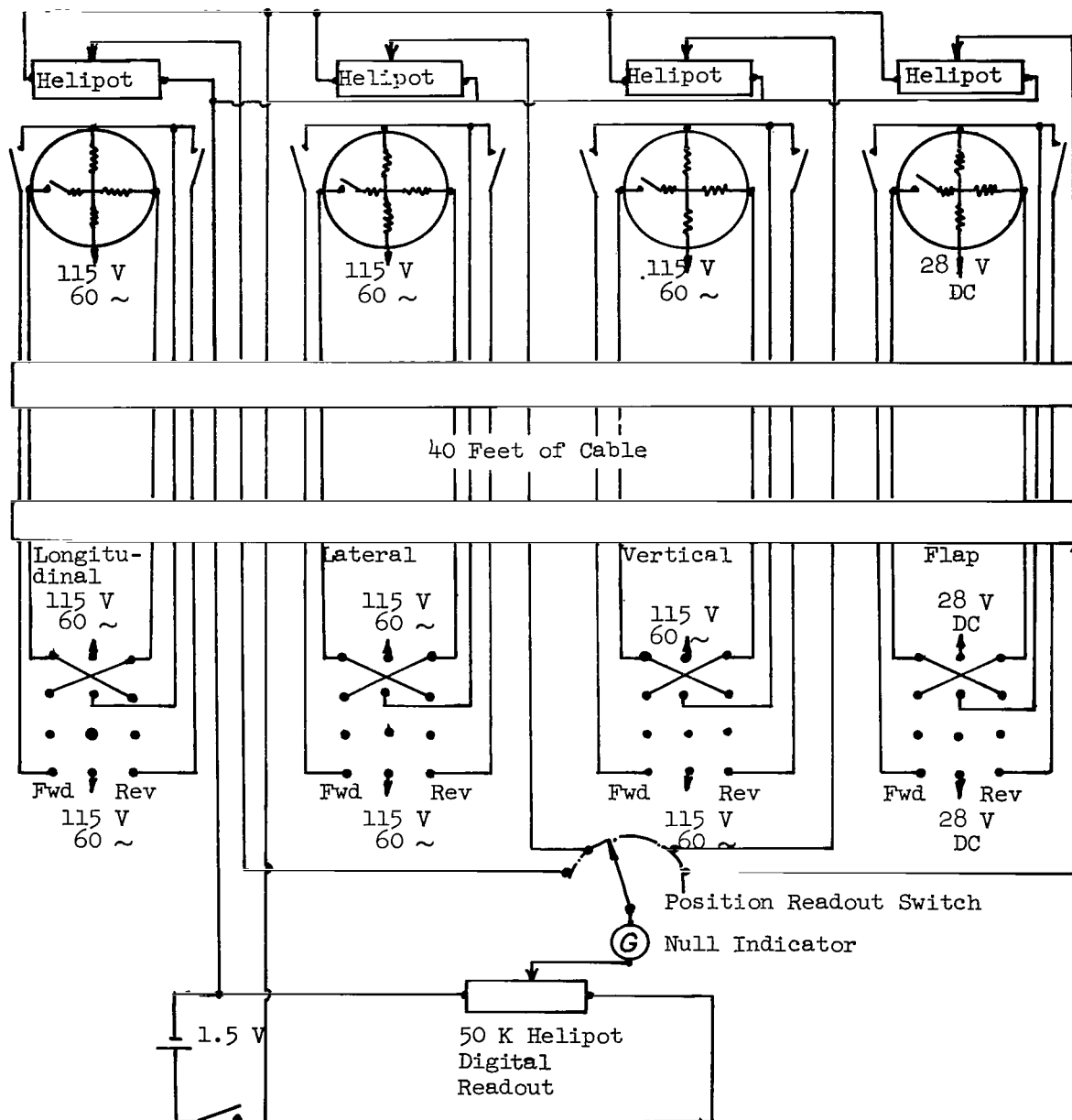


Figure 12. - Control Circuit for Probe Traverse and Flap Positioning Mechanisms.

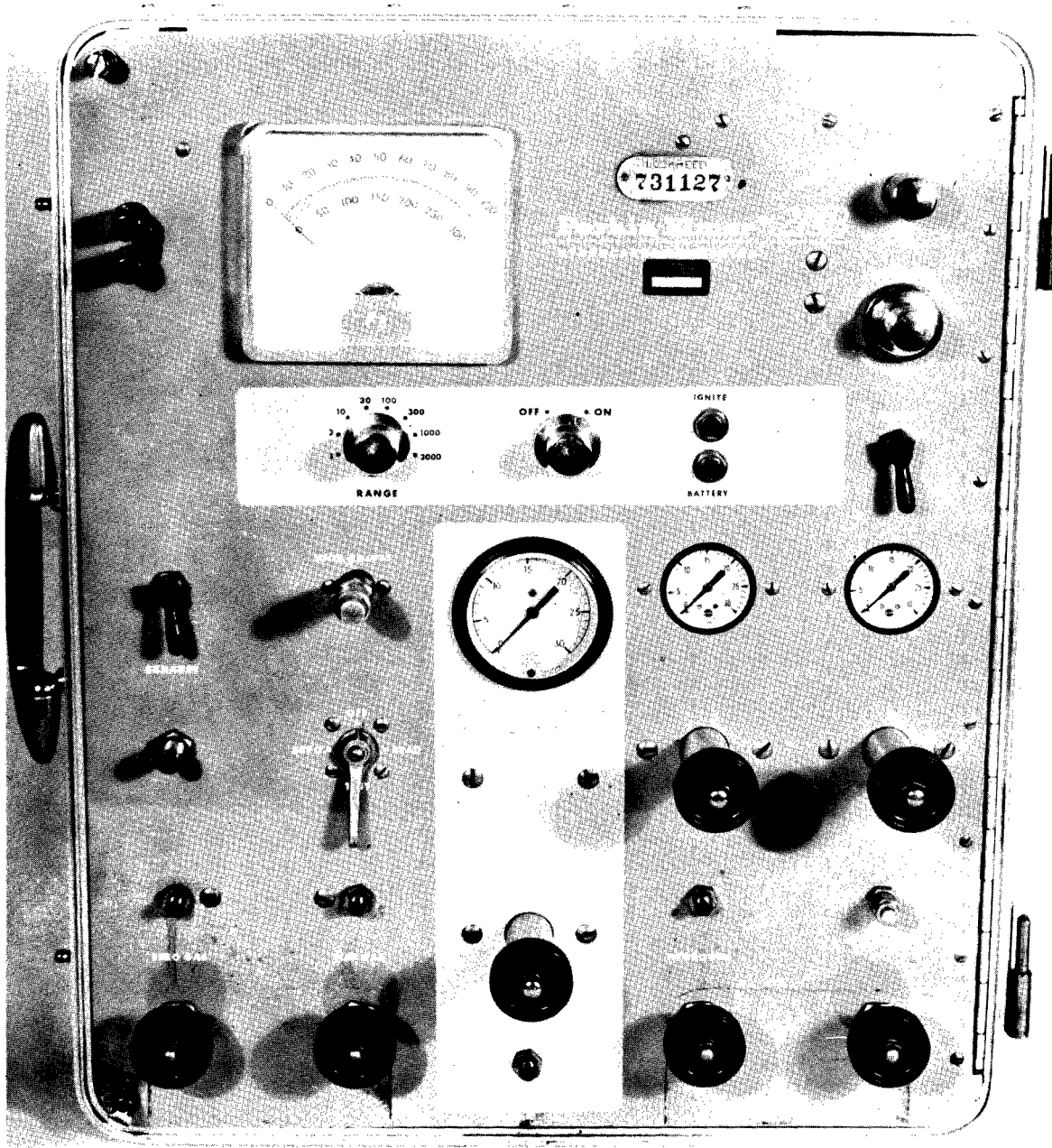


Figure 13. - Model 213B Perkin-Elmer
Hydrocarbon Detector.

$$\frac{f}{f+a} = 0.11 \quad \left(\frac{F^o}{F+A} \right)_{(WT)}$$

(VOL)

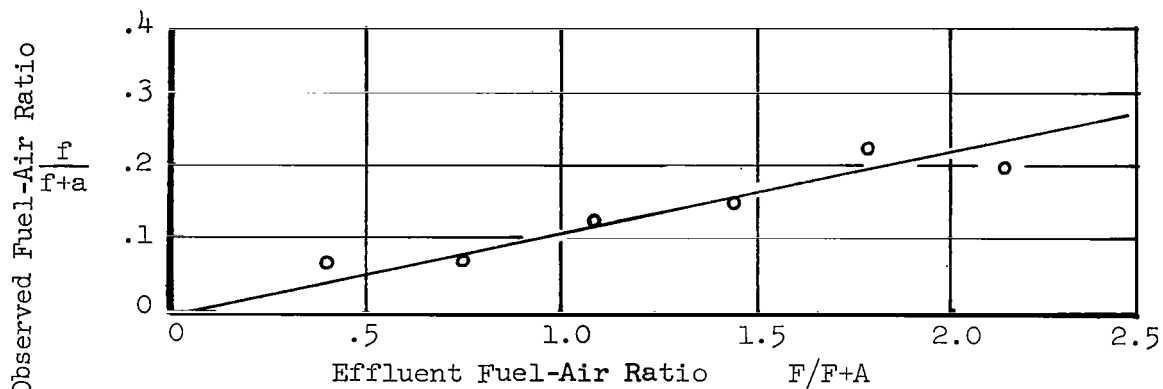


Fig. 14(a). - Effect of Effluent Fuel-Air Ratio on Observed Fuel-Air Ratio

$$\frac{f}{f+a} = 0.18 \quad (\text{No Temp. Effect})$$

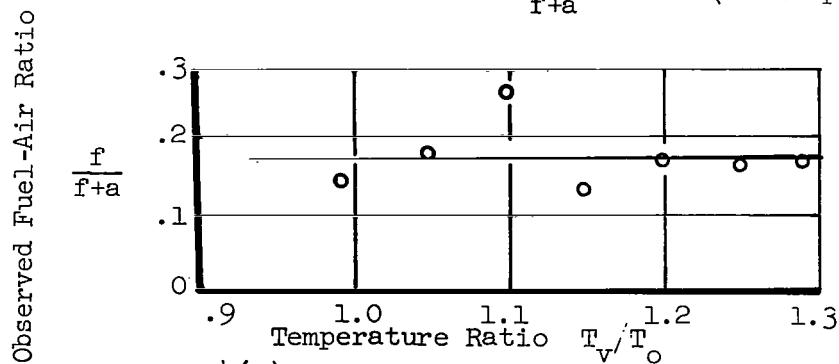


Fig. 14(b). - Effect of Temperature on Observed Fuel-Air Ratio

Figure 14. - Effect of Temperature and Effluent Fuel-Air Ratio on Observed Fuel-Air Ratio

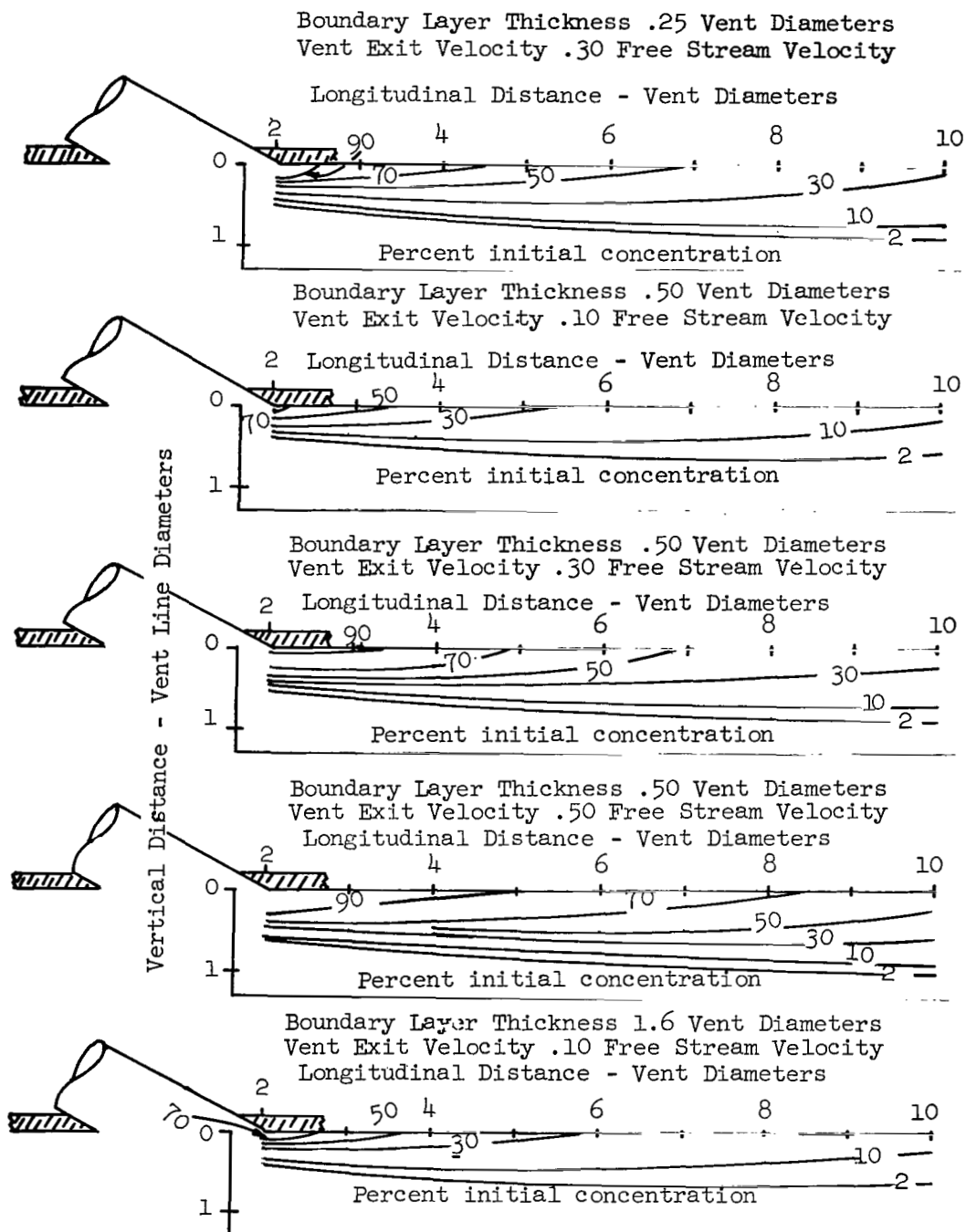


Figure 15(a).- Fuel Concentration Profiles at Vent Exit Lateral Center Line.

Figure 15. - Flush Vent Exit Fuel Concentration Profiles

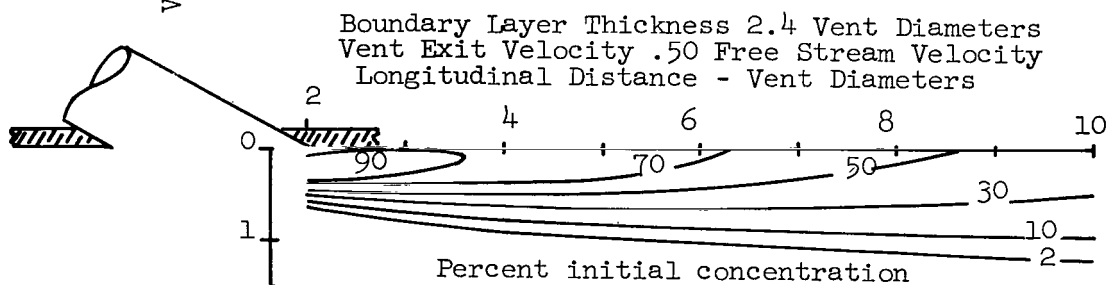
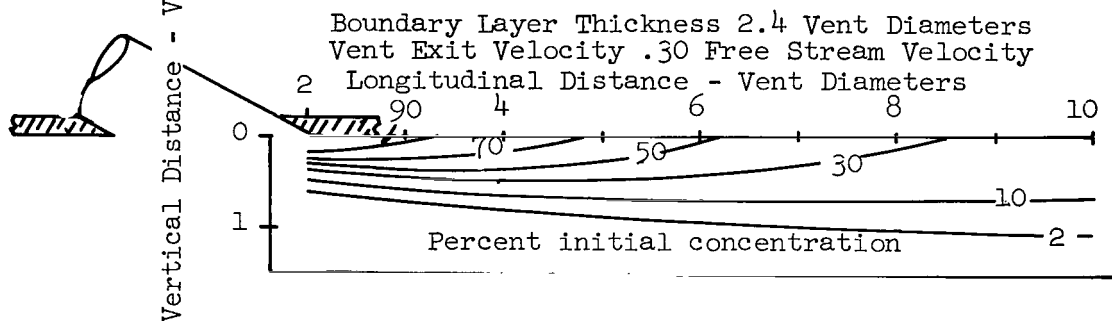
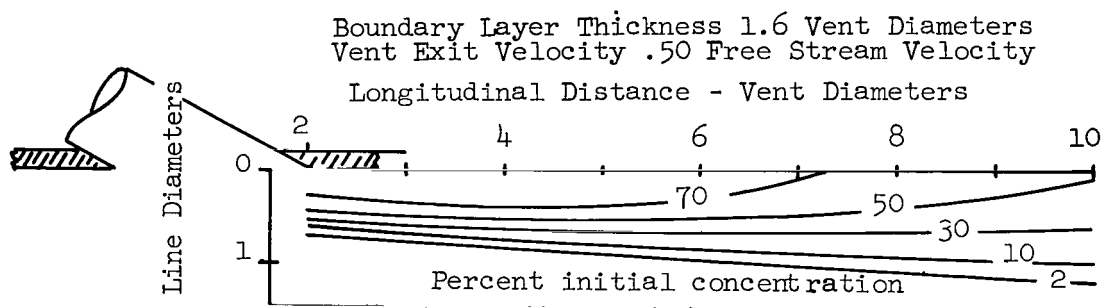
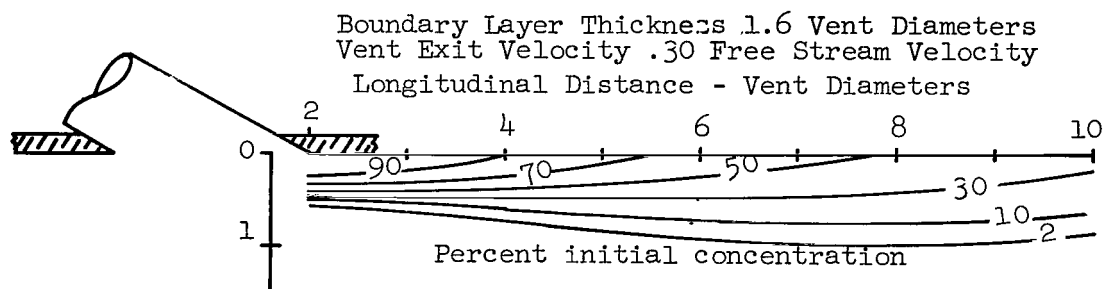


Figure 15(a). - Fuel Concentration Profiles at Vent Exit Lateral Center Line.
(cont'd.)

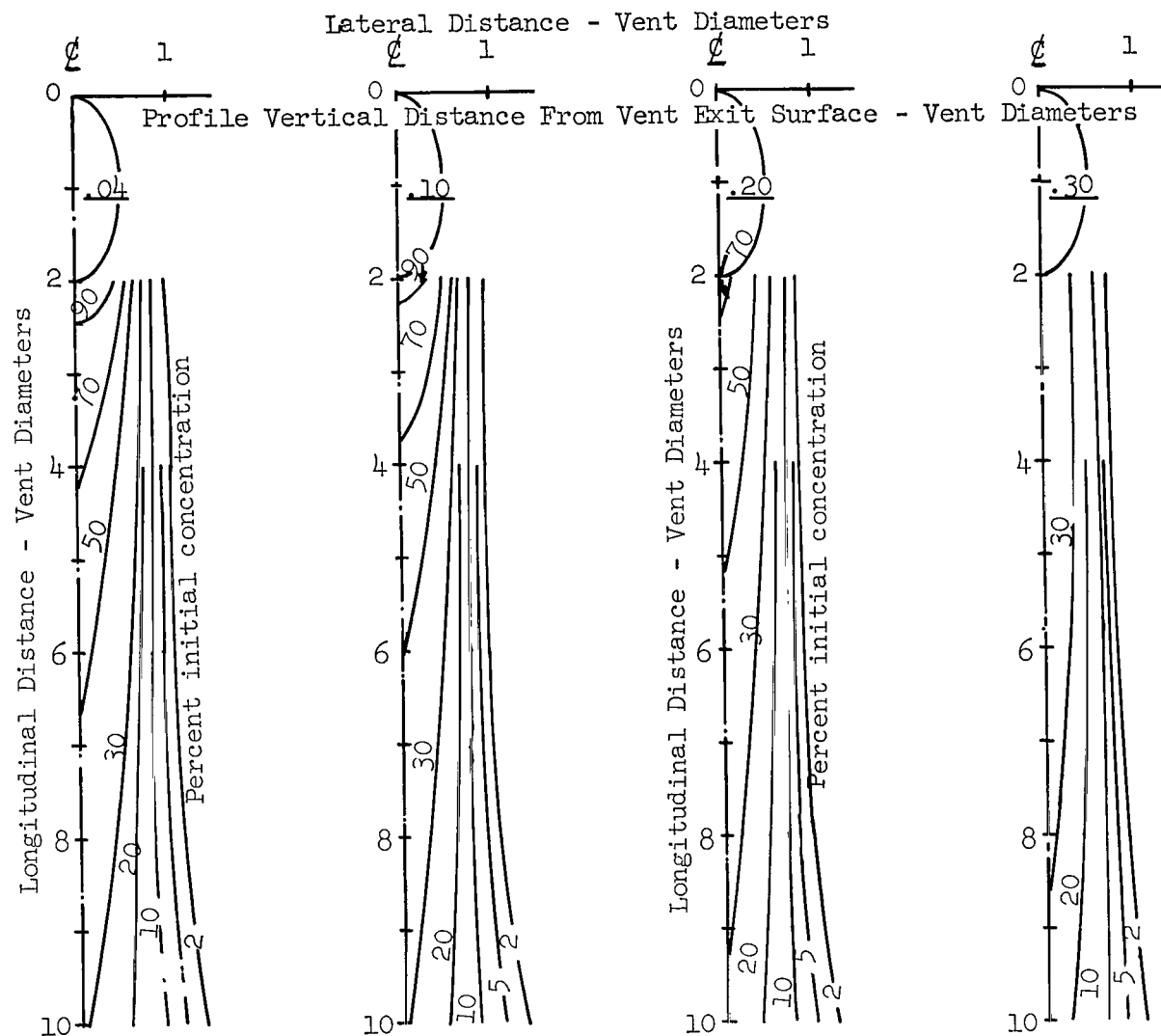


Figure 15(b).- Fuel Concentration Profiles. Boundary layer thickness 0.25 vent diameters. Vent exit velocity 0.30 free stream velocity.

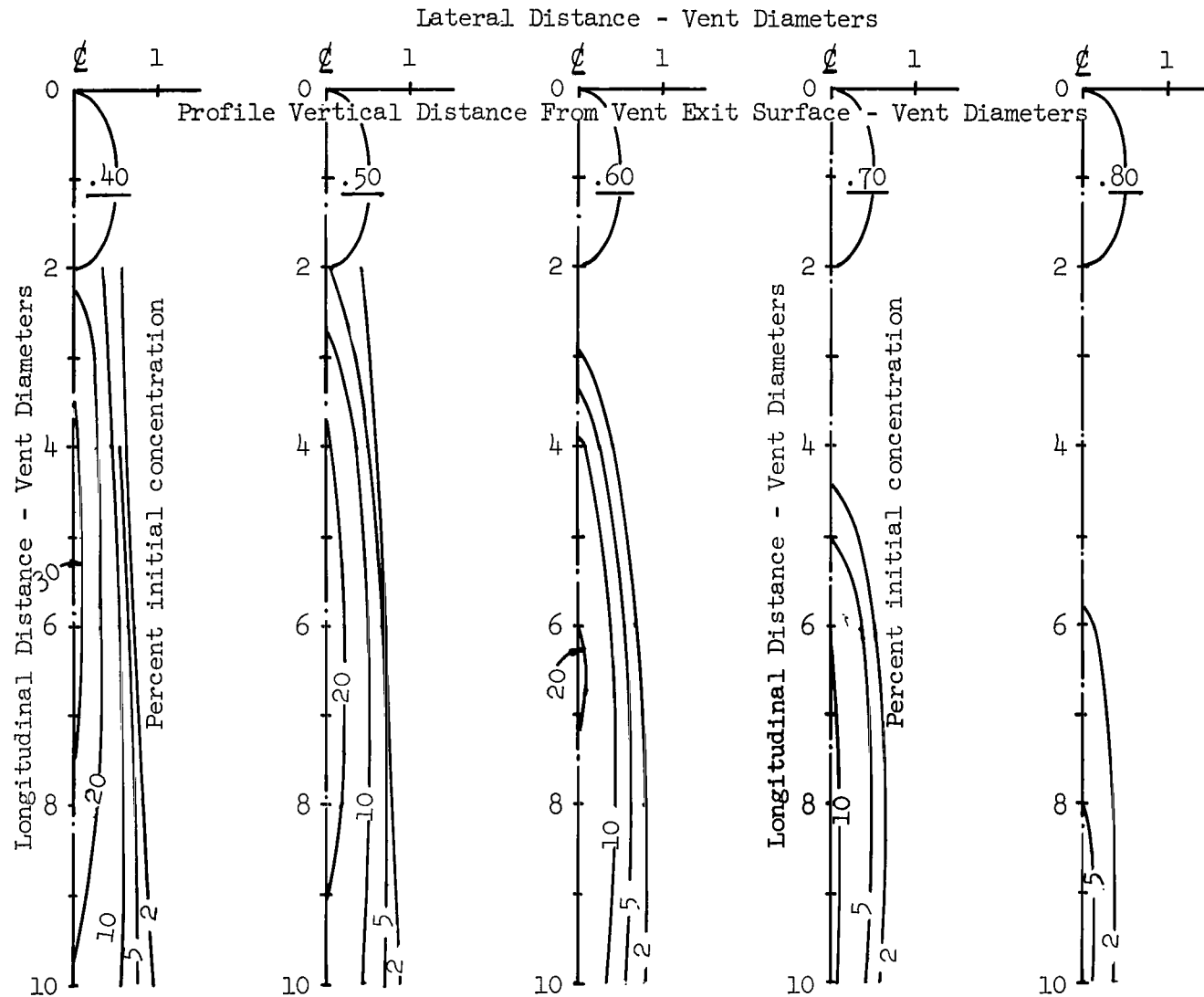


Figure 15(b).- Fuel Concentration Profiles. Boundary layer thickness 0.25 vent diameters. Vent exit velocity 0.30 free stream velocity.

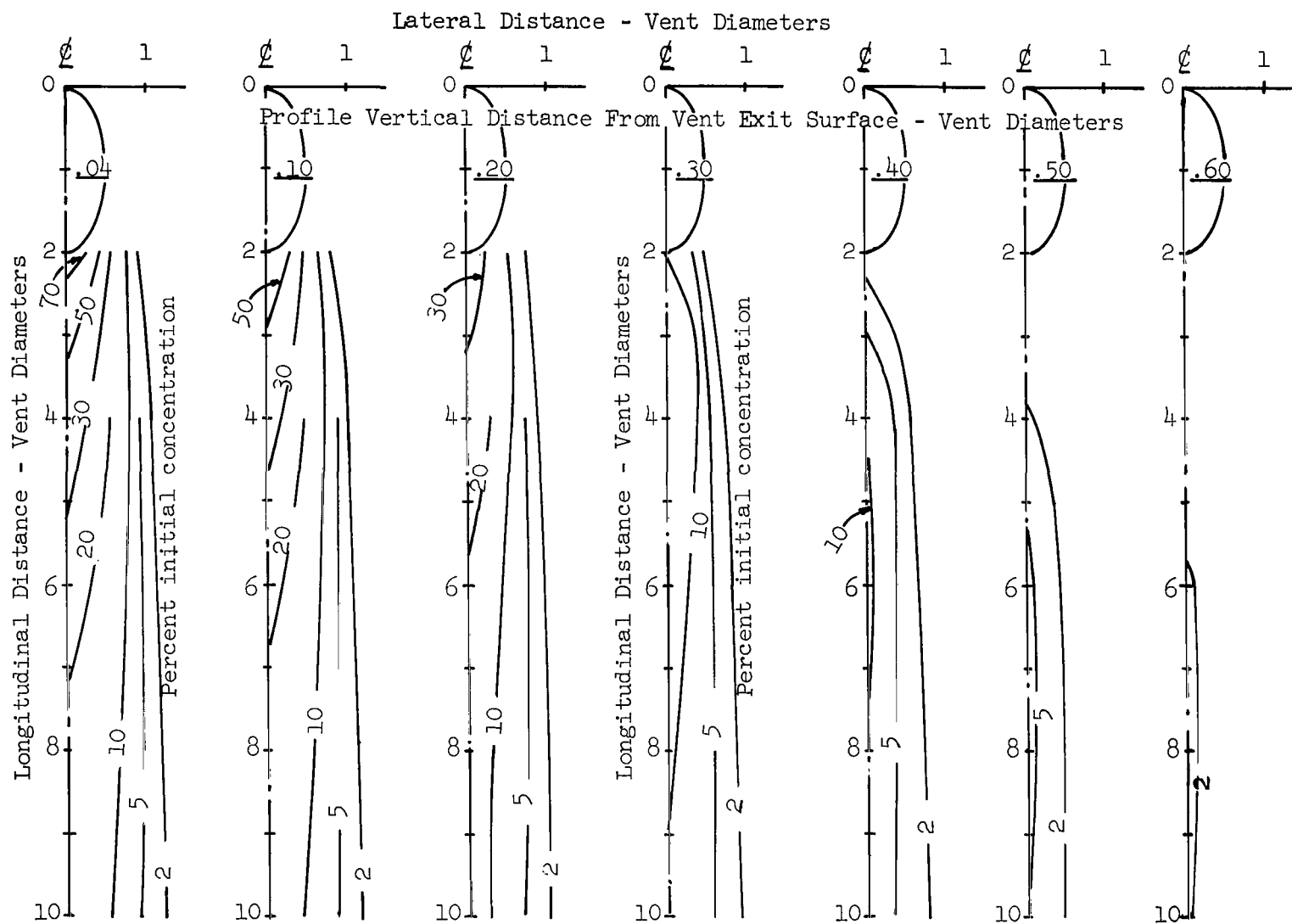


Figure 15(c).- Fuel Concentration Profiles. Boundary layer thickness .50 vent diameters. Vent exit velocity .10 free stream velocity.

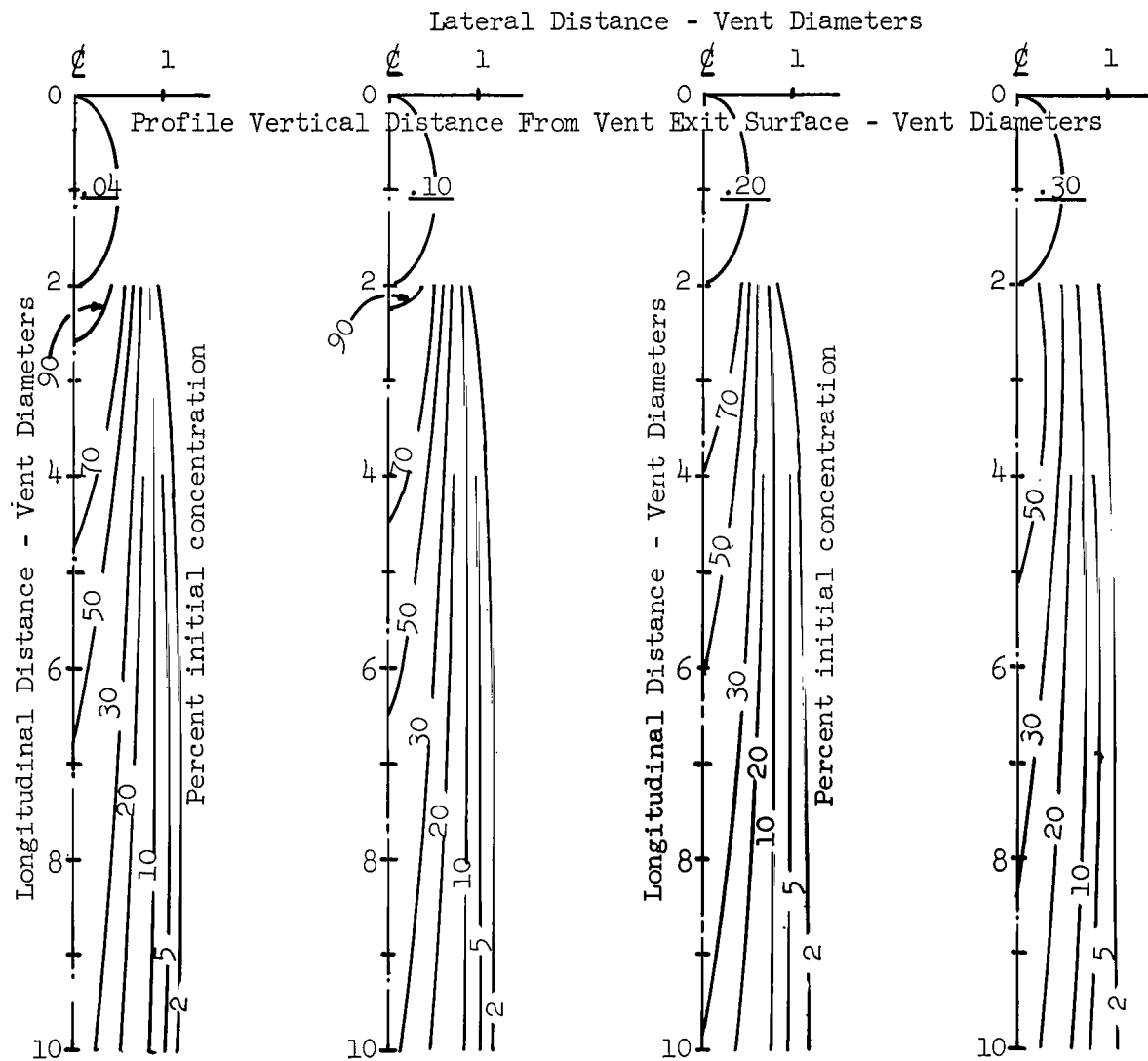


Figure 15(d). - Fuel Concentration Profiles. Boundary layer thickness .50 vent diameters. Vent exit velocity 0.30 free stream velocity.

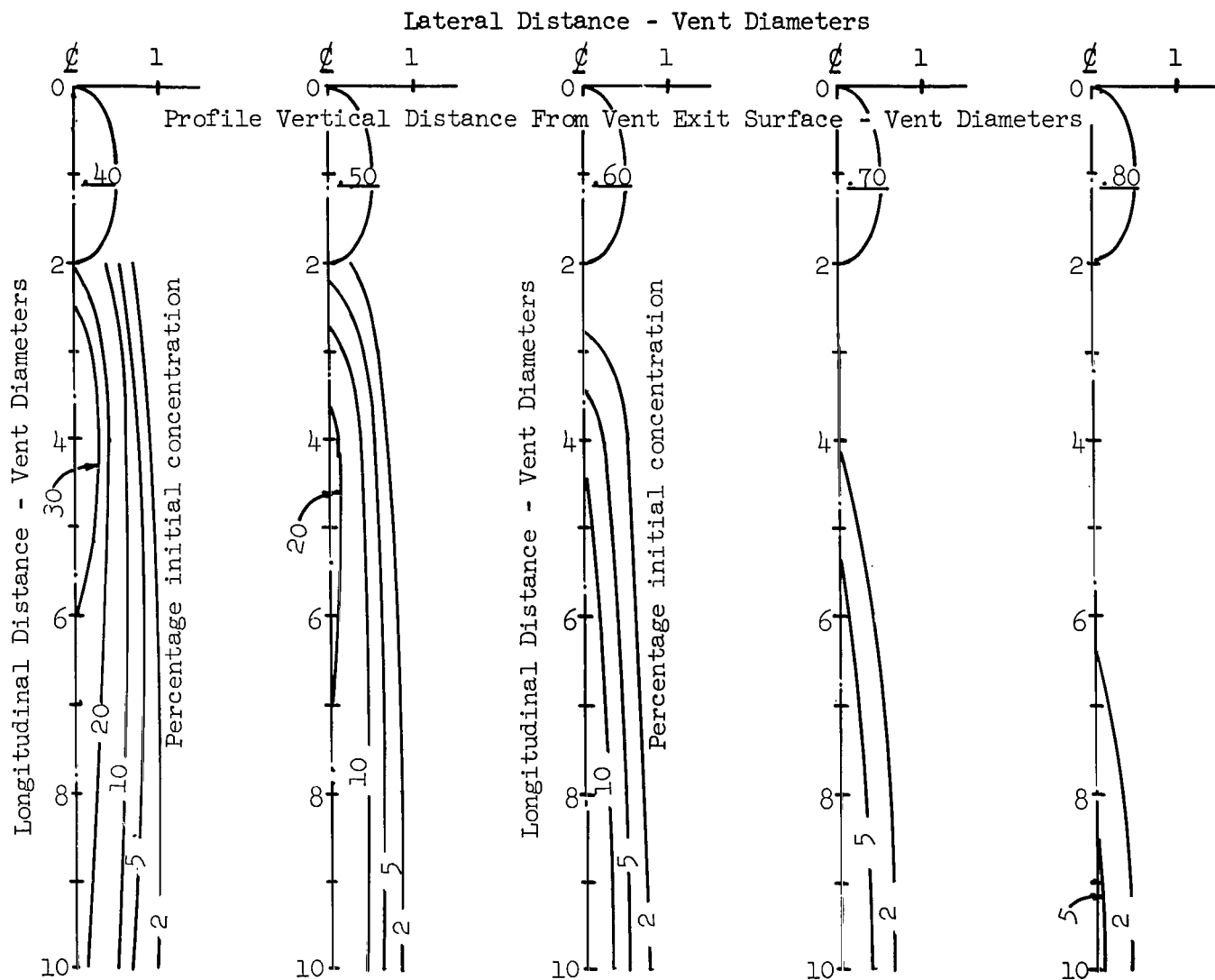


Figure 15(d).- Fuel Concentration Profiles. Boundary layer thickness 0.50 vent diameters. Vent exit velocity 0.30 free stream velocity.
(cont'd.)

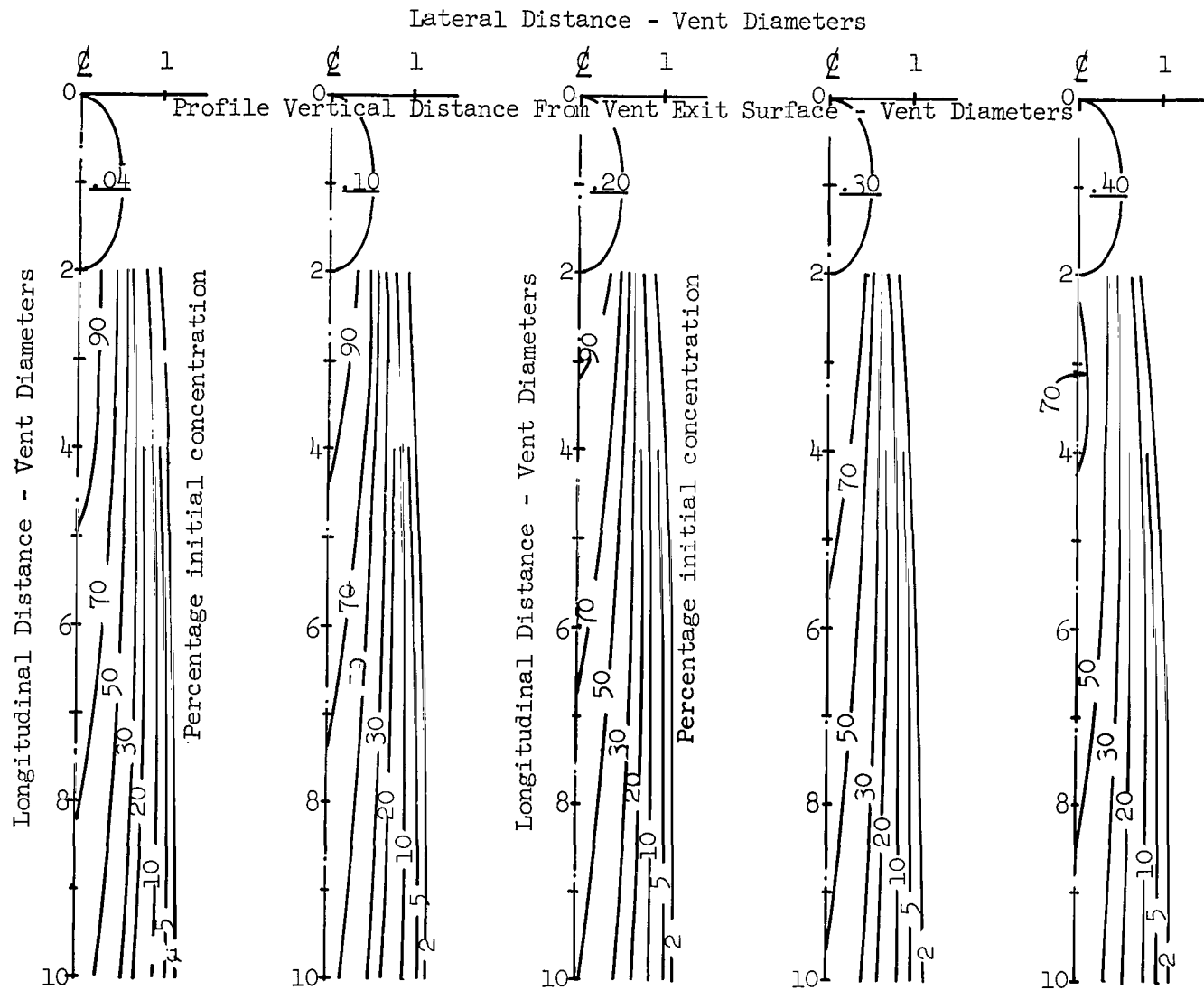


Figure 15(e).- Fuel Concentration Profiles. Boundary layer thickness .50 vent diameters. Vent exit velocity 0.50 free stream velocity.

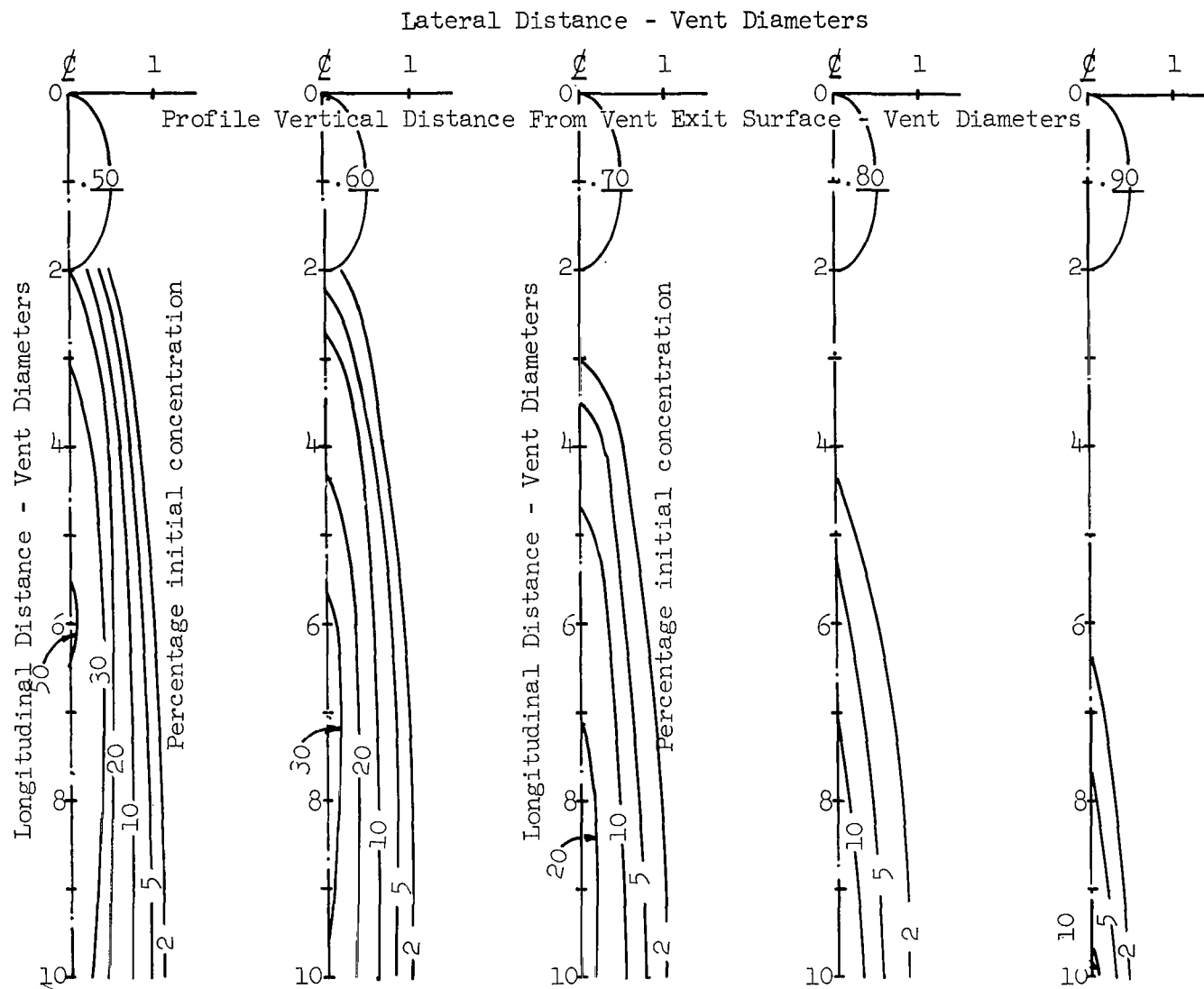


Figure 15(e).- Fuel Concentration Profiles. Boundary layer thickness 0.50 vent diameters. Vent exit velocity 0.50 free stream velocity.
(cont'd.)

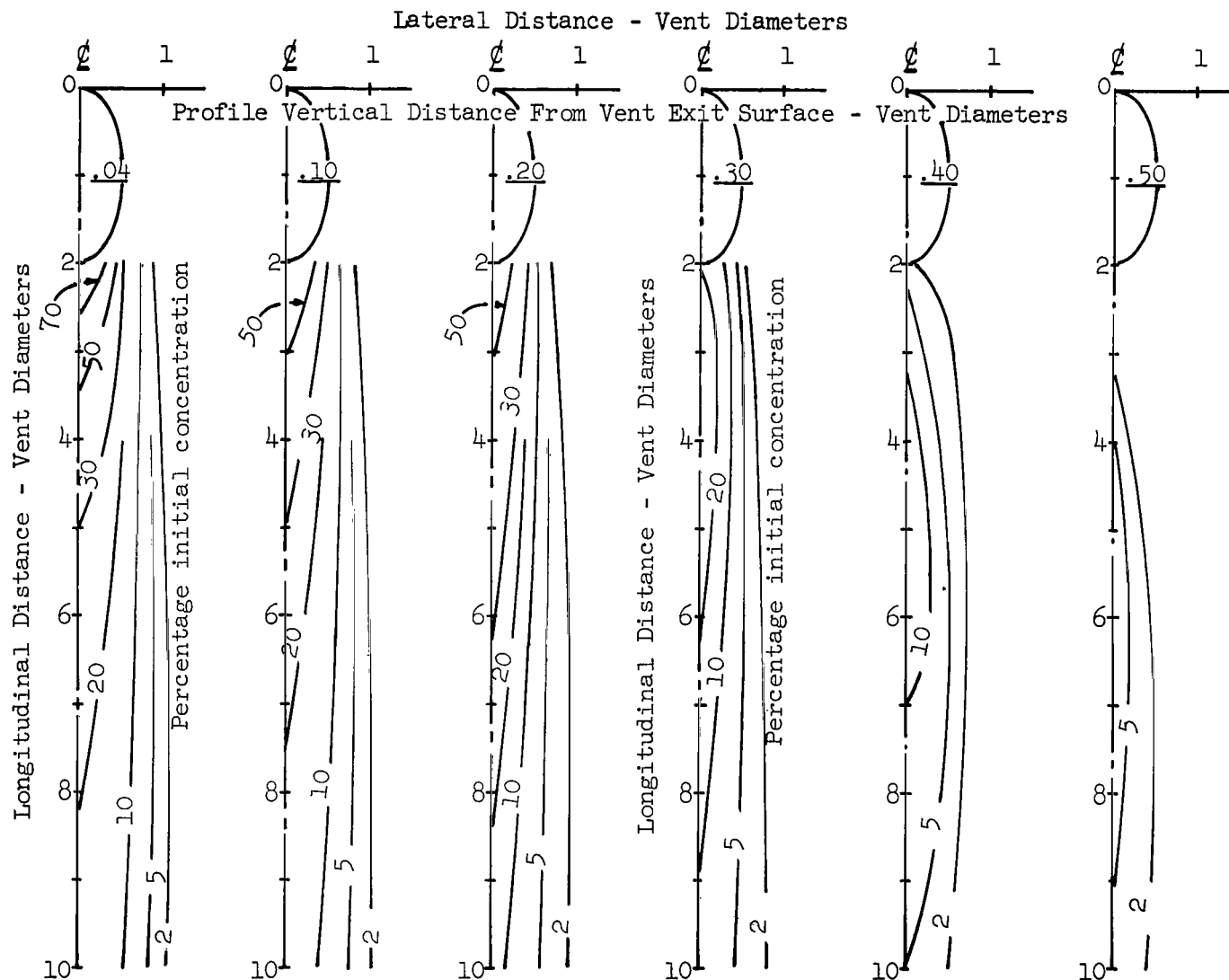


Figure 15(f).- Fuel Concentration Profiles. Boundary layer thickness 1.6 vent diameters. Vent exit velocity 0.10 free stream velocity.

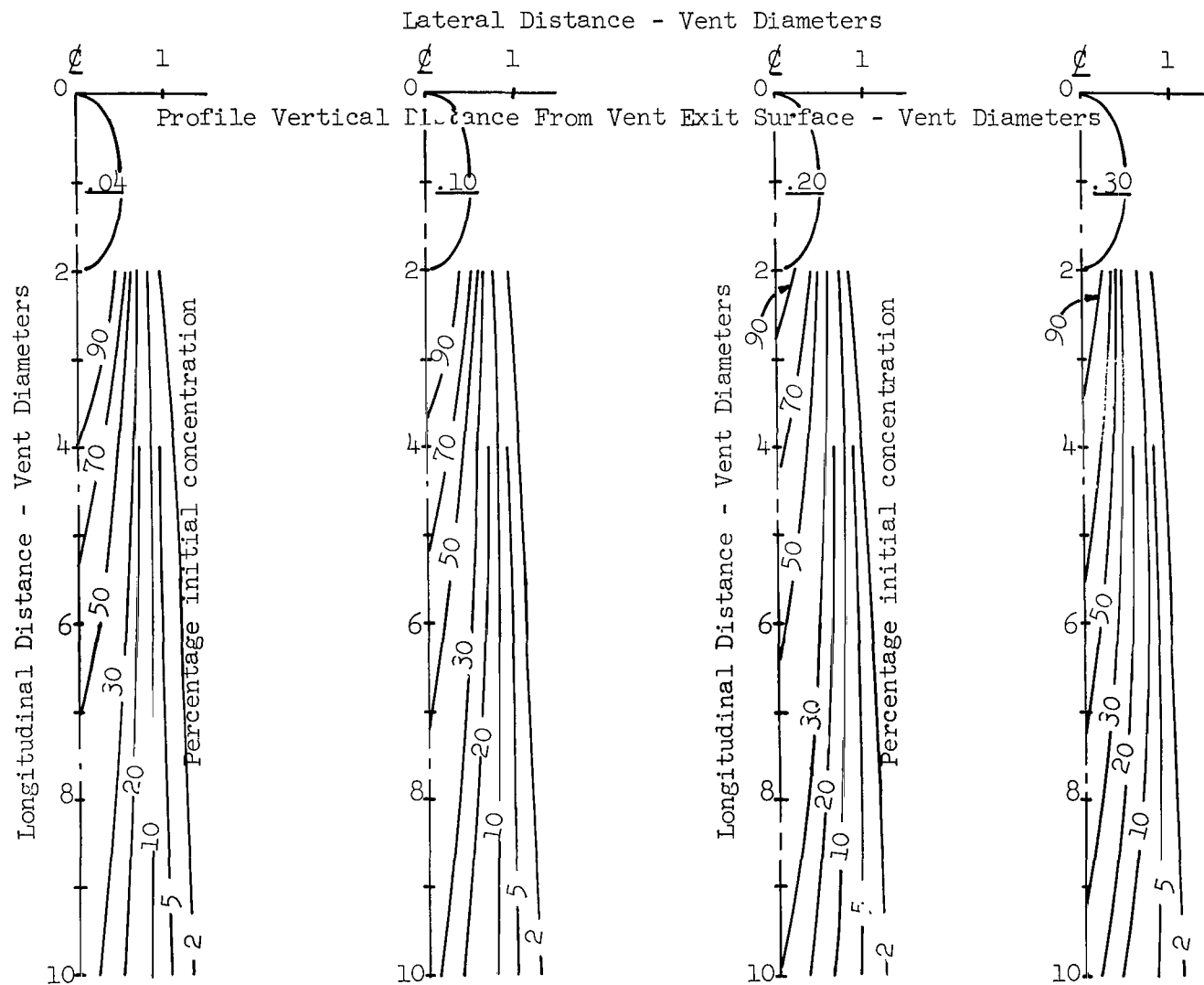


Figure 15(g).- Fuel Concentration Profiles. Boundary layer thickness 1.6 vent diameters. Vent exit velocity 0.30 free stream velocity.

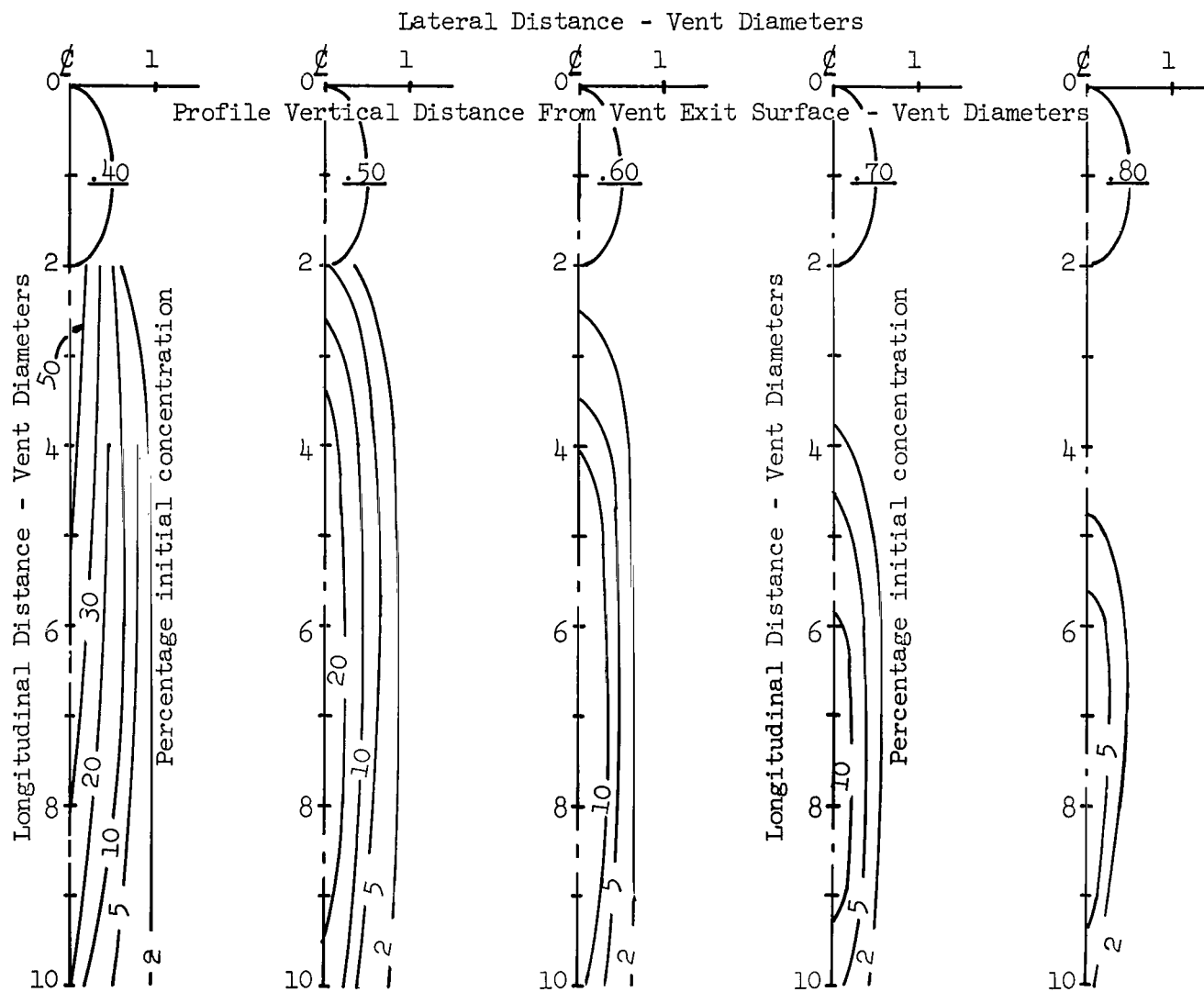


Figure 15(g).- Fuel Concentration Profiles. Boundary layer thickness 1.6 vent diameters. Vent exit velocity 0.30 free stream velocity.

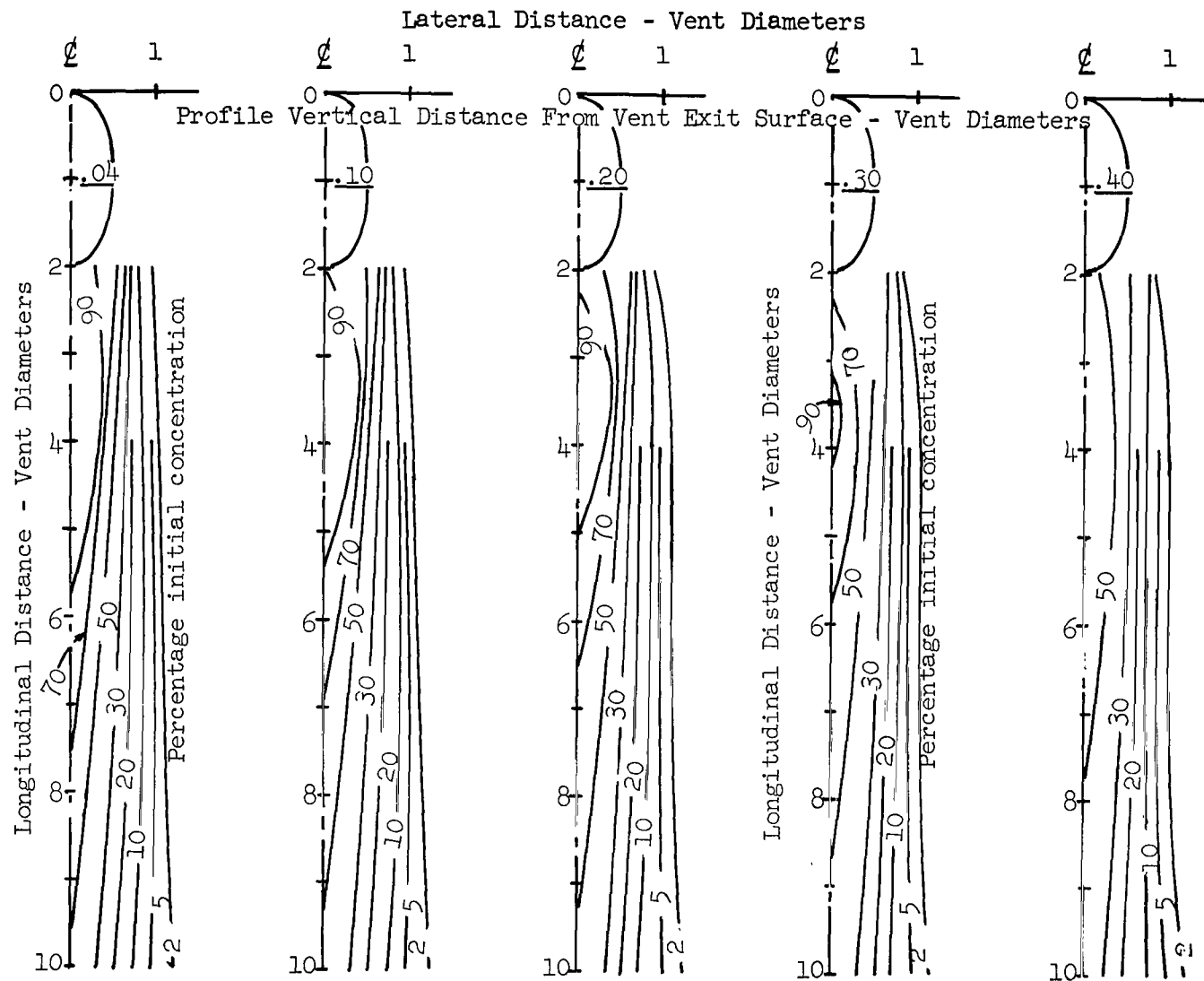


Figure 15(h).- Fuel Concentration Profiles. Boundary layer thickness 1.6 vent diameters. Vent exit velocity 0.50 free stream velocity.

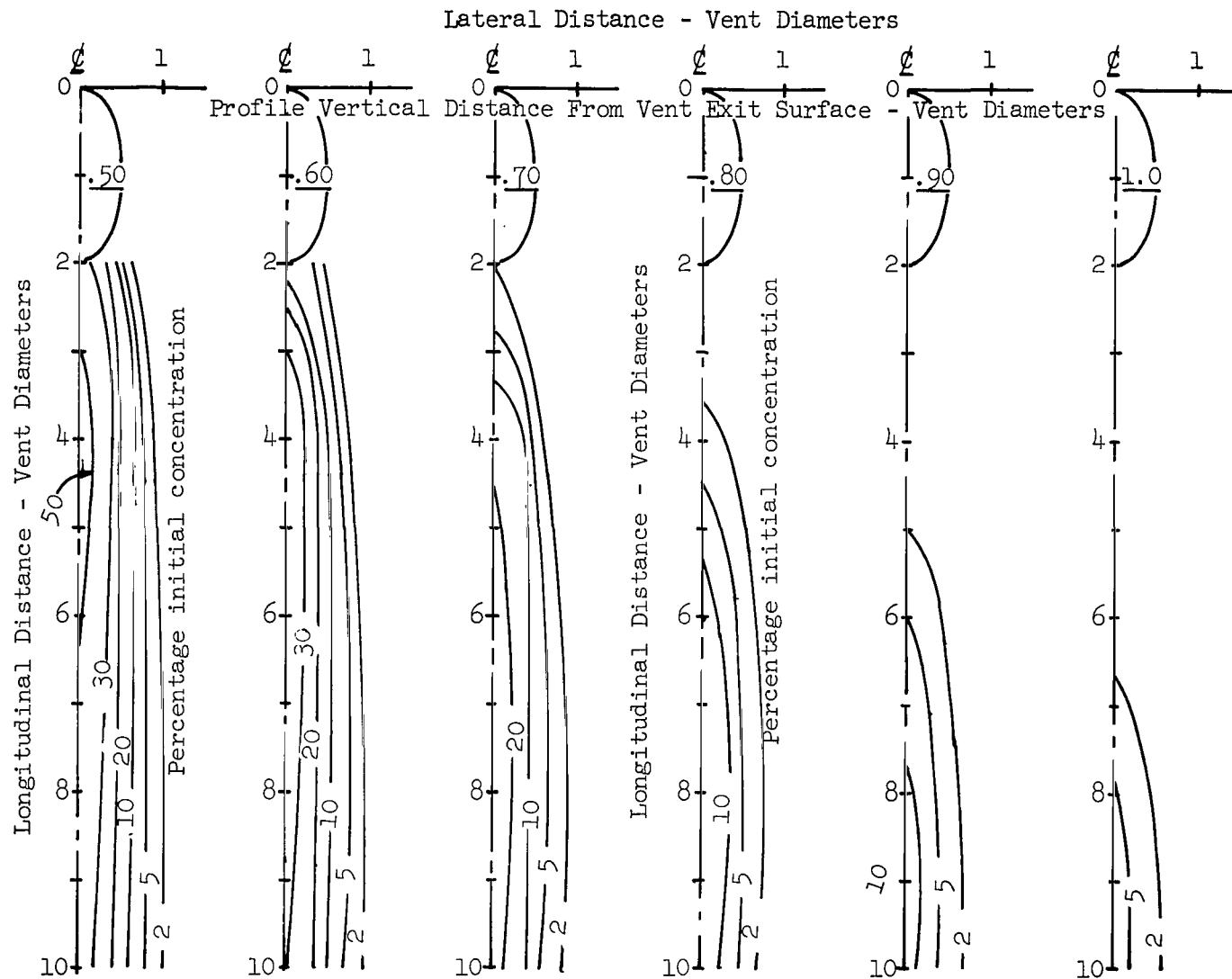


Figure 15(h).- Fuel Concentration Profiles. Boundary layer thickness 1.6 vent diameters. Vent exit velocity 0.50 free stream velocity.

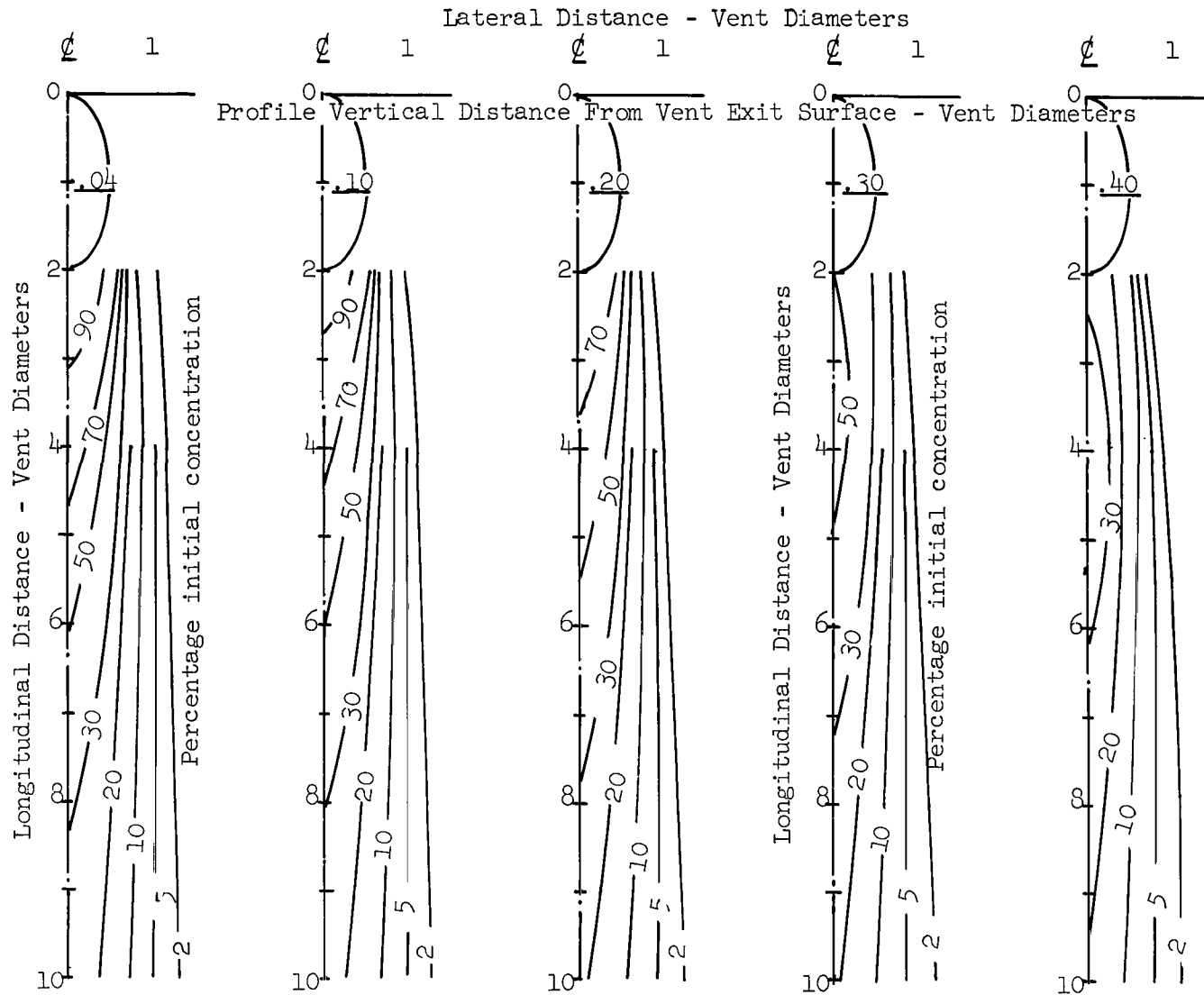


Figure 15(i).- Fuel Concentration Profiles. Boundary layer thickness 2.4 vent diameters. Vent exit velocity 0.30 free stream velocity.

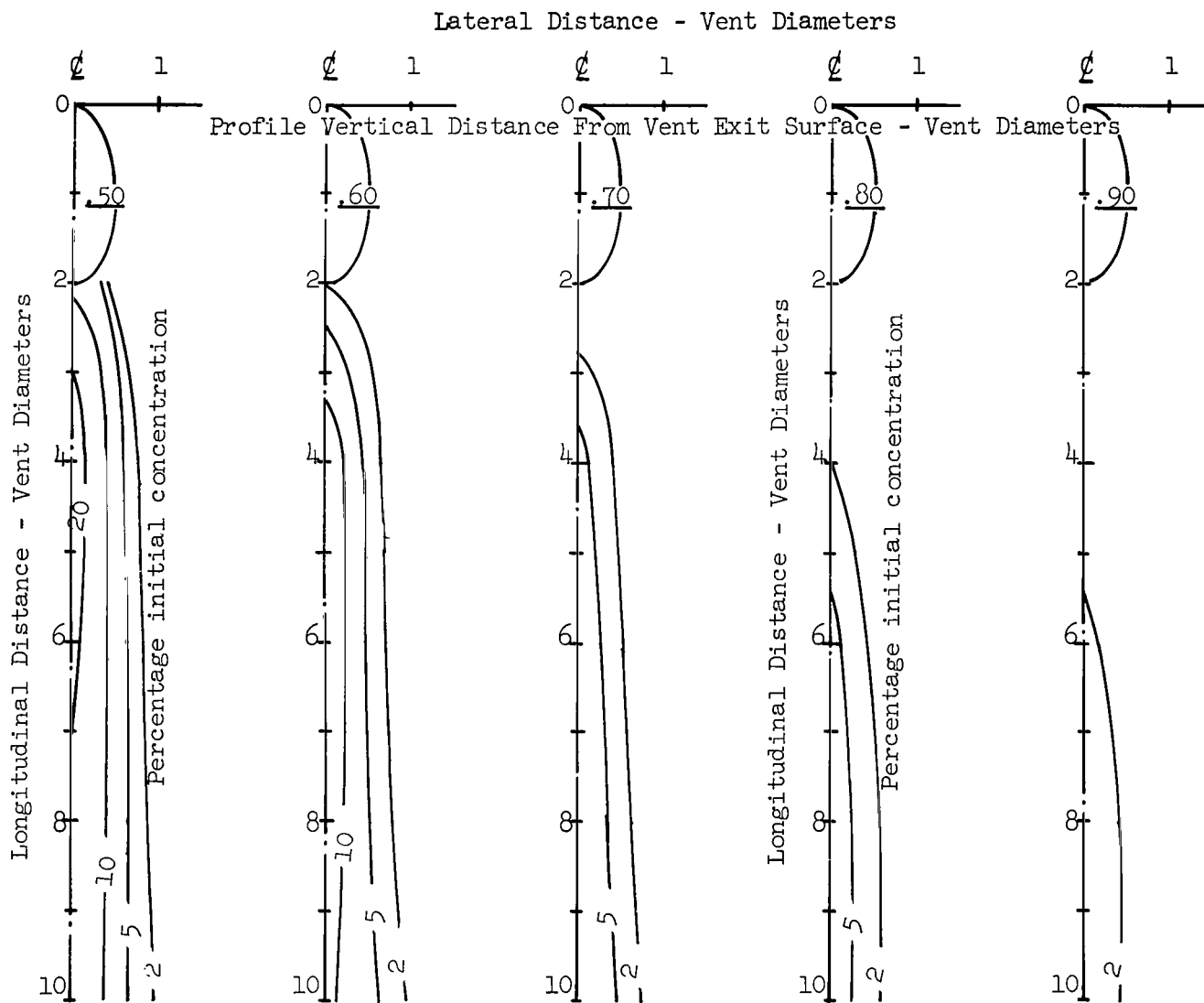


Figure 15(i).- Fuel Concentration Profiles. Boundary layer thickness 2.4 vent diameters. Vent exit velocity 0.30 free stream velocity.

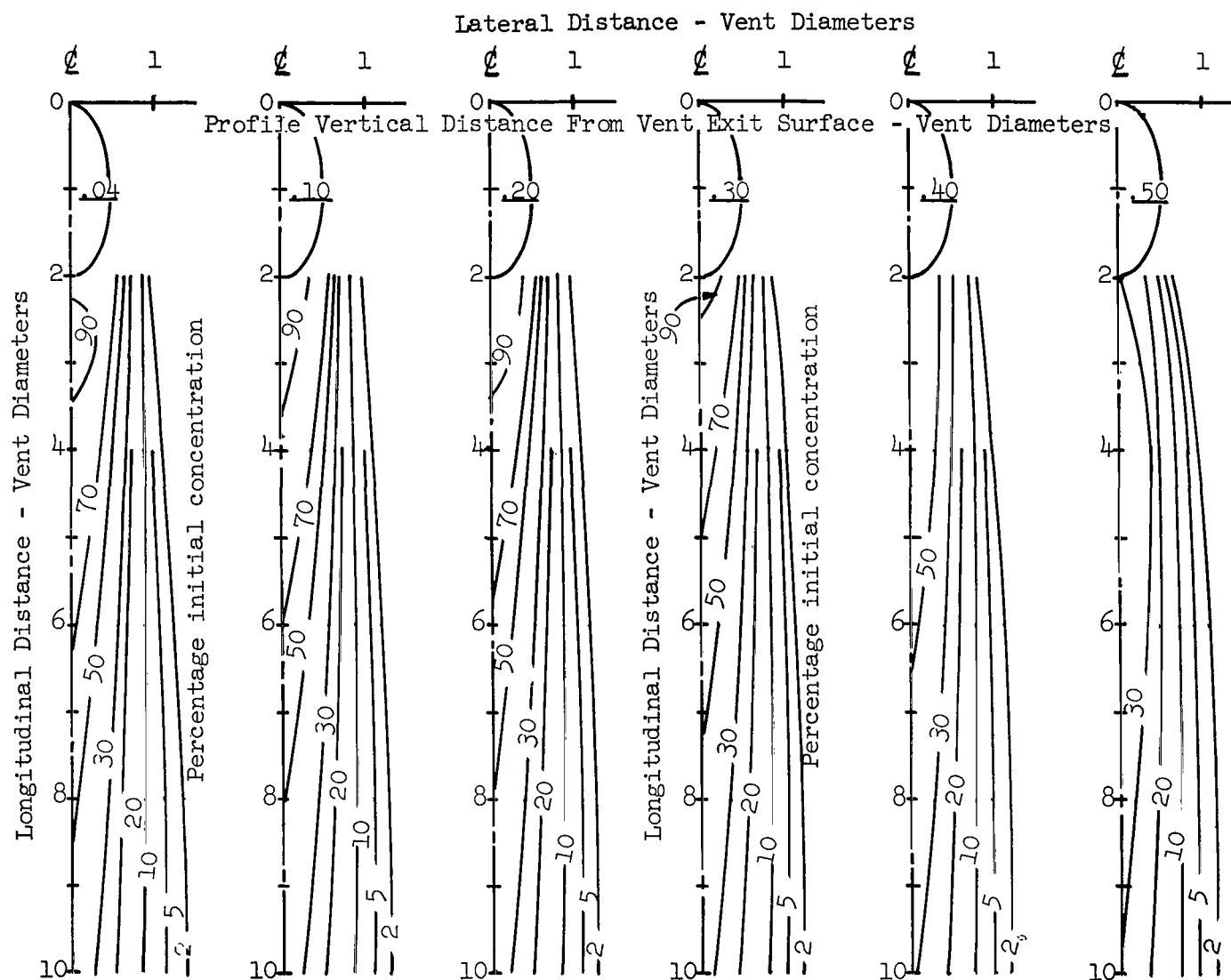


Figure 15(j).- Fuel Concentration Profiles. Boundary layer thickness 2.4 vent diameters. Vent exit velocity 0.50 free stream velocity.

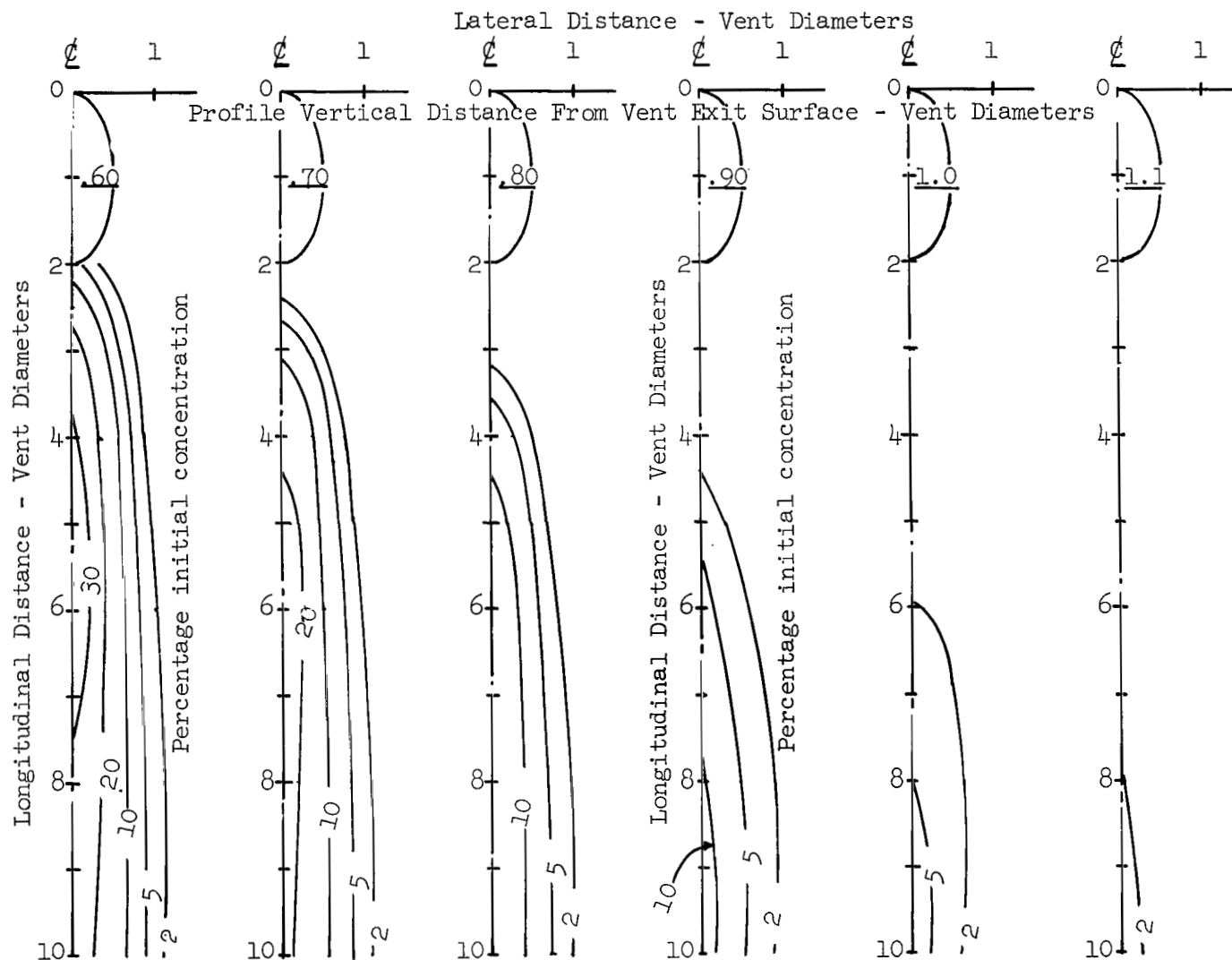


Figure 15(j).- Fuel Concentration Profiles. Boundary layer thickness 2.4 vent diameters. Vent exit velocity 0.50 free stream velocity.
(cont'd.)

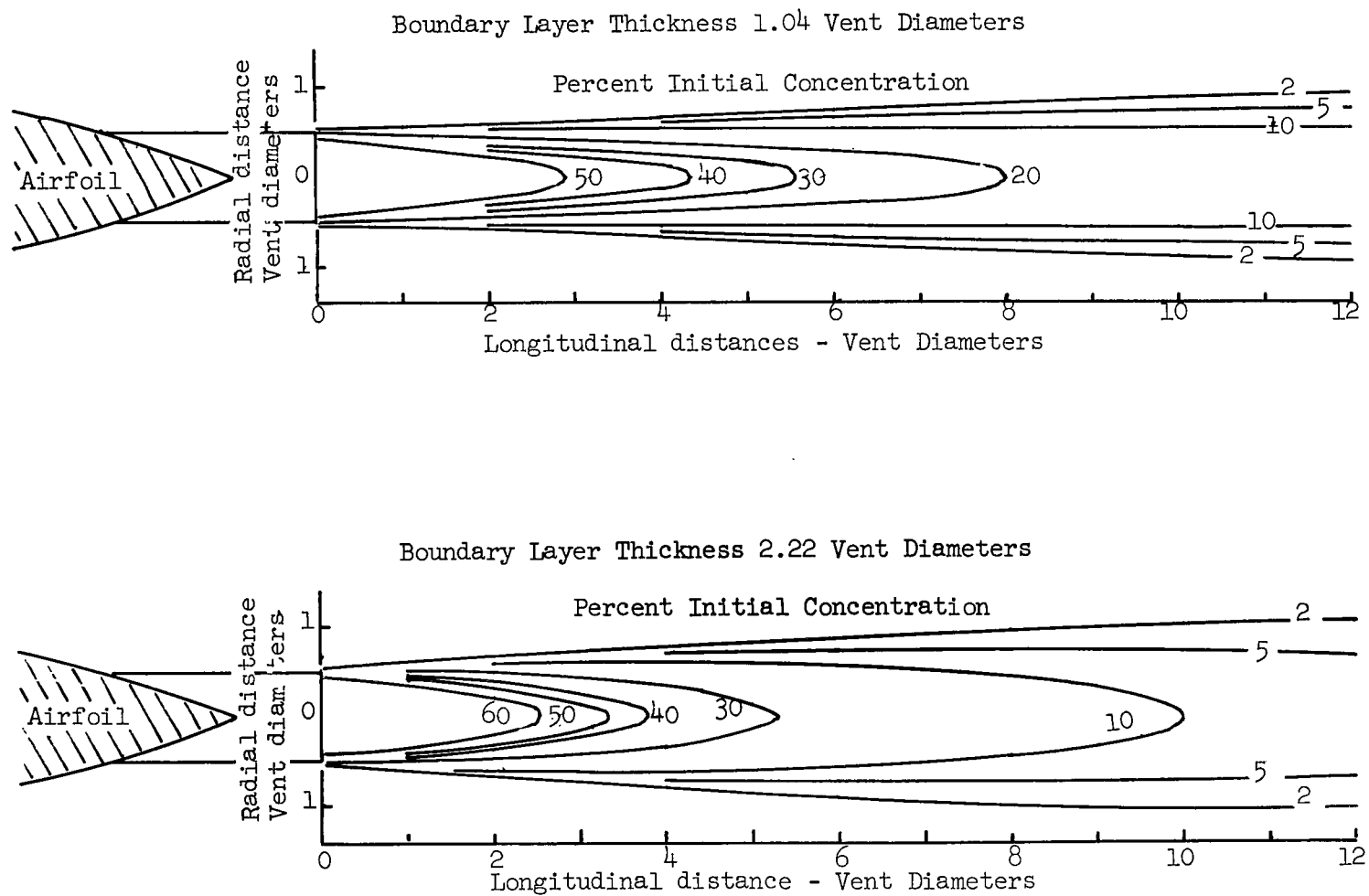


Figure 16. - Wake Vent Exit - Vent discharging into airfoil wake. Vent exit velocity 0.30 free stream velocity.

NOTE:

1. Internal Crossectional Area
Corresponds to a 1.00 x .035 Tube.
2. Profile Map Data Taken at Its
Maximum Dimensions.

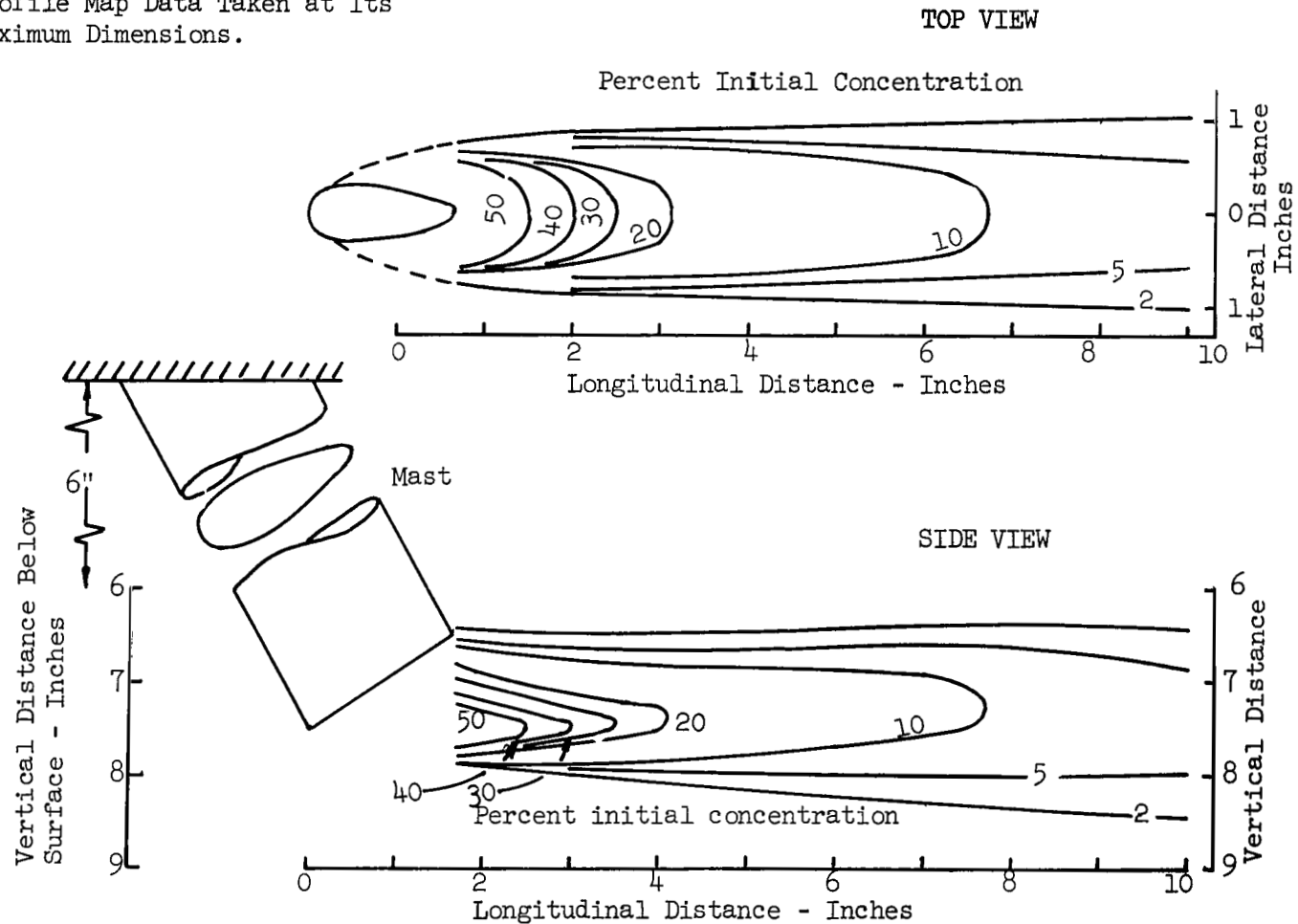


Figure 17. - Extended Vent Exit Mast Discharging Into Free Stream Airflow.
Vent Exit Velocity 0.30 Free Stream Velocity.

NOTE:

1. Internal Crossectional Area
Corresponds to a 1.00 x .035 Tube.
2. Profile Map Data Taken at Its
Maximum Dimensions.

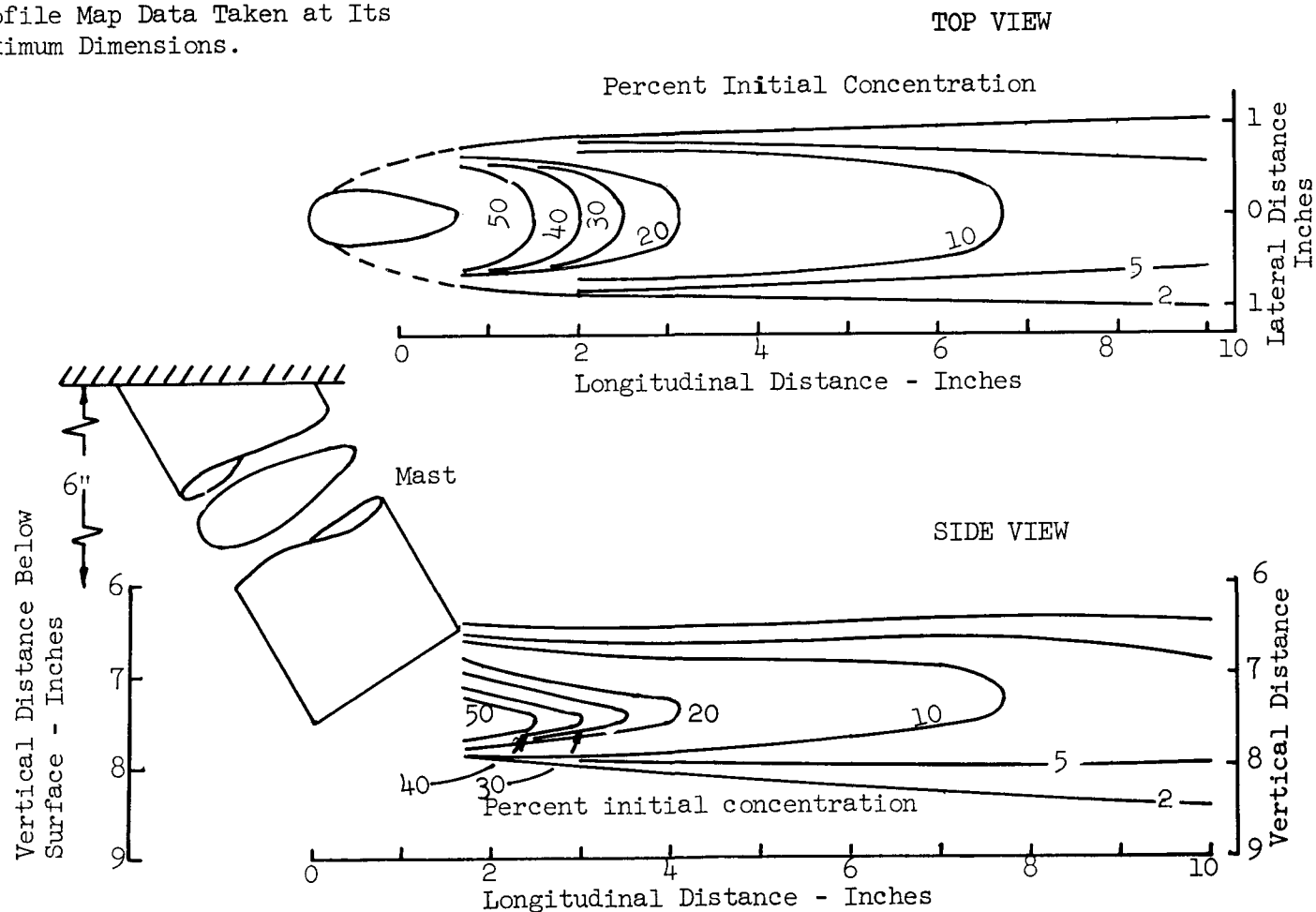


Figure 17. - Extended Vent Exit Mast Discharging Into Free Stream Airflow.
Vent Exit Velocity 0.30 Free Stream Velocity.

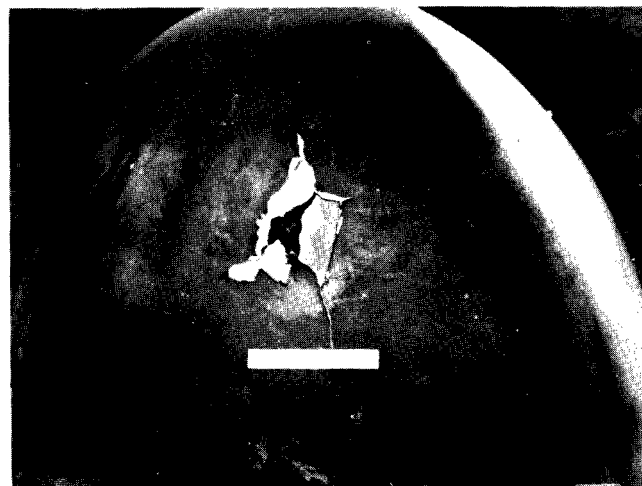
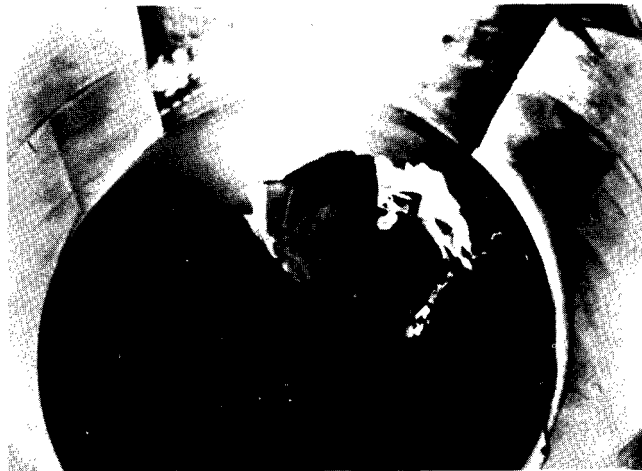


Figure 18. Comparison of natural lightning damage (above) and laboratory lightning damage (below) to same type of unprotected radome permits estimates of potential rate of rise and energy of natural lightning discharge.

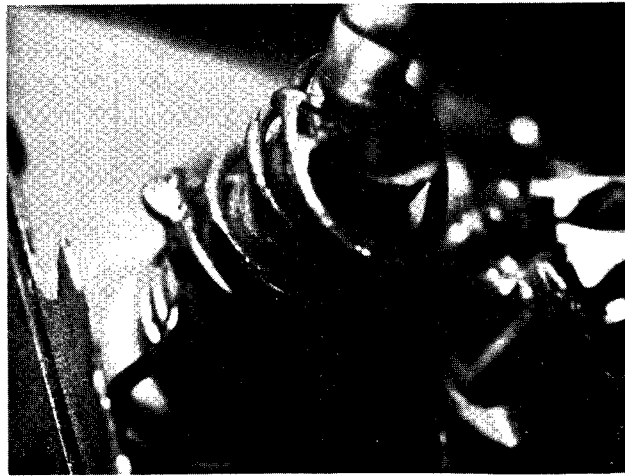


Figure 19. Damaged VHF transmitter coil illustrates magnetic forces and heating of high energy natural lightning current components.



Figure 20. Separation of vertical fin illustrates high blast pressures produced by lightning discharge arcs which entered through inadequate antenna lead-in.

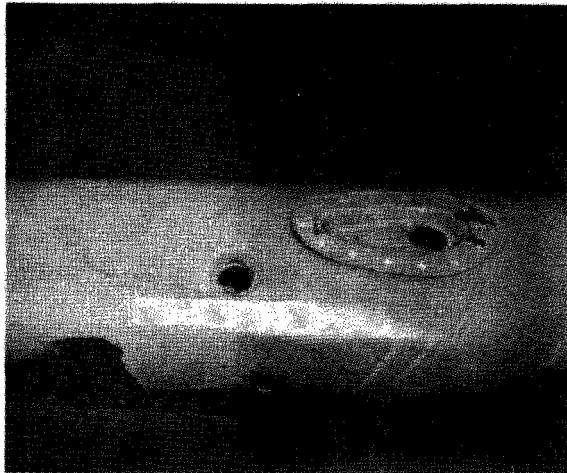
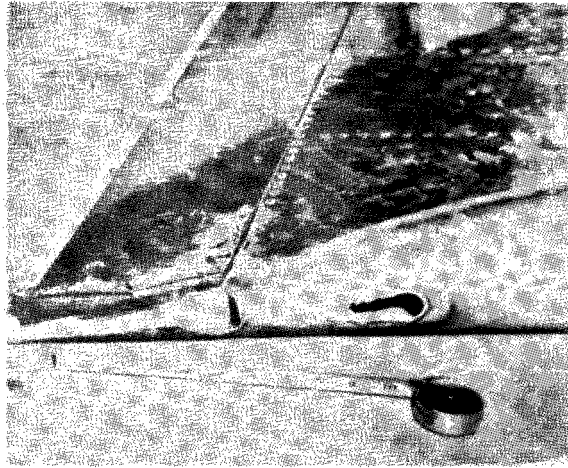


Figure 21. Natural lightning discharge to jet transport wingtip produces larger hole than 300 coulomb discharge in laboratory (lower photograph).

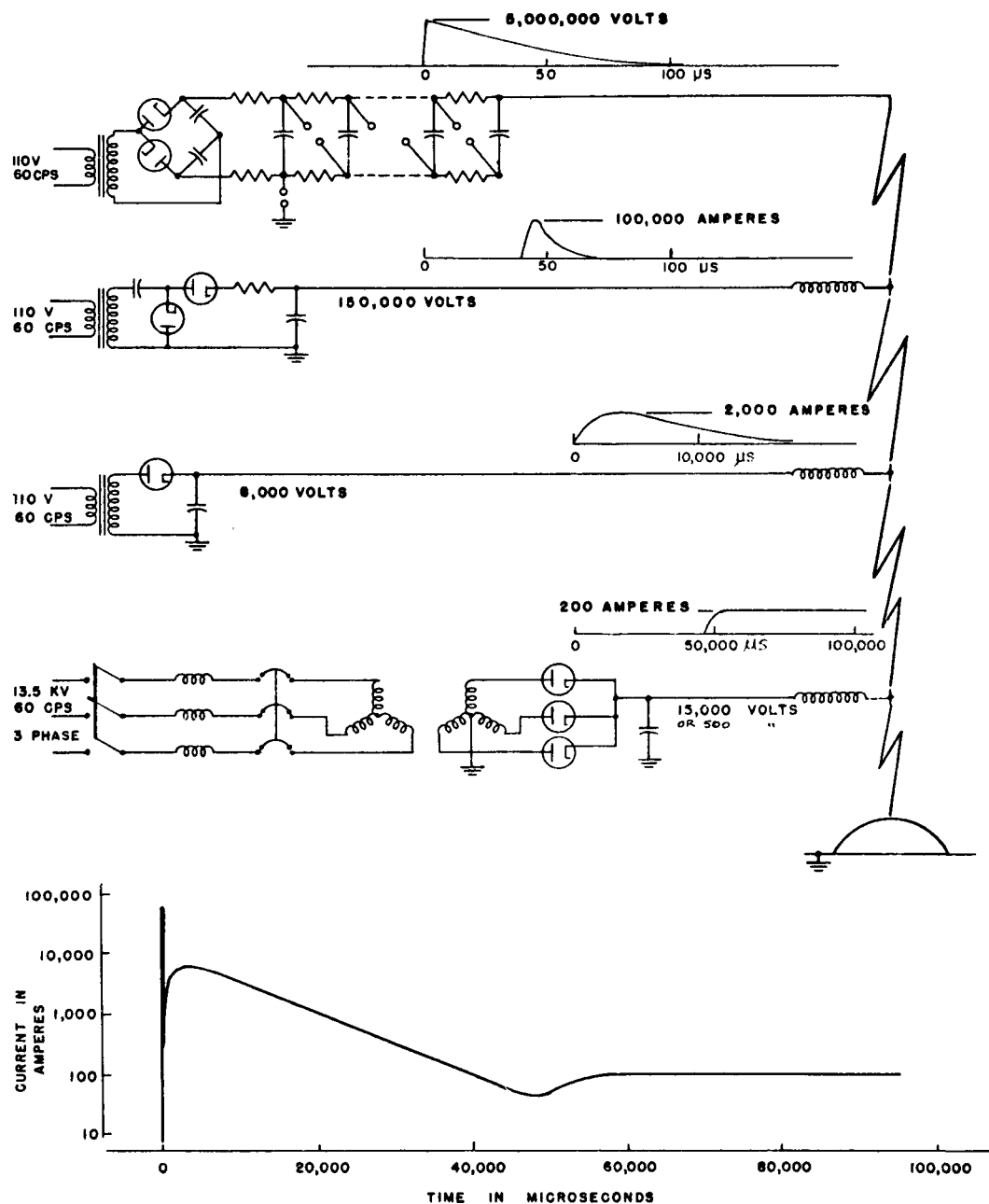


Figure 22. Diagram of multiple generators which produce typical effects of natural lightning strokes, individually or as a composite single discharge. The combined output current waveform is shown below.

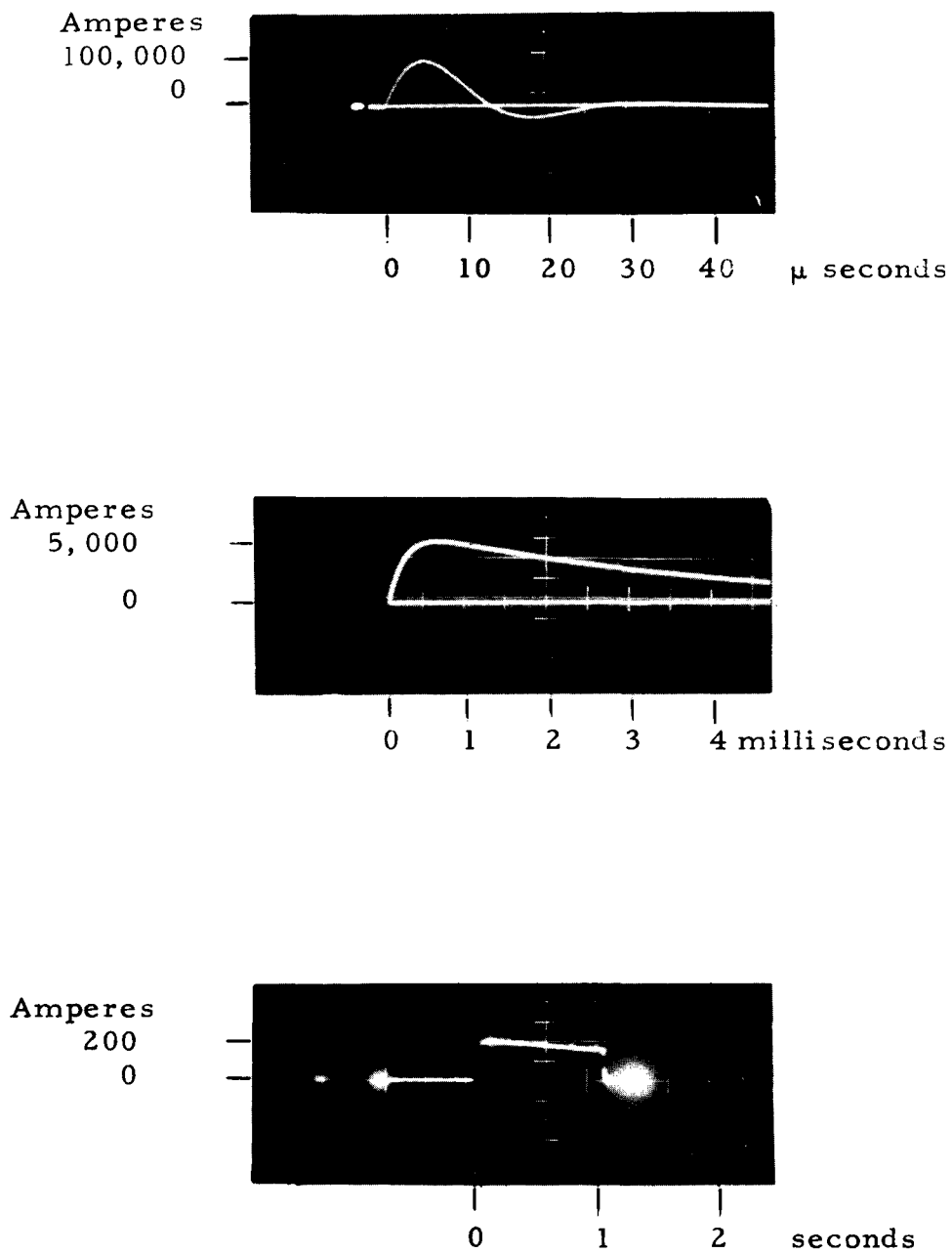


Figure 23. Oscillograms of separate current components of combined discharge for damage testing.

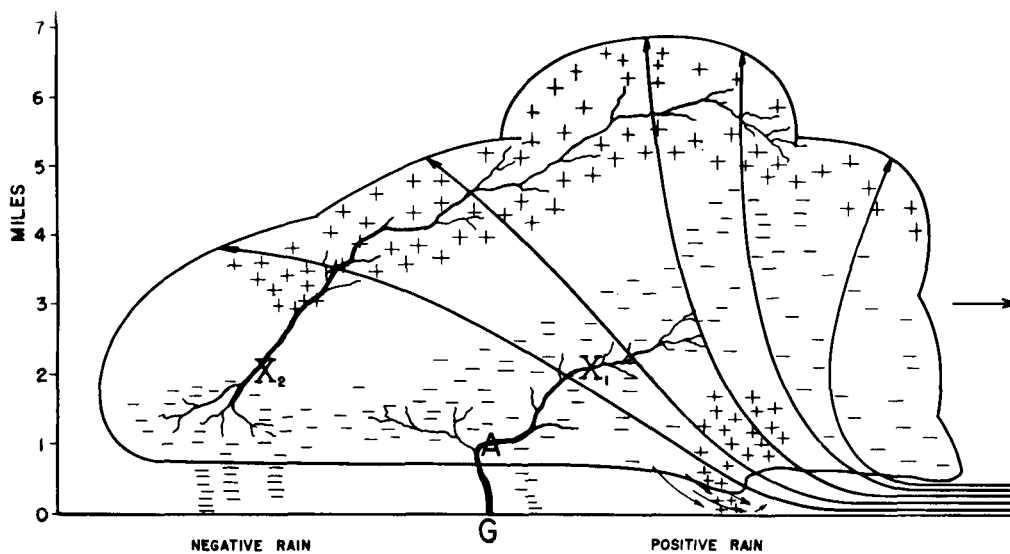


Figure 24(a). Meteorological and electrical conditions within a thundercloud, based on electric gradient measurements by Simpson and Scrase with free balloons.

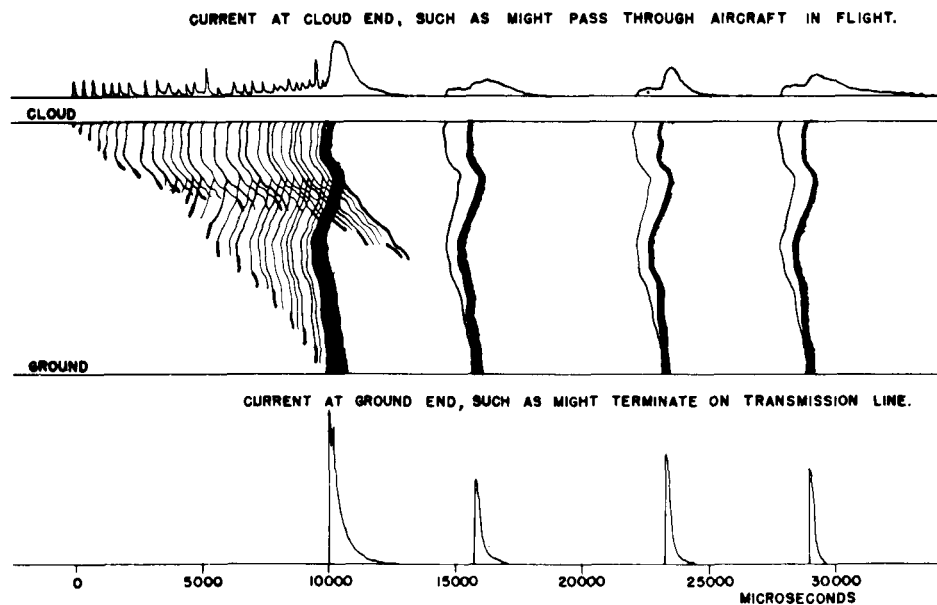


Figure 24(b). Current-time curves for the ground and cloud ends of the discharge channel, based on photographs of "successive" lightning recorded by Schonland.

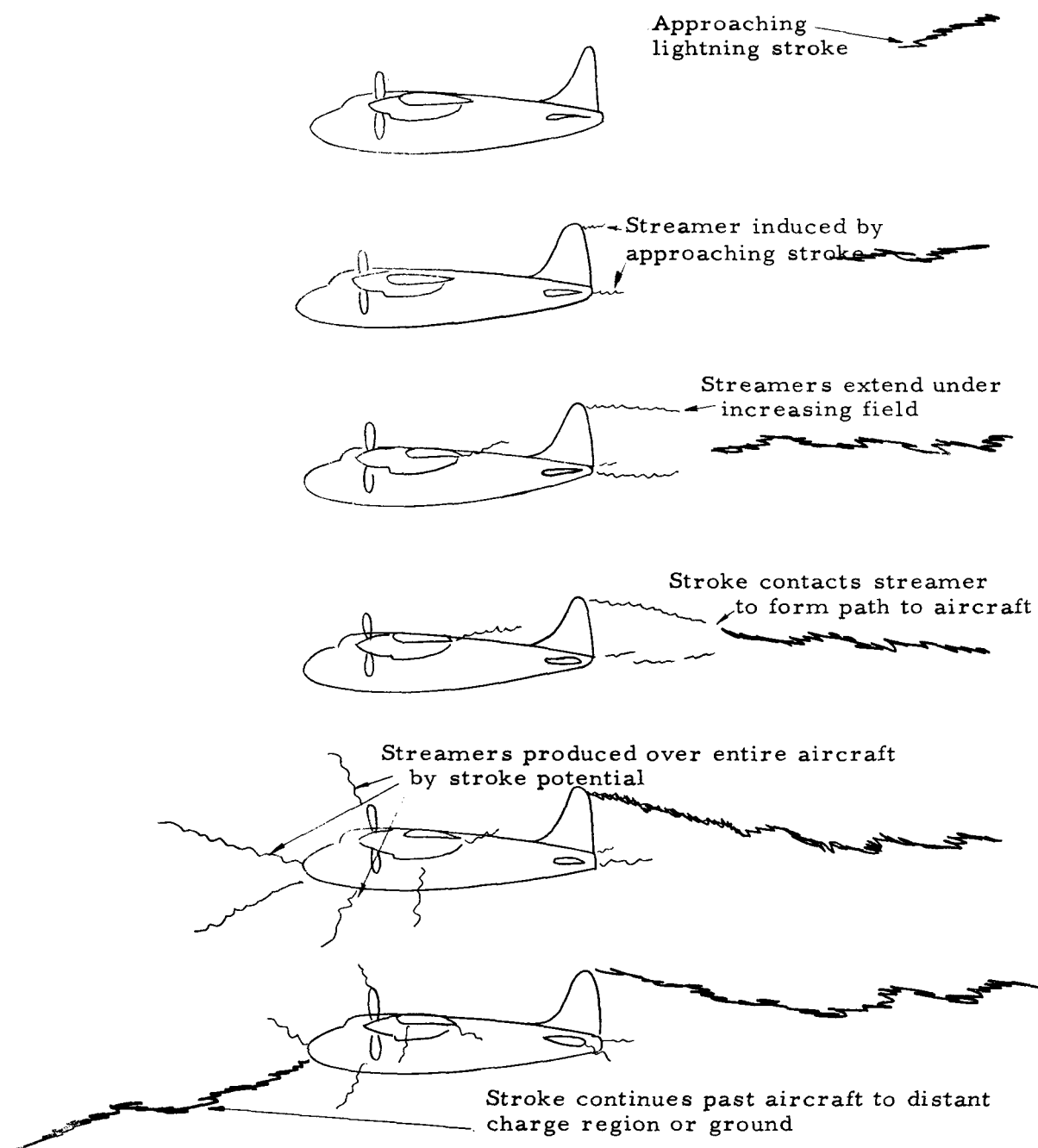


Figure 24(c). Mechanism of lightning stroke approach to aircraft illustrating streamer formation at high gradient points or extremities of aircraft.



Figure 25. Induced streamers off aircraft extremities illustrated by high impulse potential applied to model aircraft.

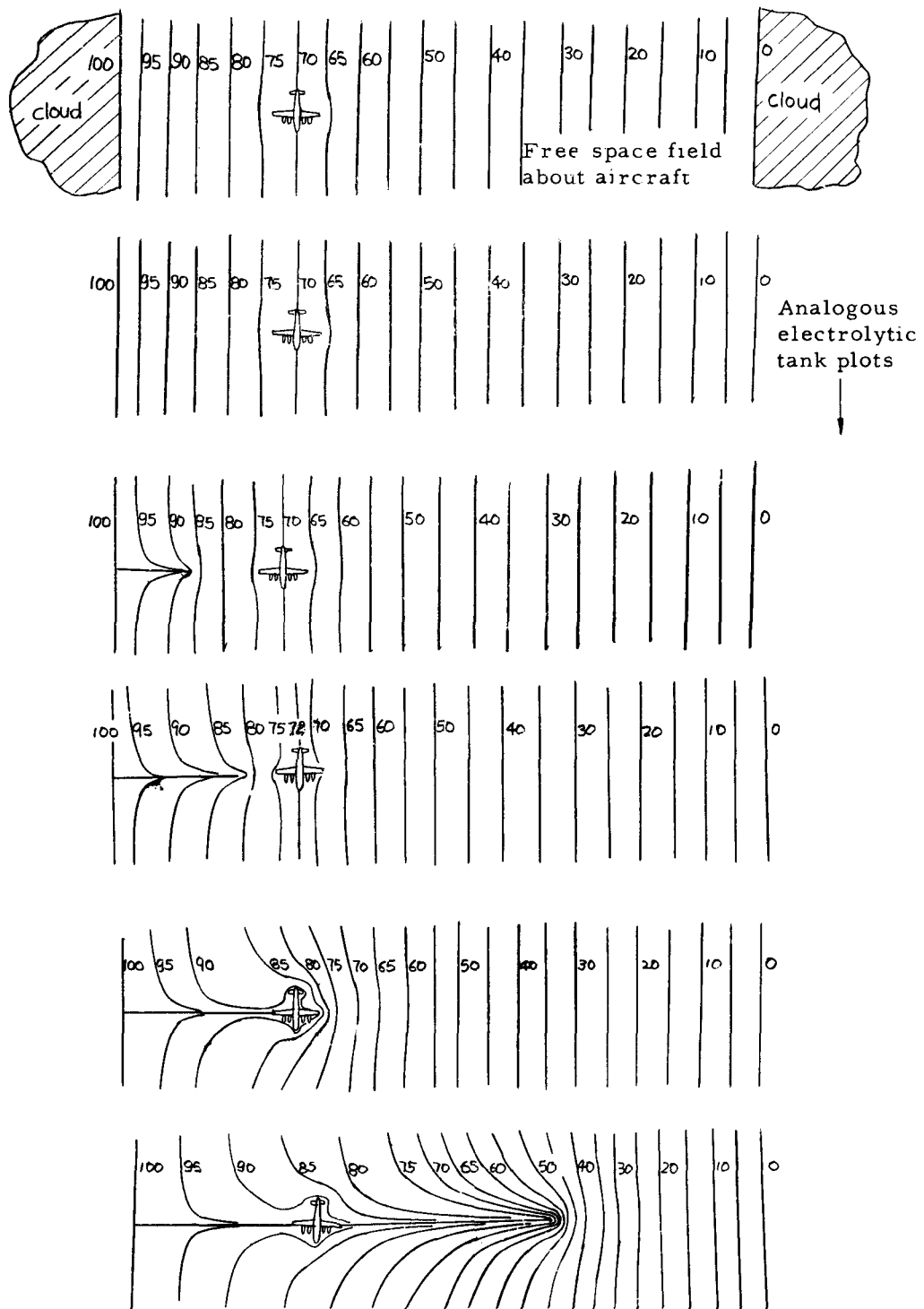


Figure 26. Gradients of different stages of lightning discharge through aircraft.

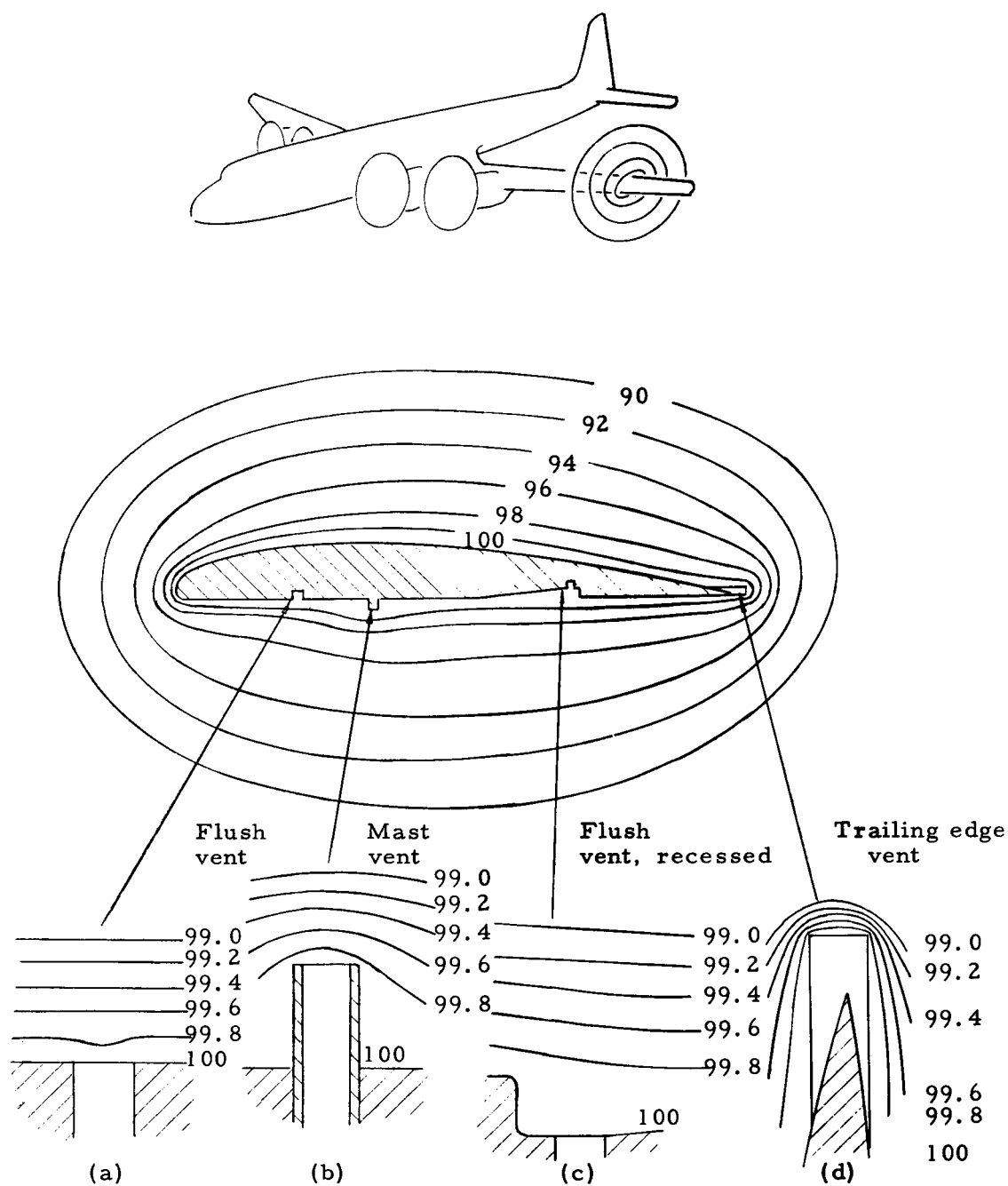
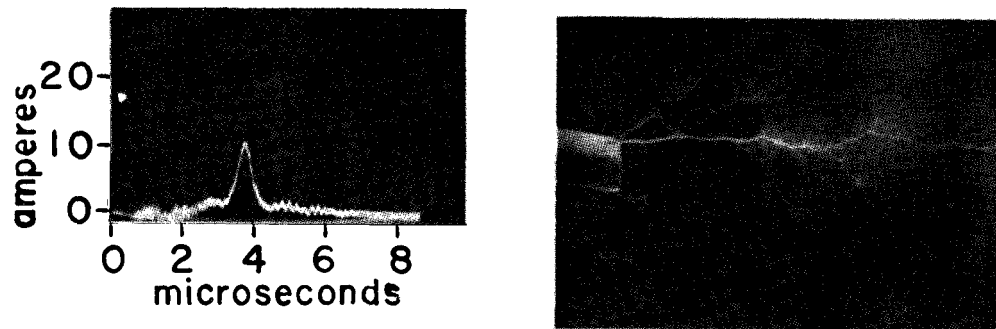


Figure 27. Electric field plots about several vent types. Closest line spacing near vent edge indicates maximum electrical gradient or lowest streamer discharge threshold for a given aircraft potential.



Current waveform and photograph of single streamer

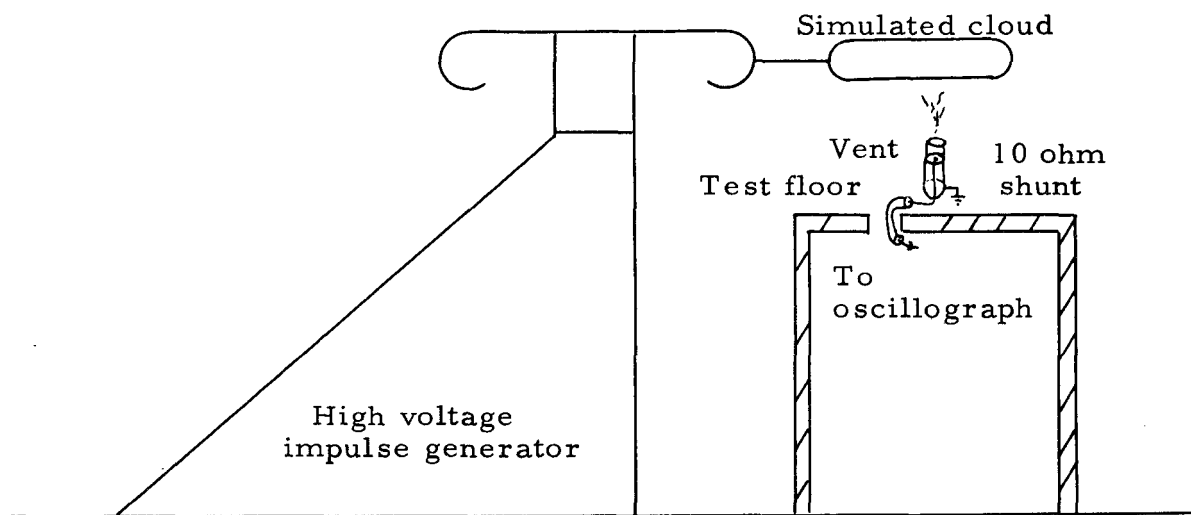


Figure 28 . Test arrangement for simulated vent tube streamer measurements.

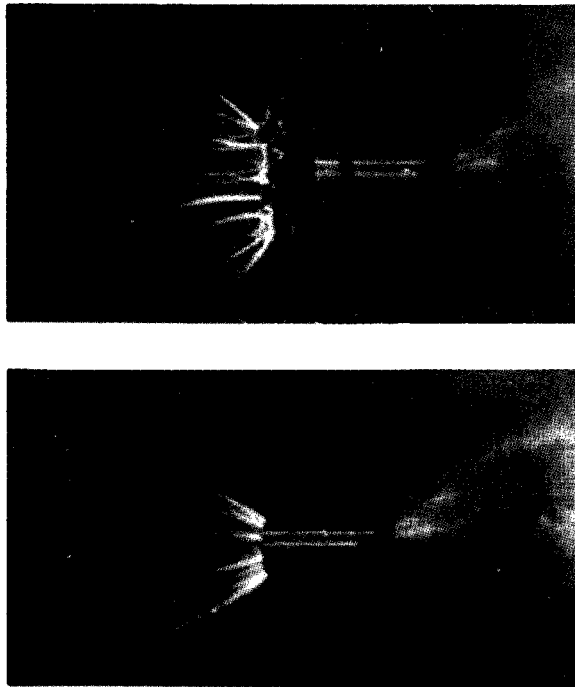


Figure 30(a). Comparison of streamering on metal vent tube with and without gradient ring.

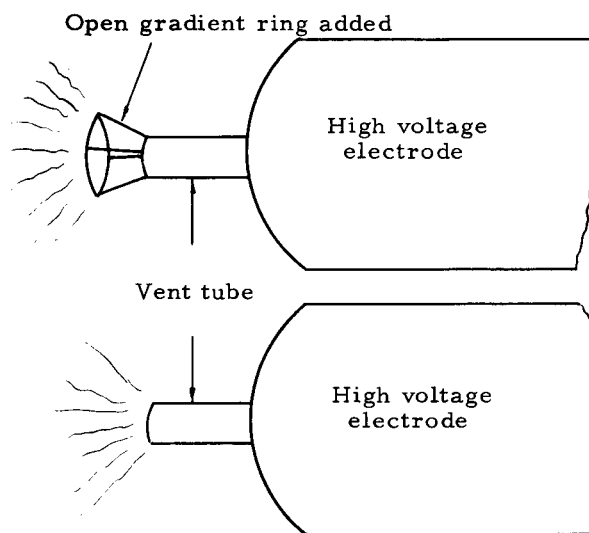


Figure 30(b). Illustration of the use of a gradient shielding ring for removing streamering from immediate vicinity of vent outlet.

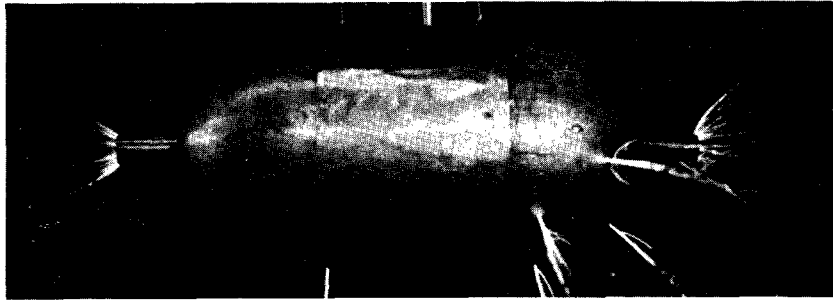


Figure 29(b). Illustration of streamering off metal vent (left) and plastic vent (right, partially obscured by streamer off front H. V. electrode).

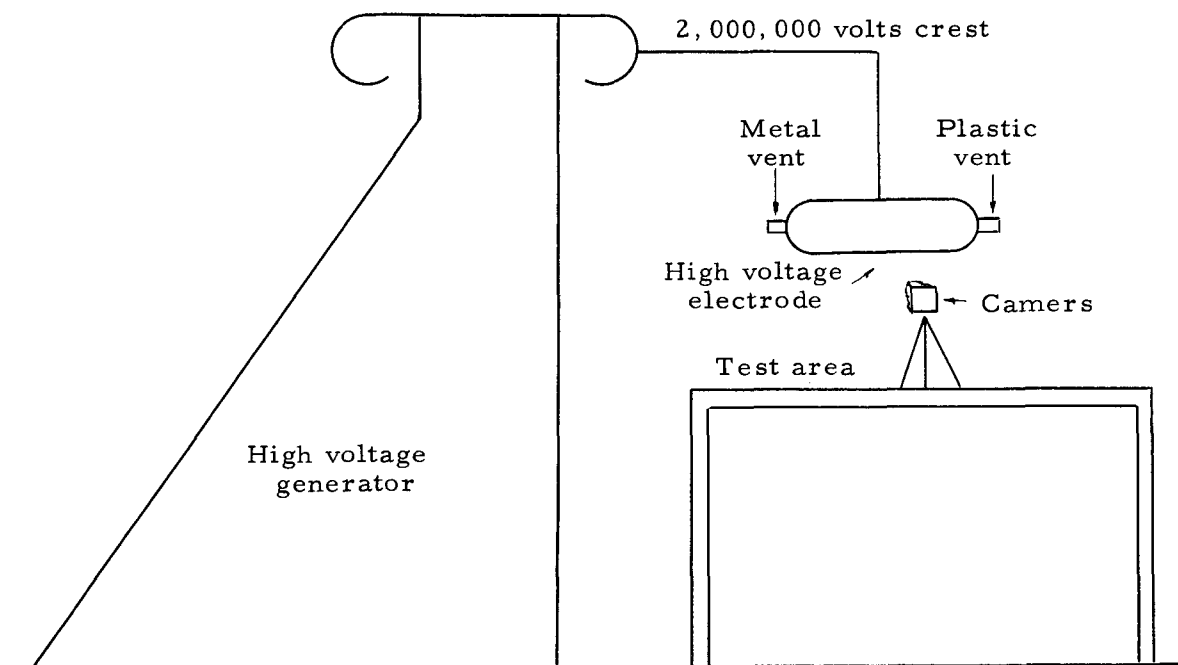


Figure 29(a). Test arrangement for photographic recording of streamer discharges off simulated metal and plastic fuel vents.

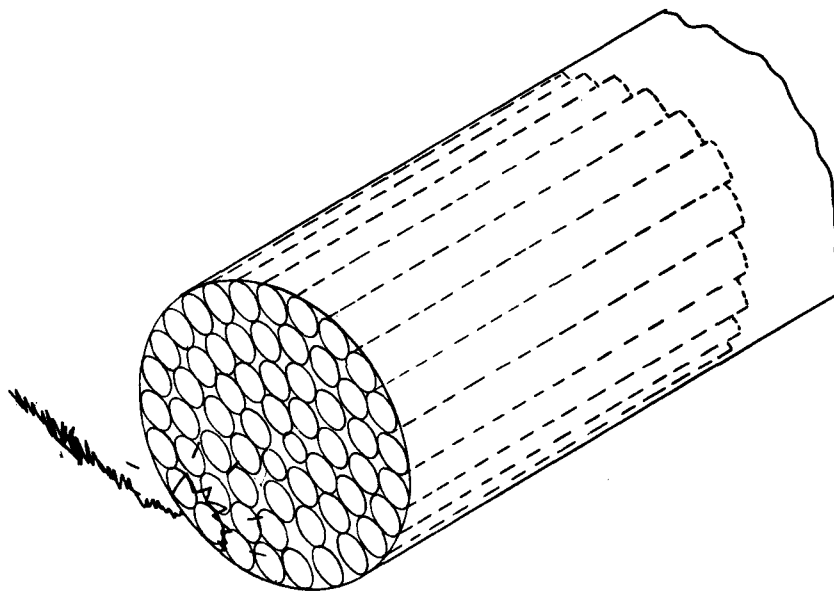


Figure 31(a). Tubular construction.

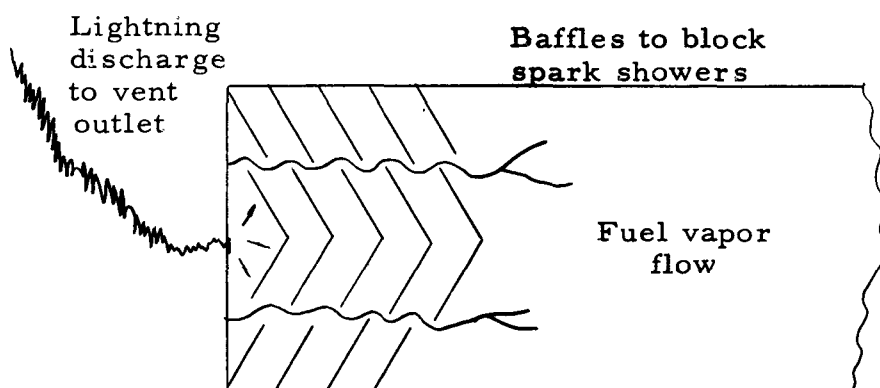


Figure 31(b). Baffle construction

Figure 31. Fuel vent outlet configurations for reducing flame propagation and spark showers.

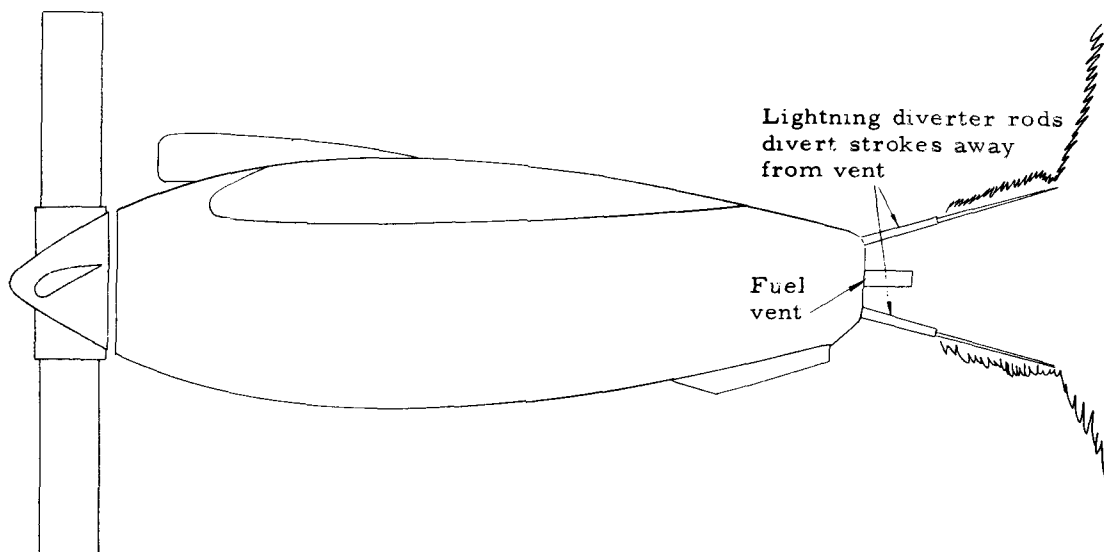


Figure 32. Illustration of diverting lightning discharges from a direct stroke to a fuel vent by application of lightning diverter rods. Diverter distances from fuel vents are still under study and should be as far as possible pending results from planned continuation of direct measurements on triggered natural lightning pressure waves.

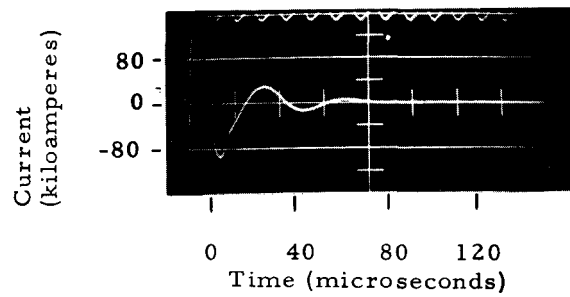


Figure 33(a). Current wave.

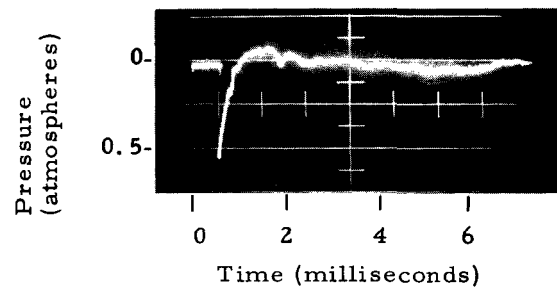


Figure 33(b). Blast pressure wave.

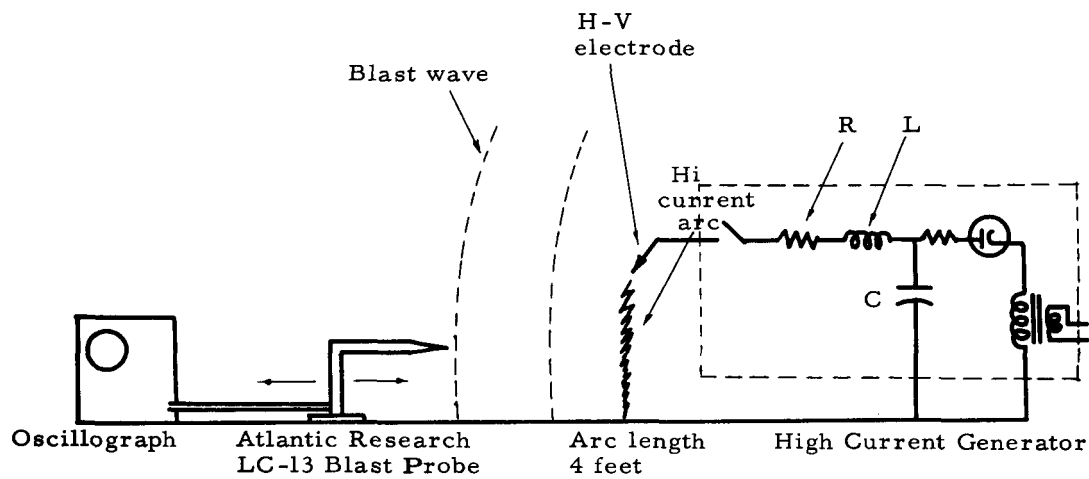
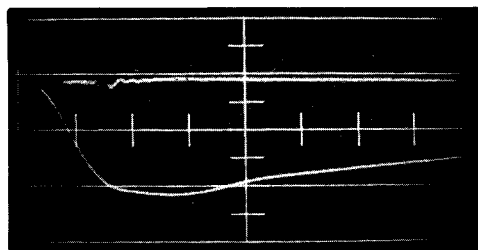
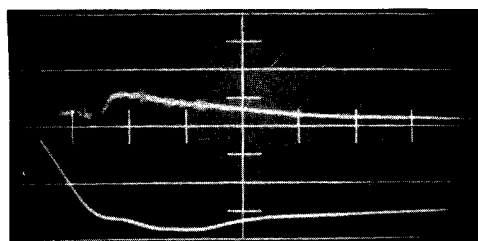


Figure 33(c). Test Arrangement.

Figure 33. Test arrangement and oscillograms of arc current and associated blast wave.



Pressure wave at 12 inches
4 psi/ division



Pressure wave at 48 inches
1 psi/ division

10 microseconds/div.

Figure 34. Blast wave front detail showing rise time of approximately 10 microseconds.

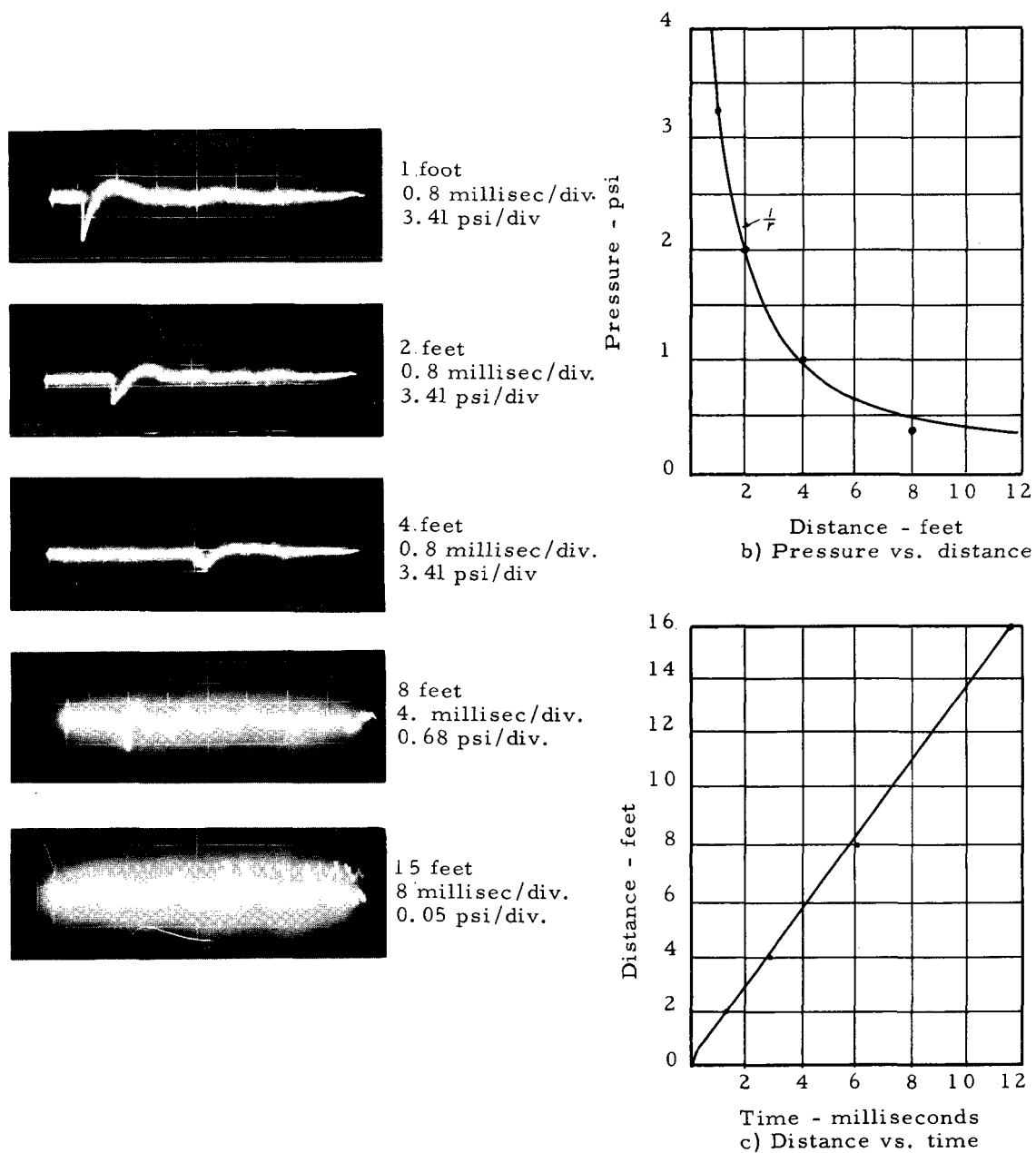


Figure 35. Blast pressure waves recorded for distance to 15 feet.
Arc triggered by 0.008 inch stainless steel wire. Energy -
100 joule/cm. arc length.

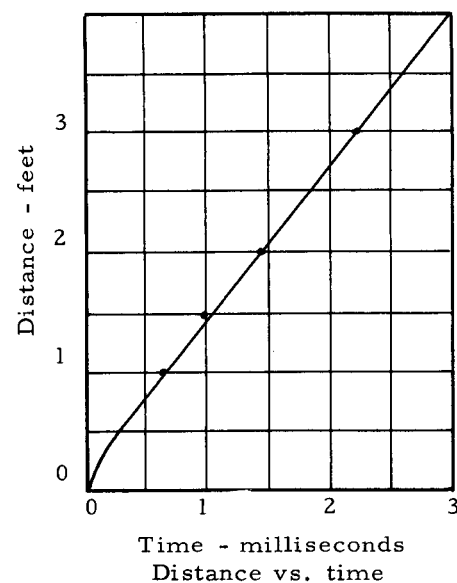
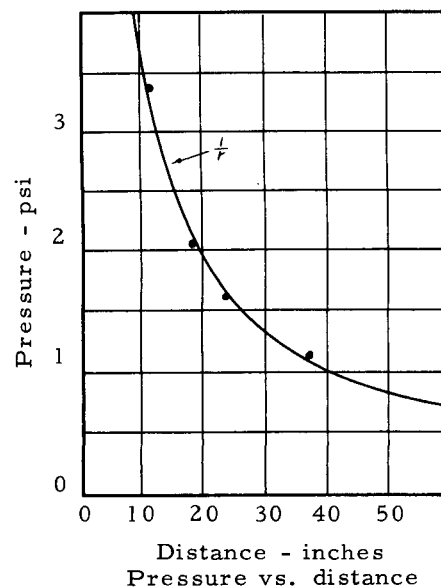
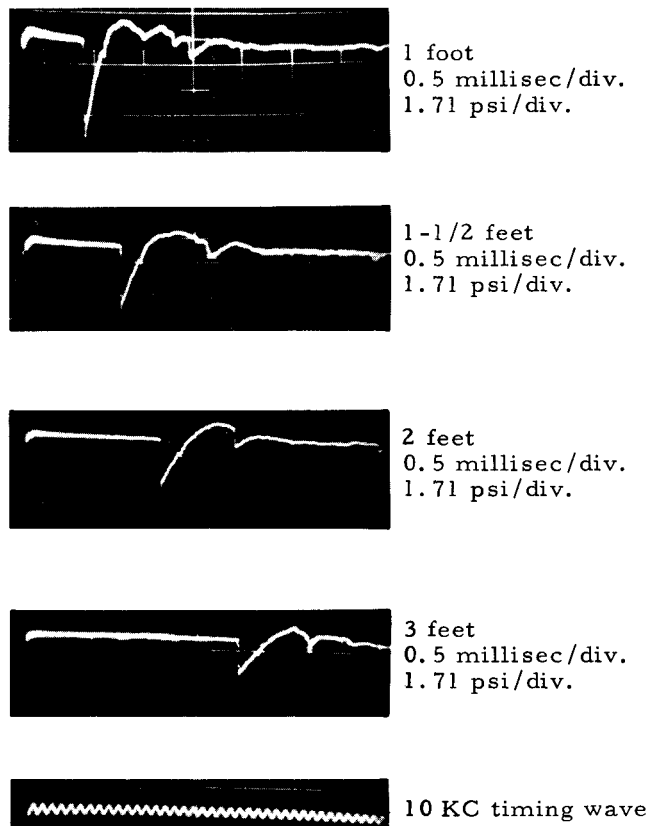


Figure 36. Blast pressure waves to distances of 3 feet. Arc triggered by 0.008 inch steel wire. Energy 100 joules/cm of arc length.

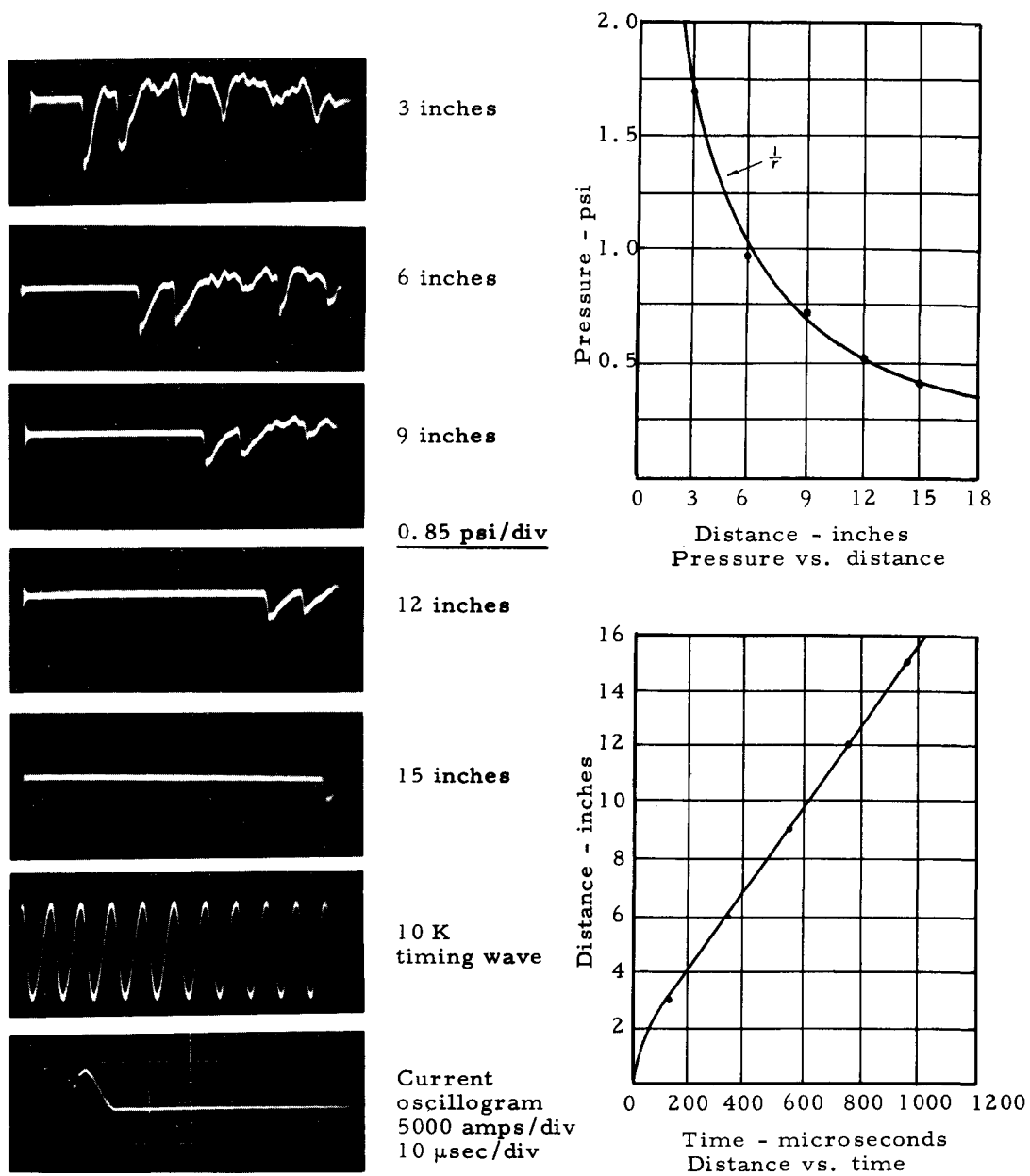


Figure 37. Blast waves from open air arc. 5000 amperes crest - 6 joules/cm of arc length.

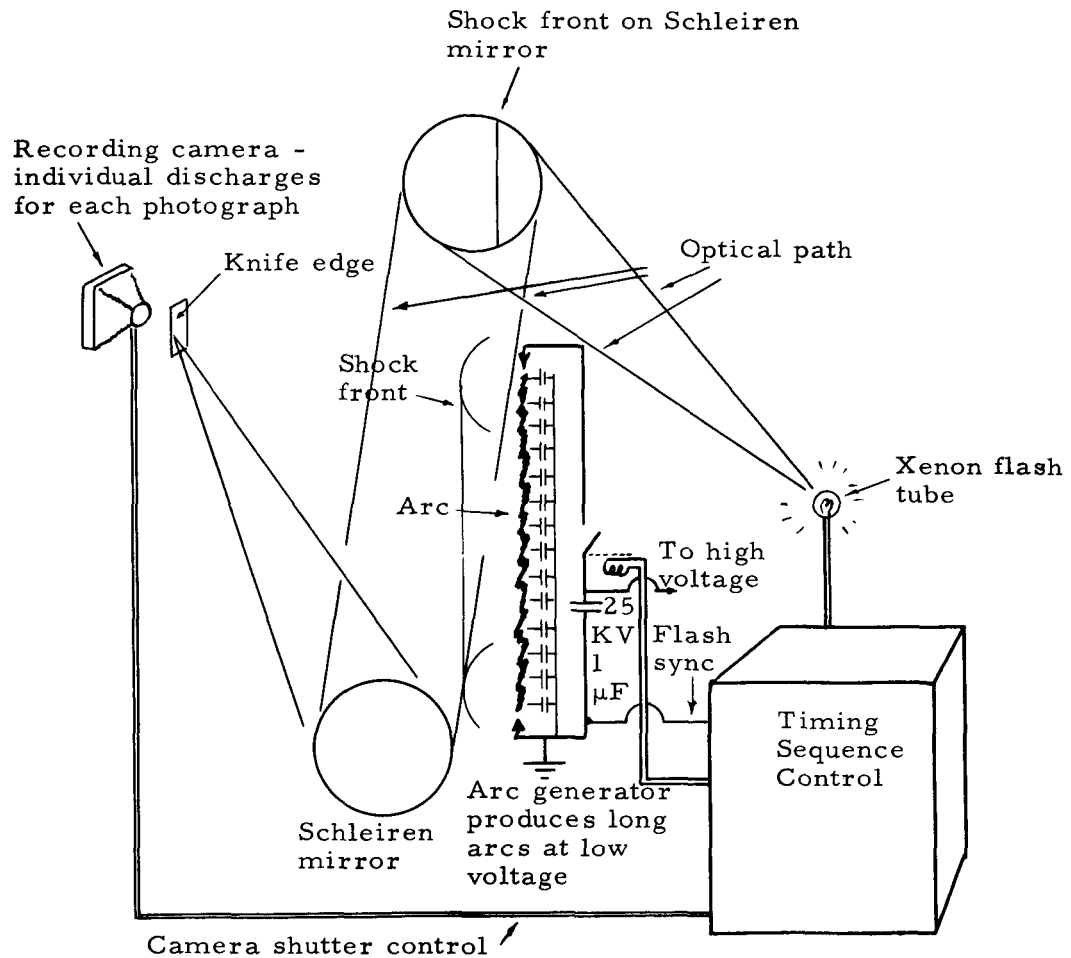


Figure 38. Test arrangement for Schleiren Measurements of shock front velocity.

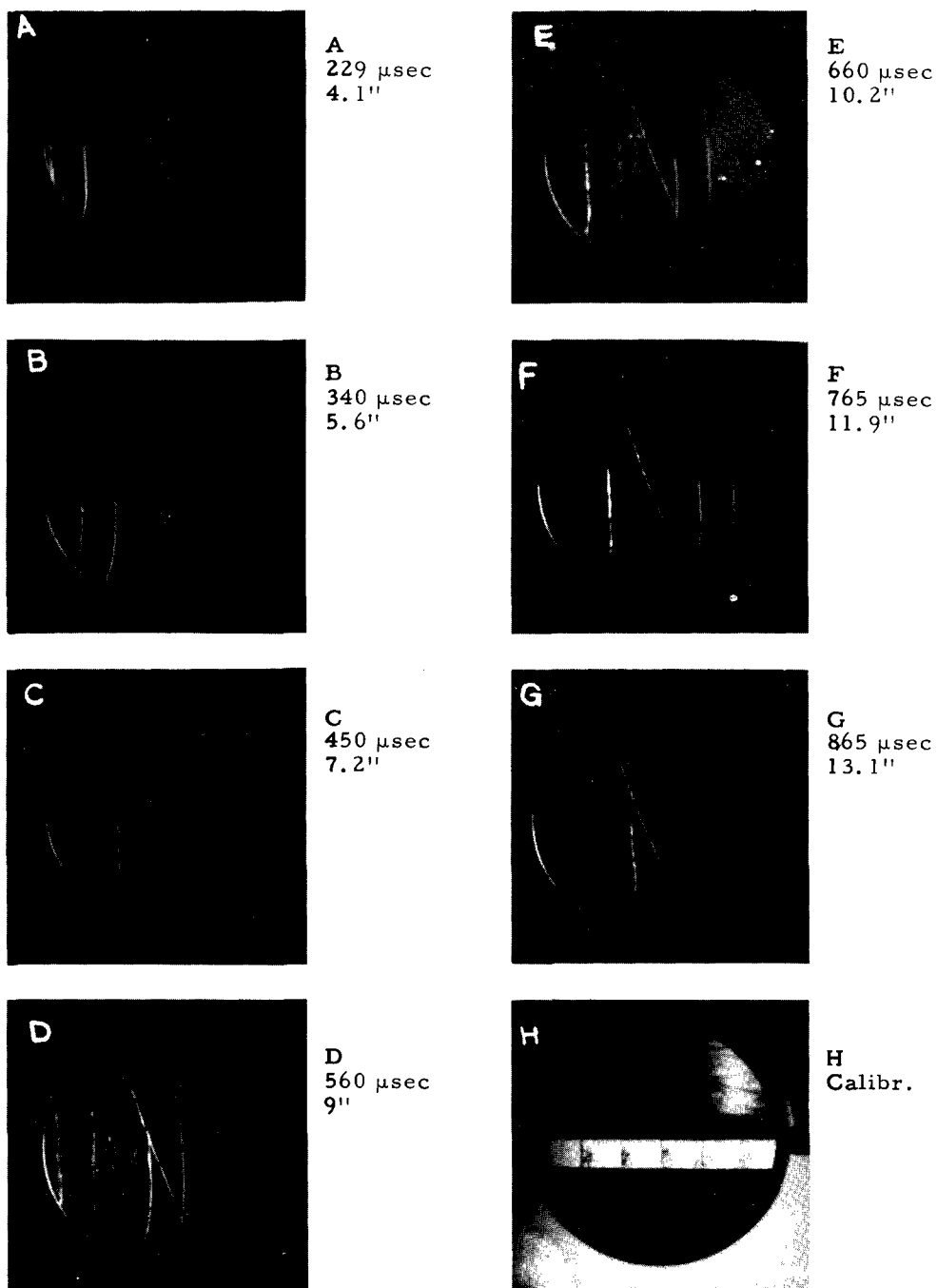


Figure 39(a). Schleiren photographs of shock wave movement away from arc. Discharge current 5000 amperes crest, 6 joule/cm of arc length. Diagonal line is caused by a scratched mirror, double shock front by reflections near arc.

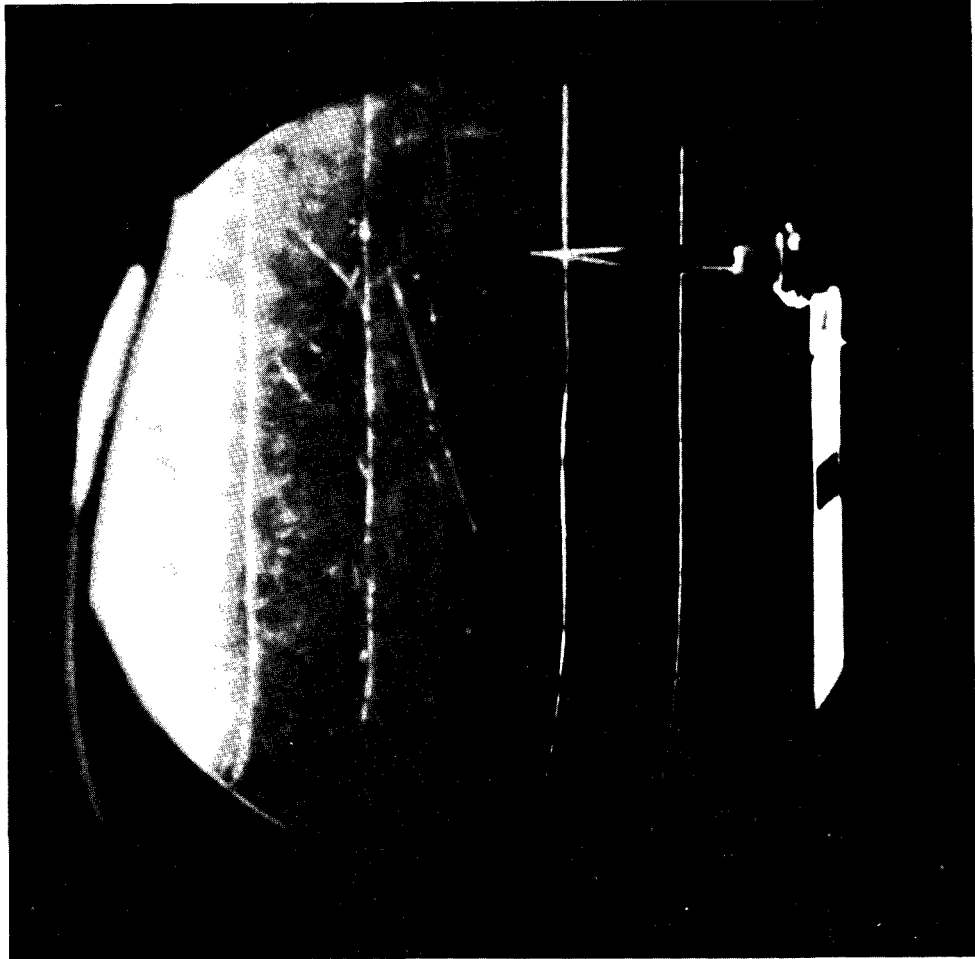


Figure 39(b). Schleiren photograph of shock wave passing blast gage transducer element.

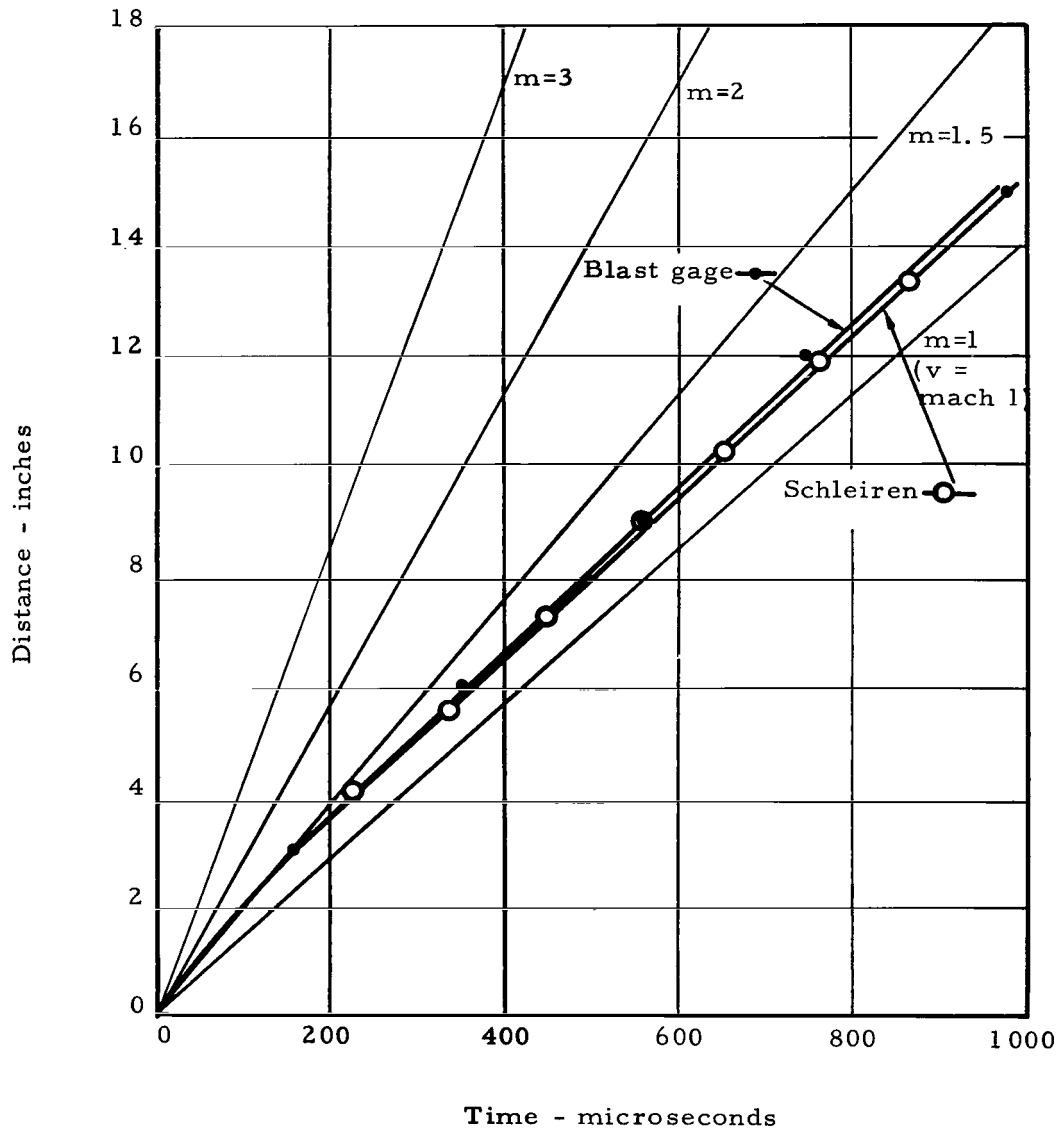


Figure 39(c) Graph of wave distance vs. time for piezo blast gage and Schleiren studies showing good correspondence between two sets of measurements.

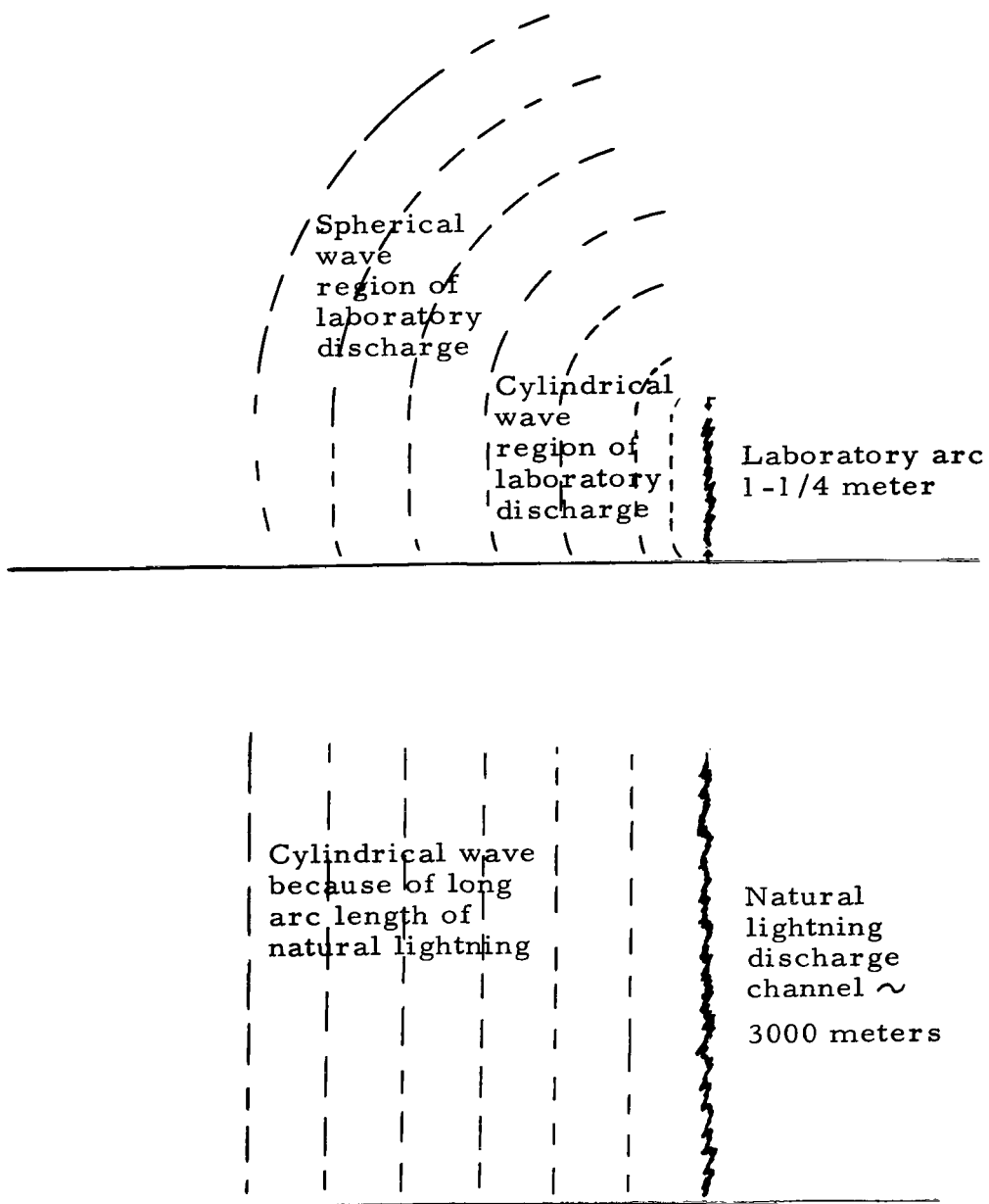


Figure 40. Illustration of cylindrical to spherical wave transition in laboratory discharge compared to natural lightning channel.

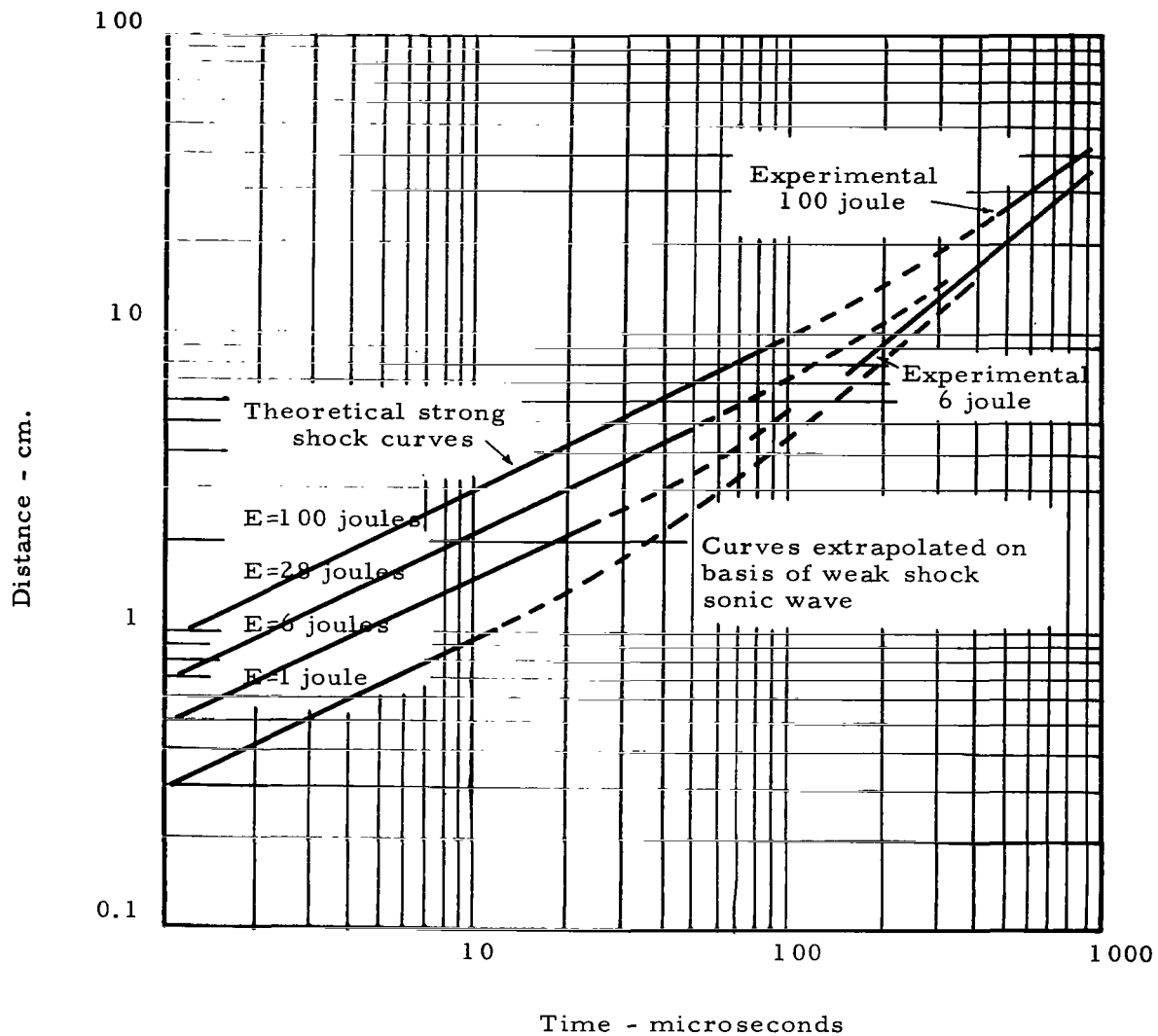


Figure 41. Graph of theoretical and experimental distance vs. time for blast waves from discharge energies of one to one hundred joules; strong shock calculations shown on left, some measured waves on right.

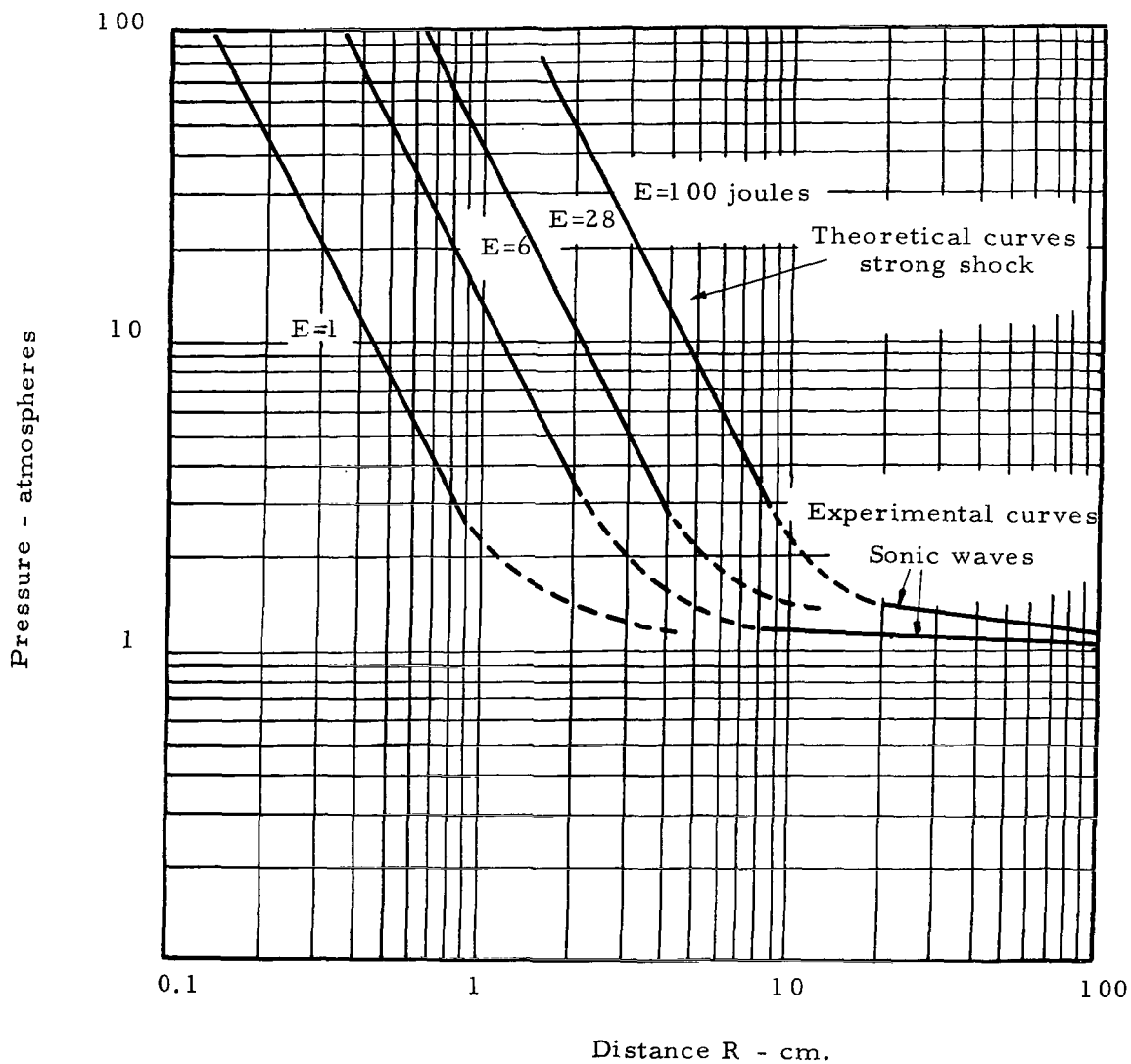


Figure 42. Theoretical and experimental curves of strong shock transition to sonic waves.

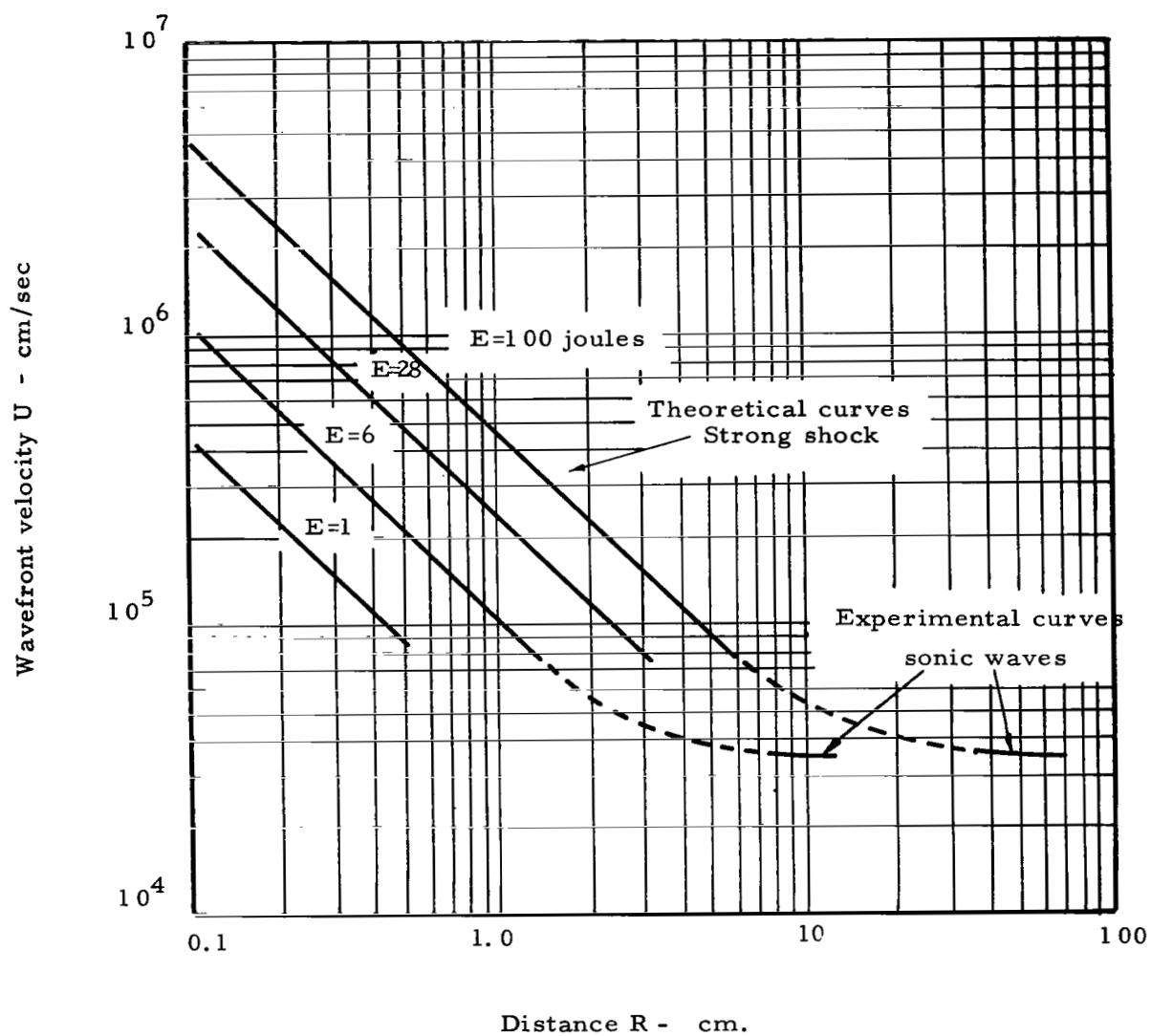


Figure 43. Theoretical curves of strong shock velocities with transitory to measured sonic waves.

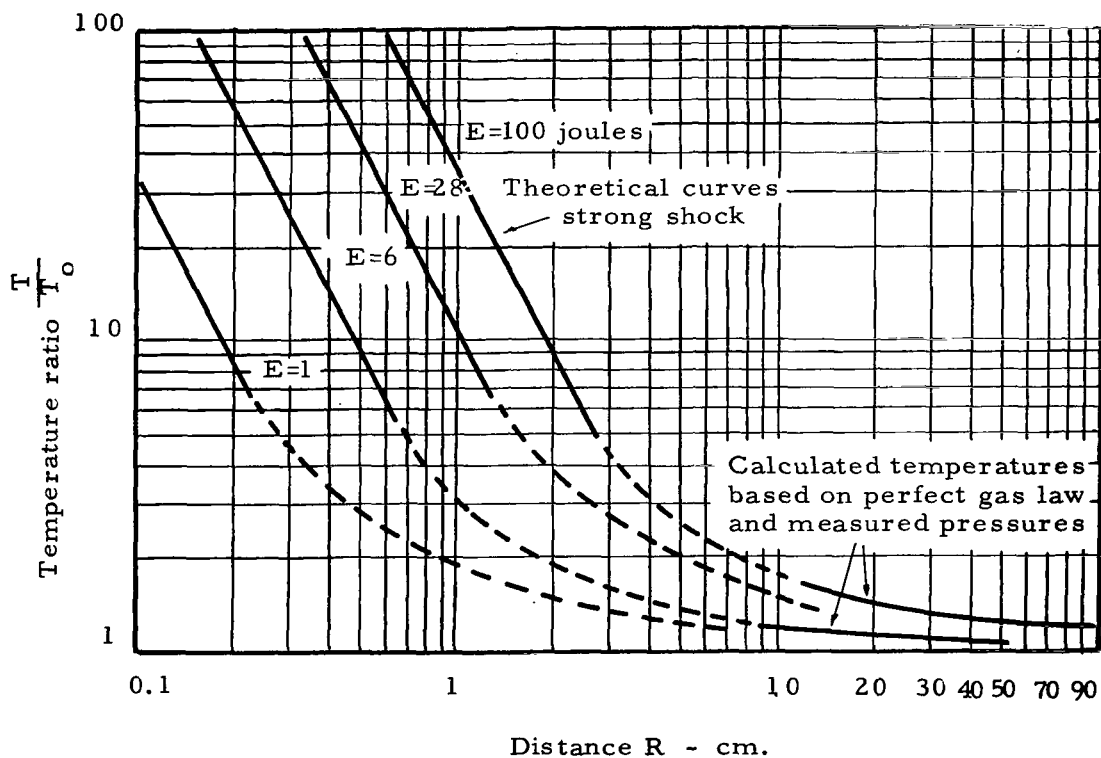


Figure 44. Theoretical curves of strong shock front temperatures with transitions to temperatures calculated on basis of perfect gas law and measured values of pressure.

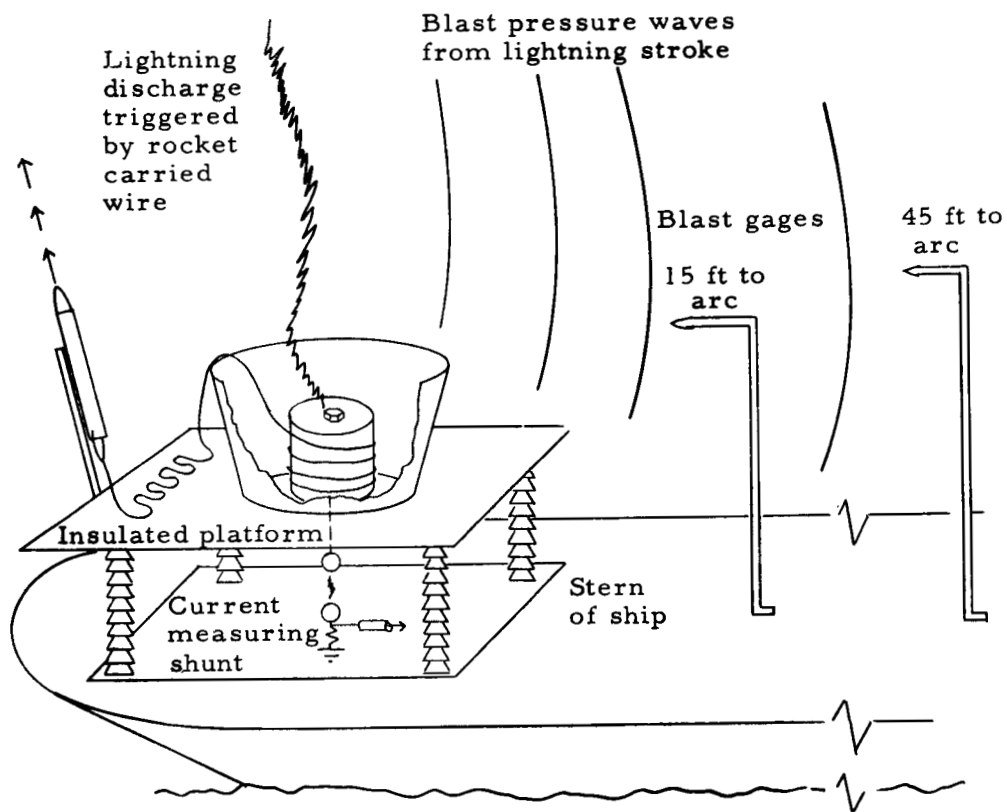


Figure 45. Rocket launching platform on stern of ship equipped with lightning current measuring shunt and blast pressure gages.

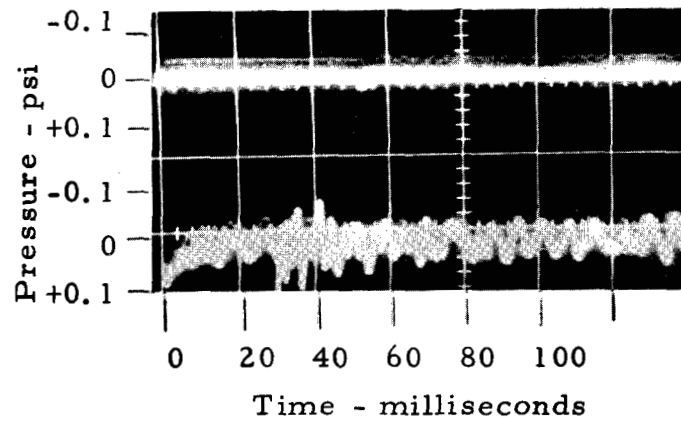


Figure 46(a). Blast wave recorded from natural lightning discharge at 40 feet (upper trace) and 9 feet (lower trace).

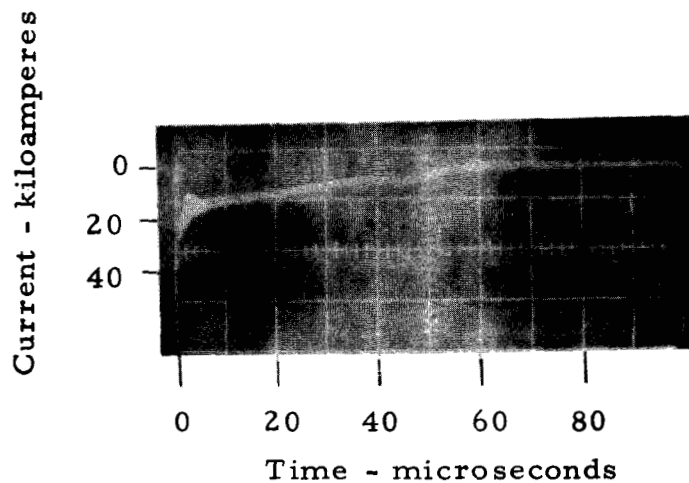


Figure 46(b). Current flow during natural lightning strike.

Figure 46. Natural lightning current oscillograms triggered by rocket supported wires.

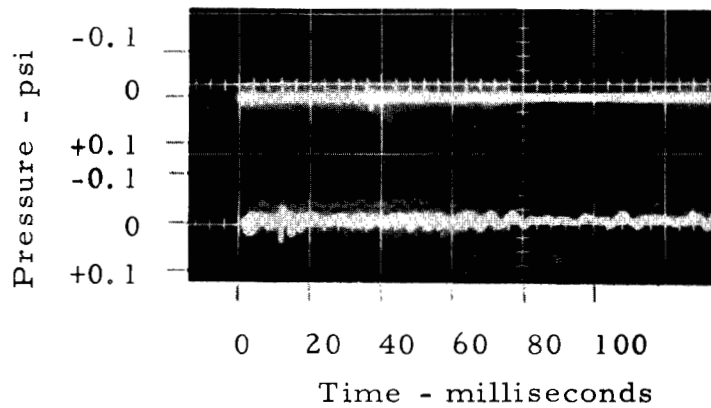


Figure 47(a). Blast wave recorded from laboratory lightning discharge at 40 feet (upper trace) and 9 feet (lower trace).

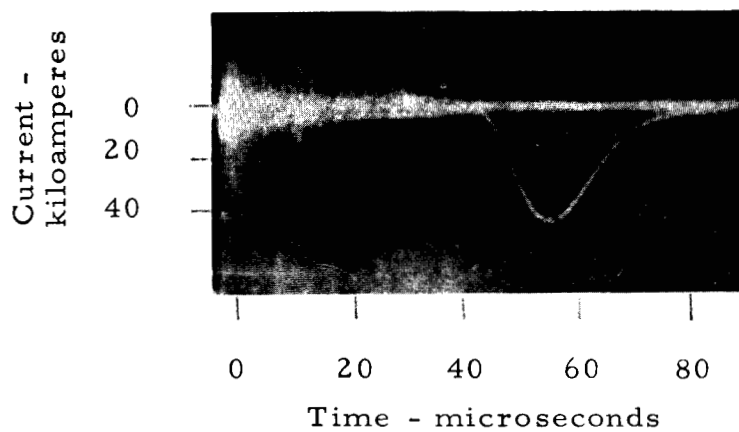


Figure 47(b). Current wave for artificial lightning discharge.

Figure 47. Oscillograms of laboratory high current discharges.

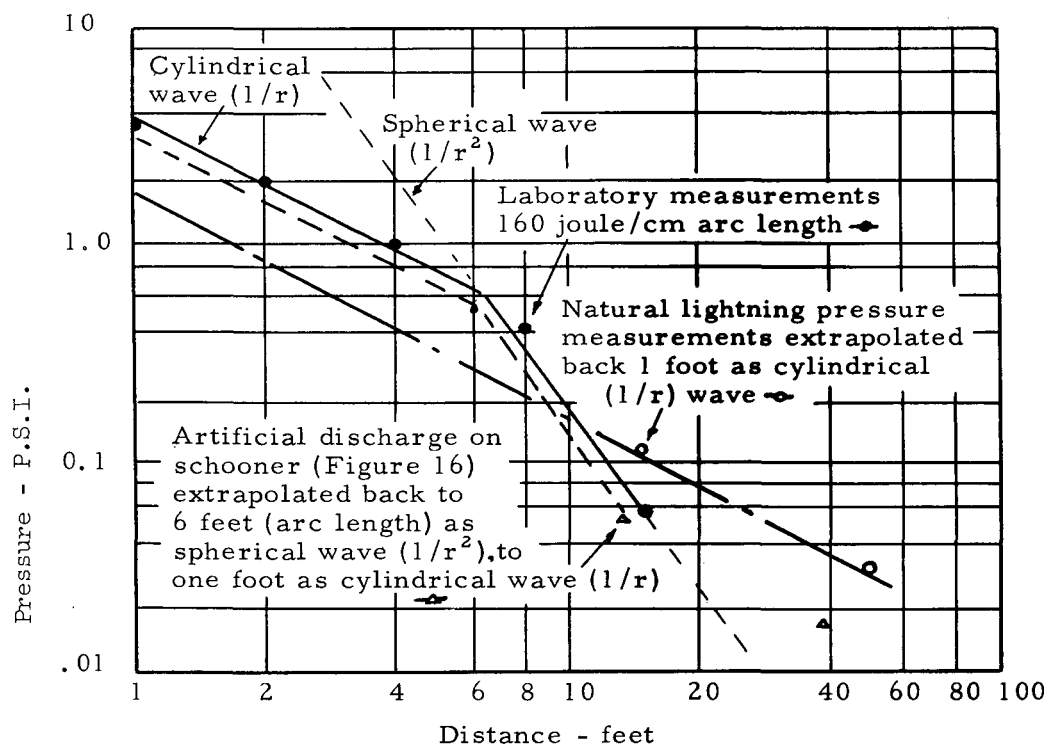
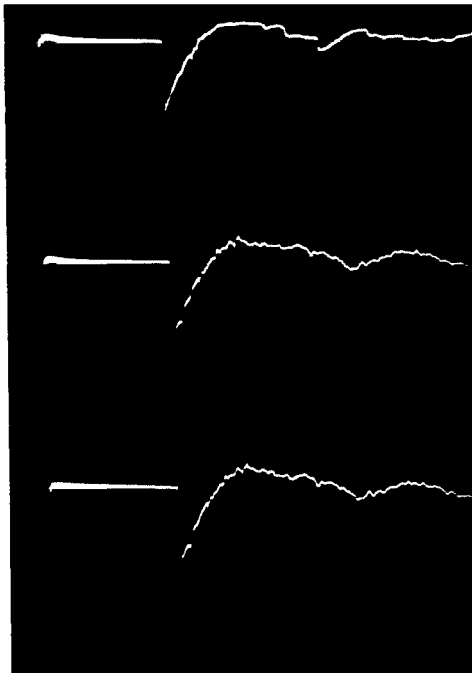


Figure 48. Pressures recorded from natural and artificial lightning discharge.



Blast probe in tube -
no screen.

Blast probe in tube -
coarse screen 3/16 inch
mesh.

Blast probe in tube -
fine screen 1/16 inch
mesh.

3.41 psi/div., pressure (ordinate)
580 microsec/div., time (abscissa)

Figure 49. Blast pressure waves measured with and without
flame arrester screens.

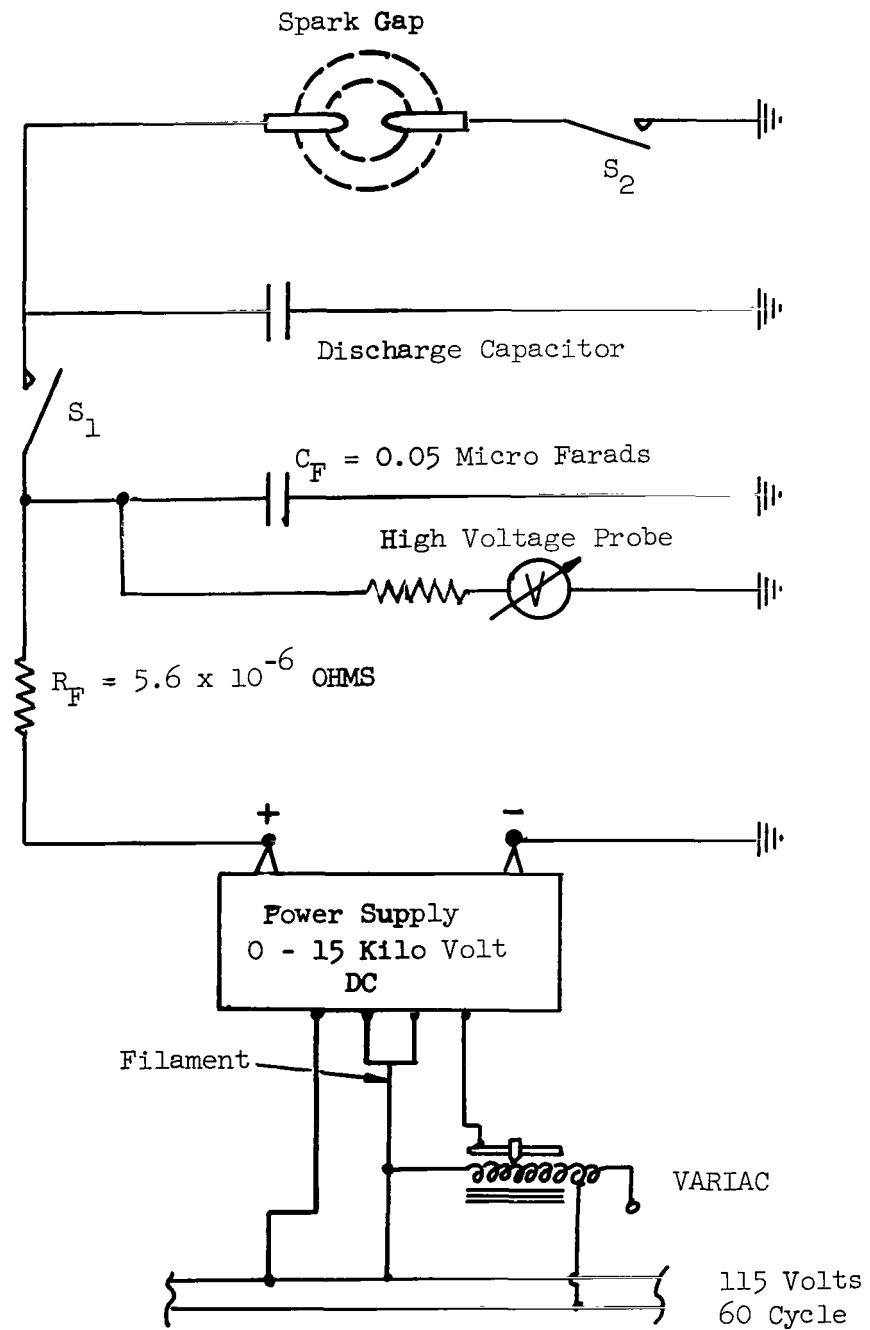


Fig. 50. - Schematic of Spark Gap Electrical Circuit Used For Dynamic Science Corporation's Test Program.

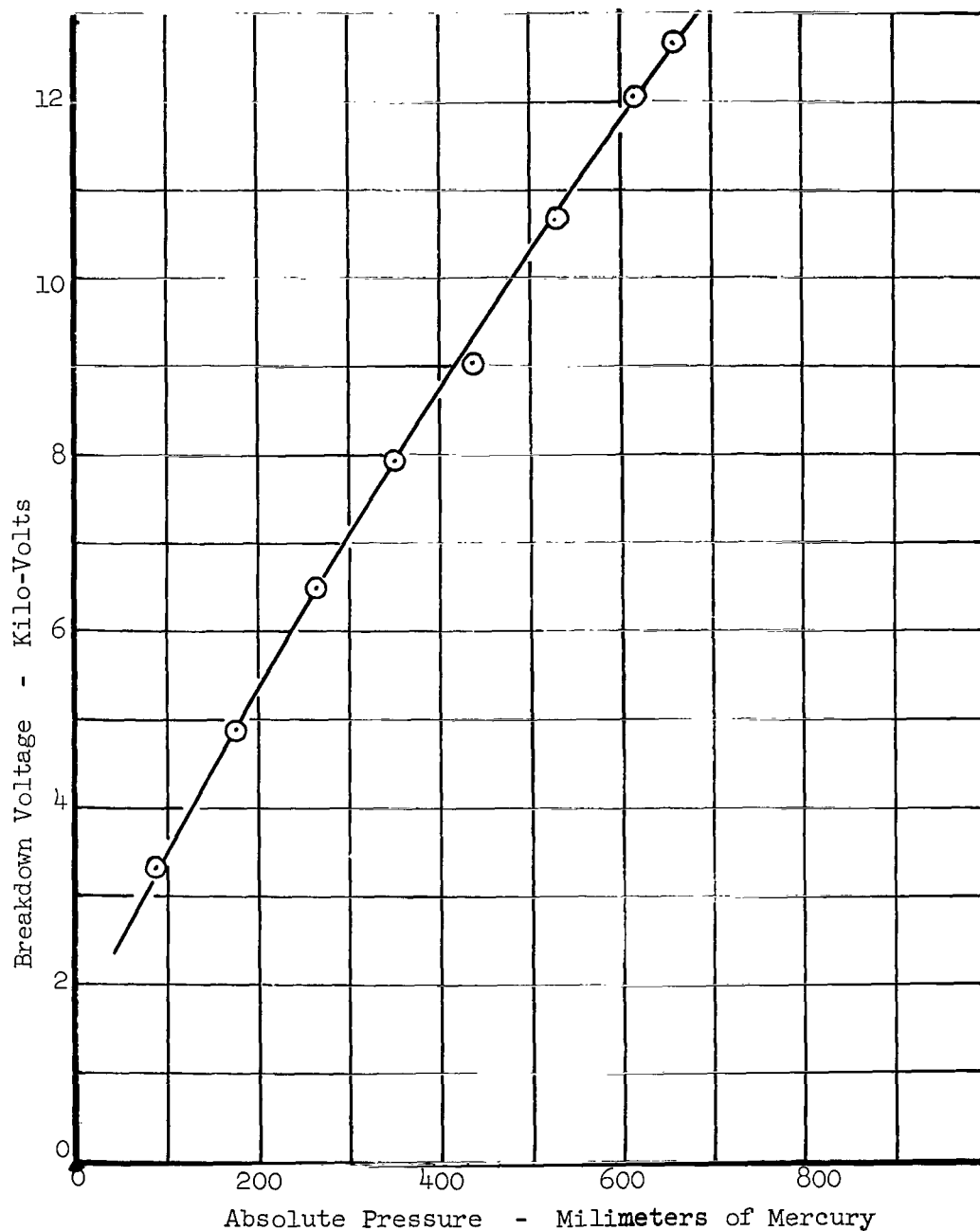


Fig. 51. - Paschen Diagram for 5% Propane-Air Mixture Measured With 8.8 Millimeter Gap.

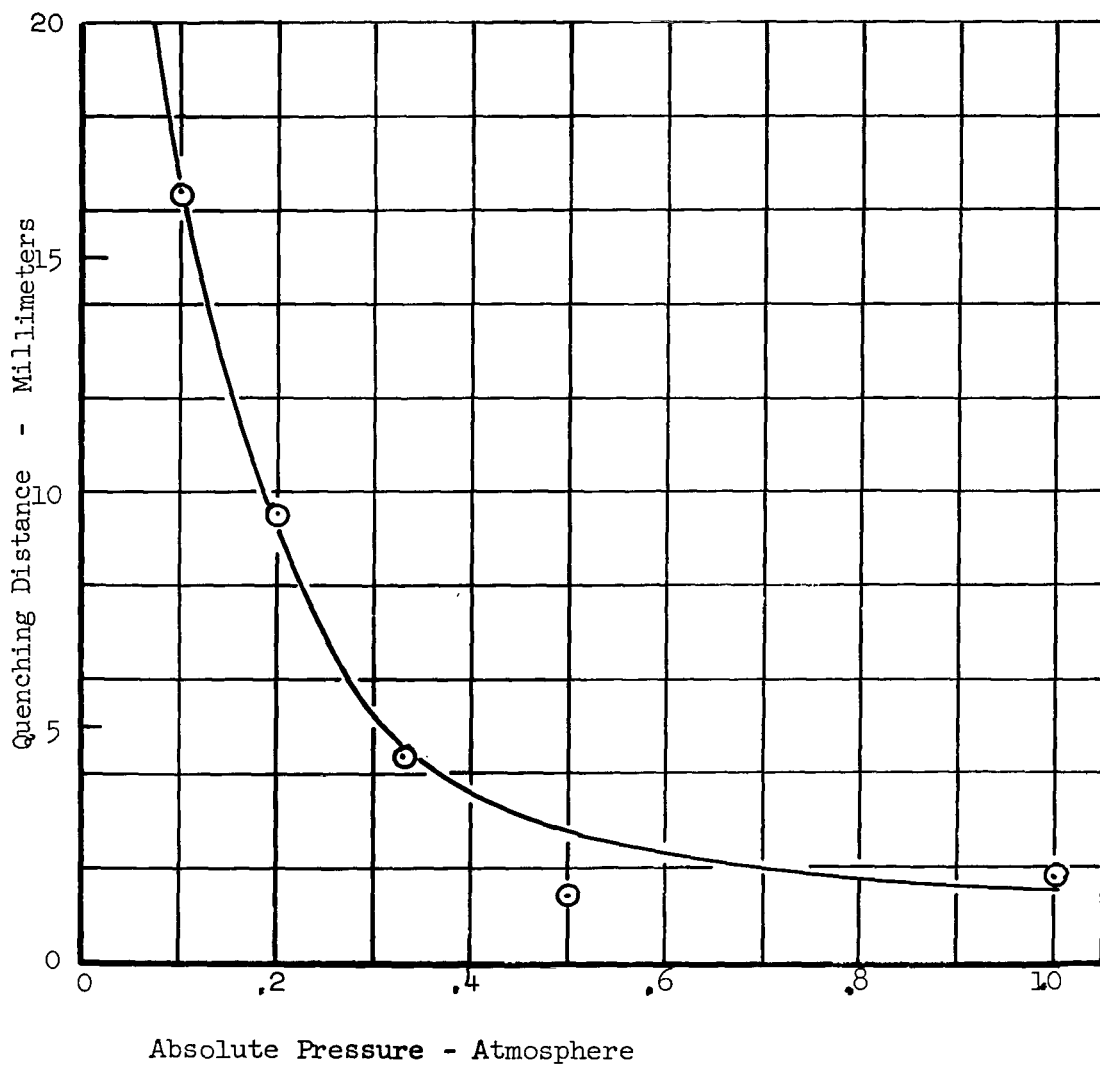


Fig. 52. - Quenching Distance for Parallel Plates, at Reduced Absolute Pressure, and 5% Propane-Air Mixture. Geometry Factor = 1.0
Ref.: B. Lewis and G. von Elbe, "Combustion, Flames, and Explosions".

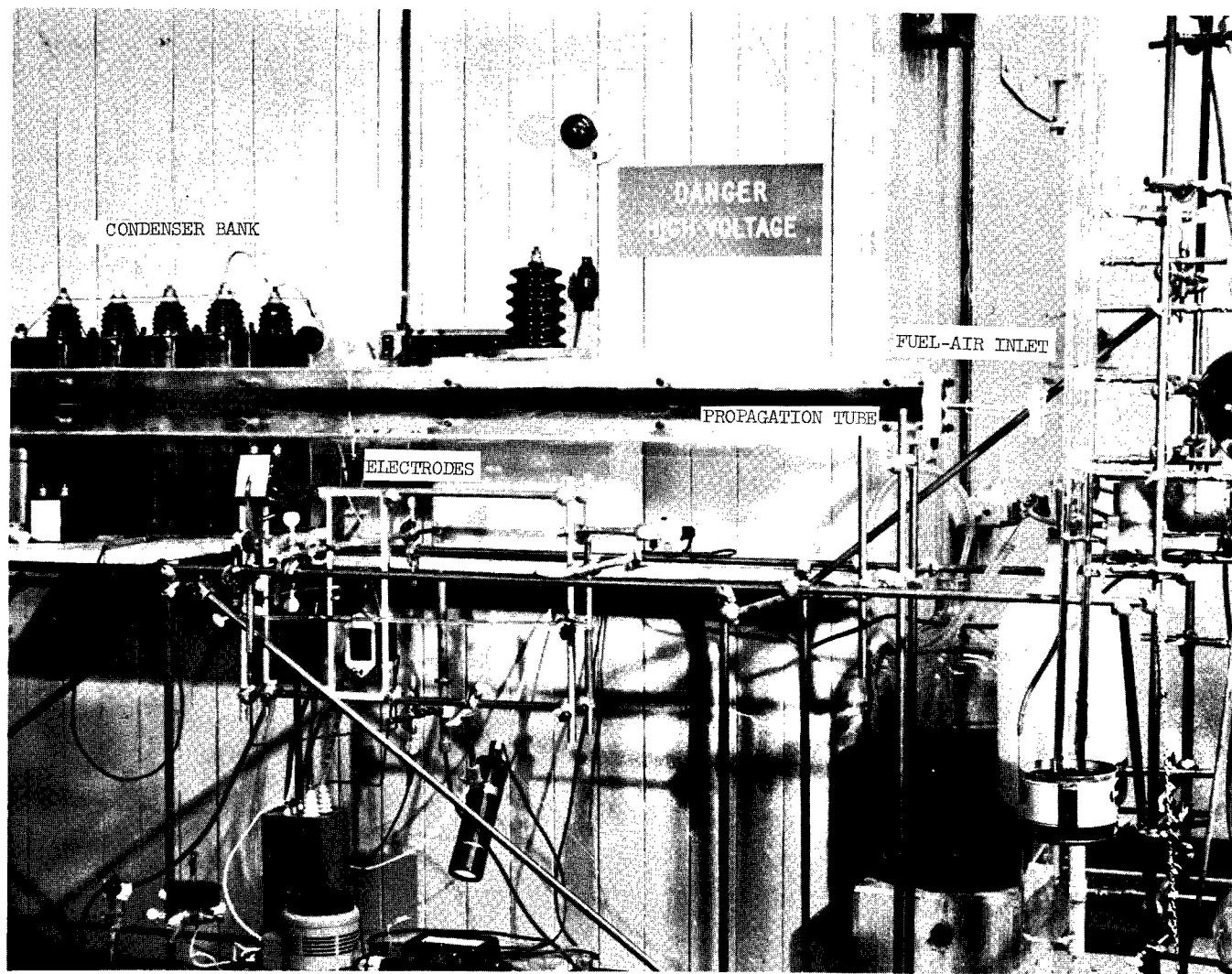


Figure 53. Ignition and Quenching Apparatus Used in Test Program
at Dynamic Science Corporation.

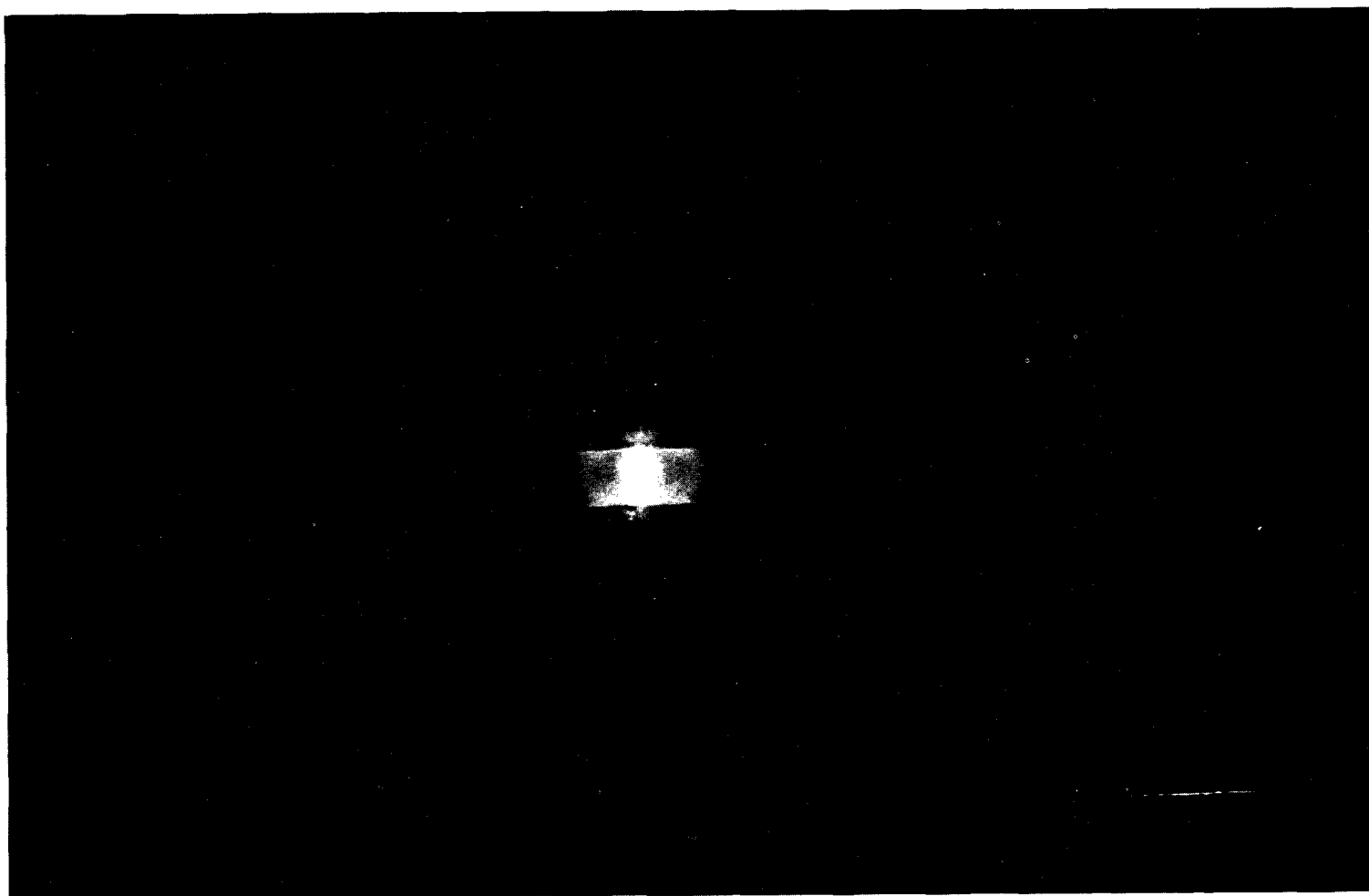


Fig. 54(a). - Discharge Energy is .081 Joule

Figure 54. - Comparison of Discharges in Air at An Absolute Pressure of 500 Millimeters of Mercury for Three Discharge Energies.



Fig. 54(b). - Discharge Energy is .504 Joule

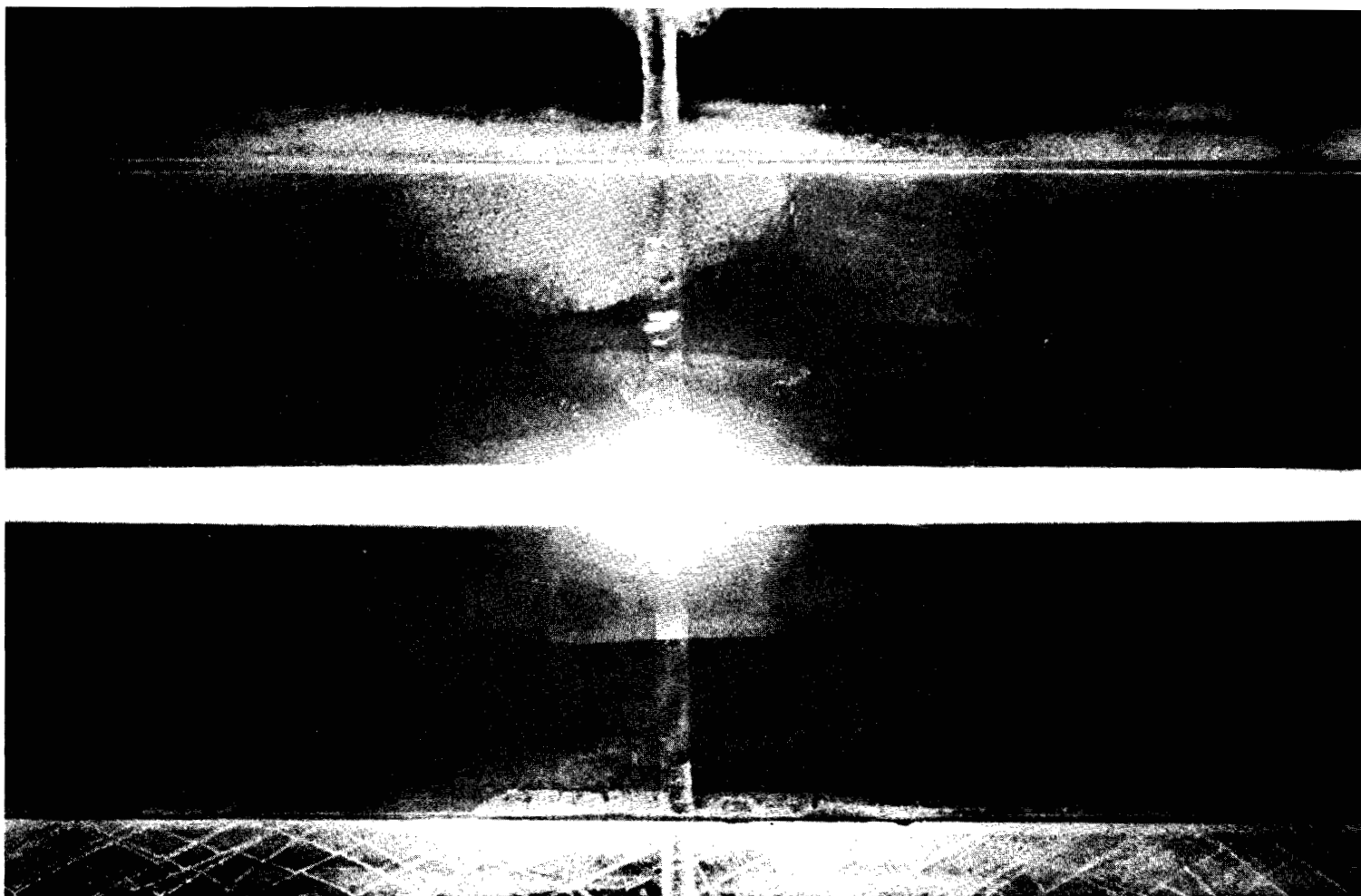


Fig. 54(c). - Discharge Energy is 364 Joules

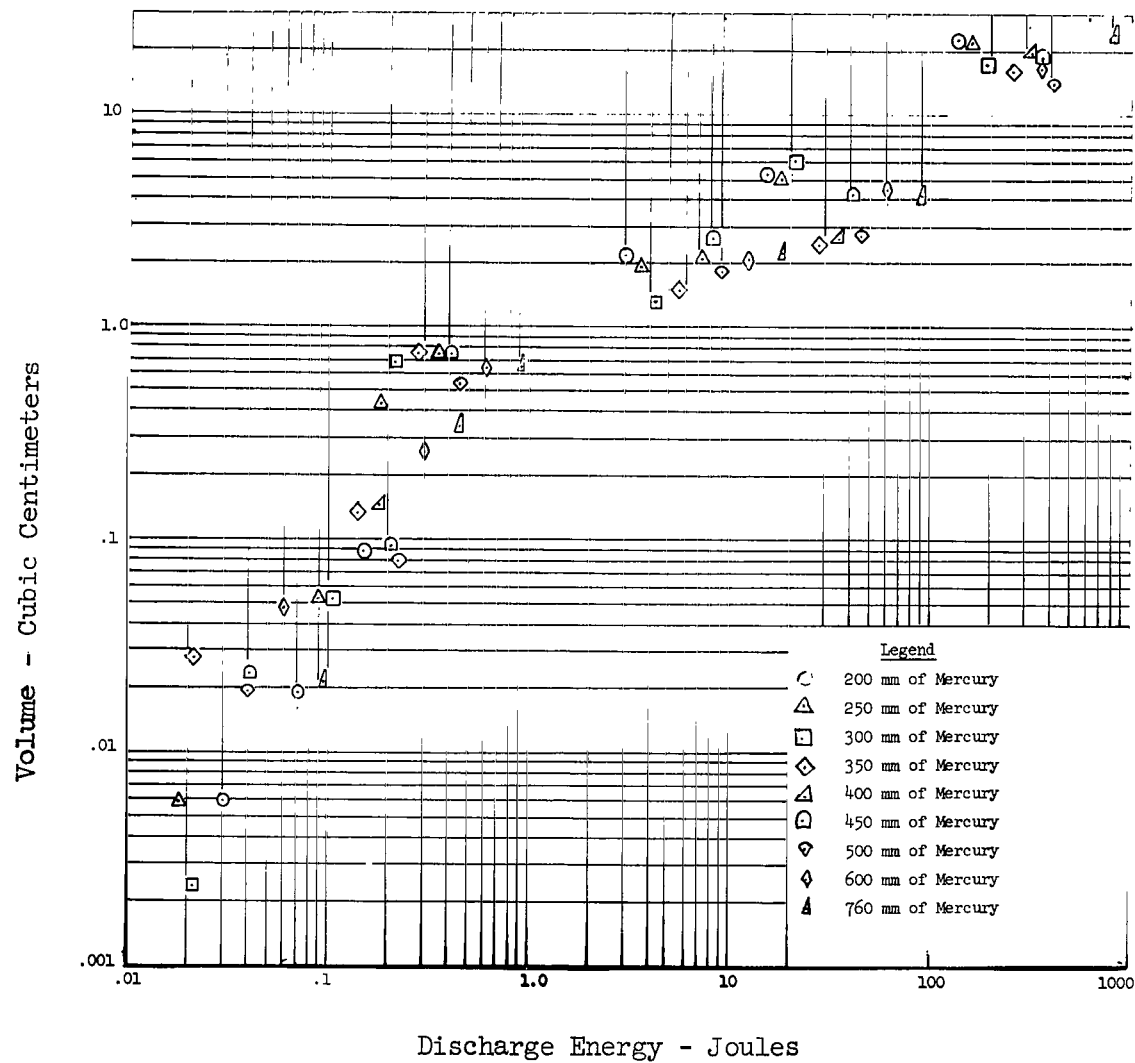


Figure 55. - Spark Volume in 5% Propane-Air Mixture for Various Discharge Energies at Several Pressures.

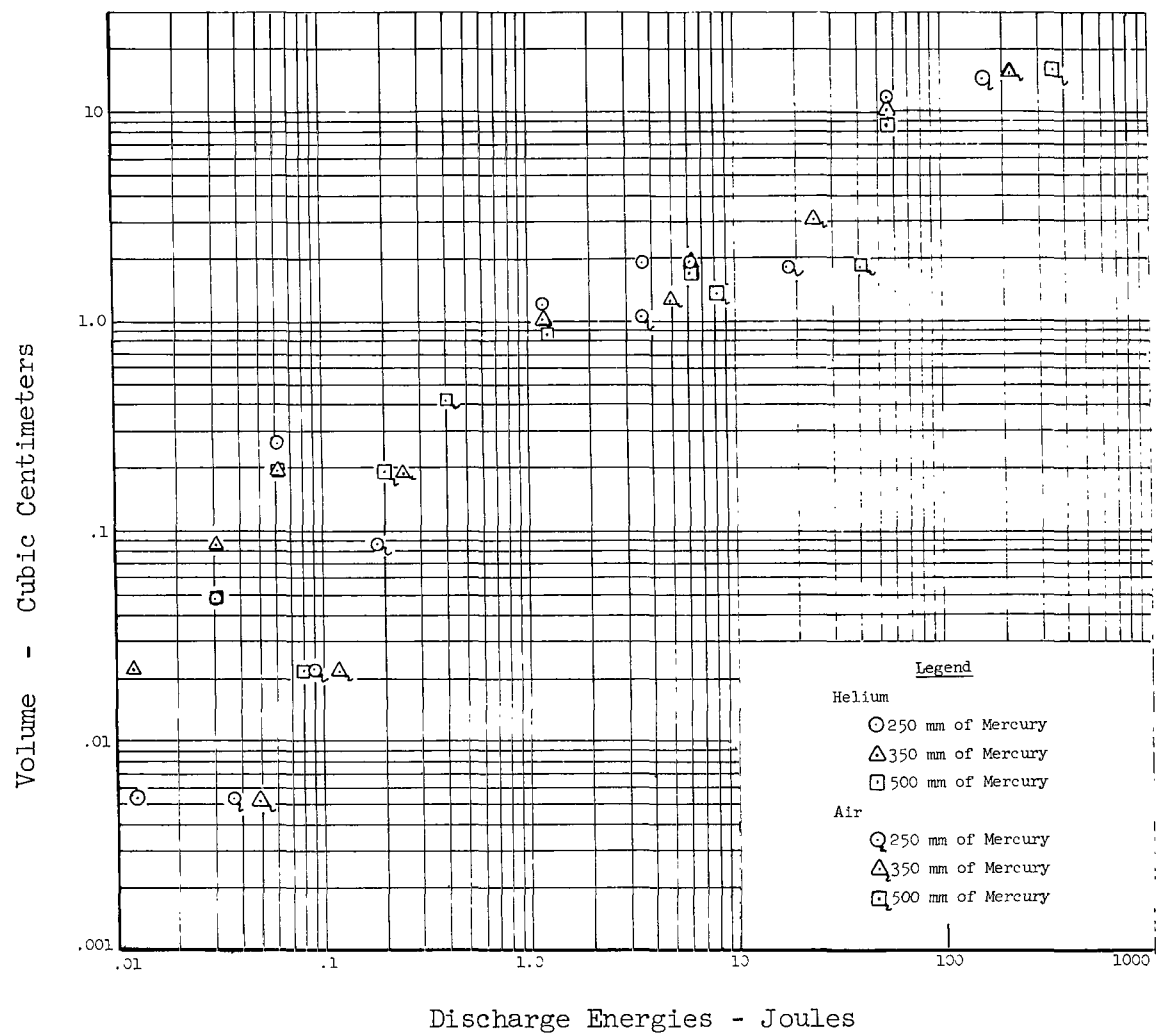


Figure 56. - Spark Volume in Helium and Air for Various Discharge Energies at Several Pressures.

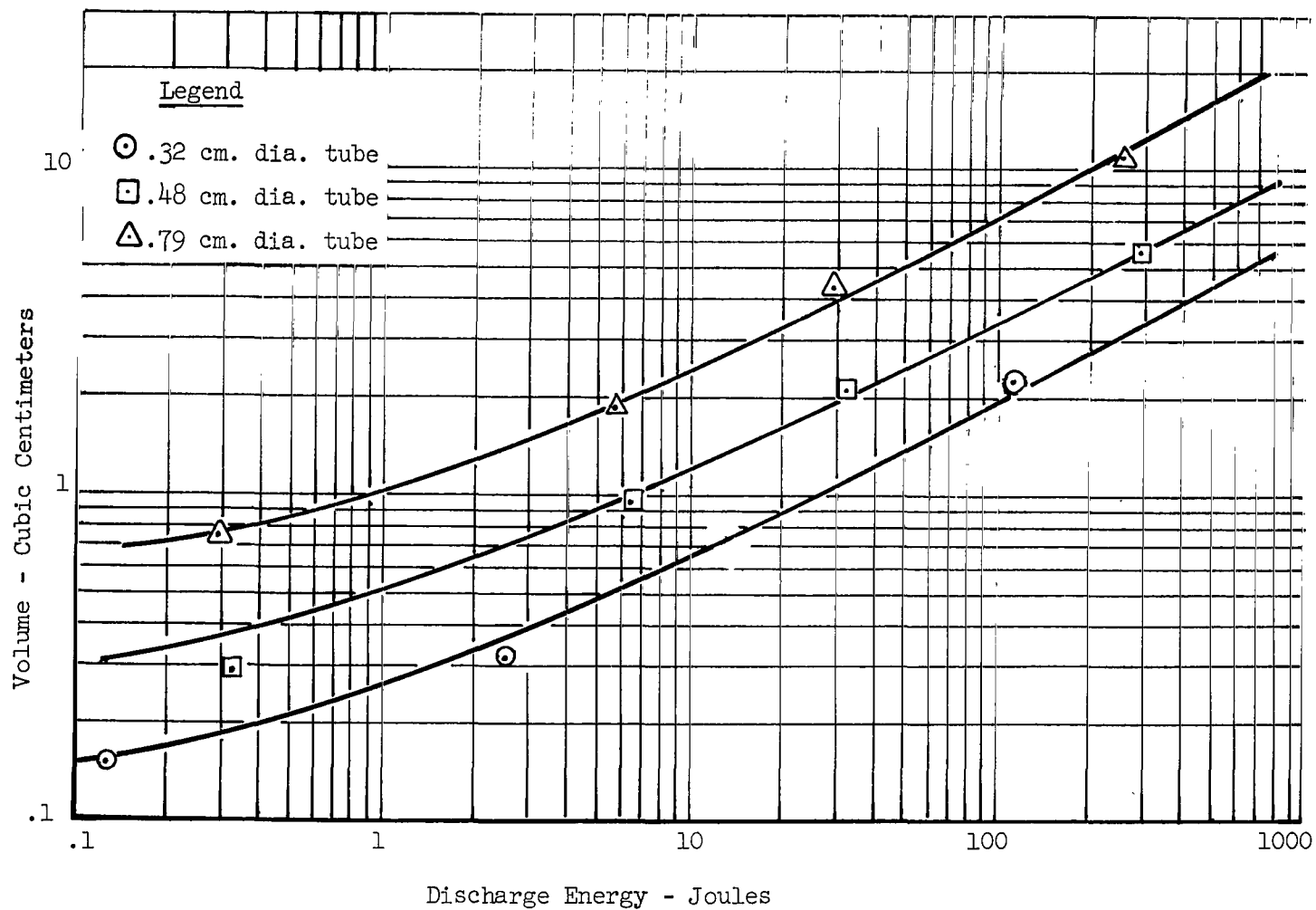


Fig. 57. - Plasma Volume in a 5% Propane-Air Mixture with 0.20 cm. diameter Electrodes for Various Discharge Energies.

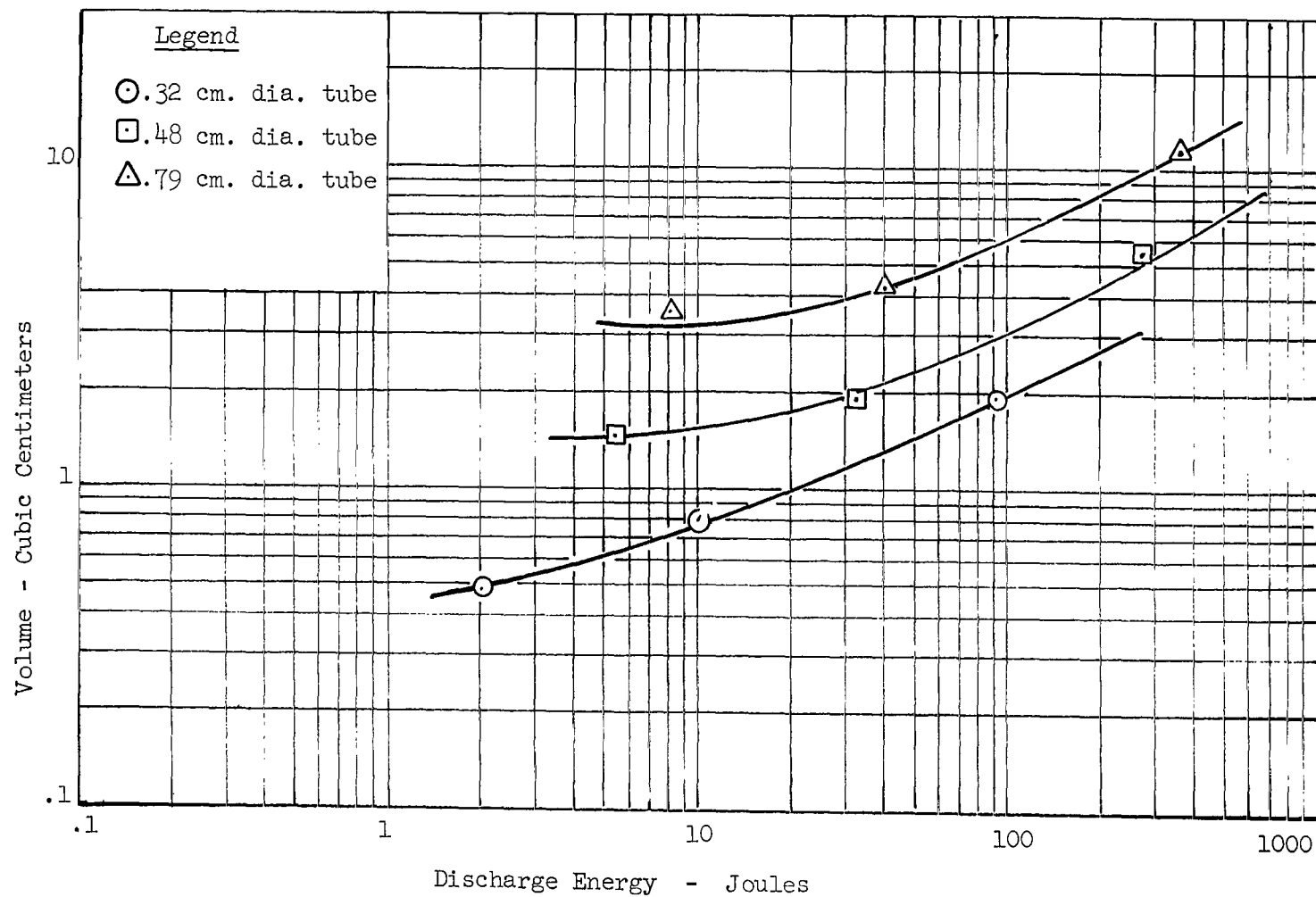


Fig. 58. - Plasma Volume in a 5% Propane-Air Mixture With a 0.40 cm. Diameter Electrode for Various Discharge Energies.

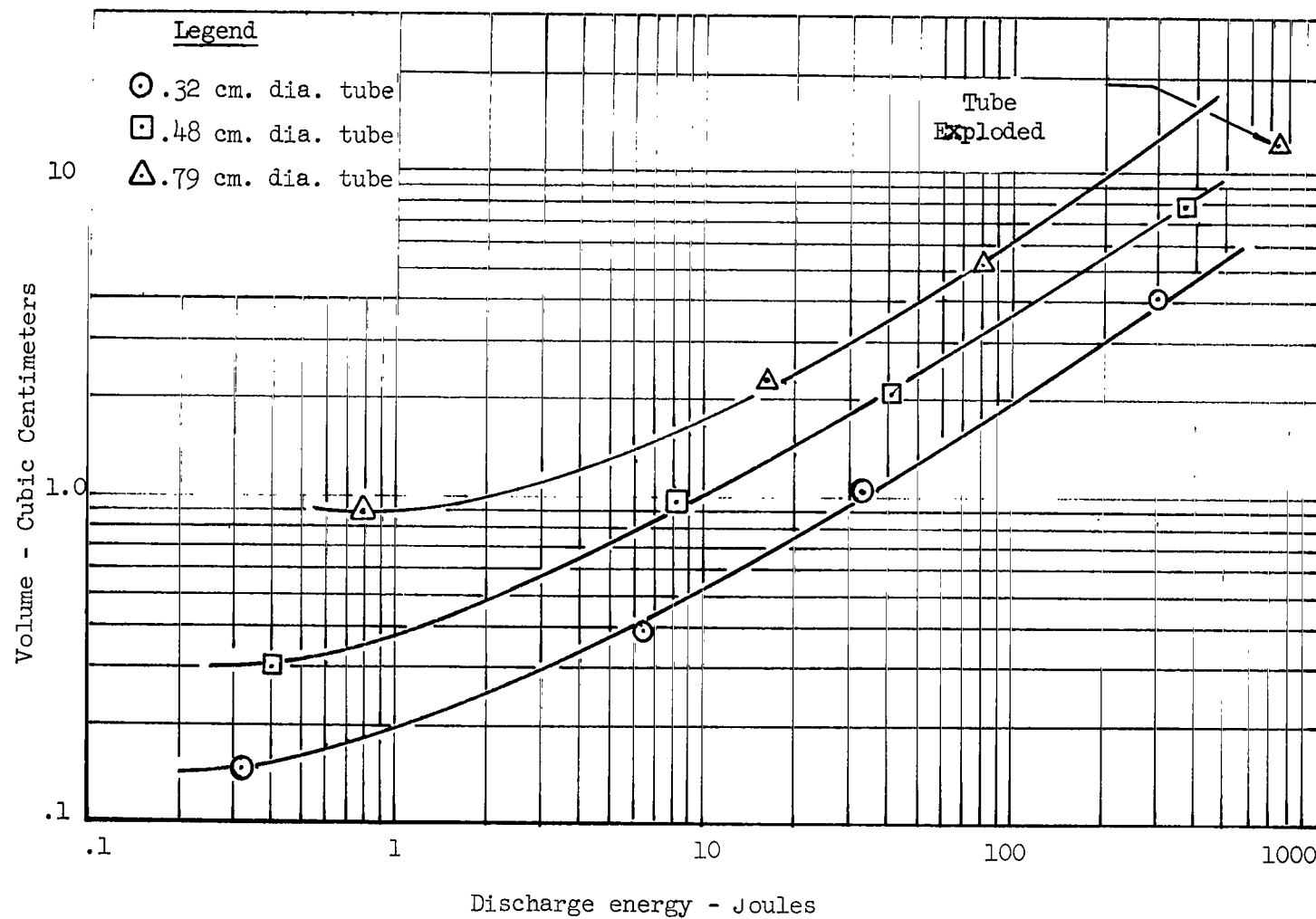


Fig. 59. - Plasma Volume in Nitrogen with a 0.20 Diameter Electrode for Various Discharge Energies.

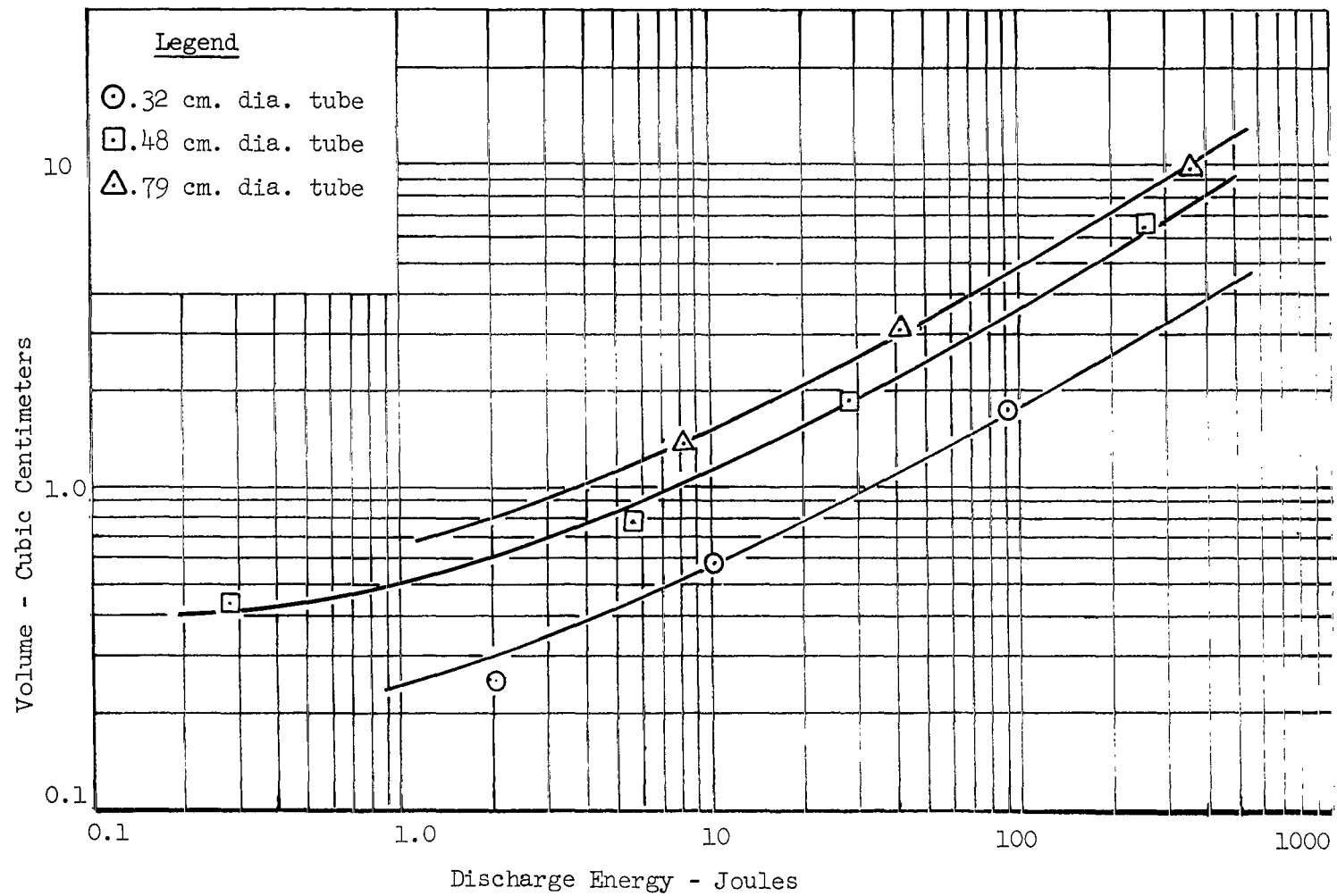


Fig.60. - Plasma Volume in Nitrogen with 0.40 cm. Diameter Electrode For Various Discharge Energies.

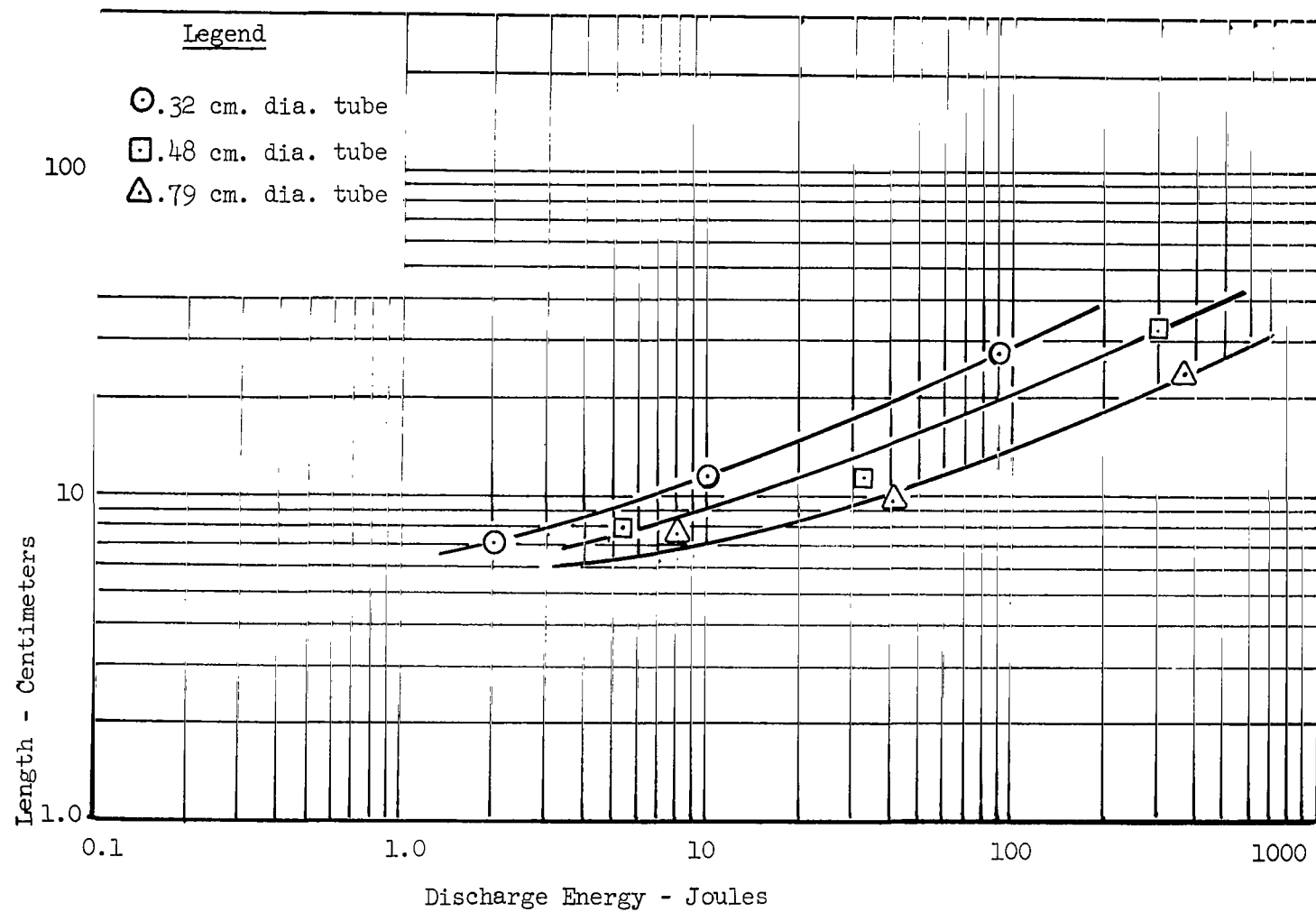


Fig. 61. - Plasma Length in a 5% Propane-Air Mixture with 0.40 cm. Diameter Electrodes for Various Discharge Energies.

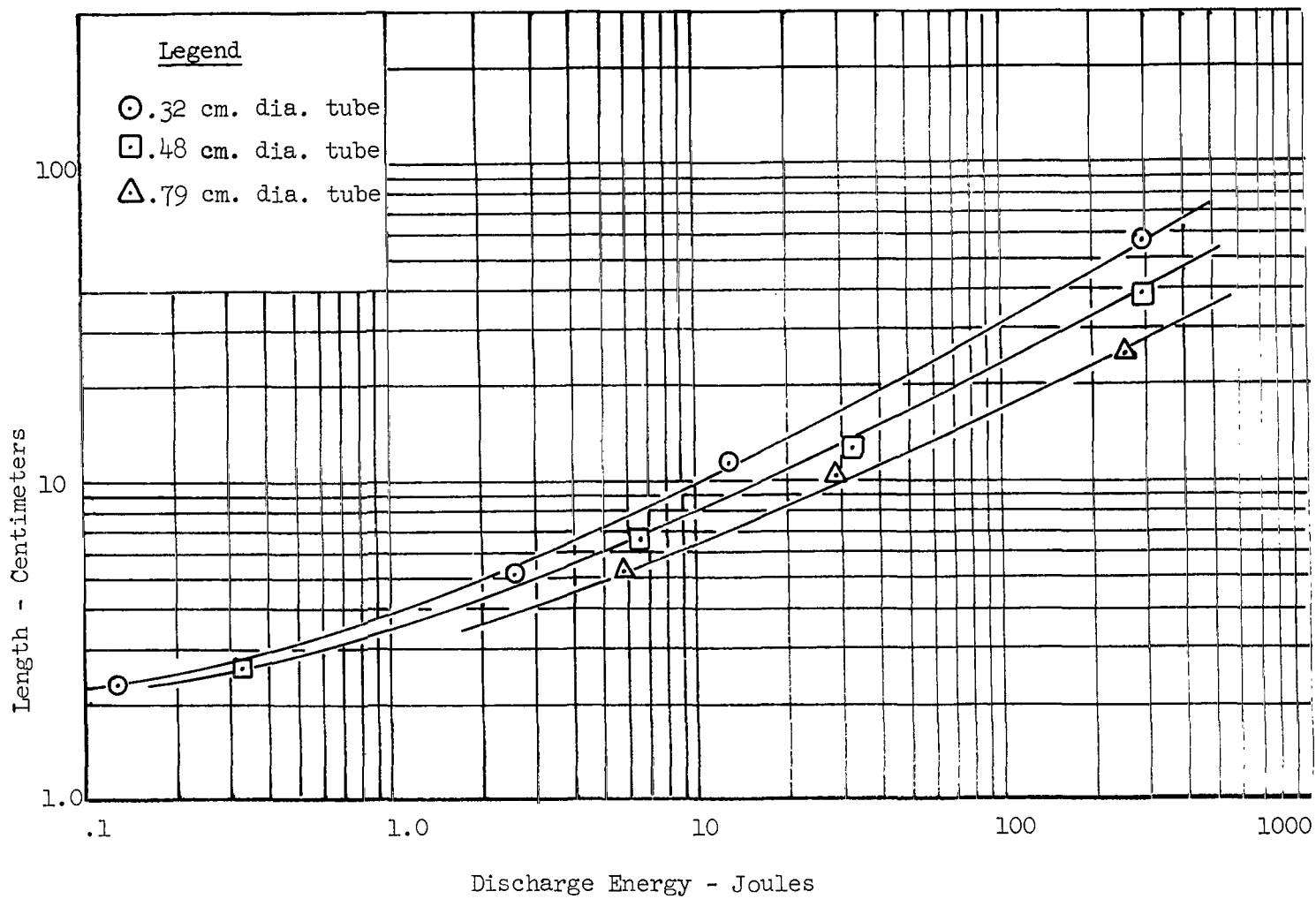


Fig. 62. - Plasma Length in a 5% Propane-Air Mixture With 0.20 cm. Diameter Electrodes for Various Discharge Energies.

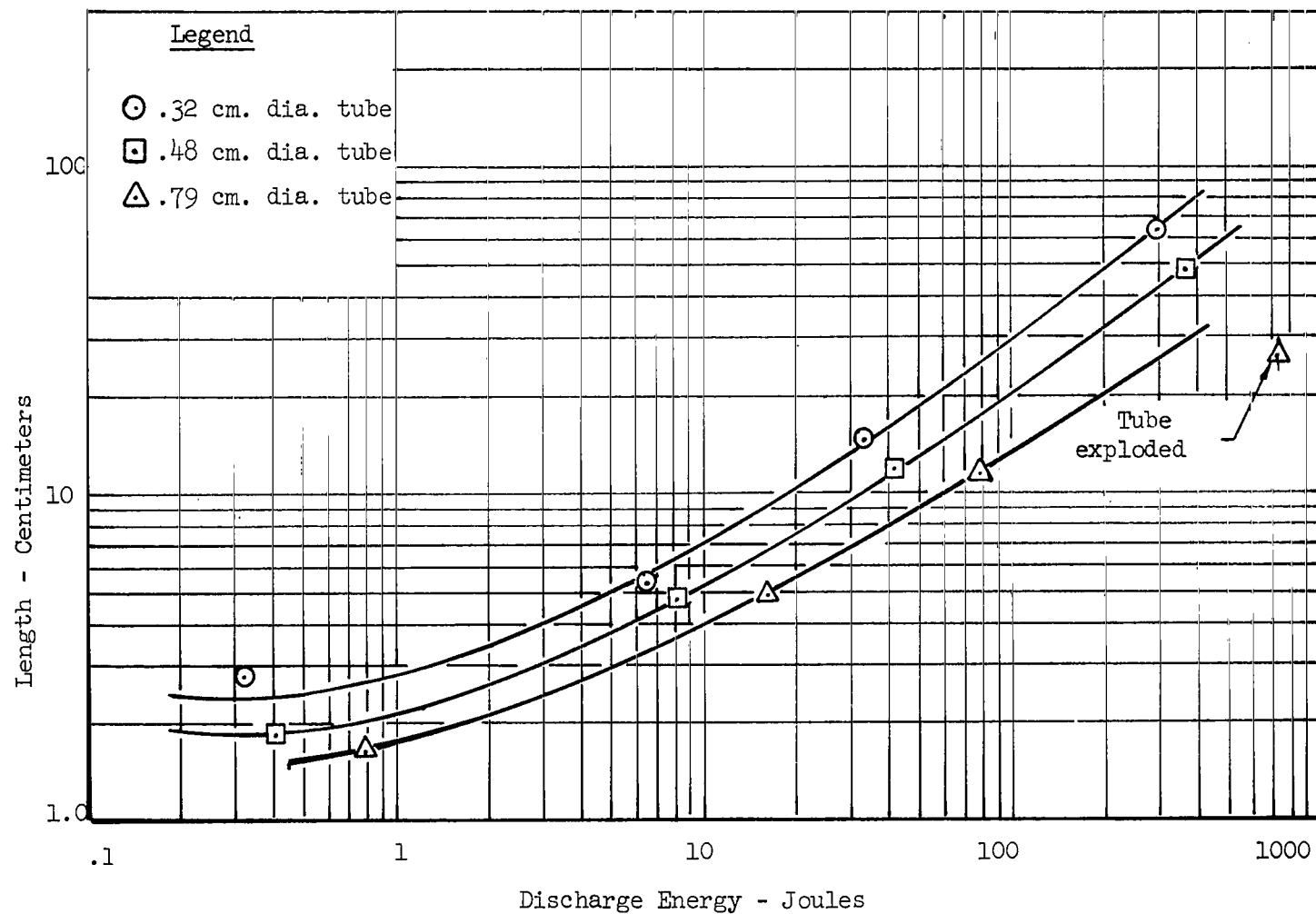


Fig. 63. - Plasma Length in Nitrogen with a 0.20 cm. Diameter Electrode for Various Discharge Energies.

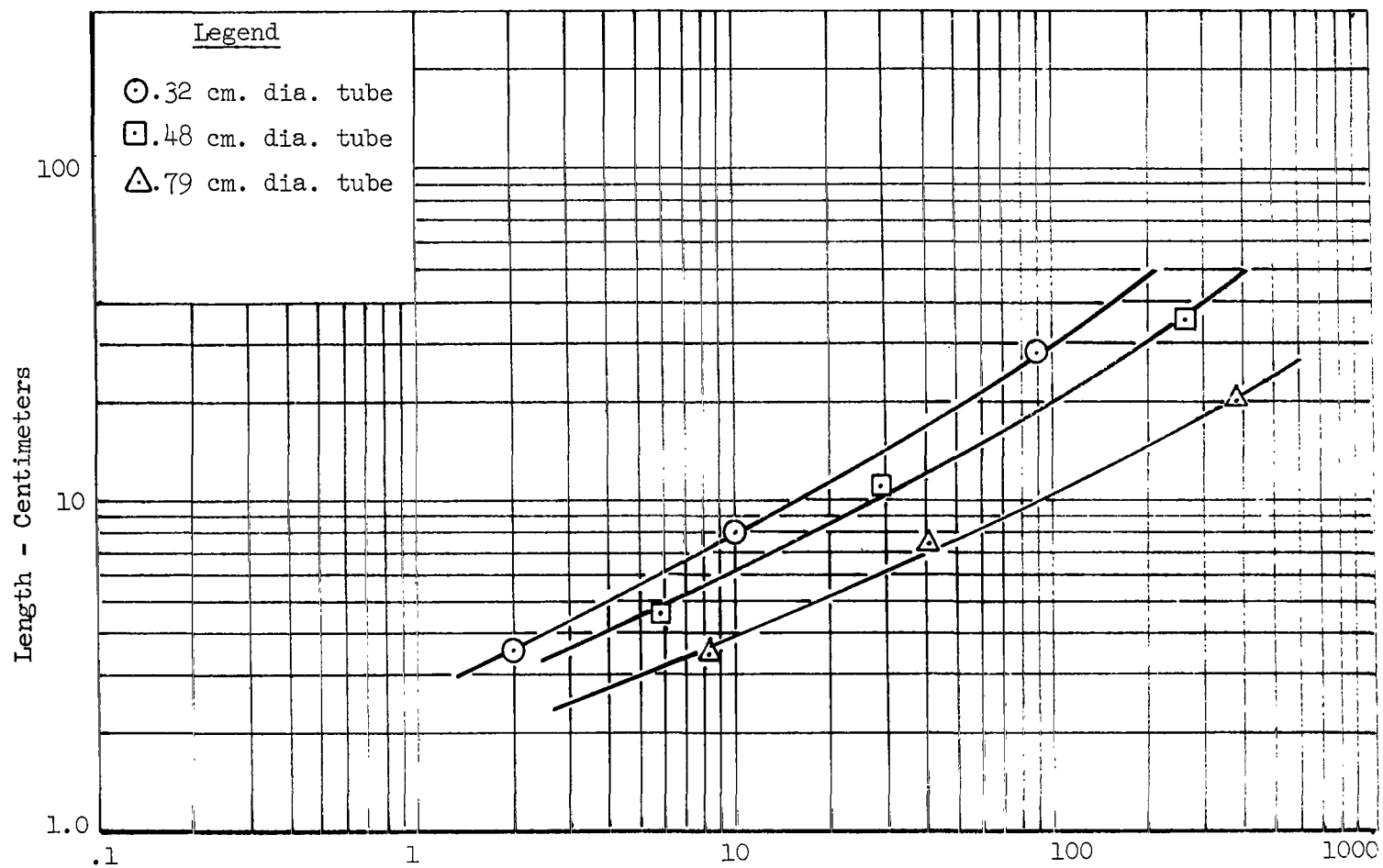


Fig. 64. - Plasma Length in Nitrogen with 0.40 cm. Diameter Electrode for Various Discharge Energies

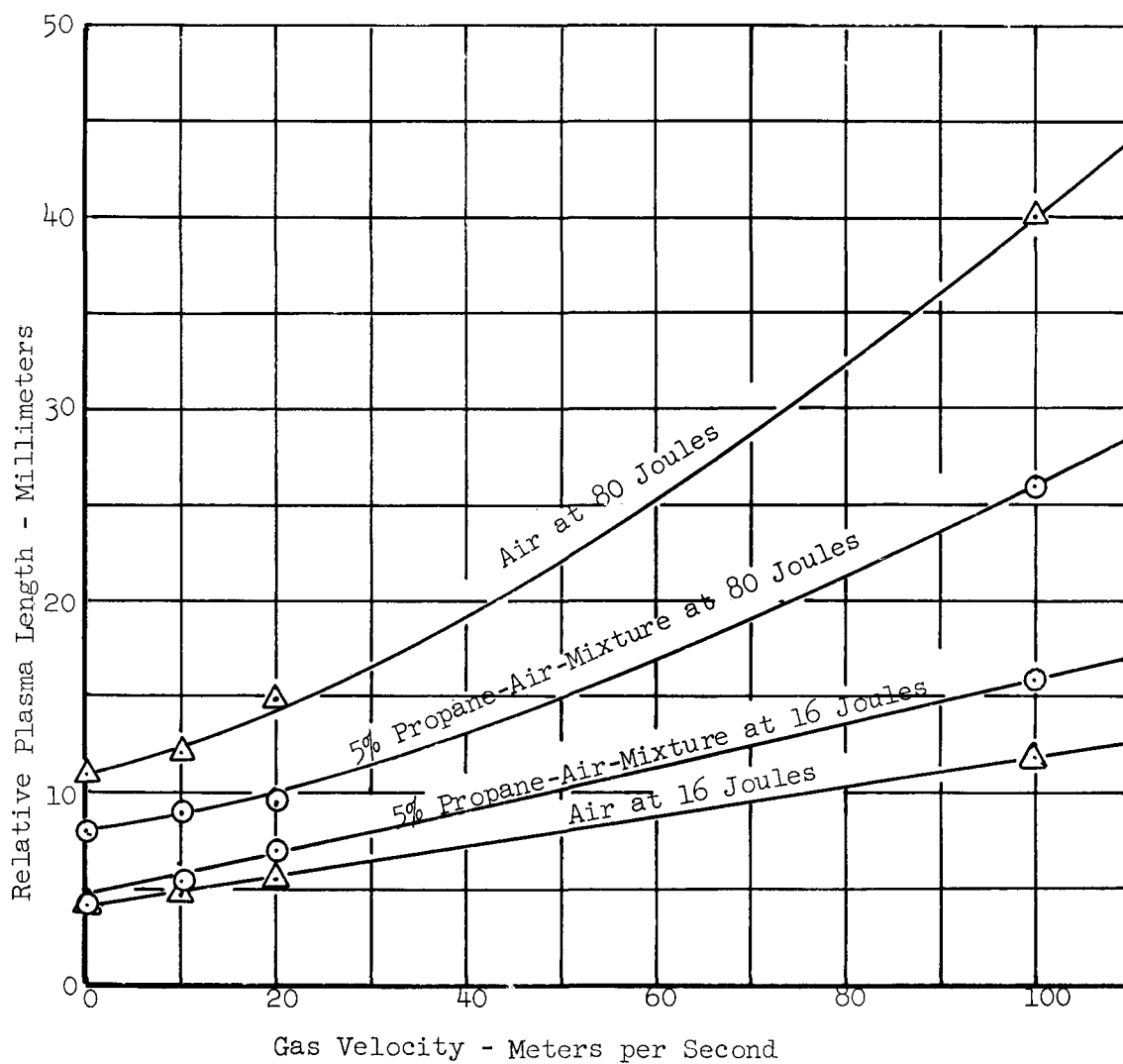


Fig. 65. - Relative plasma Length For Various Gas Velocities and Two Discharge Energies.

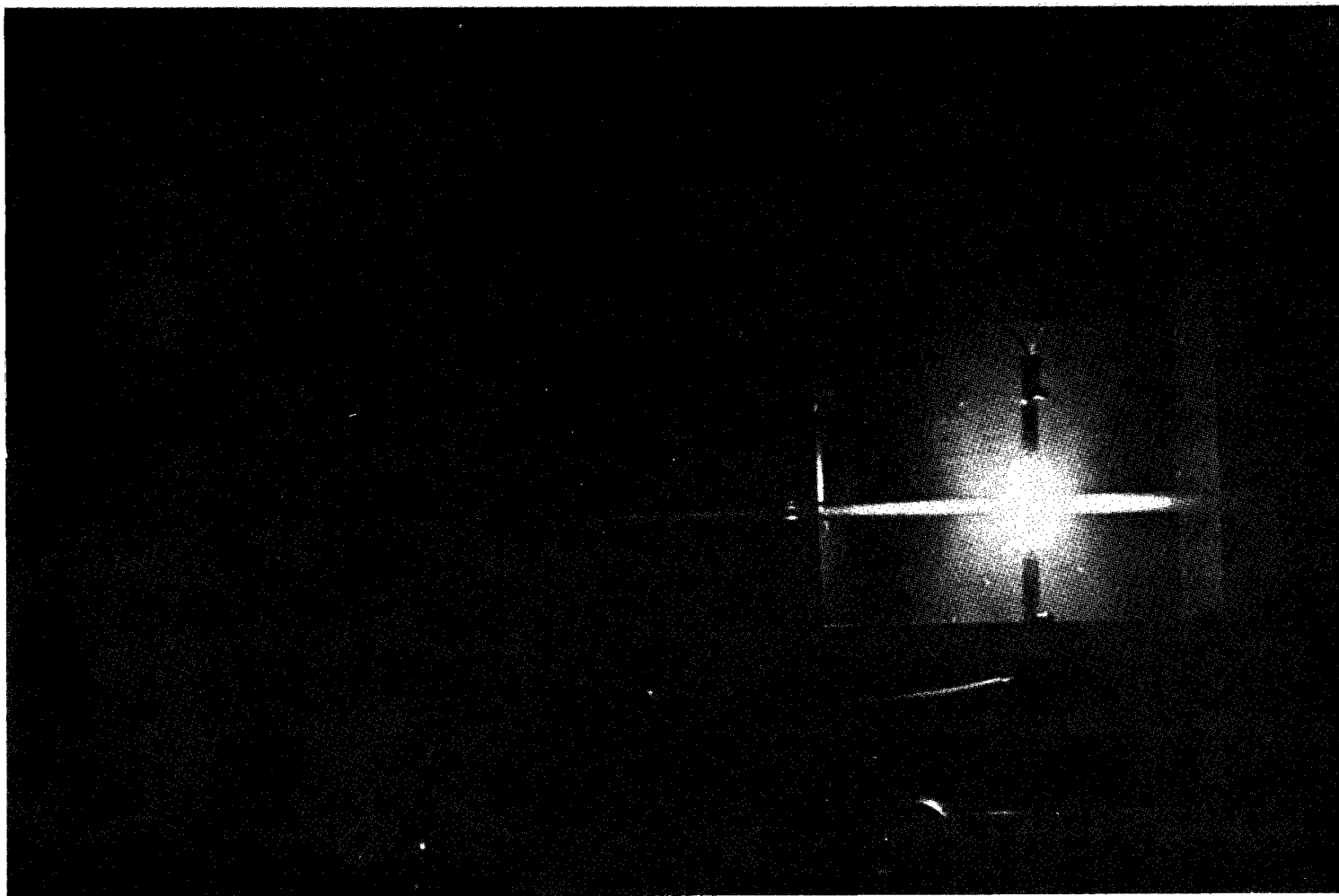


Fig. 66(a). - Discharge Energy is 16 Joules in an air environment.

Figure 66. - Comparison of Discharges in Air and 5% Propane-Air
Mixture at 16 and 80 Joules. Gas flow is 100 meters/second.

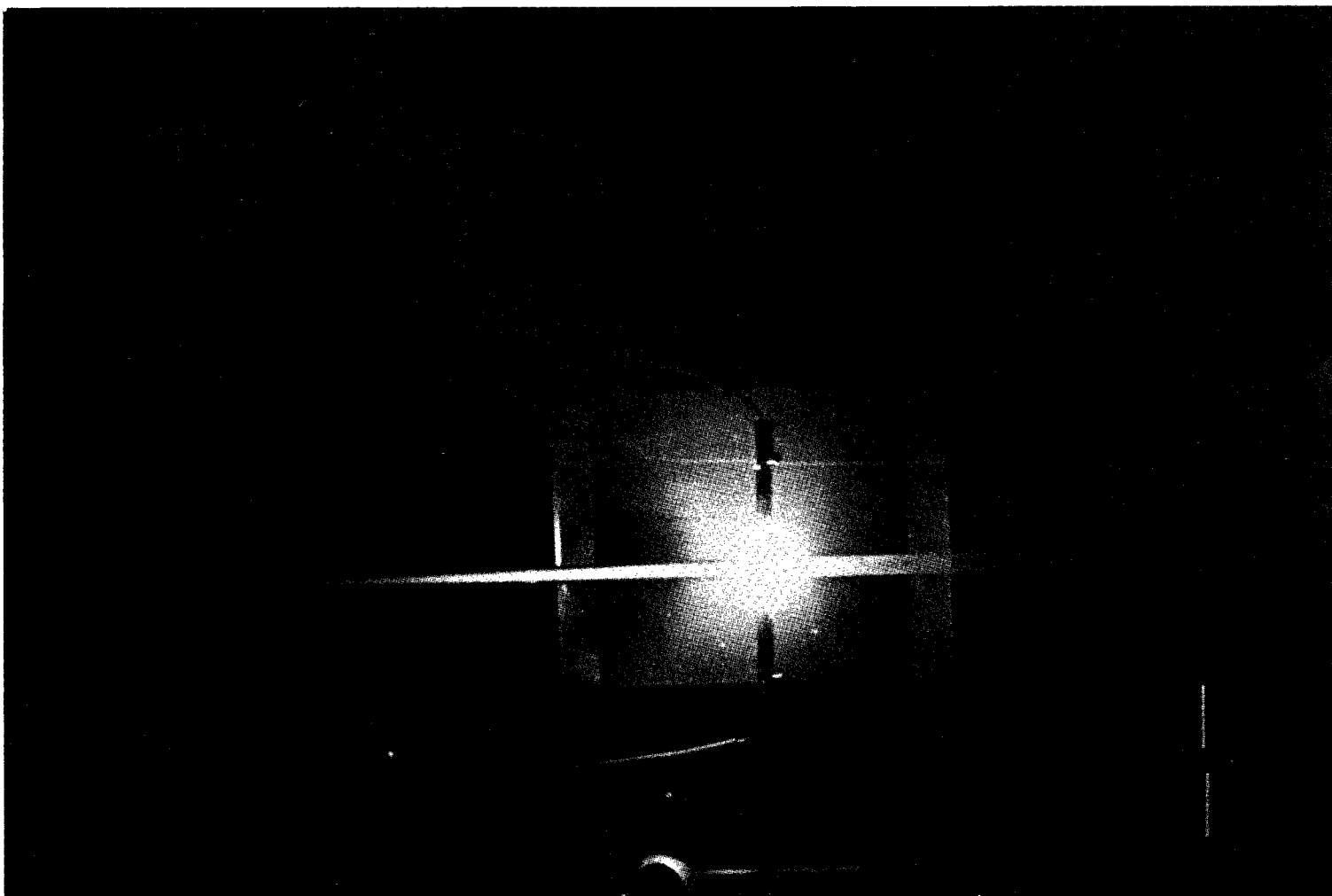


Fig. 66(b). - Discharge Energy is 16 Joules in a 5% Propane-Air Mixture.

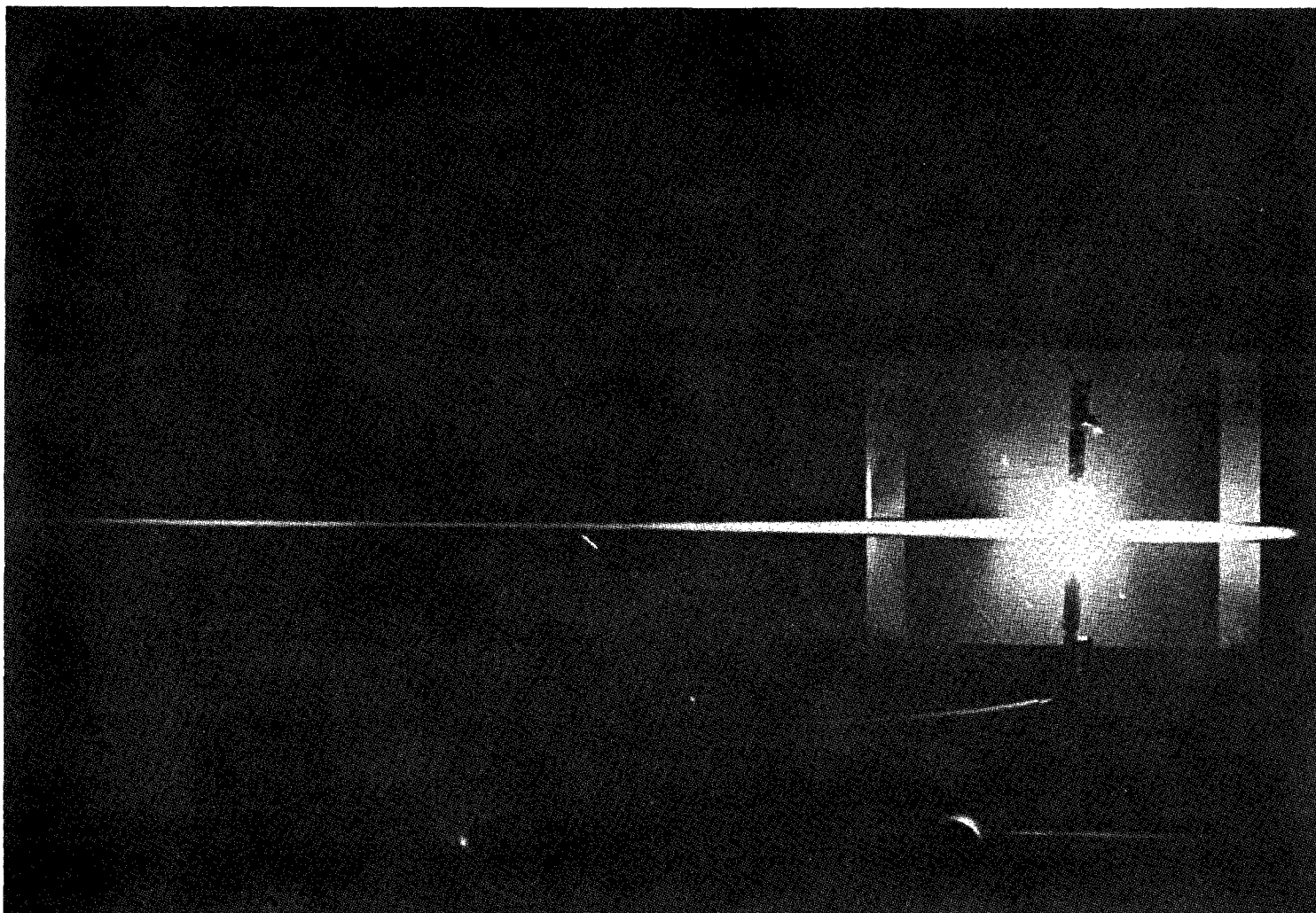


Fig. 66(c). - Discharge Energy is 80 Joules
in an Air Environment.

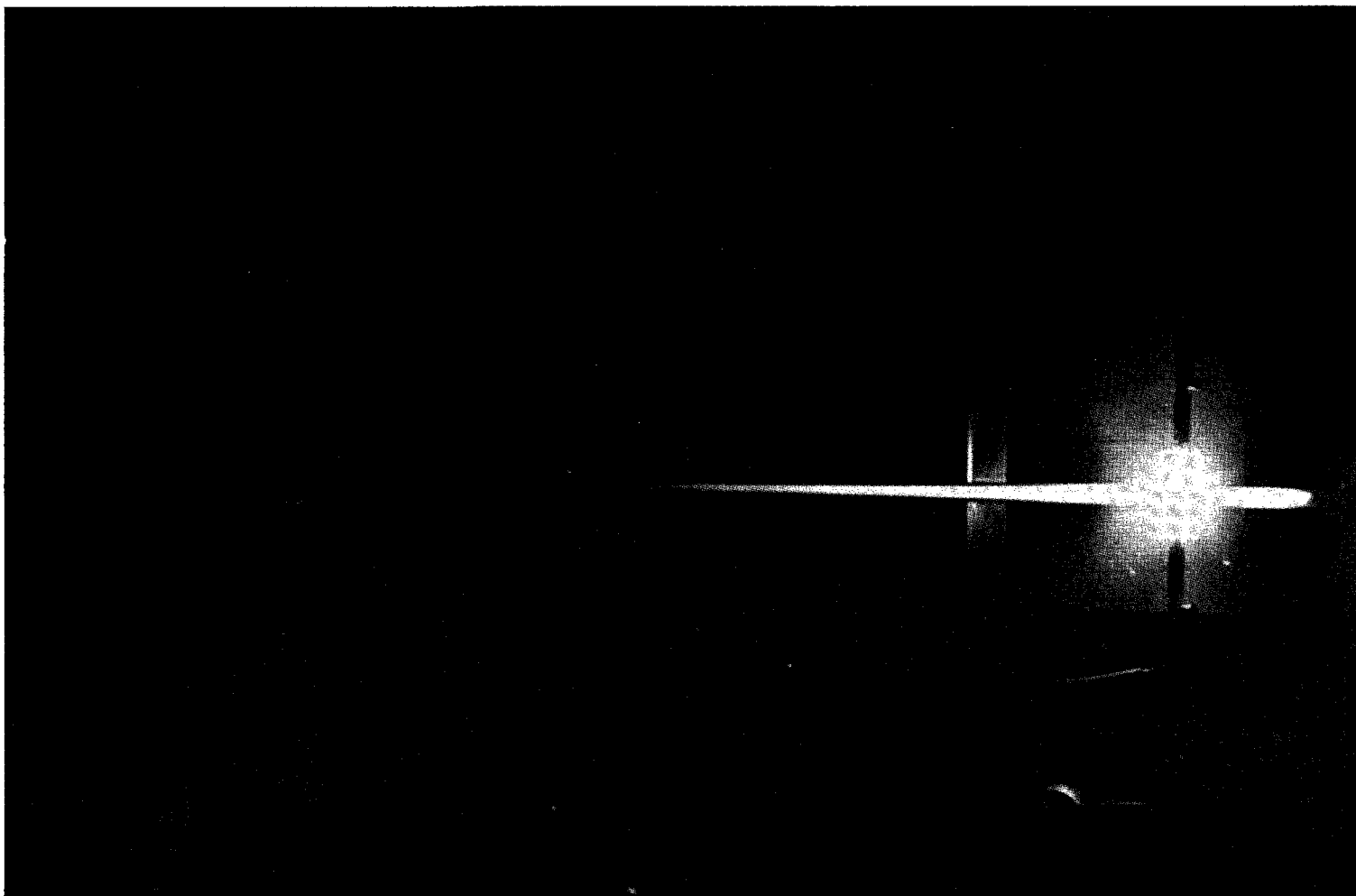


Fig. 66(d). - Discharge Energy is 80 Joules in a 5%
Propane-Air Mixture.

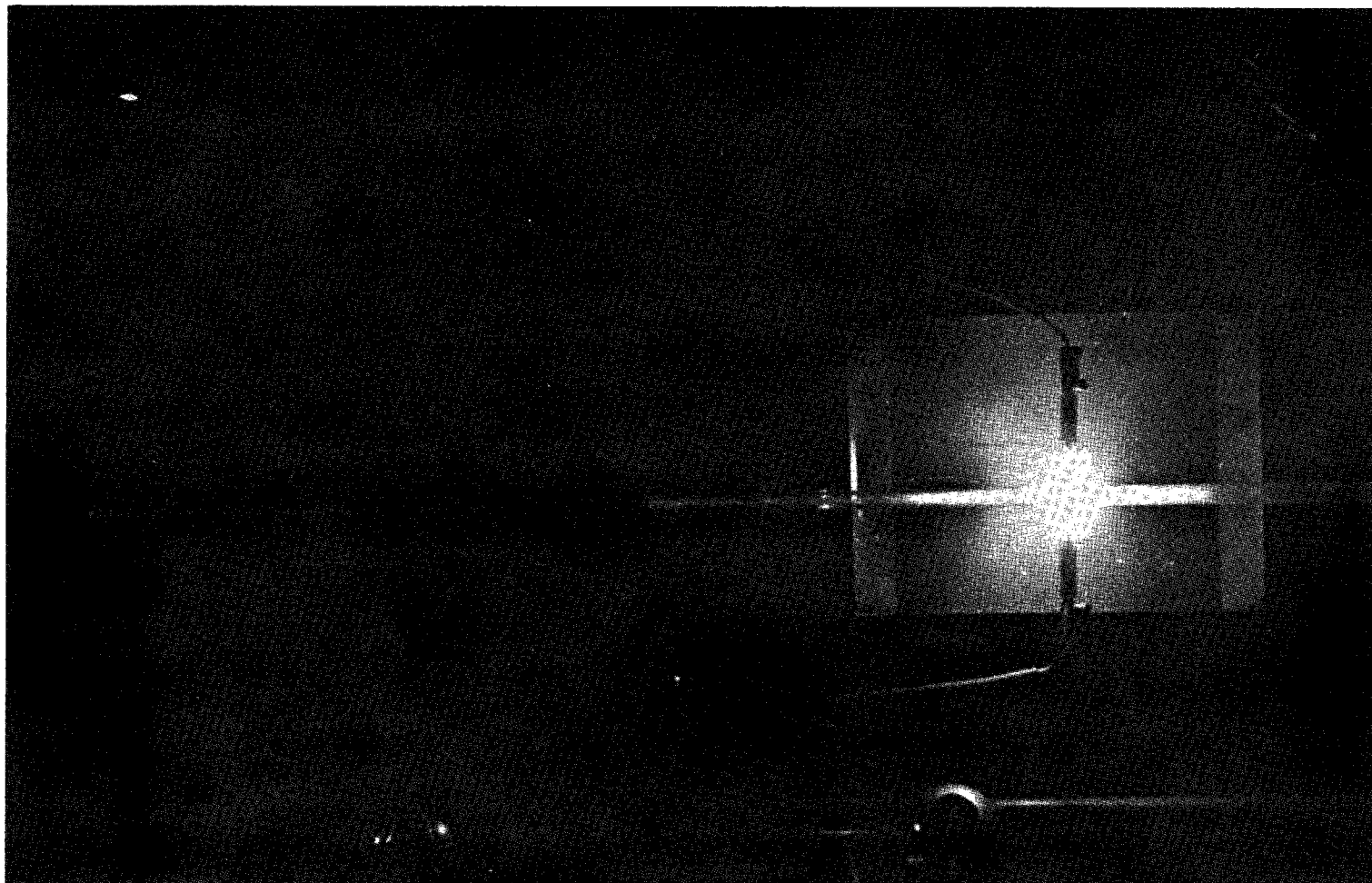


Fig. 67(a). - Flow Velocity is 10 meters per second.

Figure 67. - Comparison of Discharge at Two Velocities for 5%
Propane-Air Mixture and a Discharge Energy of 16 Joules.

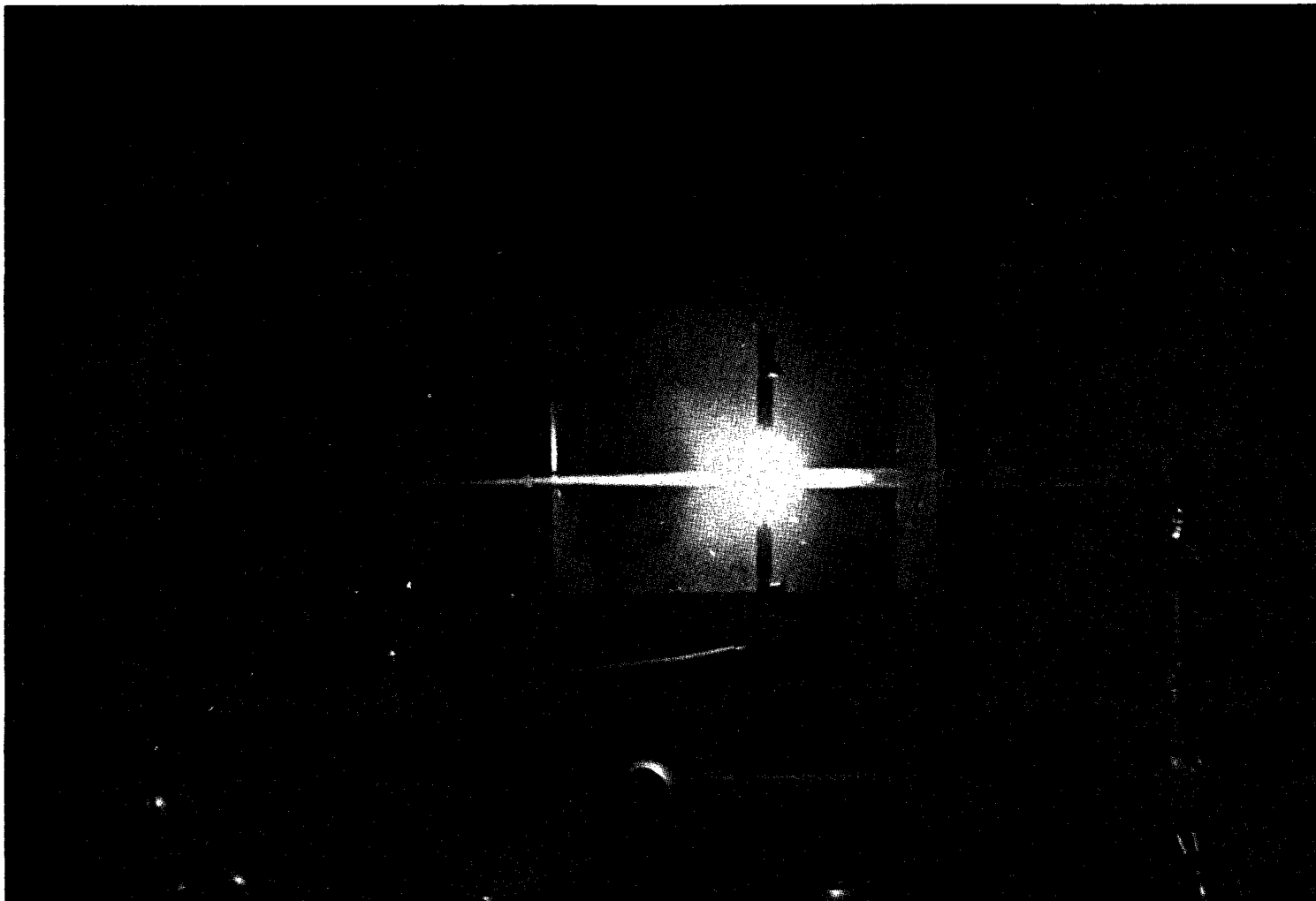


Fig. 67(b). - Flow Velocity is 20 meters per second.

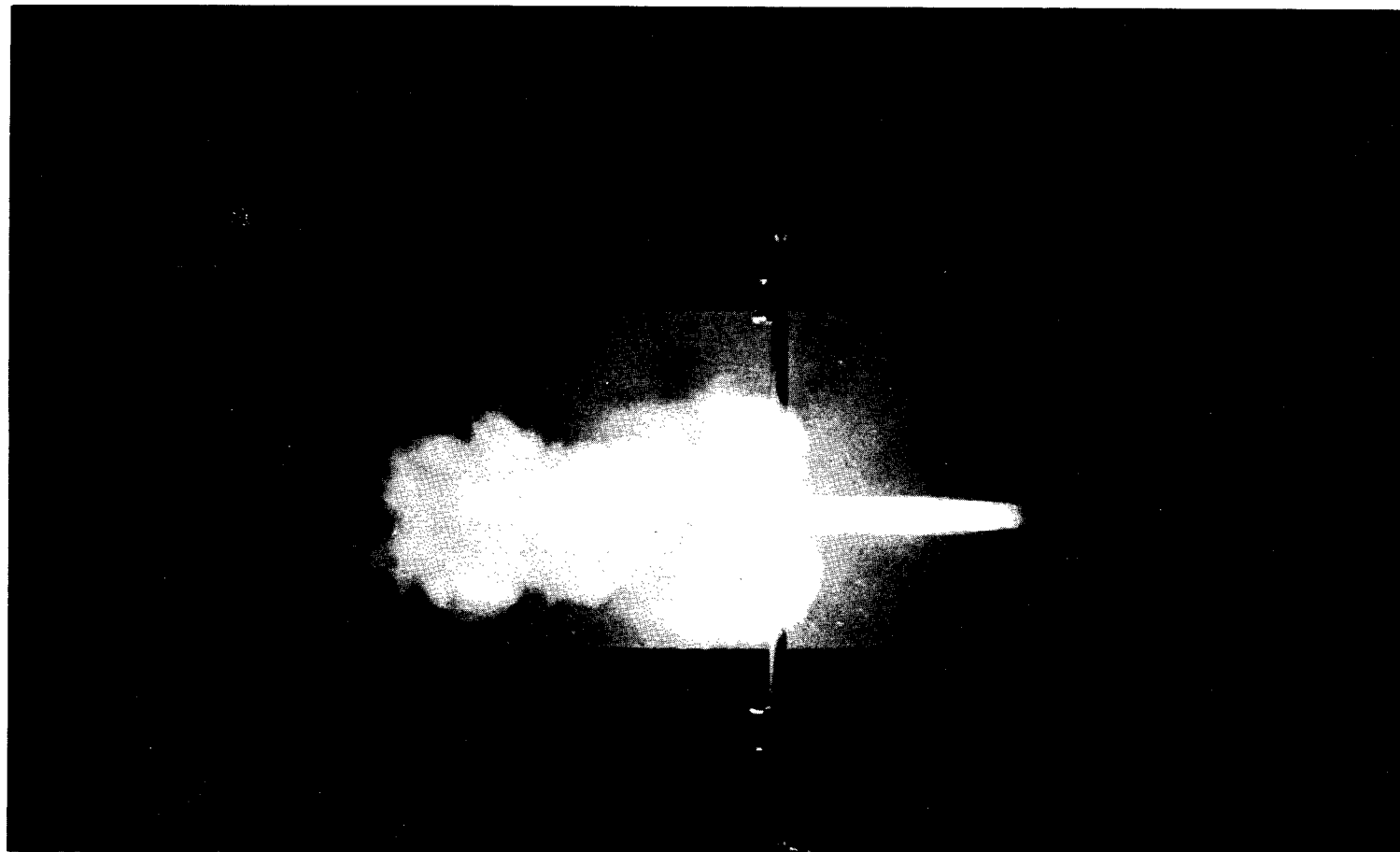


Fig. 68(a). - No Tube on Left of Electrode Holder

Figure 68. - Effect of Tube Length on Plasma Characteristics

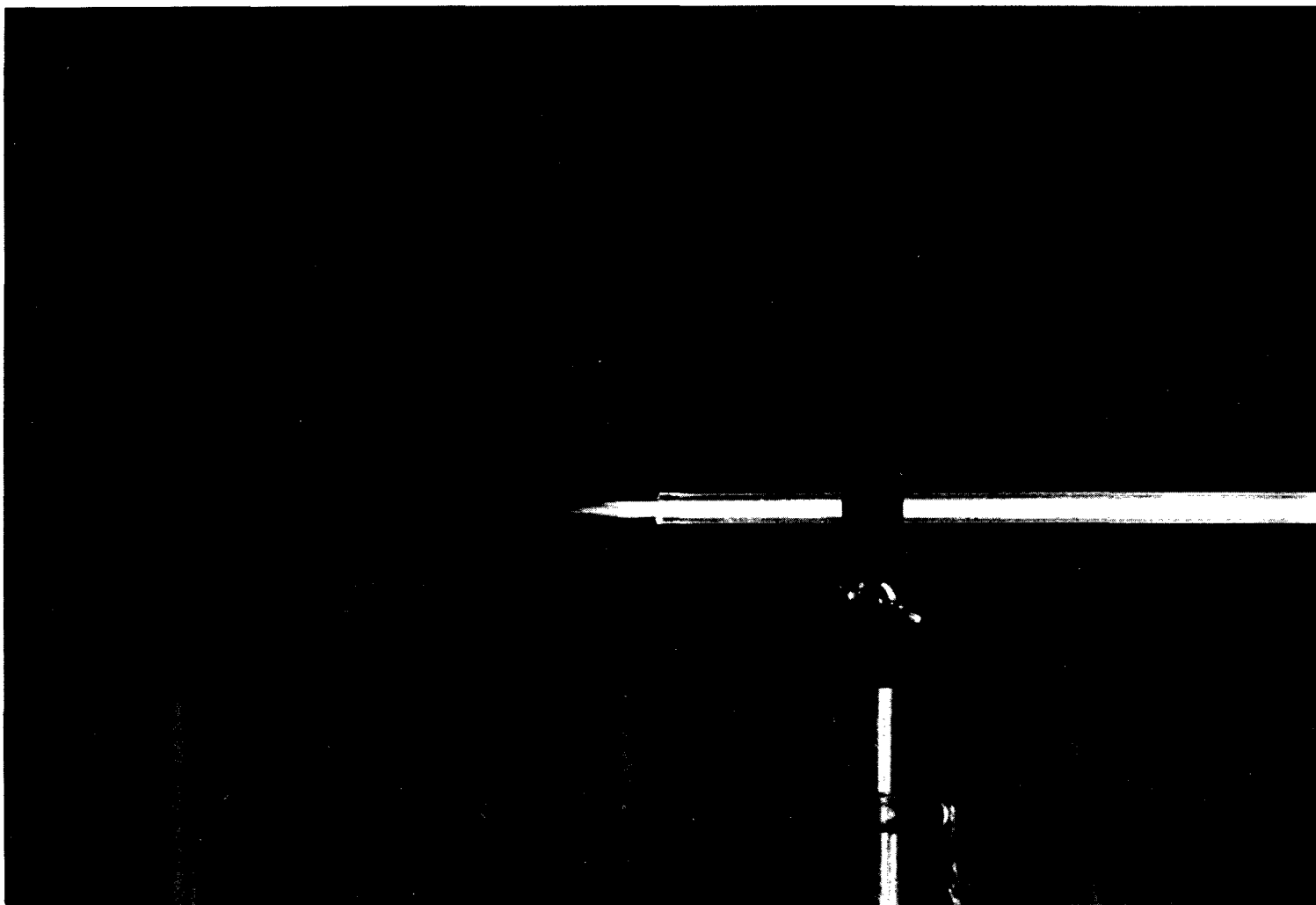


Fig. 68(b). - A 50 cm. Tube to the Left
of Electrode Holder.

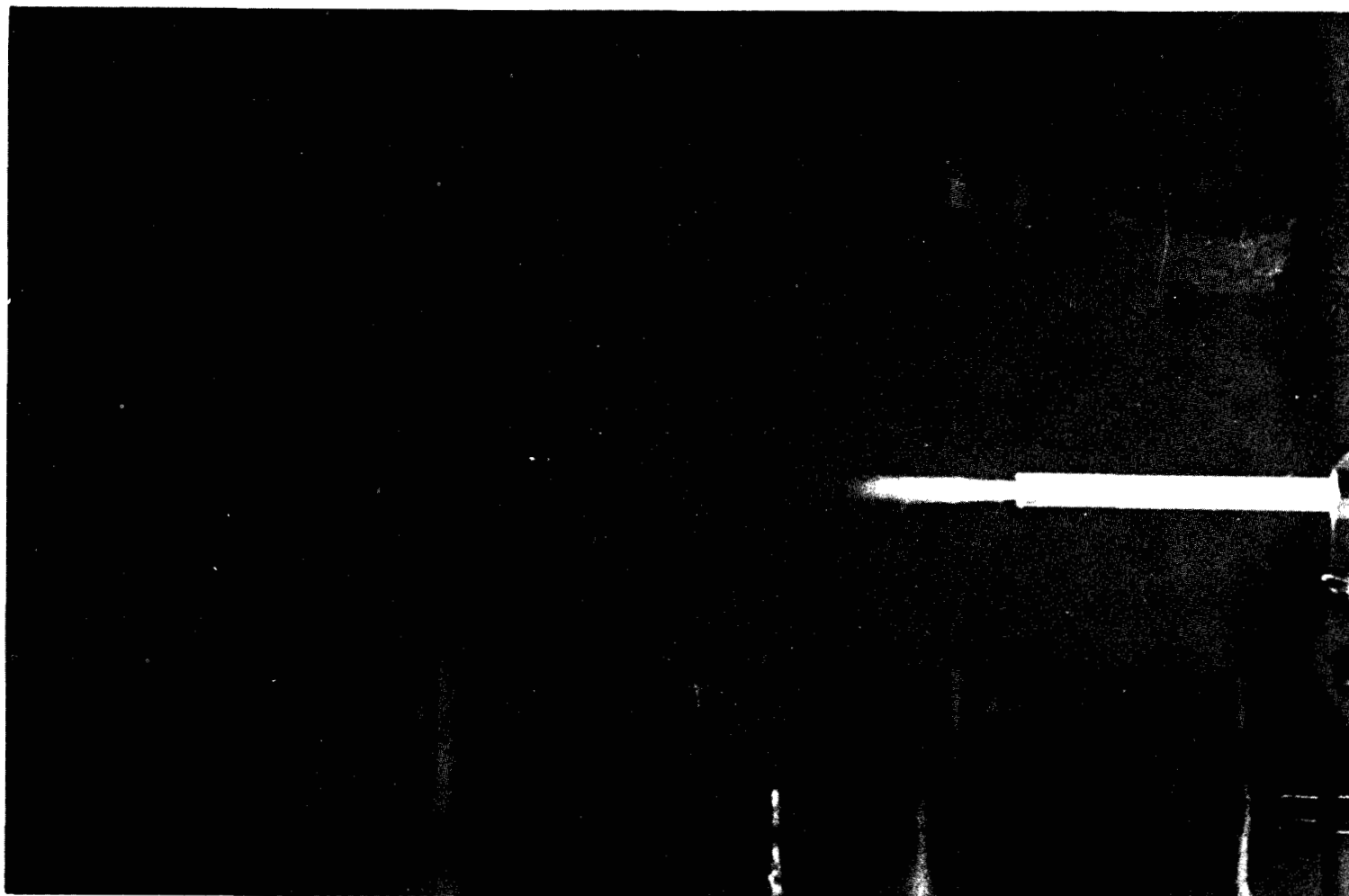


Fig. 68(c). - A 30 cm. Tube to the Left
of Electrode Holder.

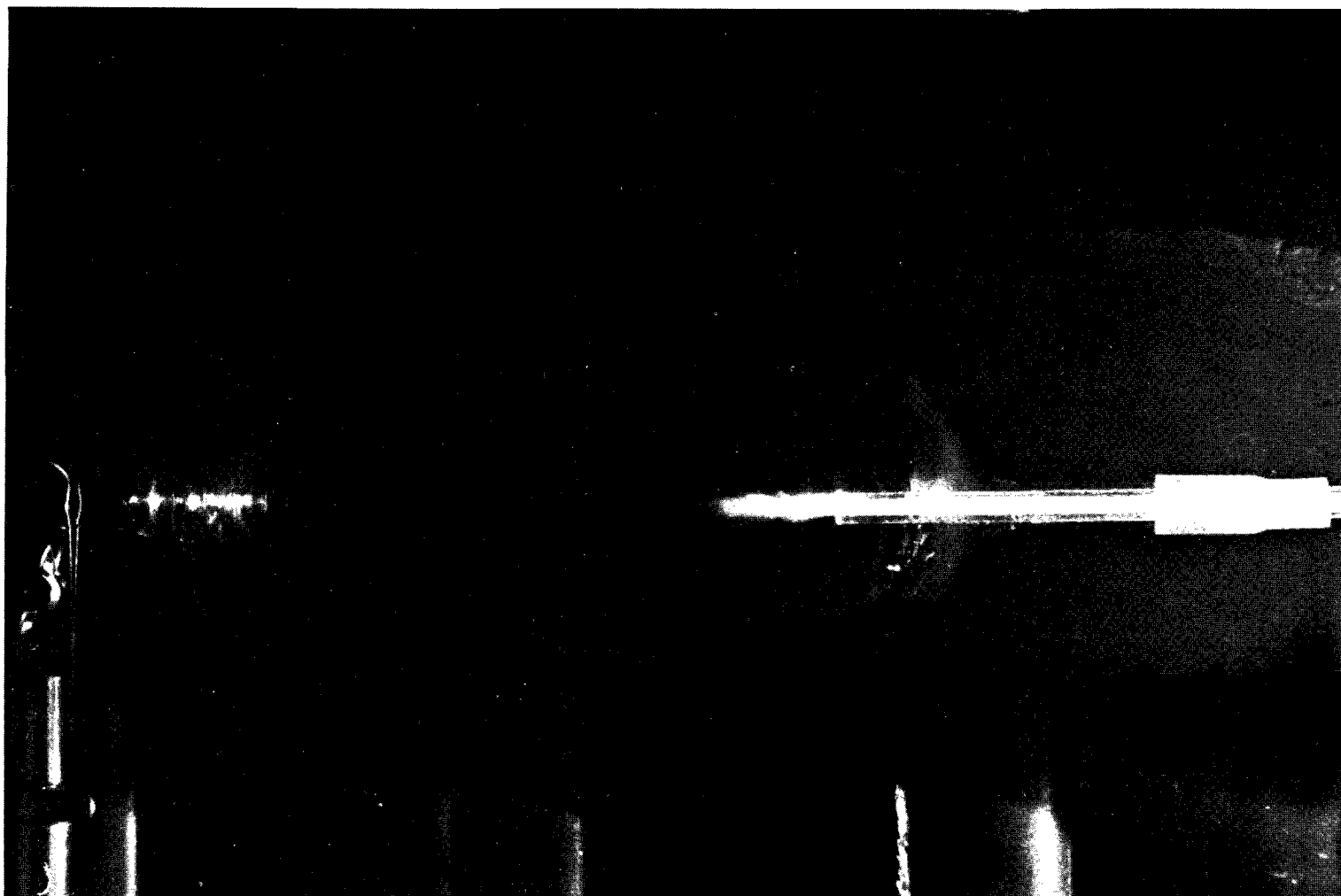


Figure 69. - Expansion of a Plasma Produced in Air
Into a Large Volume.

Test installation used for electrostatic discharge test with effluent vented vapor from a flush vent exit. Testing performed at Lightning & Transients Research Institute, at Minneapolis, Minnesota.

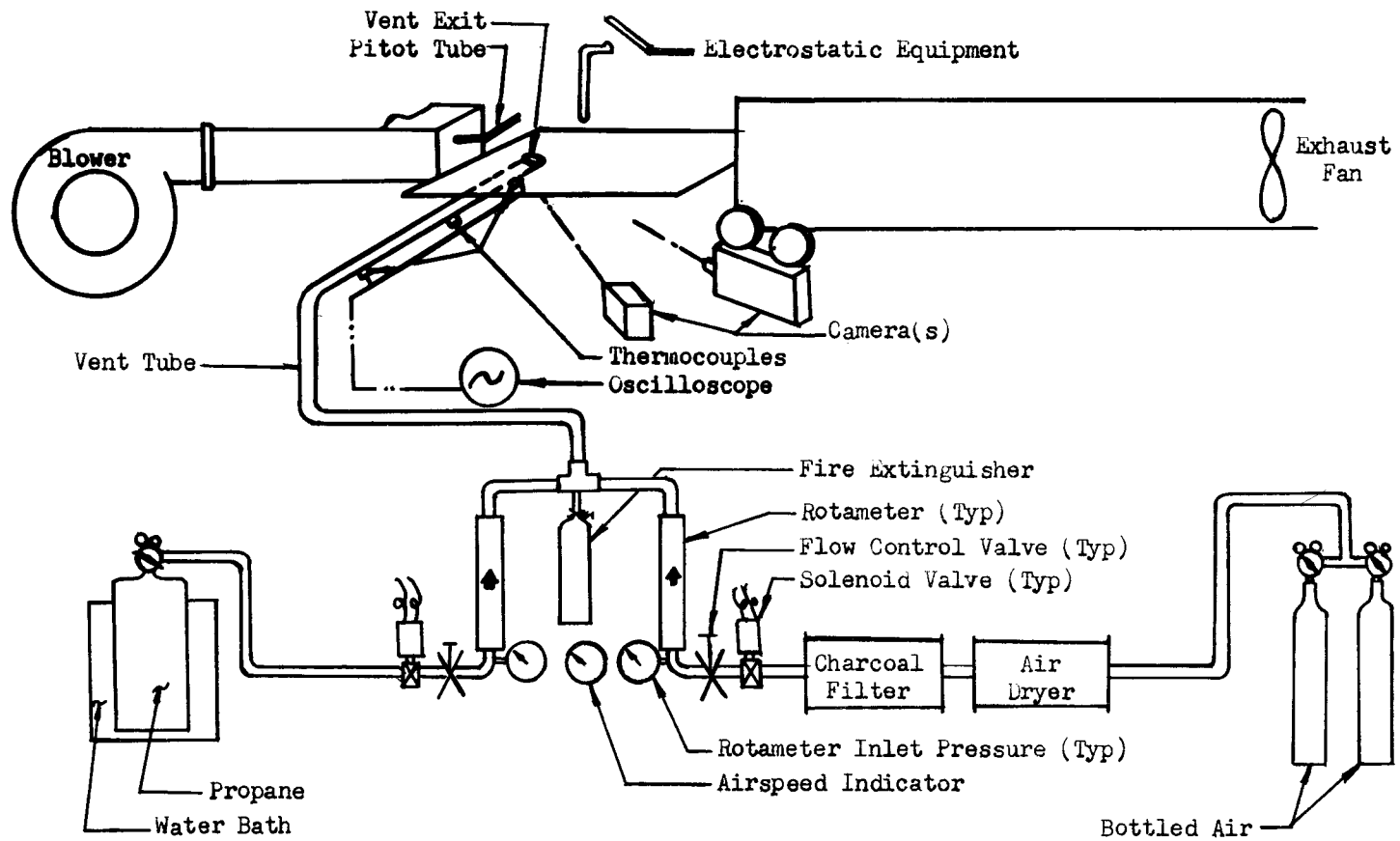


Figure 70. - Schematic - Test Installation at Lightning & Transients Research Institute.

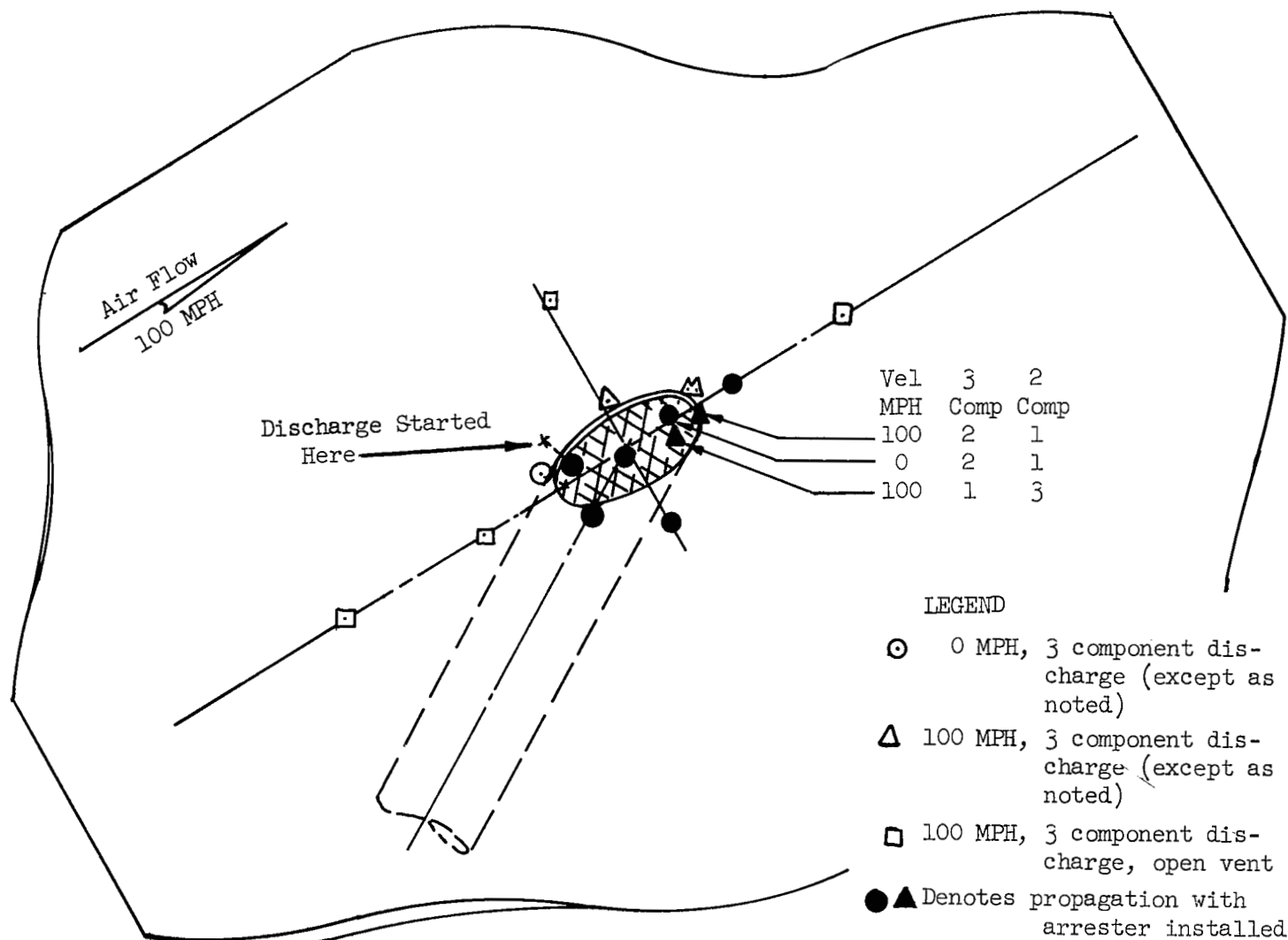


Fig. 71 - Summary of Discharge Locations for Tests with Flame Arrester Installed. Selected tests with open vent also shown.